USE OF MODIFIED SWEET POTATO STARCHES AS CORROSION INHIBITORS OF SELECTED METALS

BY

ANYIAM, CHIOMA KEZAIAH (B.ENG., M.Sc.)

REG. NO: 20104832618

A THESIS SUBMITTED TO THE POSTGRADUATE SCHOOL

FEDERAL UNIVERSITY OF TECHNOLOGY, OWERRI

IN PARTIAL FULFILLMENT OF THE REQUIREMENTS FOR THE AWARD OF THE DEGREE (DOCTOR OF PHILOSOPHY), Ph.D. IN

POLYMER SCIENCE

JULY 2016

Certification

This is to certify that the research work entitled **"Use of Modified Sweet Potato Starches as Corrosion Inhibitors of Selected Metals"** was actually carried out by ANYIAM CHIOMA KEZAIAH (REG. NO: 20104832618) in accordance with regulations governing the award of Doctor of Philosophy (PhD) in the Postgraduate School of the Federal University of Technology, Owerri.

Prof. O. Ogbobe
Principal Supervisor
..... 12/8/16
Signature and Date

Prof. E.E. Oguzie
Co-Supervisor
..... 12/8/16
Signature and Date

Engr. Prof. I.C. Madufor
Co-Supervisor
15/8/16
Signature and Date

Dr. M. U. Obidiegwu
Head of Department (PTE)
15/08/16
Signature and Date

Prof. G.I. Nwandikom
Dean, SEET
18/08/16
Signature and Date

Prof. (Mrs) N. N. Oti
Dean, PGS
.....
Signature and Date

Prof. F. E. Okieimen
External Examiner
..... 20/7/16
Signature and Date

Dedication

This work is dedicated to my father, Late Magnus Tomike Njoku who laid the foundation with which I built my educational pursuit.

Acknowledgements

My profound gratitude goes to The Almighty God for the grace and wisdom given to me to complete this work. May His name be glorified forever more.

I acknowledge with gratitude my principal supervisor, Prof. O. Ogbobe, for his guidance, understanding and encouragement. I also appreciate my co-supervisors, Prof. E. E. Oguzie of Electrochemistry and Material Science Unit, Department of Chemistry, Federal University of Technology Owerri, for guiding me in this work and for exposing me to his wealth of research experience on corrosion studies and Engr. Dr. Madu for his fatherly advice, motivation, guidance and encouragement.

I am indebted to the Head, Department of Polymer and Textile Engineering, Engr. Dr Martin Obidiegwu for his encouragement which was most valuable

Prof. C.B.C. Ohanuzue, Dr G.N. Onyeagoro, Engr. Dr. P.I. Anyanwu, Engr Dr C. Onuegbu, Engr. Dr. S. Nwanonenyi and other staff of the Department of Polymer and Textile Engineering are also appreciated for their unalloyed cooperation and contribution in making this work a reality.

I am also grateful to Mr Arinze Chidiebere of EMRU laboratory for his assistance during the course of this work, I am as well grateful to Mr Columbus of the Erosion Control Unit for his help and assistance. I am infinitely grateful to my

mum, Mrs Priscilla Njoku, and my siblings, Dr Victor Njoku, Ogo, Obinna, Ebere, Chinyere, Chiedo and Uchechi, for their prayers and moral support.

Special thanks go to my husband, Mr Kizito Anyiam, for his support, encouragement, assistance and understanding at various stages of this work, indeed he is exceptional. My children, Chimdiya, Chibuikem, Chimzuroke and Treasure, are also appreciated for their understanding.

This project is supported by the FUTO Senate Research Grants Committee and the Nigeria Tertiary Education Trust Fund (TETFund); under 2011/2012 TETFund Research Allocation for the Federal University of Technology Owerri.

CHIOMA KEZAIAH ANYIAM

Table of Contents

Chapter Four: Results and Discussions

List of Tables

List of Figures

ABSTRACT

Sweet potato starch was modified via extrusion, alkaline steeping and acid steeping to yield physically modified starch (PMS), alkaline treated sweet potato starch (ASS) and acid treated sweet potato starch (ATS). The unmodified and modified starches were characterized using the Fourier transform infrared spectroscopy and assessed for corrosion inhibition efficacy on mild steel and galvanised steel in 0.25 M H_2SO_4 and 1 M HCl using gravimetric (weight loss) measurements and potentiodynamic polarization techniques. All the starch samples inhibited corrosion of the metals in the acidic media, with maximum efficiency ranging from 22.86 to 62.76 % for mild steel and 24.27 to 63.48 % for galvanised steel. Introduction of potassium iodide notably increased inhibition efficiency up to 85.59 %, 85.09 %, 83.64 %, 87.72 % for NS, PMS, ASS, and ATS respectively for mild steel and for galvanised steel 92.60 %, 95.62 %, 93.67 % and 93.94 % respectively for NS, PMS, ASS and ATS. Fourier transform infrared spectroscopy was used to analyse the scrapped metal after corrosion in presence and absence of the additives in the acidic media. Atomic force microscopy was used to analyse the surface morphology of the corroded metals in the presence and absence of the additives in the acidic media. The inhibitor adsorption characteristics were found to obey Langmuir isotherms. Temperature studies (30-60^{O}C) investigated showed higher inhibition efficacy at lowest temperatures, thus suggesting physiosorption adsorption mechanism. These results were in agreement with the kinetic and activation energy parameters investigated. Potentiodynamic polarization measurements showed that NS, PMS, ASS and ATS are mixed-type inhibitors.

Keywords: Corrosion, steel, biopolymers, inhibitive behaviour, starch.

CHAPTER ONE

INTRODUCTION

1.1 Background Information

Corrosion of metals and alloys occur due to chemical and electrochemical reactions with their environment, which often results in drastic deterioration in the properties of the metal or the material. The preliminary steps to reduce, combat or completely eradicate corrosion require the elimination or suppression of the corrosive activity by the use of inhibitors, pigments, coatings and others providing barrier properties, corrosion reducing activity and overall an active anticorrosion effect. In the past two decades, there has been a vigorous effort to develop efficient, economically viable and environmentally compliant methods to prevent metallic corrosion.

The use of inhibitors remains one of the most effective, economic and practical methods of protecting metallic surfaces against corrosion in aggressive media. Studies on inhibitors have evolved since 1950. At the beginning, the investigations were focused on the evaluation of corrosion prevention efficiency of chromates, nitrates, and borates, which showed high efficiency, but has a negative effect of high toxicity for human being (Kàlmàn, 1990). Recent studies as elucidated in section 2.1 have focused on the evaluation and development of "environmental friendly" compounds as corrosion inhibitors. Inhibitors of polymeric origin have drawn considerable attention in recent times due to their

inherent stability, cost effectiveness, unusual deformation, functional groups, the presence of multiple adsorption sites as well as the presence and nature of the heteroatoms attached to the polymers which enable them form complexes with metal ions on the metal surfaces. These complexes occupy a large surface area, blanketing the surface and protecting the metal from the corrosive agent present in the solution. The resulting adsorbed film acts as a barrier that separates the metal from the corrodent and efficiency of the inhibitor depends on the mechanical, structural and chemical characteristics of the adsorption layer formed under particular conditions (Oguzie 2004, 2008). Owing to the growing interest and attention of the world towards the protection of the environment, corrosion researches are geared towards finding alternative green corrosion inhibitors to replace synthetic corrosion inhibitors which in spite of their high efficiency are expensive, toxic and harmful to the environment when compared to the green corrosion inhibitors.

Green polymeric inhibitors are natural biopolymers obtained from plants and animals and they include the following lignin, starch, cellulose, cashew nut shell liquid, rice husks, sucrose, caffeic acid, lactic acid, chitosan to mention but a few. These green polymers contain functional groups which impart good adhesion and corrosion resistance performance to the substrate. Polymeric plant extracts have become important because they are environmentally acceptable, inexpensive, readily available and renewable sources of materials. However effective these

biopolymers are, their performance are further enhanced by physical modification, chemical modification or addition of modifiers (halides and surfactant).

1.1.1 Polymers

Polymers are long chain, macro molecules built up from smaller repeat unit's molecules called monomers**.** Polymers consist of tens or hundreds of thousands of monomer repeating units in its chain, sometimes with branching or cross-linking between the chains. The properties of polymers are dependent on many factors including inter- and intrachain bonding, the nature of the backbone, processing events, presence/absence of additives including other polymers, chain size and geometry, and molecular weight distribution. They are basically classified into two, namely synthethic and natural polymers.

1.1.2 Synthethic Polymers

These are man made polymers obtained from the synthesis of chemicals in the laboratories. They include polystyrene. polyester, polythene, nylon, et.c. They are made mostly to check the demerits and enhance the qualities of natural polymers depending on their use as well as impart a particular functionality. Plastic materials which are suitable for use in combating corrosion and several which have suitable characteristics such as good resistance to chemicals, heat and

environmental degradation, serve in place of scarce expensive metals and alloys include vinyl for piping, sheet graphite for parts of heat exchangers, et.c.

1.1.3 Natural Polymers

Natural polymers are polymers that occur in nature and include lignin, starch, cellulose, cashewnut shell liquid, rice husk, sucrose, caffeic acid, lactic acid, tannic acid, furan, proteins, glycerol, and vegetable oils et.c. They contain functional groups such as hydroxyls, aldehydes, ketones, carboxyls, double bonds, ester, and ether et.c. that imparts good adhesion and corrosion resistance performance to the substrate. Also, their performance can be further improved by chemical transformations and use of modifiers (inorganic reinforcements, nanomaterials).

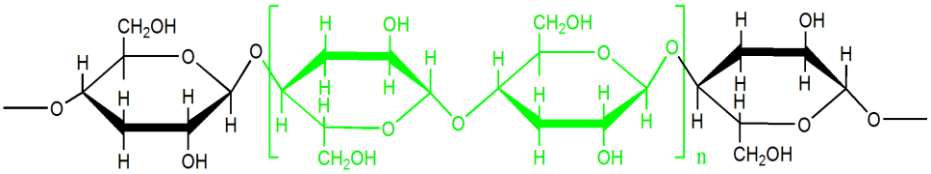

Cellulose

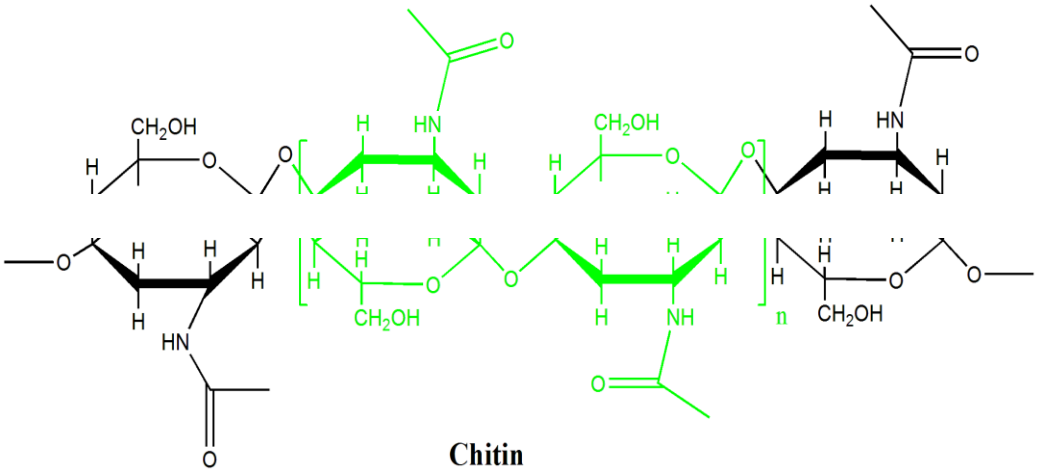

Chitin

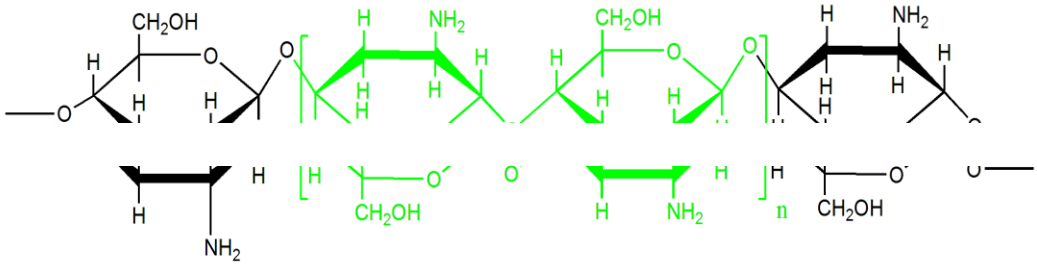

Chitosan

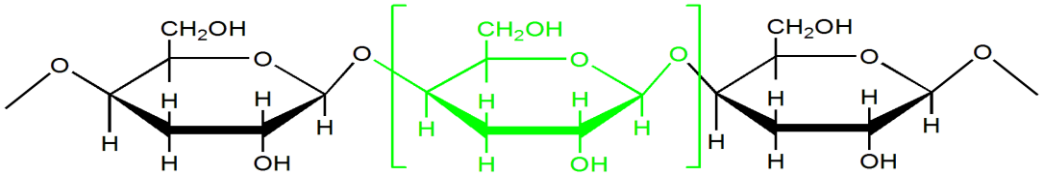

Starch

Figure 1.1. Structures of some natural polymers [Cellulose, Chitosan Chitin and Starch]. (Sharmin *et. al*. 2012)

1.1.4 Polymers and Corrosion Control

Polymers are unique materials with exceptional functionality and characteristics for corrosion control. They have been utilised in the control of corrosion as nonmetallic and chemically stable materials, in the form of individual structural materials or linings, protective coatings, coatings, et.c. They are used for the purpose of economizing on nonferrous metals and highly alloyed steels used by various industries in the role of anticorrosion materials (Klinov 1962). An anticorrosion coating for the corrosion protection of metals, liquid Nairit (chloroprene rubber; Yerevan, Armenia), have been used for the replacement of deficit metals. This coating was tested, especially, in ship construction and for the protection of screws (propellers), subjected not only to corrosion but to erosion and cavitations in thermal power equipment and they are also used for the lining of devices and equipment, and in the composition of protective coatings.

They are used as corrosion inhibitors because of their vast functional groups, through these functional groups they form complexes with metal ions and on the metal surface these complexes occupy a large surface area, thereby blanketing the surface and protecting the metal from corrosive agents present in the solution (Ranjedran *et al*. 2005). The inhibitive power of these polymers is related structurally to the cyclic rings, heteroatom (oxygen, sulphur and nitrogen) that have been found to increase basicity and electron density and acts as major active

centres of adsorption. It is widely accepted that inhibitors especially the organic ones work by an adsorption mechanism. The resultant film of inhibitor is then responsible for protection either by physically blocking the surface from the corrosion environment or by retarding the electrochemical processes. Fluorocarbonic polymers and polyorganosiloxanes are other classes of polymers that are suitable for the protection against corrosion of smoke pipes, pumps for pumping hot liquids, cracking installations, and other equipment under conditions of high temperatures and under the action of aggressive media.

1.1.5 Starch

Starch is a morphologically complex polymer substance, consisting of loose amorphous regions that are interspersed with highly regular crystalline regions, resulting from the formation of hydrogen bonds between the starch molecules. It is the major energy reserve of plants; it is extracted and refined by wet grinding, sieving and drying. After its extraction from plants, starch occurs as a flour-like tasteless and odorless white powder insoluble in cold water. This powder called native starch consists of microscopic granules with diameters depending on the botanic origin, ranging from 2 (for wheat and rice) to 100 μm (for potato), and with a density around 1.5 g.cm−3. The amylopectin content ranges between 72 and 82%, while the amylose content ranges between 18 and 28%. However, some mutant types of starch have very high amylopectin content (99% for waxy maize),

and some very high amylose content (up to 70% and more for amylomaize). Other trace elements are lipids, proteins, minerals, phosphorous, enzymes, amino acids, and nucleic acids. Amylose is essentially a linear polymer consisting of glucose units linked by α-(1→4) glycosidic bonds, slightly branched by α-(1→6) linkages. Amylopectin is a highly branched polymer constituted of relatively short branches of α-D-(1→4) glycopyranose that are interlinked by α-D-(1→6) glycosidic linkages. The starch granule displays a multiscale structure as shown in Fig. 1.2. It consists of the starch granule (2–100 μm), into which we find growth rings (120–500 nm) composed of blocklets (20–50 nm) made of amorphous and crystalline lamellae containing amylopectin, and amylose chains (0.1–1 nm). When observed under a microscope and polarized light, starch shows birefringence. The refracted characteristic "Maltese cross" corresponding to the crystalline region is typical of a radial orientation of the macromolecules. The so-called onion-like structure of starch granule with more or less concentric growth rings is composed of alternating hard crystalline and soft less ordered shells growing by apposition from the hilum (center of the granule). The thickness of the combined repeated crystalline and amorphous lamellae is 9 nm regardless the botanic origin. Native starches contain between 15% and 45% of crystalline material (Christopher, 1997; Tang *et al*. 2004). Depending on their X-ray diffraction pattern, starches are categorized in three crystalline types referred to A, B and C. A-type is characteristic of cereal starches (wheat and maize starch). B-type is typical of tuber and amylose-rich cereal starches. C-type is

characteristic of leguminous starches and corresponds to a mixture of A and B crystalline types. V-type is observed during the formation of complexes between amylose and a complexing molecule (iodine, alcohols, cyclohexane, and fatty acid). The appearance of starch X-ray diffraction pattern depends on the water content of granules during the measurement. The more starch is hydrated, the thinner the diffraction pattern rings up to a given limit. Water is therefore one of the components of the crystalline organization of starch. The crystalline composition consists of around 15–45% of the starch granules.

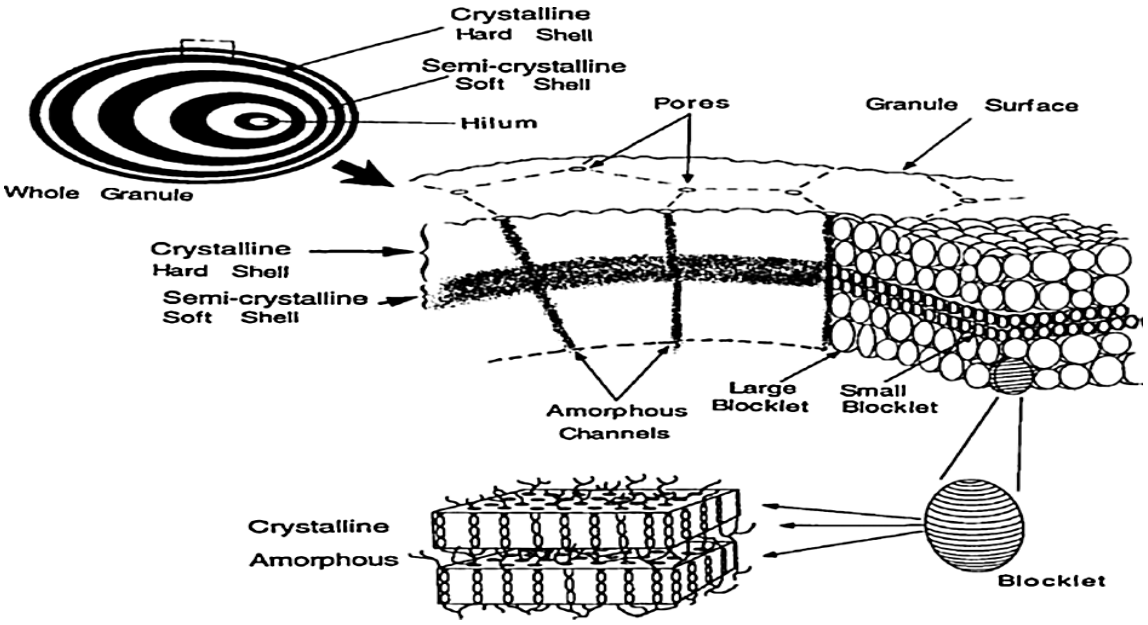

Figure 1.2 Schematic drawing of hierarchical structure of starch granule. (Gallant *et. al. 1997*).

The scope of starch application is both enhanced and limited by its unique molecular structure. For instance, the compact arrangements of molecules in the crystalline regions inhibit water or chemical reagents from making contact with

the molecules in the crystalline region. As a result, the gelatinization temperature is higher and chemical reactivity of starch is decreased. Meanwhile, the relative large molecular weight and the extensive network formed by hydrogen bonds lead to high gelatinization temperature and lower fluidity.

1.1.6 Modification of Starch

Native starch exhibits some drawbacks that restrict its use, such as insolubility in cold water and sensitivity to shearing and low pH (Burrell 2003). The objective of starch modification is to alter the physico-chemical characteristics of native starch to improve functional characteristics. Modification is important for the continued and increased use of starch to provide thickening, gelling, binding, adhesiveness and film forming characteristics. The physical and/or chemical modification of starch may, therefore, enhance its applications range. Several methods have been developed to produce modified starches with a variety of characteristics and application. These techniques alter the starch polymer, making it highly flexible and changing its physicochemical properties and structural attributes to increase its value for food and non-food industries (Lopez *et al*., 2010). Drying methods to make starches cold water soluble are extrusion, drum drying or spray drying. For many purposes, the market prefers starch with less extensive crystalline regions, resulting in improved physico-chemical properties and increased reactivity for planned applications. Therefore, there is great interest

in methods to modify the structure in the crystalline region, or decrease the size of crystalline regions (Fiedorowicz *et al.* 2001; Liang *et al.* 2004). The main methods of decreasing starch crystalline regularity include chemical processes, such as acidolysis, oxidation (Wang & Wang, 2003), enzymatic degradation processes (Zhang & Oates, 1999; Yiu *et al*., 2008) and physical processes, such as heat-moisture treatment, radioactive degradation, microwave degradation, ultrasonic degradation and extrusive degradation processes. . Sweet potato starch is composed of a mixture of amylose and amylopectin and is reported to possess A-type (high swelling) pattern and its starch granules are medium sized with a smooth round oval shape (Morothy, 2002).

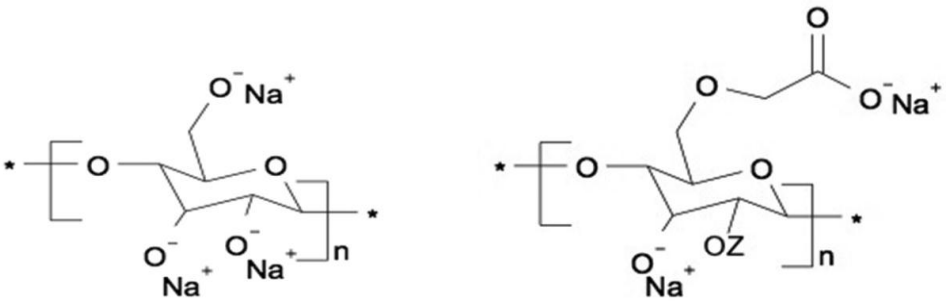

AS CMS

Figure 1.3 Chemical structures of activated starch (AS) and carboxymethylated starch (CMS), where Z indicates a Na+ cation or a carboxymethyl group (Ochoa *et. al.* 2013).

1.1.6.1 Acid Modification of Starch

Acid modification of starch is the treatment/ exposure of starch to acids under controlled conditions. Treatment of starch with acids at any concentration, results in hydrolysis of the starch which reduces the granule size and paste viscosity. It

is carried out using hydrochloric or sulfuric acid and the concentration of the acid affects the degree of hydrolysis. During acid hydrolysis, the amylopectin is depolymerised and this increases the quantity of linear chains similar to amylose, favouring gel formation and its strength (Ulbrich *et al*., 2014, Jenkins and Donalds 1997 & Wang *et al.* 2003). After acid hydrolysis, the molecular mass of the starch grannules decreases. Manmeet *et al*. (2011) investigated the acid hydrolysis of sweet potato starch, result obtained revealed that swelling power, solubility and water binding capacity of the starch decreased and tended to appear fused and less smooth than the native starch granules after acid modification.

1.1.6.2 Physical Modification of Starch (Extrusion)

Extrusion is defined as a process at high temperature and in short amounts of time, where in starch granules are subjected to mechanical shearing forces in a relatively low moisture environment (Camire *et al*., 1990). Extrusion improves water solubulity, reduces the size of the starch grannules and increases the T_{gel} of starch, changing the molecular extension and its associations, such as the amylose-lipid complex structure hence, reducing the crystallinity of thr starch and increasing its amorphous nature. The extrusion process also affects starch digestibility and can reduce the RS content (Martinez *et al*., 2014).

1.1.6.3 Alkaline Modification of Starch

Alkaline treatment of starch is carried out with inorganic alkalis such as sodium hydroxide or potassium hydroxide, which is later neutralised by the addition of an acid like hydrochloric acid. This causes the starch to partially hydrolyse. Alkaline treatment of starch results in cold water-soluble starch that still possesses the granular assembly (Chen and Jane 1994a). It has been suggested that alkali condition opens up the starch granule structure, resulting in breaking the intermolecular hydrogen bonds thereby enhancing the water solubility (Han and Lim 2004).Singh and Singh (2003) observed that alkaline treatment brought substantial changes in physico-chemical, morphological, thermal and rheological properties of corn and potato starches. Reduction in amylose content, increase in swelling capacity of starch granules, increase of viscosity at high temperatures, and rapid development of viscosity at cooling temperatures are attributes of alkali treated starch (Berski *et al.*, 2011).

1.2 Problem Statement

Corrosion of metals and alloys is a significant challenge of modern civilization with adverse economic environmental and safety consequences. Again majority of the additives used for corrosion protection are rather costly and often times

toxic to man and the environment. Hence there is a need to develop a new class of effective, inexpensive and non-toxic corrosion inhibiting additives.

1.3 Objectives of Study

The main objective is to evaluate the effectiveness of modified sweet potato starch as corrosion inhibitor for mild steel and galvanised steel in acidic medium.

Specific Objectives

I. To modify sweet potato starch by extrusion, alkaline steeping and acid steeping to obtain physically modified starch (PMS), alkaline treated starch (ASS), acid treated starch (ATS).

II. To characterize the functionalities of the modified and unmodified starches.

III. To determine the influence of structural modifications on the corrosion inhibition performance of sweet potato starch.

IV. To study the effect of potassium iodide and modified sweet potato starches on mild steel and galvanised steel in acidic medium.

V. To determine the inhibition and adsorption mechanisms.

1.4 Justification of Study

Bioploymers have been studied as acid corrosion inhibitors and were found to be good corrosion inhibitors of metals in acidic and alkaline environments. Also, previous works reported that biopolymers having the –COOH- group are one of

the effective polymer based systems. However, these naturally occurring polymers have limitations which can be enhanced by various methods of modification which improves their functionality. The effects of the addition of halides (KCl, KBr, and KI) have also been studied, and the results obtained indicated that the increase in efficiency was due to synergism.

1.5 Scope of Study

The study is restricted to the following;

The modification of sweet potato starch by; extrusion, alkaline steeping and acid steeping to obtain physically modified sweet potato starch (PMS), alkaline treated sweet potato starch (ASS) and acid treated sweet potato starch (ATS) respectively.

Characterisation of the unmodified and modified starch samples using the FTIR spectrophotometer.

Determination of the corrosion rates, inhibition efficiency and degree of surface coverage.

Study of the effect of the modified and unmodified starches with potassium iodide.

Determination of adsorption mode and adsorption mechanism.

Determination of thermodynamic properties.

CHAPTER TWO

LITERATURE REVIEW

2.1 Corrosion Inhibitors

Corrosion inhibitors are chemical substances or combination of substances that when present in the environment, inhibits or reduces corrosion without a significant reaction with the components of the environment (Raja & Sethuraman,

2008). Corrosion inhibitors may be organic or inorganic, and their effectiveness or efficiency is a function of many factors such as fluid composition.

Corrosion inhibitors have been classified in many ways, but one of the most common is the classification into groups, based on how they control corrosion, which is as follows; adsorption or film - forming inhibitors, precipitation inhibitors, oxidizing or anodic passivation inhibitors, cathodic corrosion inhibitors, environmental conditioners or scavengers, volatile or vapor - phase inhibitors. These groupings and others are shown in Fig.2.1.

Inhibitors often work by adsorbing themselves on the metallic surface, protecting the metal surface by film formation. They are normally distributed from a solution or dispersion. They slow down corrosion processes by either; increasing the anodic or cathodic polarization behaviour, reducing the movement or diffusion of ions to the metallic surface or increasing the electrical resistance of the metallic surface.

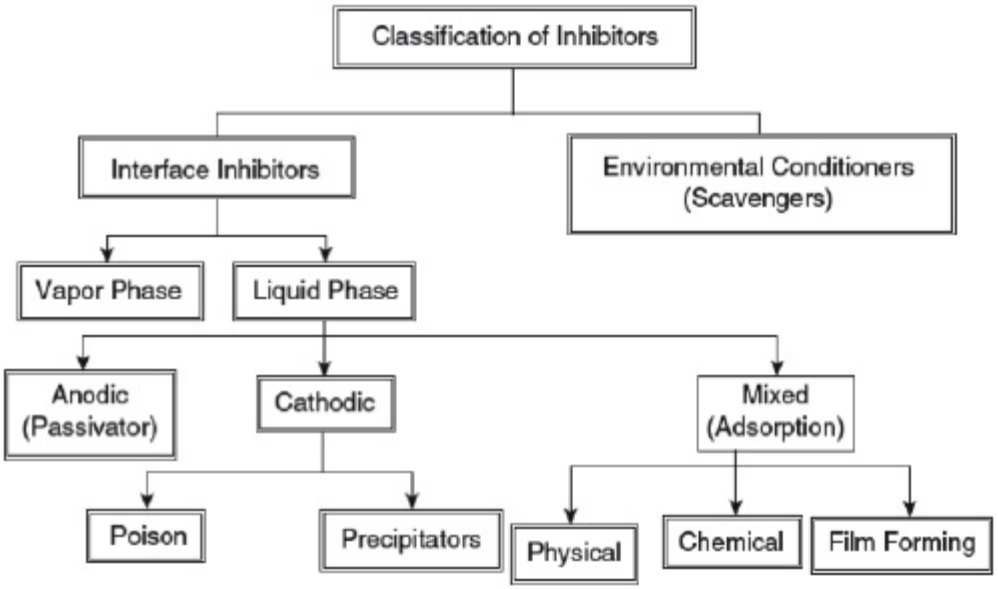

Fig. 2.1 Corrosion Inhibitors classification

2.2 Polymers as Corrosion Inhibitors

Polymers, both naturally occurring and synthetic ones, have been studied as metal corrosion inhibitors. Polymers especially the water soluble ones are efficient corrosion inhibitors in different aqueous media. Mechanism of inhibition are mainly attributed to adsorption and depends on the metal, physicochemical properties of the molecule such as functional groups, steric factors, aromaticity at the donor atom and p orbital character of donating electrons, as well as the electronic structure of the molecules. In other words, the efficiency of polymers as corrosion inhibitor depends not only on the characteristics of the environment in which it acts, the nature of the metal surface, and electrochemical potential at the interface, but also on the structure of the inhibitor itself, which includes the number of adsorption active centers in the molecule, their charge density, the

molecular size, the mode of adsorption, the formation of metallic complexes, and the projected area of the inhibitor on the metallic surface. The results of the series of investigations have revealed that the processes involved in corrosion inhibition are not uniform with respect to all classes of compounds so far investigated and are not even constant or consistent with one inhibitor in a given system (Abdel-Gaber *et al*., 2006). Indeed, the overall process is a function of the metal, corrodent, inhibitor structure, and concentration, as well as temperature.

Interest in the use of polymers as inhibitors, arose from their stability in acid media, low cost, and the presence of multiple adsorption sites in their molecular structure for bonding with a metal surface (Yurt *et al*., 2007). They combine good chemical resistance with impermeability to different media and unusual deformation characteristics. Through their functional groups they form complexes with metal ions and on the metal surface these complexes occupy a large surface area, thereby blanketing the surface and protecting the metal from corrosive agents present in the solution (Rajendran *et al*., 2005). The inhibitive power of these polymers is related structurally to the cyclic rings, heteroatom (Oxygen and Nitrogen) that are the major active centres of adsorption. The inhibitive characteristics of such components derive from the adsorption ability of their molecules with the polar group acting as the reaction centre for the adsorption process. The resulting adsorbed film acts as a barrier that separates the metal from the corrodent and efficiency of inhibition depends on the mechanical,

structural and chemical characteristics of the adsorption layers formed under particular conditions (Oguzie, 2004; Oguzie , 2008).

The use of polymers as corrosion inhibitors has been reported, among those studied to date include polyethylene glycol, polyvinyl alcohol, polyacrylamide, carboxyl methylcellulose, poly (aminoquinone), polyethylene glycol methyl ether (PEGME), polyvinylpyrrolidone and polyethylenimine, poly (4-vinylpyridne), and poly (diphenylamine) (Shinde et al, 2005; Pawar et al, 2007; Torresi et al, 2005; Souza de, 2007 and Vera et al, 2007), to mention but a few.

2.2.1 Synthetic Polymers as Corrosion Inhibitors

Synthetic polymers have received considerable attention as metal corrosion inhibitor. They have polar functional groups, which is one of the requirements for an organic compound to qualify as a metal corrosion inhibitor.

Chetouani *et al.* (2003) studied the effect of poly (4-vinylpyridine isopentyl bromide) (P4VPIPBr) in three degrees of quaternisation (6, 18 and 79%) on the corrosion of pure iron in molar sulphuric acid by potentiodynamic, polarisation resistance and weight loss measurements. The inhibition efficiency of P4VPIPBr increased with its concentration to attain 100% around 5 x 10^{-6}M. IE% values obtained from the various methods are in good agreement. Polarisation measurements show also that the compound acts as a cathodic inhibitor and

adsorbs on the pure iron surface according to the Frumkin adsorption isotherm model. In a related study on the influence of poly (4-vinylpyridine-poly (3-oxide-ethylene) tosyle) P4VPPEO5000Ts, on the corrosion inhibition of iron in molar sulphuric acid solution was investigated using weight-loss, polarisation resistance, potentiodynamic and EIS measurements. P4VPPEO5000Ts exhibited excellent inhibition on the iron and its inhibition efficiency attained 100% at a concentration of 2.5×10^{-8} M. Potentiodynamic polarisation studies clearly reveal that it acts as a mixed-type inhibitor. Adsorption of this compound on iron surface has an S-shaped adsorption isotherm with two consecutive steps indicating Frumkin adsorption isotherm (Chetouani *et al*., 2004).

Khairou and El-Sayed (2003) investigated the effects of poly(vinyl alcohol) (PVA), on the corrosion of cadmium in a 0.5M hydrochloric acid (HCl) solution with both electrochemical impedance spectroscopy and Tafel plot techniques. Measurements carried out at cathodic, open-circuit, and anodic potentials showed that PVA had inhibitory effects on both the cathodic and anodic processes, with a predominant anodic inhibiting action. The hydroxy groups contained in PVA, effected the bridging between the polymer and the surface, resulting in an inhibiting effect in the HCl solution. PVA was greatly adsorbed at the anodic potential and obeyed the Temkin adsorption isotherm. Umoren et al (2007) also investigated the corrosion inhibition of polyvinyl alcohol (PVA) on mild steel in H_2SO_4 at 30 – 60°C by using weight loss and hydrogen techniques. The inhibition

efficiency of the inhibitor increased with increase in concentration and temperature. The inhibitors were found to obey Temkin, Freudlich and Langmuir adsorption isotherms from the fit of the experimental data at all concentrations and temperature studied. Further studies carried out by Umoren and Gasem (2013) on the inhibition efficiency of three different molecular weights of polyvinyl alcohol (PVA) designated PVA-I, PVA-II, and PVA-III corresponding to 14,000, 72,000, and 125,000 g/mol respectively, on mild steel in hydrochloric acid solution using electrochemical impedance spectroscopy (EIS), linear polarization resistance (LPR), and potentiodynamic polarization (PDP) techniques at 25^{o}C. Indicated that the different molecular weights of PVA inhibits the corrosion of mild steel in HCl environment and the extent of inhibition was dependent on concentration and molecular weight of the polymer. PVA was found to be a mixed-type inhibitor and its adsorption on the surface of mild steel followed Langmuir adsorption model. Physical adsorption mechanism was proposed for the mode of adsorption of the polymer on the mild steel surface.

The composite form of PVA has been investigated by (Karthikaiselvi *et al*., 2012). The performance of Poly (vinyl alcohol-aniline) PVAA composite in protecting mild steel against corrosion in 1 M HCl by means of weight loss, electrochemical polarization, and electrochemical impedance methods was studied. Results indicate that the addition of PVAA to the acid retards the dissolution of the metal. Inhibition was found to be due to the adsorption of

PVAA on the mild steel surface and increased with increasing concentration of the inhibitor. Polarization results indicate that PVAA is a mixed type inhibitor and its adsorption onto the metal surface follows Langmuir and Temkin adsorption isotherms. Studies carried out by Karthikaiselvi and Subhashini (2013), reports the influence of poly (vinyl alcohol-o-methoxy aniline) PVAMOA composite on the corrosion behavior of mild steel in 1 M HCl at 303-343K. The inhibition efficiency of the polymer increased with temperature rise from 303-323K but tends to decrease at higher temperatures. The adsorption of the composite on the mild steel surface was established by scanning electron microscope and obeyed Langmuir and El- Awady adsorption isotherms.

Shukla *et al.* (2003) investigated the mechanism of corrosion of aluminium and the effect of polyethylene glycol (PEG) polymer as corrosion inhibitor in acidic medium using the weight loss method, potentiodynamic and galvanostatic polarization measurements. Differential pulse polarography (DPP) and differential pulse anodic stripping voltammetry was used to study the corrosion rates for the corrosion of aluminium in acidic medium at short time intervals. Results obtained showed that the corrosion inhibition efficiency of PEG was 94% after 24 h of immersion period. In a related study of PEG as an effective corrosion inhibitor, Khairou and El-Sayed (2003) investigated the effects of polyethylene glycol (PEG) on the corrosion of cadmium in a 0.5M hydrochloric acid (HCl) solution with both electrochemical impedance spectroscopy and Tafel plot

techniques. Results obtained indicate that at cathodic, open-circuit, and anodic potentials. All the investigated polymers had inhibitory effects on both the cathodic and anodic processes, with a predominant anodic inhibiting action. The adsorption of most PEG obeyed the Temkin adsorption isotherm, indicating that the main process of inhibition was adsorption.

Ashasszi and Galebsaz (2005) studied the inhibitive effects of different polyethylene glycols of varying molecular weight (200 – 10,000 g/mol) on carbon steel corrosion in 3N H_2SO_4 using weight loss, polarization and electrochemical impedance spectroscopy. Results obtained showed that the PEGs were effective corrosion inhibitors for carbon steel in the acidic environment. It was found that PEG has an inhibiting effect on the corrosion process and the inhibition efficiency was more than 90 %. The studied polymers were physically adsorbed on the carbon steel surface in the acid medium. The results from the three independent methods employed were in good agreement. In a related study reported by Ashassi *et al.* (2006), the inhibition effect of some Polyethylene glycols (PEGs) on carbon steel corrosion at 25°C in 0.5N HCl as corrosive medium by weight loss, polarization and electrochemical impedance spectroscopy techniques was evaluated. In order to study the effect of PEGs' structure on the inhibition efficiency, different molecular weights: 400, 1000, 4000 and 10,000 gmol-1 was selected. Results obtained show the effectiveness of polyethylene glycols on corrosion inhibition of C- steel in HCl solution. The inhibition efficiency

increases with increase in mean molecular weight of the polymer and its concentration. The adsorption of the studied polymers on C – steel obeys Langmuir isotherm. Comparative studies on the corrosion inhibition of mild steel in H_2SO_4 at 30 – 60°C by polyethylene glycol (PEG) and polyvinyl alcohol (PVA) using weight loss and hydrogen techniques has been reported by Umoren *et al.* (2007). The inhibition efficiency of the inhibitor increased with increase in concentration and temperature. The inhibitors were found to obey Temkin, Freudlich and Langmuir adsorption isotherms from the fit of the experimental data at all concentrations and temperature studied. The phenomenon of chemical adsorption was proposed from the activation parameters obtained. PEG was found to be a better inhibitor than PVA. In a related study by the same authors, comparative studies on the corrosion inhibition of Aluminium in H_2SO_4 at 30 – 60°C by polyethylene glycol (PEG) and polyvinyl alcohol (PVA) using gravimetric (weight loss), gasometric (hydrogen evolution) and thermometric techniques. It was observed that inhibition efficiency (IE%) increased with increase in concentration of both PEG and PVA. Increase in temperature increased the corrosion rate in the absence and presence of the inhibitors but decreased the inhibition efficiency. Both PEG and PVA were found to obey Temkin adsorption isotherm at all concentrations and temperature studied. PEG and PVA inhibited aluminum corrosion by virtue of adsorption which was found to follow physiosorption mechanism. The study revealed that PEG was a better corrosion inhibitor for Al than PVA.

Dubey and Singh (2007) studied the corrosion inhibition of mild steel in sulphuric acid solution by polyethylene glycol methyl ether (PEGME) using electrochemical polarization (galvanostatic and potentiostatic) techniques It was found that PEGME is a very effective corrosion inhibitor for mild steel in acidic medium. Inhibition efficiency increased with increase in the concentration of PEGME but almost remains the same with increasing temperature. Adsorption of PEGME was found to follow the Langmiur's adsorption isotherm. PEGME was also found to function as an inhibitor of mixed type acting by blocking the active sites on the cathodic and anodic regions.

The effect of two polyamide compounds on the corrosion behavior of aluminum metal in oxalic acid solution was investigated using potentiostatic and potentiodynamic anodic polarization techniques has been investigated by Abdallah *et al*. (2004). The inhibition efficiency increases with increasing polyamide concentration until a critical value and then starts to decrease in high polymer concentrations, indicating low inhibition efficiency. The inhibitive behavior of these compounds was discussed in terms of adsorption of the polyamide compounds on the metal surface and formation of insoluble complexes. The adsorption process was found to obey Temkin adsorption isotherm. The pitting potential varies with concentration of chloride ions according to a linear relationship. The addition of polyamide compounds shifts

the pitting potential of aluminum electrode to more positive potentials, indicating an increased resistance to pitting attack.

The inhibition efficiency of polyvinyl pyrrolidone (PVP) in controlling corrosion has been reported. Selvaraji *et al*. (2004) studied the inhibition efficiency of polyvinyl pyrrolidone (PVP) on carbon steel immersed in an aqueous solution containing 60 ppm of Cl-, in the absence and the presence of Zn2+ using weight loss method. Influence of pH, immersion period, N-cetyl- N,N,N-trimethyl ammonium bromide and sodium dodecylsulphate on the inhibition efficiency of the inhibitor system was also investigated. The nature of the protective film was analyzed by FTIR and fluorescence spectroscopy. In the presence of PVP, the protective film consists of Fe^{2+} - PVP complex; the film was found to be UV-fluorescent. In the presence of PVP and Zn^{2+}, the protective film consists of Fe^{2+} - PVP complex and $Zn(OH)_2$; it was found to be UV-fluorescent.

Al Fuhaiman *et al.* (2013) investigated the corrosion inhibition of carbon steel using polyvinyl pyrrolidone (PVP) in an aerated alkaline medium containing 0. 1 M NaCl at pH 9 and 10. The influence of KI and untreated Saudi clay (UC) as additives on the inhibition efficiency of PVP was also studied. The results reveal that inhibition efficiencies of corrodent solutions with 1000 ppm PVP ranged from 66- 78% for weight loss results and 23-66% for the electro- chemical measurements. It was found from electrochemical impedance results that the adsorption of PVP led to the formation of a protective film on the carbon

steel/NaCl solution interface. PVP was found to be a mixed type inhibitor. However, the addition of KI to PVP and the blank significantly enhanced the inhibition efficiency while the addition of UC affects the inhibiting ability of PVP negatively.

The inhibition of mild steel corrosion in aerated acid mixture of 0.05 N H_2SO_4 and 0.5 N HCl solutions by polyvinyl pyrrolidone (PVP) and polyethylene glycol (PEG) has been assessed using potentiodynamic polarization, linear polarization, electrochemical impedance spectroscopy, adsorption, and surface morphological studies by John *et al.* (2013). It was found that the presence of PEG and PVP decreases the double - layer capacitance and increases the charge-transfer resistance. Inhibition efficiency increased significantly with increase in the additives concentration. The inhibitor molecules were found to adsorb on the metal surface following Langmuir adsorption isotherm model. Both PEG and PVP were found to afford good inhibition of mild steel corrosion in acidic medium and act as mixed type inhibitors. Surface analysis which was done with the aid of scanning electron microscope and atomic force microscope reveal that PVP offer better inhibition to mild steel surface than PEG.

Karthikaiseli and Subhashini (2012) in an attempt to overcome the limitation of insolubility of polymethyl aniline (PMA) converted PMA into a water-soluble composite by using supporting polymer polyvinyl pyrrolidone to get higher solubility and corrosion inhibition efficiency. The corrosion inhibitive effect of

the water-soluble composite poly (vinyl pyrrolidone-methyl aniline) on mild steel in 1 M HCl was assessed by weight loss and electrochemical techniques. The water-soluble composite was found to affect both the anodic and cathodic processes and acts as a mixed type inhibitor. The adsorption of the inhibitor obeys the Langmuir adsorption model and more strictly follow El-Awady adsorption isotherm. Also, the inhibition efficiency of the inhibitor was found to increase as the temperature increases from 303-333K but decreases at temperature exceeding 333K.

The effect of the addition of poly (4-vinylpyridine- hexadecyl bromide) P4VP-Alkyl 50% newly synthesized on the corrosion of mild steel in 1 M HCl has been assessed by weight loss, linear potential scan voltammetry (I - E), and electrochemical impedance spectroscopy (EIS) Belkaid *et al.* (2012). It was found that the polymer reduces the corrosion rate of mild steel in 1 M HCl and the inhibition efficiency increased with increase in the polymer concentration and attained 95% at a concentration of 300 mg/L. The polymer was found to adsorb on the metal surface according to Langmuir adsorption isotherm model and influences specifically the cathodic reactions.

The corrosion and inhibition behaviour of aluminium in HCl in the presence of polyvinyl pyrrolidone (PVP), polyacrylamide (PA) and their blends in the temperature range of 30 – 60^{o}C using weight loss, hydrogen evolution and thermometric techniques has been reported by Umoren *et al.* (2008). Inhibition

efficiency increased with increase in inhibitors concentration and decreases with increase in temperature. PVP was found to have higher inhibition efficiency than PA which was attributed to their differences in molecular structures. Inhibition efficiency was enhanced on blending the two polymers and the optimum inhibition was obtained at 3:1 blending ratio of PVP: PA. Umoren and Obot (2008) evaluated the corrosion inhibition of mild steel in I M H_2SO_4 in the presence of polyvinyl pyrolidone (PVP) and polyacrylamide (PA) as inhibitors at 30 – 60°C using gravimetric and gasometric techniques. Results obtained indicate that increase in temperature increases the corrosion rate in the absence and presence of the inhibitors but decreased the inhibition efficiency. The inhibition efficiency increased with increase in concentration of the inhibitors. Both PVP and PA were found to obey Temkin and El- Awady et al. Kinetic-thermodynamic adsorption isotherm at all the concentrations and temperatures studied. Physiosorption mechanism was proposed from the activation parameters obtained. PVP was found to be a better inhibitor than PA.

Umoren and Solomon (2010) studied the influence of bromide and iodide ions on the inhibitive effect of polyacrylamide on aluminium corrosion in HCl solution using weight loss, hydrogen evolution, and thermometric techniques at 30 and 60^{o}C. The results show that the halide additives synergistically increased the inhibition efficiency of polyacrylamide. The increase in inhibition efficiency (%IE) was found to be more pronounced in I- than Br- ions. The observed

difference in behaviour of both halide additives could be linked to the differences in their atomic radii as well as electronegativity. The values of synergism parameter (S1) obtained for the halides are greater than unity, suggesting that the improved inhibition efficiency of polyacrylamide caused by the addition of the halide ions is due to synergistic effect. Corrosion inhibition could be attributed to adsorption of inhibitor molecules on the Al surface via physical mechanism. The adsorption process followed the kinetic-thermodynamic model of El-Awady adsorption isotherm. These results were further corroborated by kinetic and thermodynamic parameters for corrosion and adsorption processes evaluated from experimental data.

Yan *et al.* 2014 investigated the application of water-soluble polyacrylamide modified by β-cyclodextrin (ACDPAM) as a corrosion inhibitor on X70 steel in 0.5 M H_2SO_4 solution using electrochemical measurements, weight loss, and scanning electron microscopy (SEM). The polarization curves results reveal that the copolymer acts as a mixed-type inhibitor. The inhibition efficiency is found to increase by the increase in copolymer concentration and decreases by the rise in temperature, and it also exhibits effective inhibition even at a higher temperature. The adsorption of ACDPAM on X70 steel surface obeys the Langmuir adsorption isotherm and is governed by chemisorption. The SEM results demonstrate that X70 surface is protected by ACDPAM.

Khairou and El-Sayed (2003) investigated the effects of poly (acrylic acid) (PAA) and sodium polyacrylate (NaPA) on the corrosion of cadmium in a 0.5M hydrochloric acid (HCl) solution with both electrochemical impedance spectroscopy and Tafel plot techniques. Results obtained indicated inhibitory effects on both the cathodic (except for NaPA) and anodic processes, with a predominant anodic inhibiting action. However, NaPA exhibited a slight cathodic inhibiting action only at higher polymer concentrations. This behavior may be attributed to the very weak adsorbability of the polymers on the cathodic sites. The adsorption of both polymers obeyed the the Temkin adsorption isotherm.

Mekki and Chelali (2004) studied two forms of polymers namely red form with molecular weight of (800,000 g mol-1) insoluble in alcohol and green form with low molecular weight (44,000 g mol-1) and soluble in alcohol obtained by polymerization of ortho-ethoxyaniline were tested as corrosion inhibitor for mild steel in acidic media. The obtained results showed the adsorption of the polymer alcoholic form obeys Temkin adsorption isotherm with no significant change as function with inhibition efficiencies for a series of molecular weights ranging from 123,000 to 124,000 g mol-1.

Jeyaprabha *et al.* (2006) studied the performance of water soluble polyaniline as corrosion inhibitor for iron in 0.5M H_2SO_4 has been evaluated by potentiodynamic polarization, linear polarization, and electrochemical impedance spectroscopy and compared with the performance of the aniline

monomer. It has been found that polyaniline is an efficient inhibitor, since the maximum efficiency of 84% has been observed at a concentration of 100 ppm, whereas the monomer accelerated the corrosion. FTIR studies have shown that the polyaniline is strongly adsorbed on the iron surface and inhibits the corrosion effectively. However, aniline has been found to improve the passivation tendency of iron at higher concentrations. Adsorption of polyaniline onto iron surface follows Temkin adsorption isotherm.

Vera *et al.* (2007) studied the influence of polyaniline (PANI) and poly (orthomethoxyaniline (POMA) on corrosion inhibition of copper in 0.1M NaCl. Best result was obtained for polyaniline which was attributed to the fact that the polymer film was involved in the formation of oxide film on the polymer – metal surface. This oxide film increases the barrier effect of the polyaniline film hence greater corrosion inhibitor efficiency. The phenomenon of oxide formation was not observed with POMA.

Benabdellah *et al.* (2007), in their investigation on the inhibiting abilities of two copolymers namely, poly (vinyl caprolactone-co- vinyl pyridine) and poly (vinyl imidazol-co-vinyl pridine) on the corrosion behavior of steel in phosphoric acid at different temperatures, concluded that these copolymers have excellent inhibitive effects.

Migahad *et al.* (2010) synthesized and evaluated recycled poly (ethylene terphethalate) as a possible corrosion inhibitor. In their work, Polyethylene

terephthalate waste (PET) was depolymerized by triethanolamine into glycolyzed product (GT), followed by esterification with bromacetic acid in the presence of manganese acetate as a catalyst to give (GT-Br). The obtained ester was reacted with thiourea to give thiol derivative (GT-SH). The effectiveness of the synthesized compound as corrosion inhibitor for API XL65 carbon steel, in 2 M hydrochloric acid solution was investigated by various electrochemical techniques such as open circuit potential, potentiodynamic polarization and electrochemical impedance spectroscopy (EIS). The results of these investigations showed enhancement in inhibition efficiencies with the increasing of inhibitor concentration. The protective film formed on carbon steel surface was analyzed using an energy dispersive X-ray analysis (EDX) technique. Also, scanning electron microscope (SEM) was used to study the surface morphology of steel surface in the absence and presence of 400ppm of the additive.

Qian *et al*. (2013), modified polyaspartic acid (PASP) which was used as inhibitor for mild steel corrosion in 0.5 M H_2SO_4 solution by adding KI. The inhibition efficiency PASP was found to be significantly enhanced by this modification. Result of the zero charge potential measurements shows that iodide ions promote the film formation of PASP greatly.

In recent years, polymer amines have been studied as an efficient corrosion inhibitor for iron in acid media. Sathiyanarayanan *et al.* (2005) studied the influence of poly (aminoquinone) (PAQ) on corrosion inhibition of iron in 0.5 M

H_2SO_4 using potentiodynamic polarization and electrochemical impedance spectroscopy measurement. The inhibitive performance of PAQ was compared to that of its monomer o-phenylenediamine (OPD) and was found that the inhibition performance of PAQ was better than OPD which was attributed to the presence of extensive delocalized electrons. Inhibition efficiency of 90% at 100ppm was obtained for PAQ while inhibition efficiency of 80% at 1000ppm was obtained for OPD. PAQ was found to be a mixed inhibitor. Besides, PAQ was able to improve the passivation tendency of iron in 0.5 M H_2SO_4 markedly. Adsorption of PAQ followed Temkin adsorption isotherm.

Jeyaprapha *et al.* (2005) evaluated the performance of poly (diphenylamine) as corrosion inhibitor for iron in 0.5 M H_2SO_4 by potentiodynamic polarization, linear polarization and electrochemical impedance spectroscopy and compared with the performance of the diphenylamine monomer. It has been found that poly(diphenylamine) is an efficient inhibitor since the maximum efficiency of 96% has been observed at very low concentration of 10 ppm whereas the monomer gave an efficiency of 75% at 1000 ppm. Besides, poly(diphenylamine) has been found to improve the passivation characteristics of iron in 0.5 M H_2SO_4. FTIR studies have shown that the poly(diphenylamine) is strongly adsorbed on the iron surface and inhibits the corrosion effectively.

Manivel and Venkatachari (2006) investigated the inhibitive effect of poly(p-aminobenzoic acid) on iron in 1 M HCl solution by polarization and

electrochemical impedance spectroscopy and compared with that of monomer p-aminobenzoic acid .Results obtained shows the effectiveness of poly(p-aminobenzoic acid) being very high in comparison with that of the monomer. The cathodic and anodic processes were suppressed by p- aminobenzoic acid and poly (p-aminobenzoic acid) of iron dissolution in 1 M HCl by their adsorption on the iron surface. The inhibition efficiency of both p-aminobenzoic acid and poly(p-aminobenzoic acid) were found to increase with the inhibitor concentrations. Ultraviolet (UV) reflectance studies of the iron surface after exposure to inhibitor in the acid environment show that poly(p- aminobenzoic acid) is strongly adsorbed on iron surface.

Yurt et al (2007) investigated the inhibitive performance of novel synthesized water soluble triblock copolymers-2-(diethylamino) ethyl ethacrylate- block-2-(dimethylamino) ethyl methacrylate – block-2-(N-mor- pholino) ethyl methacrylate [PDEA-PDMA-PMEMA] and 2- (diisopropylamino) ethyl methacrylate-block-2-(dimethylamino) ethyl methacrylate – block-2- (N-morpholino)ethyl methacrylate [PDPA-PDMA-PMEMA] of two different molecular weight on the corrosion behaviour of mild steel in 0.5 M HCl using potentiodynamic polarization, electrochemical impedance spectroscopy and linear polarization methods. Polarization methods indicate that all studied copolymers were acting as mixed type inhibitors. Inhibition efficiencies increase with increase in inhibitor concentration. This reveals that inhibitive actions of

inhibitors were mainly due to adsorption on steel surface. Adsorption of the inhibitors was found to follow Langmuir adsorption isotherm. The correlation between the inhibition efficiencies of the studied copolymers and their molecular structures based on quantum chemical calculations indicate that adsorption of the triblock copolymers depend on the charge density of adsorption centres and dipole moments.

The inhibition properties of the electro-prepared Poly (o-phenylenediamine), P(oPD), on the corrosion rate of mild steel (MS) in HCl solutions have been investigated under different experimental conditions using weight loss and potentiodynamic polarization techniques by Abd el Rehim *et al*. (2010). The data obtained from the two techniques showed that the presence of P(oPD) in the acid solutions suppresses the corrosion rate of MS indicating that the polymer acts as corrosion inhibitor. The inhibition performance of the polymer was found to improve with increasing its concentration and decreasing the reaction temperature. The inhibition of mild steel corrosion was proposed to occur through adsorption and formation of barrier film of P(oPD) on the metal surface which separates the metal from direct contact with the corrosive medium and hence protects the metal against the corrosion.

Finsgar *et al.* (2009) studied the effect of polyethyleneimine (PEI) as corrosion inhibitor for ASTM 420 stainless steel in 30% aqueous NaCl. The results of linear polarization and cyclic polarization measurements indicate high inhibition

effectiveness of the selected organics. Moreover, from cyclic measurements, it was deduced that PEI acts as an inhibitor against pitting corrosion. Immersion test in the presence of PEI showed remarkable corrosion protection against uniform corrosion. Film persistency immersion testing indicated that once the protective layer is formed, it is very stable in non- inhibited NaCl solution. X-ray photoelectron spectroscopy measurements showed that PEI binding is mediated by electrostatic interactions between PEI and the substrate. A decrease layer of PEI might be effective either in preventing diffusion of ionic species from film or in preventing attack by chlorine from salt water.

Hasanov *et al.* (2010) studied the corrosion inhibitive efficiencies of two crown type polyethers, namely dibenzo-bis-imino crown ether (C-1) and dibenzo-diaza crown ether (C-2), which are macrocyclic Schiff base and its reduced form (macrocyclic amine), respectively, for steel in sulphuric acid solution by Tafel extrapolation and linear polarization methods. Corrosion and adsorption isotherm parameters were determined from current-potential curves. The studies show that C-1 and C-2 inhibit the corrosion of the steel in corrosive environment induced by sulphuric ions. Semi-empirical AM1 method was used for theoretical calculations and the result obtained from the calculations for the compounds were found to be consistent with the experimental findings.

Two novel class of interesting polyurea derivatives designated as 6(a-c) and 7 (a-c) have been synthesized using solution polycondensat- ion technique by the

interaction of one mole of bis (2- aminothiazol-4-ylbenzylidene) cycloalkanones monomers with one moles of diisocyanate compounds in pyridine. The corrosion inhibition behaviors of the synthesized polymers on steel in 0.5 M H_2SO_4 solution at 40^oC were tested by Aly and Hussien (2010). It was found that polyurea designated 6a gives approximate constant values of inhibition efficiency at all the selected concentrations except in 1 and 2 ppm while the designated 7a polyurea derivative inhibit the corrosion of steel in 0.5 M H_2SO_4 solution at low concentration but accelerate at higher concentration.

Atta *et al.* (2011) have synthesized novel dispersed magnetite core-shell nanogel polymers and their effectiveness as corrosion inhibitors for carbon steel in 1 M HCl tested by potentiodynamic polarization and electro- chemical impedance spectroscopy techniques. The results showed enhancement in inhibition efficiencies with increasing the inhibitor concentrations and temperatures. It was found that the nanogel particles act as mixed inhibitors and their mode of adsorption on the metal surface fit well into Langmuir adsorption isotherm.

Khairou and El-Sayed (2003) investigated the effects pectin (P), and carboxymethyl cellulose (CMC) on the corrosion of cadmium in a 0.5M hydrochloric acid (HCl) solution with both electrochemical impedance spectroscopy and Tafel plot techniques. Measurements were carried out at cathodic, open-circuit, and anodic potentials. All the investigated polymers had inhibitory effects on both the cathodic (except for NaPA, P, and CMC) and anodic

processes, with a predominant anodic inhibiting action. However, NaPA, P, and CMC exhibited a slight cathodic inhibiting action only at higher polymer concentrations. This behavior may be attributed to the very weak adsorbability of the polymers on the cathodic sites. Because PVA and PEG had hydroxy groups, there could be bridging between the polymer and the surface, resulting in an inhibiting effect in the HCl solution. However, PVA had much greater adsorbability on the surface than PEG at the anodic potential. The adsorption of most of the polymers obeyed a Temkin adsorption isotherm, and this indicated that the main process of inhibition was adsorption.

2.2.2 Natural Polymers as Corrosion inhibitors

In the continued effort to contribute to the search for environmentally friendly inhibitors to replace the toxic fossil origin organic inhibitors, the use of natural products otherwise tagged "green corrosion inhibitors" has been advocated. More so, they are readily available, cheap and a renewable source of materials.

Abdallah (2004) studied the use of guar gum a naturally occurring polysaccharide as a corrosion inhibitor for carbon steel in sulphuric acid solution, results indicated that increase in inhibitor concentration increased the resistance to pitting corrosion. Comparative studies were conducted on the inhibition efficiencies of guar gum and polyethylene glycol as corrosion inhibitors for mild

steel in sulphuric acid solution by Umoren et al (2008). Results obtained shows that guar gum exhibited good inhibition efficiency. The authors have also reported the inhibitive properties of exudate gum for aluminium corrosion inhibition in acidic medium.

In a related study, corrosion inhibition of aluminium using the same inhibitor in an alkaline medium (NaOH) at 30 and 40°C has been reported by Umoren *et al.* 2006 using hydrogen evolution and thermometric techniques. It was found that GA inhibited the alkaline induced corrosion of aluminium. Inhibition efficiency increases with increase in concentration of GA and also with temperature rise. Maximum inhibition efficiency of 76% was obtained at 40°C using 0.5g/L GA concentration. Phenomenon of chemical adsorption was proposed for the inhibition process and GA was found to adsorb onto aluminium surface following Frendich, Temkin and Langmiur adsorption isotherms.

Gum Arabic (GA) (a naturally occurring polymer) has also been reported as an inhibitor for inhibition of mild steel corrosion in H_2SO_4 at 30 – 60°C using weight loss, evolution and thermometric measurements Umoren (2008). Inhibition process was afforded by virtue of chemical adsorption of GA components onto mild steel surface following Temkin adsorption isotherm. Inhibition efficiency increases with increase in GA concentration as well as temperature rise. It was also found from the kinetic/thermodynamics studies that adsorption of GA onto mild steel surface was spontaneous.

Bentrah *et al.* (2014) studied the inhibiting ability of gum arabic (GA) on the corrosion of API 5L X42 pipeline steel in 1 M HCl solution using electrochemical impedance spectroscopy and potentiodynamic polarization methods. Results shows that gum arabic could afford 92% protection at 2 g/L to API 5L X42 steel in 1 M HCl. The adsorption of GA on the steel surface was found to obey Langmuir adsorption isotherm and involves physical adsorption. GA was also found to act as a mixed-type inhibitor.

The inhibitive effect of the gum exudate from Acacia seyal var seyal on the corrosion of mild steel in drinking water was investigated by Buchweishaija and Mhinzi (2008) using the potentiodynamic polarization and electrochemical impedance spectroscopy (EIS) techniques. The result obtained showed that gum exudates could serve as effective inhibitors for the corrosion of steel in drinking water network. The percentage inhibition increases with increasing the concentration of the gum at 30oc.The percentage inhibitor efficiency above 95% was attained at gum concentration greater or equal to 400ppm. The corrosion rates of steel and inhibition efficiencies of the gum exudates obtained from impedance and polarisation measurements were in good agreement. Potentiodynamic polarisation studies clearly reveal that the gum behaves predominantly as an anodic inhibitor. The study also shows that the inhibition efficiency was insignificantly affected by the temperature rise of the medium. In a similar study, Buchweishaija (2009) studied the inhibitive performance of gum exudates from

Acacia drepanolobium and Acacia senegal from Tanzania, towards the corrosion of mild steel in fresh water studies. The results indicate that gum exudates (Acacia drepanolobium and Acacia senegal) exhibits good inhibition characteristics to corrosion on mild steel under fresh water medium and the inhibition efficiency of up to 90.7% and 99.7% respectively was attained at 30^{o}C. Furthermore, the studies have shown that the inhibition performance remained above 90% on both Acacia exudates independent of the raise in temperature.

The inhibitive effect of exudate gum from Dacroydes edulis on the corrosion of aluminium in HCl solutions was studied using weight loss and thermometric methods at 30°C to 60°C by Umoren *et al.* 2008, and the results revealed that the exudate gum acted as an inhibitor for the corrosion of aluminum in HCl solution. The inhibition efficiency increases with an increase in the concentration of the exudate gum but decreases with increase in temperature.

The effect of naturally occurring exudate gum from Raphia hookeri on the corrosion of mild steel in H_2SO_4 between 30°C and 60°C has also been investigated by Umoren *et al.* (2006) using weight loss and hydrogen evolution techniques. Results obtained revealed that the exudate gum is a good inhibitor for the corrosion of mild steel in acidic media. The inhibition efficiency increased with an increase in exudate gum content and decreases with increase in temperature. The adsorption of exudate gum from R. hookeri on the mild steel follows Langmuir adsorption isotherm.

Glucose, gellan gum, and hydroxylpropyl cellulose have been assessed as green inhibitors for cast iron in acidic environment by means of chemical and electrochemical techniques Rajeswari (2013). It was found that inhibition efficiency increased with increase in the concentration of the inhibitors. Also the protective effect of glucose and hydroxylpropyl cellulose decreased as the temperature was raised while the inhibition ability of the gellan gum increase gradually with rise in temperature. The polymers were seen to influence both the anodic and cathodic reactions and the mode of their adsorption on the cast iron followed Langmuir adsorption isotherm.

Fares *et al.* (2012) investigated the inhibiting effect of naturally occurring pectin polymer on aluminum corrosion in acidic media. The result obtained shows that the inhibition efficiency of pectin first increased linearly and then exponentially with concentration until a plateau was reached. Temperature was found to have profound effect on the inhibition efficiency; a severe decline from 91% at 10^{o}C to 31% at 40^{o}C with the same concentration of pectin was reported.

The inhibitive influence of chitosan as a green corrosion inhibitor for mild steel in 0.1 M HCl was studied by Umoren *et al*. (2013) using gravimetric, potentiodynamic polarization, electrochemical impedance spectroscopy, scanning electron microscopy, and UV-visible techniques. The polymer was found to moderately inhibit the corrosion of mild steel in the studied environment even at low concentration and had influence on both the anodic and cathodic

reactions. 68.0% inhibition efficiency was obtained with the highest concentration of the inhibitor used (4 µM) from potentiodynamic measurements.

El-Haddad (2013), has reported that chitosan retard the dissolution of copper in 0.5 M HCl effectively. The investigation was carried out using weight loss, potentiodynamic polarization, electrochemical impedance spectroscopy (EIS) and electrochemical frequency modulation (EFM) measurements. It was found from potentiodynamic polarization measurements that the chitosan acts essentially as a mixed-type inhibitor. Results of EIS indicated that the value of constant phase elements (CPEs) tends to decrease and both charge transfer resistance and inhibition efficiency tend to increase by increasing the inhibitor concentration. The studied inhibitor was found to show good inhibition efficiency in 0.5 M HCl. El-Haddad noted that the value of adsorption energy (ΔG_{ads}) indicated that the adsorption of chitosan on the copper surface was more of chemical mechanism than physical one. Chemical adsorption of chitosan was taken to arise from the donor acceptor interactions between free electron pairs of heteroatoms and vacant d-orbitals of copper. The adsorption of inhibitor on the copper surface was also seen to obey Langmuir adsorption isotherm.

The corrosion behavior of mild steel (MS) sheets in 0.5 M H_2SO_4 in the presence of chitosan extracted from shrimp shells (CSS) has been studied using electrochemical techniques by Ubong and Mazen (2014). The optimum concentration (10 µM) of this carbohydrate polymer inhibited MS corrosion up

to 85 % in the solution of the acid electrolyte. Results reveal that CSS reduced the dissolution of MS linearly with its concentration, and this reduction could be attributed to the interfacial formation of CSS film at the MS-electrolyte boundary. CSS is a mixed-type inhibitor and the shapes of Nyquist capacitive and inductive loops obtained from the impedance results could be associated with double layer reactions and relaxation of corrosive ions adsorption in the presence of CSS, respectively, at the MS/solution interface. Surface analytical studies with atomic force microscope, scanning electron microscope and Fourier transform infra-red also confirm the adsorption of CSS on MS.

In an attempt to improving the inhibitive performance of naturally occurring polymers on the corrosion of metals in different aggressive environments, several modifications have been done. Ferkry and Mohamed (2010) modified chitosan by incorporating acetyl thiourea and then evaluated the corrosion inhibition performance of the acetyl thiourea chitosan (ATUCS) on the corrosion behavior of mild steel in naturally aerated 0.5 M H_2SO_4 solution. ATUCS was found to show very good inhibition efficiency in 0.5 M H_2SO_4 solution and reaches 94.5% at 0.76 mM concentration.

Also, Li *et al.* (2014) have modified chitosan with thiosemicarbazide (TSFCS) and thiocarbohydrazide (TCFCS). TSFCS and TCFCS were tested for protective ability on 304steel corrosion in 2% acetic acid using potentiodynamic

polarization measurements. The results show that both compounds act as mixed-type anticorrosion inhibitors for 304 steel in 2% acetic acid.

Banerjee *et al.* (2012), chemically modified natural polysaccharide by grafting polyacrylamide with Okra mucilage and tested the modified polymer as corrosion inhibitor for mild steel in 0.5 M H_2SO_4 solution using gravimetric and electrochemical techniques. The inhibition efficiency was found to increase with increasing inhibitor concentration up to maximum of 96.6% for 100 ppm at 25^{o}C.

Iota-carrageenan a natural polymer has been reported as a corrosion inhibitor for aluminum in the presence of pefloxacinmesylate, acting as zwitterionic mediator, in acidic medium by Fares *et al.* (2012). Significant improvement in inhibition efficiency of iota-carrageenan was observed in the presence of the mediator. Activation energy of corrosion and other thermodynamic parameters such as standard free energy, standard enthalpy, and standard entropy of the adsorption process revealed better and well-ordered physical adsorption layers in presence of pefloxacin. The adsorption of iota-carrageenan in the presence of pefloxacin mediator was found to follow the Langmuir isotherms. The adsorption of the inhibitor on the aluminum surface was confirmed with the aid of a scanning electron microscope (SEM).

Arukalam *et al.* 2011 The inhibitive effect of hydroxyethylcellulose (HEC) on Mild steel and Aluminium corrosion in 0.5M HCl solution under atmospheric exposure was studied using weight loss method. From the results obtained, it was

observed that the corrosion rate was higher in Aluminium than in Mild steel. Inhibition efficiency and surface coverage were however, found to be higher in Mild steel than in Aluminium. In addition, corrosion current was determined. From our results, the corrosion current was higher in Mild steel than in Aluminium.

Arukalam and Obidiegwu 2011 investigated the inhibitive property of hydroxyethylcellulose to corrosion of aluminium in an acidic medium using weight loss method under atmospheric exposure. The results revealed that HEC inhibited the rate of corrosion attack on the metal. Corrosion rates increased with increase in acid concentration. The inhibition efficiencies increased from 27.74% for the lowest inhibitor concentration to 57.317% for the highest concentration of the inhibitor for aluminium corrosion in 1.0MHCl. Similarly, the inhibitor (HEC) showed efficiencies in the range from 35.893% to a maximum of 58.157% for aluminium corrosion in 1.5M HCl. The corrosion current was also studied and it decreased with increase in inhibitor concentration.

In a related work, Arukalam *et al.* (2014) investigated the inhibition performance of hydroxyethyl cellulose on the acid corrosion of copper. Weight loss measurements results revealed that HEC effectively inhibits copper corrosion in the studied acid media, with maximum inhibition efficiency ~95%. Maximum efficiency in 1 M HCl was obtained after 1 day of immersion and that in 0.5 M H_2SO_4 after 5 days. The impedance response revealed two capacitive time

constants and this mechanism was not altered on addition of HEC, which functioned by adsorption onto the copper surface. The potentiodynamic polarization profile in 1 M HCl shows features of active-passive transition, whereas that in 0.5 M H_2SO_4 shows spontaneous passivation. These mechanisms were not modified by the inhibitor. The computational studies confirmed the corrosion inhibiting potential of HEC. The HEC/Cu adsorption energy estimated by means of molecular dynamics simulation (-55.09 kJ/mol) suggests a spontaneous physical adsorption process.

Solomon *et al*. (2010) studied the use of chemical methods to assess the inhibitive and adsorption behaviour of carboxymethyl cellulose (CMC) for mild steel in H_2SO_4 solution at 30–60°C. Results obtained show that CMC act as inhibitor for mild steel in H_2SO_4. The inhibition efficiency was found to increase with increase in CMC concentration but decreased with rise in temperature, which is suggestive of physical adsorption mechanism. The adsorption of the CMC onto the mild steel surface was found to follow Langmuir and Dubinin–Radushkevich adsorption isotherm models. The inhibition mechanism was further corroborated by the values of activation parameters obtained from the experimental data.

Manimaran *et al.* 2013 has investigated the inhibition efficiency (IE) of carboxymethyl cellulose (CMC)-Zn^{2+} system in controlling corrosion of carbon steel in ground water in the absence and presence of Zn^{2+}has by weight loss method. The formulation consisting of 250 ppm CMC and 50 ppm Zn^{2+} has 98 %

IE. A synergistic effect exists between CMC and Zn^{2+}. Synergism has been confirmed by synergism parameter. AC impedance spectra confirm the formation of protective film on the metal surface. The nature of the protective film has been characterized by scanning electron microscopy (SEM).

Kalaivani *et al.* 2013 studied the Inhibition efficiency (IE) of carboxymethylcellulose in controlling corrosion of aluminium in well water at pH11 by weight loss method in the presence and absence of Zn^{2+} ion. The formulation consisting of 250 ppm of carboxymethylcellulose (CMC) and 25 ppm of Zn^{2+} has 95% inhibition efficiency. Polarisation study revealed that this formulation controls the cathodic reaction predominantly. AC impedance spectra revealed that a protective film is formed on the metal surface and the protective film was analysed by the technique of scanning electron microscope (SEM) and atomic force microscopy (AFM).

Lignin a natural polymer that contains hydroxyl, carboxyl, benzyl alcohol, methoxyl, aldehydic and phenolic functional groups is being studied as a corrosion inhibitor. It adsorbs on metal surfaces and is capable of forming a barrier between the metal and corrodents (Altwaiq *et al*., 2011). Extracted alkali lignin as investigated by Altwaiq *et al.* exhibited corrosion inhibition behaviour in the corrosion of different alloys immersed in HCl solutions. This was investigated by weight loss analysis, surface analysis on the corroded metals by scanning electron microscope (SEM), and micro- beam X-ray fluorescence (μ-

XRF), inductively coupled plasma−optical emission spectroscope (ICPOES) and others. Ren et al (2008) investigated the corrosion inhibition properties of lignin terpolymer, results showed that the highest corrosion inhibition percentage was over 95% in 10% HCl medium at 25^{o}C, the lignin terpolymer inhibitor adsorption followed Temkin isotherm at 25 and 80 and the adsorption capability was in reverse proportion to the temperature. Lignin doped conductive polymers [polyaniline-PANI] are used in corrosion protection. Electrochemical analysis revealed that Ligno-PANI is an efficient corrosion inhibitor. A very low loading (1-2%) of the inhibitor brings much (10-20 fold) reduction in corrosion, presumably by the formation of a passive oxide layer (Xu, 2002).

Oki *et al.* (2011) studied the corrosion inhibition of mild steel in hydrochloric acid by tannins from rhizophora racemosa. Weight loss measurements show that a maximum concentration of 140 ppm of tannin from Rhizophora racemosa is required to achieve 72% corrosion inhibition. Similar concentration of tannin: H_3PO_4 in ratio 1:1 gave 61% inhibition efficiency, whereas efficiency obtained for phosphoric acid as inhibitor in the same environment was 55%. Corrosion rates obtained over six hours of exposure in 1 M HCl solution at inhibitor concentrations of 140 ppm are 2 mA/cm2, 2.4 mA/cm2, 2.6 mA/cm2 and 6 mA/cm2 for tannin, tannin/H_3PO_4 and H_3PO_4-inhibited and uninhibited specimens respectively. Natural atmospheric exposure studies revealed that

specimens treated in H_3PO_4 resisted corrosion for three weeks, while tannin treated specimens suffered corrosion attack after one week of exposure tests.

Hassan and Zafaraany (2013) investigated the corrosion inhibition of aluminum (Al) in hydrochloric acid by anionic polyeletrolyte pectates (PEC) as a water-soluble natural polymer polysaccharide using both gasometric and weight loss techniques. The results drawn from these two techniques are comparable and exhibit negligible differences. The inhibition efficiency was found to increase with increasing inhibitor concentration and decrease with increasing temperature. The inhibition action of PEC on Al metal surface was found to obey the Freundlich isotherm. Factors such as the concentration and geometrical structure of the inhibitor, concentration of the corrosive medium, and temperature affecting the corrosion rates were examined. The kinetic parameters were evaluated and a suitable corrosion mechanism consistent with the kinetic results was discussed in the work.

Bello *et al.*, (2010) used modified cassava starch as corrosion inhibitor of carbon steel in an alkaline 200mg/L NaCl solution (chemical composition of tap water) in contact with air at 25^{o}C. One was cassava starch modified through gelatinization and activation [GAS] and carboxymethylated starch [CMS] with different degrees of substitution [DS]. These were characterized by NMR spectroscopy; estimation of DS was also performed, which was about 0.13±0.03 (CMS 0.13) and 0.24±0.04 (CMS 0.24). The studies confirmed that starch acts as

corrosion inhibitor of carbon steel; the extent of protection against corrosion depended on the amount and type of active groups present [Carboxylic (-COO−) and Carbonyl (–O−) groups for CMS, and Carbonyl (–O−) groups for GAS] and also on DS.

Ochoa *et al.* (2013) studied the use of activated (AS) and carboxymethylated ($CMS_{0.24}$) cassava starch derivatives as corrosion inhibitors for carbon steel XC35 in a 200 mgL^{-1} NaCl solution. They were characterized by back titration and Fourier Transform Infrared Spectroscopy (FTIR). Electrochemical techniques were used to evaluate the inhibitive properties of starches at room temperature and the chemical composition of the protective films was determined by X-Ray Photoelectron Spectroscopy (XPS). Electrochemical measurements revealed that AS acts as mixed inhibitor, whereas $CMS_{0.24}$ mainly inhibits the anodic reaction. In both cases, the protection increased with the inhibitor concentration; nevertheless, after 24 hours of immersion, the $CMS_{0.24}$ loses its properties, while AS molecules still maintains them. XPS analyses show that the inhibitive films are composed of an iron oxide/hydroxide mixture in which starch molecules are incorporated. Results were explained taking into consideration the hydrophilicity and the strength of the ionic interaction of the starches with the metal surface.

Rosliza and Nik (2010) studied the corrosion resistance conferred by tapioca starch [TS] to AA6061 alloy in seawater. The weight loss of AA6061 alloy specimens in seawater diminished with increasing TS concentration as a result of

corrosion deposits. PD results revealed that as the concentration of TS increased, corrosion potential [Ecorr] values shift to more positive value, corrosion current density (icorr) reduced remarkably, the numerical values of both anodic and cathodic Tafel slopes decreased, polarization resistance [Rp] value of AA6061 alloy increased (higher the Rp value, lower the corrosion rate), double layer capacitance value [Cdl] decreased, indicating that anodic and cathodic processes are suppressed by TS, that acts as corrosion inhibitor, preferentially reacting with Al^{3+} to form a precipitate of salt or complex on the surface of the aluminium substrate. Inhibition efficiency [IE (%)] values obtained from all the measurements viz. gravimetric, PD, linear polarization resistance [LPR] and EIS were in close agreement with each other. IE (%) of TS increased with the corrosion inhibitor concentrations ranging from 200 to 1000 ppm. The protection conferred by TS is attributed to the adsorption on AA6061 alloy surface through all the functional groups present in starch (linear amylose constituted by glucose monomer units joined to one another head to tail forming alpha-1, 4 linkage, and highly branched amylopectin with an alpha-1, 6 linkage every 24–30 glucose monomer units).

Mobin *et al.* 2011 studied the corrosion inhibition of mild steel in 0.1 M H_2SO_4 in presence of starch (polysaccharide) using weight loss and potentiodynamic polarization measurements in the temperature range of 30–60°C. Starch inhibits the corrosion rates of mild steel to a considerable extent; the maximum inhibition

efficiency (%IE) being 66.21% at 30^{o}C in presence of starch concentration of 200 ppm. The effect of the addition of very small concentration of sodium dodecyl sulfate and cetyl trimethyl ammonium bromide on the corrosion inhibition behavior of starch was also studied. The IE of starch significantly improved in presence of both the surfactants. The effect of surfactants on the corrosion inhibition behavior of starch appears to be synergistic in nature. Starch alone and in combination with surfactants is found to obey Langmuir adsorption isotherm from the fit of the experimental data of all concentration and temperature studied. Phenomenon of physical adsorption is proposed from the trend of IE with temperature and also the values Ea, ΔGads, and Qads obtained. The results obtained by potentiodynamic polarization measurements are consistent with the results of the weight loss measurement.

Synergism is one of the most important effects in inhibition process and serves as basis for modern corrosion inhibiting formulations. Synergism of corrosion inhibitors is either due to interaction between constituents of the inhibitor or due to interaction between the inhibitor and one of the ions present in aqueous solution Eddy and Odiongenyi (2007). In most cases, the mechanism of synergism differs from the mechanism of the individual inhibitors. By taking advantage of synergism the amount of inhibitor applied can be decreased or an environmental friendly but less effective corrosion inhibitor can be used more effectively. Though the synergistic influence of halide ions on different organic

compounds has been adequately investigated there remains relatively few works directed towards the synergistic between the different organic compounds and surfactants (Rafiqee *et al.* 2008).

Zhang *et al.* (2011) investigated the inhibition behavior of methionine combined with cetrimonium bromide (CTAB) and cetylpyridinium bromide (CPB) for Cu corrosion in 0.5 M HCl solution. Results obtained shows that combination of methionine with CTAB or CPB provides strong synergistic inhibition effect.

Mobin *et al.* 2011 investigated the corrosion inhibition characteristics of nitrogen containing amino acid L-tryptophan on mild steel in 0.1 M HCl solution, in the temperature range of 30-50^{o}C, by weight loss and potentiodynamic polarization measurements. L-tryptophan significantly reduces the corrosion rates of mild steel; the maximum inhibition efficiency being 83% at 50^{o}C in presence of inhibitor concentration of 500 ppm. The effect of the addition of very small concentrations of anionic surfactant, sodium dodecyl sulfate (SDS), and of cationic surfactant, cetyl trimethyl ammonium bromide (CTAB), on the corrosion inhibition behavior of L-tryptophan was also studied. The inhibition efficiency (IE) of L-tryptophan significantly improved in presence of both surfactants. The effect of SDS and CTAB on the corrosion inhibition behavior of L-tryptophan appears to be synergistic in nature, the values of synergism parameter being greater than unity. The adsorption of inhibitors on mild steel surface obeyed Langmuir's adsorption isotherm. The calculated thermodynamic parameters for

adsorption reveal a strong interaction between the inhibitors and the mild steel surface. The results obtained by electrochemical studies are consistent with the results of the weight loss measurements. L-tryptophan acts more anodic than cathodic inhibitor.

The adsorption and corrosion inhibition behaviors of polyethylene glycol (PEG) alone and in the presence of surfactants sodium dodecyl benzene sulfonate and cetyltrimethyl ammonium bromide on mild steel in 0.1 M H_2SO_4 in temperature range of 30-60°C was investigated by Mobin and Khan 2014 using weight loss method, solvent analysis of iron ions, scanning electron microscopy (SEM), energy dispersive x-ray analysis (EDAX), atomic force microscopy (AFM) and determination of kinetic/thermodynamic parameters. The inhibition efficiency (IE) of PEG increased with increasing concentration showing a maximum IE of 86.91% at 30 °C at 25 ppm but decreased with increasing temperature. Inhibiting action of PEG is synergistically enhanced on addition of small amount of surfactants. Surface morphology of the corroded mild steel specimen as evaluated by SEM, EDAX and AFM confirmed the existence of an adsorbed protective film on the mild steel surface. The calculated thermodynamic/kinetic parameters reveal that adsorption process is spontaneous and obey Langmuir adsorption isotherm.

Sohelia *et al.* 2013 studied the corrosion inhibition characteristics of cation-rich and anion-rich catanionic mixtures of cetyltrimethyl ammonium bromide

(CTAB) and sodium dodecyl sulfate (SDS), as corrosion inhibitor of mild steel (MS), in aqueous solution of 3.5% NaCl using electrochemical impedance spectroscopy (EIS), potentiodynamic polarization and scanning electron microscopy (SEM). Solutions of CTAB/SDS mixtures showed more appropriate inhibition properties compared to the solutions of the individual surfactants, due to strong adsorption on the metal surface and formation of a protective film. Potentiodynamic polarization investigations indicated that the inhibitors studied were mixed type inhibitors. Adsorption of the inhibitors on the mild steel surface obeyed the Flory–Huggins adsorption isotherm. Furthermore, the values of the adsorption free energy (ΔG°ads) in both mixtures decreased compared with a single surfactant which is attributed to stronger interactions in mixtures.

Mobin *et al.* 2013 studied the corrosion inhibition behavior of nitrogen-containing amino acid l-Histidine (LHS) on mild steel in 0.1 M H_2SO_4 solution in the temperature range of 30-60°C was studied by weight loss measurements, and potentiodynamic polarization measurements. The effect of the addition of very small concentration of surfactants, sodium dodecyl sulfate (SDS), and cetyltrimethyl ammonium bromide (CTAB), respectively on the corrosion inhibition behavior of LHS was also studied. The surface morphology of the corroded steel samples was evaluated by scanning electron microscopy (SEM) and atomic force microscopy (AFM). LHS significantly reduces the corrosion rates of mild steel, with the maximum inhibition efficiency (IE) being 71.09% at

30°C in the presence of 500 ppm of LHS. The IE of LHS is synergistically increased in the presence of SDS and CTAB. The SEM and AFM photographs show a clearly different surface morphology in the presence of additives. LHS alone and in combination with surfactants obeys Langmuir adsorption isotherm from the fit of the experimental data of all concentration and temperature studied. The calculated thermodynamic parameters for adsorption reveal strong interaction between the inhibitors and the mild steel surface, and suggest physical adsorption. The results obtained by potentiodynamic polarization measurements are consistent with the results of the weight loss measurement. LHS acts more anodic than cathodic inhibitor.

Parveen and Mobin 2013 carried out studies on inhibiting formulations consisting of amino acids and surfactants for mild steel corrosion in 0.1 M H_2SO_4 in the temperature range of 30-60^{o}C. The aim of the surfactants addition was to improve the inhibition efficiency of environment friendly but less effective amino acids as inhibitor for mild steel corrosion in acidic medium. The concentration of surfactants was fixed taking into account that environmental safety of inhibitive formulation is least compromised. The techniques used are weight loss measurements, potentiodynamic polarization measurements, scanning electron microscopy (SEM) and atomic force microscopy (AFM). Inhibition efficiency of selected amino acids is synergistically improved in presence of surfactants.

Synergism between N-containing amino acid and surfactants is more pronounced than S-containing amino acids and surfactants.

CHAPTER THREE

MATERIALS AND METHODS

3.1 Materials

The materials for the work include the following:

Inhibitors: Natural sweet potato starch (NS), Alkaline treated sweet potato starch (ASS), Acid treated sweet potato starch (ATS), and physically modified sweet potato starch (PMS).

Halide: Potassium Iodide (KI)

Corrodents: Sulphuric acid (H_2SO_4) and Hydrochloric acid (HCl).

Metals: Mild steel sheets and galvanised steel sheets.

Other Materials: The other materials for the research are distilled water, absolute ethanol, acetone, bristle brush, beakers, glass rod, hooks, plastic thread, water bath, weighing machine, stopwatch, hand drying machine, potentiostat/galvanostat, FTIR spectroscopy and atomic force microscopy.

3.1.2 Material Preparation

3.1.2.1 Extraction of Starch from tubers

The sweet potato tubers were washed, peeled and trimmed to remove defective parts. The tubers were then sliced, diced and blended in distilled water in a food blender. The mixture was sieved through an 80-mesh sieve and the retained solids were rinsed on the sieve with distilled water. The filtrate was allowed to stand overnight at 15^{o}C, the precipitate was collected and the supernatant discarded.

The re-suspension and sedimentation operation was repeated until white starch was obtained. The starch was dried at 50ºC for 6 hours. Finally, the dried sweet potato starch was ground and sieved through a 100-mesh sieve (Nattapulwat *et al* 2009).

3.1.2.3 Modification of Starch

3.1.2.3.1 Physical modified starch

The extracted sweet potato starch was modified physically by extrusion. The extracted sweet potato starch was processed by an extruder which combines several unit operations, including mixing, kneading, shearing, heating, cooling, shaping, and forming. The temperature in the extruder was set at 150°C and the residence time was 60 seconds.

3.1.2.3.2 Alkaline Treatment of Starch

The alkaline treated granular starch was prepared following the method of Chen and Jane (1994) with slight modifications. 10 g starch was suspended in 40 g ethanol (40 % w/v) at 25ºC and stirred mechanically for 10 min. This was followed by adding 12 g NaOH at rate of 4 g/min. The suspension was gently stirred for 15 min; afterwards 40 g ethanol (40 % w/v) was slowly added and stirred for 10 min. The slurry was left at room temperature (25 °C) for 30 min in order to give sufficient time for the treated starch to settle down. The settled granules were washed with fresh ethanol solution (40 % w/v), neutralized with 3

M HCl in absolute ethanol, and then washed with 60 % and 95 % ethanol solutions. The obtained starch was dehydrated with absolute ethanol, and finally oven-dried at 80 °C for 3 h.

3.1.2.3.3 Acid treatment of Starch

Dry starch (100 g) was taken in a beaker and 150 ml of 6% (w/v) HCl at 40 °C was added in batches over 48 h with occasional stirring. Acid addition was done carefully to accomplish a uniform dispersion of starch throughout the acid. After hydrolysis, the suspension was neutralized with 2% (w/v) NaOH solution and washed three times with distilled water. The water was then removed by centrifugation at 3000 rpm for 10 min and decantation. The wet acid-modified starch was dried in hot-air-oven at temperature not exceeding 40 °C. The dried powder was ground and sieved through 100-mesh sieve to obtain acid-modified starch powder.

3.1.2.3 Preparation of Molar Acid Solution and Inhibitor/Acid Solution

Stock solutions of 0.25 M H_2SO_4 and 1M HCl were first prepared and thereafter other concentrations were obtained respectively using serial dilution principle.

Similarly, stock solutions of NS, PMS, ASS and ATS was prepared by weighing the appropriate amount of the respective inhibitors and dissolving in 1litre of 0.25 M H_2SO_4 and 1 M HCl solutions respectively. Other concentrations (700mg/L,

500mg/L, 300mg/L and 100mg/L) for all the inhibitors were obtained using the serial dilution method.

Stock solution of potassium iodide was prepared by weighing 400mg and dissolving in one litre of 0.25 M H_2SO_4 and 1 M HCl solution.

3.1.2.4 Preparation of Metal Coupon

Mild steel and galvanised steel were used for the study. Each sheet was 10 mm (mild steel) and 5 mm (galvanised steel) in thickness and was mechanically press cut into 3 cm x 3 cm coupons. The percentage composition of mild steel and galvanized steel are presented in Table 3.1:

Table 3.1; Composition of Mild Steel and Galvanised Steel

ELEMENT / METAL	C	Mn	P	S	Ti	Zn	Fe	Cr	Cu
Galvanised Steel	≤0.04	≤0.20	≤0.011	≤0.008	≤0.036	Balance	Balance	-----	-------
Mild Steel	0.25	0.25	0.045	0.02	0.04	------	Balance	0.05	0.06

These coupons were used without further polishing. However, for surface treatment, they were degreased in absolute ethanol, dried in acetone, and stored in desiccators free from moisture before being used in the corrosion studies. The hydrochloric acid (HCl) and sulphuric acid (H_2SO_4) (Sigma-Aldrich) concentration were prepared from analytical grade reagent. All preparations were made using doubly distilled water. The study was conducted under ambient

conditions and at 30 to 60°C, and the temperature was maintained using a thermostated water bath.

3.2 Experimental Methods

3.2.1 Gravimetric Measurement Method

In the gravimetric method, clean weighed metal coupons were used. For the temperature dependent tests, the beakers were placed in a constant thermostated bath maintained between 30 to 60°C for 6 hours. The time dependent gravimetric tests were conducted under ambient conditions for mild steel and galvanised steel in 0.25 M H_2SO_4 and 1 M HCl respectively, the coupons were immersed completely in 250ml beakers containing 200ml of the test solutions with the aid of glass rods and hooks. The coupons were retrieved after 24-hours interval progressively for 120 hours, immersed in 70% nitric acid for 2 minutes at room temperature, scrubbed with a bristle brush under running water, dried in acetone, and weighed. The differences in weight of the coupons before and after immersion in different test solutions would be taken as the weight loss, which was used to calculate the corrosion rate.

$$CR = \frac{[\Delta W \times 87600]}{DAt} \qquad (3.1)$$

Where CR- corrosion Rate (mm/y), ΔW – change in weight (g), D- Density of the coupon (g/cm^3), A-Area of exposed surface of the coupon (cm^2) and T- Time of immersion (h).

The inhibitor efficiency was at each concentration of starch samples were calculated by comparing the corrosion rate in the absence (CR_0) and presence (CR_1) using the relationships:

$$\%IE = \frac{CR_o - CR_1}{CR_o} \times 100 \quad (3.2)$$

where, CR_o = corrosion rate of mild steel in blank corrodent; CR_1 = corrosion rate of mild steel in presence of the inhibitor.

The degree of surface coverage by the adsorbed inhibitor (Ɵ) is related to I.E% by:

$$\theta = 1 - \frac{CR_1}{CR_o} \quad (3.3)$$

3.2.2 Adsorption Studies

The degree of surface coverage (θ) for various concentrations of the inhibitors, and inhibitors in combination with Potassium iodide was used to explain the best isotherm to determine the adsorption process. The data were tested graphically by fitting to the Temkin isotherm, Langmuir isotherm and Freundlich isotherm respectively to determine the best adsorption isotherm. For Langmuir's isotherm, plots of C/Ɵ against C were drawn. Langmuir's adsorption isotherm is given by equation:

$$\frac{C}{\theta} = \frac{1}{K} + C \quad (3.4)$$

For Temkin's isotherm, plots of θ against log C were drawn and its equation is given by:

$$exp(-2a\theta) = K_{ads}C \quad (3.5)$$

Freundlich adsorption isotherm is given by Equation 3.4 and the linearized version by Equation 4.5. Plots of the logarithm of surface coverage (In θ) against logarithm of the concentration of the extract (ln C) were drawn.

$$\theta = KC^n \quad (3.6)$$

$$\ln\theta = \ln K + n \ln C \quad (3.7)$$

3.2.3 Kinetic and Thermodynamic Studies

The apparent activation energy Ea, enthalpy of adsorption, ΔH entropy of adsorption, ΔS and free energy of adsorption (ΔGads) for the corrosion of mild steel and galvanised steel in the corrodents (H_2SO_4 and HCl) in the presence of the inhibitors alone and in combination with the halide was obtained.

Activation Energy E_a

Plots of the logarithm of corrosion rate (log CR) versus reciprocal of absolute temperature (1/T) for the corrosion of the metals in the presence and absence of the four inhibitors in both acidic media were drawn. The apparent activation energy was calculated using Arrhenius equation:

$$\log CR = \log A - \frac{E_a}{2.303RT} \qquad (3.8)$$

CR is the corrosion rate, A is the Arrhenius constant, Ea is the apparent activation energy, R is the molar gas constant and T is the absolute temperature.

Enthalpy (ΔH) and Entropy of Adsorption (ΔS)

Plots of logarithm of corrosion rate/absolute temperature (log CR/T) versus reciprocal of absolute temperature (1/T) for the corrosion of mild steel and galvanised steel i the presence and absence of the four inhibitors in acidic media were drawn. Enthalpy of adsorption, ΔH and entropy of adsorption, ΔS for the corrosion of the metals were obtained by the equation:

$$CR = \frac{RT}{Nh} exp\left(\frac{\Delta S}{R}\right) exp\left(-\frac{\Delta H}{RT}\right) \qquad (3.9)$$

From the slope the values of ΔH was calculated and from the intercept of the linear plot, the values of ΔS was obtained (Mobin *et al.* 2011).

3.2.4 Potentiodynamic polarization measurements

The potentiodynamic polarization measurements was carried out using an EG and G potentiostat/galvanostat, model 263A. The experiments was carried out using

a corrosion cell from EG and G; model K0047 with Ag/AgCl electrode (saturated KCl) as reference electrode, Platinum wire as counter electrode and steel coupons as working electrode. The experiments will be performed using a scan rate of 0.166m V/S, commencing at a potential above 250 mV more active than the stable open circuit potential. All the measurements were carried out at room temperature (30 ± 1^{o}C). Before starting the measurements the specimen was left to attain a steady state indicated by a constant potential. The inhibition efficiency will be calculated using the relationship:

3.2.3 Fourier infrared spectroscopy.

Fourier transform infrared (FTIR) spectra (KBr) were recorded using a Nicolet Magna-IR 560 FTIR spectrophotometer at a frequency of 4000 to 400 cm^{-1}. The spectra for the inhibitors under investigation, as well as the protective film formed on the mild steel surface after 72 h immersion in both acidic environments was recorded by carefully removing the film, mixing it with KBr, and making the pellets.

3.2.4 Atomic Force Microscopy

The inhibitive layer formed in the presence of the starch molecules was also analyzed by means of AFM with an Agilent 5500 Scanning Probe Microscope. AFM images were obtained using Acoustic AC Mode (AAC Mode) with a cantilever oscillation frequency of 155 kHz. The mild steel and galvanised steel samples were immersed during 6 and 24 h in the solution containing the inhibitor. The surface was scanned with a very sharp tip that applies Van der Waals attractive forces. When the tip is close enough then electrostatic repulsive forces apply. The bending of the cantilever is then monitored with a laser beam that is focused on the cantilever and reflected into the detector. Images were taken at the centre and periphery of the surface and processed with Picoscan Image 5 software obtaining topography.

CHAPTER FOUR

RESULTS AND DISCUSSIONS

Sweet potato starch was extracted and modified via extrusion, acid steeping and alkaline steeping to obtain physically modified starch, acid modified starch and alkaline modified starch. The starch samples were characterized using FTIR spectroscopy to determine the functional groups present and subsequently analysed for corrosion inhibiting efficacy using gravimetric and the potentiodynamic polarization methods, including FTIR and atomic force microscopy.

Section 4.1 describes the FTIR characterization of the unmodified and modified starch samples, in this section the starch samples were analysed via FTIR to ascertain the functional groups present after modification. Section 4.2 describes the time dependent gravimetric measurements conducted under ambient conditions for mild steel and galvanised steel in 0.25 M H_2SO_4 and 1 M HCl respectively, calculated values of corrosion rate, inhibition efficiency and degree of surface coverage were deduced. Section 4.3 describes the synergistic effect of the use of the starch samples with potassium iodide. Section 4.4 describes the potentiodynamic polarization measurements conducted on the metals in both acidic media. Section 4.5 describes the FTIR analysis carried out on the metal surfaces to predict whether the starch samples were adsorbed or not adsorbed. Section 4.6 describes morphological studies conducted on the mild steel and

galvanised steel coupons after immersion in the inhibitor / acid media with the aid of the atomic force microscopy. Section 4.7 describes the adsorption mode of the starch samples as well as the isotherm that gave the best fit. Section 4.8 describes the effect of temperature on the inhibition efficacy of the starch samples as well as the kinetics and mechanism of adsorption.

4.1 FTIR Characterization of Inhibitor Samples

The unmodified and modified starches were characterised with the Fourier Transform Infrared Spectroscopy (FTIR) and the spectra for each starch sample is presented in Figures 4.1 to 4.3.

Figure 4.1 presents the FTIR spectra for unmodified starch and acid treated starch. Initially, the FTIR spectra of the unmodified starch showed complex vibrational modes due to the pyranose ring of the glycosidic unit in the region below 800 cm^{-1} which is in line with research works reported by Kizil and Seetharaman (2002) and Vasco et al. (1972). At the 1000–1200 cm^{-1} region, the common features of polysaccharides were observed. This region was dominated by ring vibrations overlapped by stretching vibrations of C–OH side groups and the C–O–C glycosidic bond vibration (Kacurakova et al., 2000). Within this wavenumber range, the C–O and C–C stretching vibrations contribute to modes related to the bands at 994, 1084, and 1163 cm^{-1} and the C–O–C glycosidic band at 860 cm^{-1}. The spectrum also displays C–H bending bands at 1465, 1425, and

1366 cm^{-1}. The starch spectrum shows characteristic O–H bending and stretching bands at 1649 and 3430 cm^{-1}, respectively which is attributed to the complex vibrational stretches associated with free, inter - and intra - molecular bound hydroxyl groups that make up the gross structure of starch. Characteristic peaks were observed at 2929 cm^{-1} for C-H stretches associated with the ring hydrogen atoms.

For the acid treated starch spectra, it is observed that there are slight shifts in the peaks, reductions in the intensity of the peaks as presented in Table 4.1, and narrowing of the O–H broad band at 3430 cm^{-1}. Most authors have used infrared spectroscopy to estimate the amount of ordered or crystalline regions by analyzing the bands at 1047 and 1022 cm^{-1}. Thus, the crystalline state can be identified by the appearance of a band at 1047 cm^{-1}, while the starch amorphous region is characterized by an absorption band around 1022 cm^{-1}(Cael et al., 1975; Soest et al., 1995; Sevenou et al., 2002; Liu et al., 2004). From the acid treated starch spectra it is observed that the band at 1022cm became narrower indicating disappearance of the amorphous region of the starch which is characteristic with acid hydrolysis of starch.

The Ftir spectrum for the physically modified starch is presented in Fig 4.2. From the spectra, it is observed that there are slight shifts in the peaks, reductions in the intensity of the peaks as presented in Table 4.1, and broadening of the O–H band at 3430 cm-1. At the 1022cm^{-1} wavelength, which denotes the starch amorphous

region, a broader band is observed indicating increase in the amorphous region of the starch which could be as a result of the shearing force the starch granules have to pass through during extrusion.

The FTIR spectrum of the alkaline treated starch is presented in Fig 4.3. From the spectra, it is observed that there are slight shifts in the peaks, increase in the intensity of some peaks, and narrowing of the O–H band at 3430 cm^{-1} as well as a sharper peak being observed 1649 cm^{-1} which simply indicates the loss of the bound water in starch due to its modification (Fang *et al.* 2004). At the 1022cm^{-1} wavelength, which denotes the starch amorphous region, a slightly narrowed peak is observed indicating decrease in the amorphous region of the starch which could be as a result of the alkaline effect on the starch granules. Mehdi *et al.* (2014) also showed that the spectral patterns of alchoholic-alkaline treated starch were similar to natural starch and no new functional groups were found in the FTIR spectra. They also reported that characteristic peaks of hydroxyl groups were of low transmittance in spectrum of treated starch compared with that of native counterpart implying in participation of hydroxyl groups in interactions with modifying agents.

Table 4.1 Peaks and bonds observed at the absorption bands in the FTIR spectra of the starch samples

	Unmodified Starch	Acid Treated Starch	Physically Modified Starch	Alkaline Treated Starch
O-H	3430	3422	3434	3425
C-H	2929	2936	2930	2932
O-H	1649	1656	1647	1655
$C\text{-}H_s$	1465	1465	1455	1465
C-H, COO	1425	1424	1426	1423
C-O, O-H	1163	1160	1161	1162
C-O	1084	1080	1085	1078
C-C	994	989	984	993
C-O-C	860	862	863	863

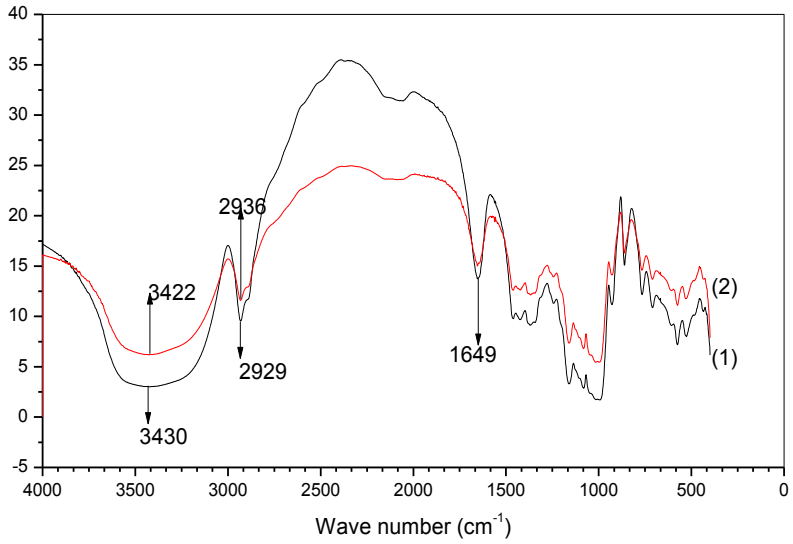

Figure 4.1: *FTIR spectra of sweet potato natural starch (1), and acid treated starch (2)*

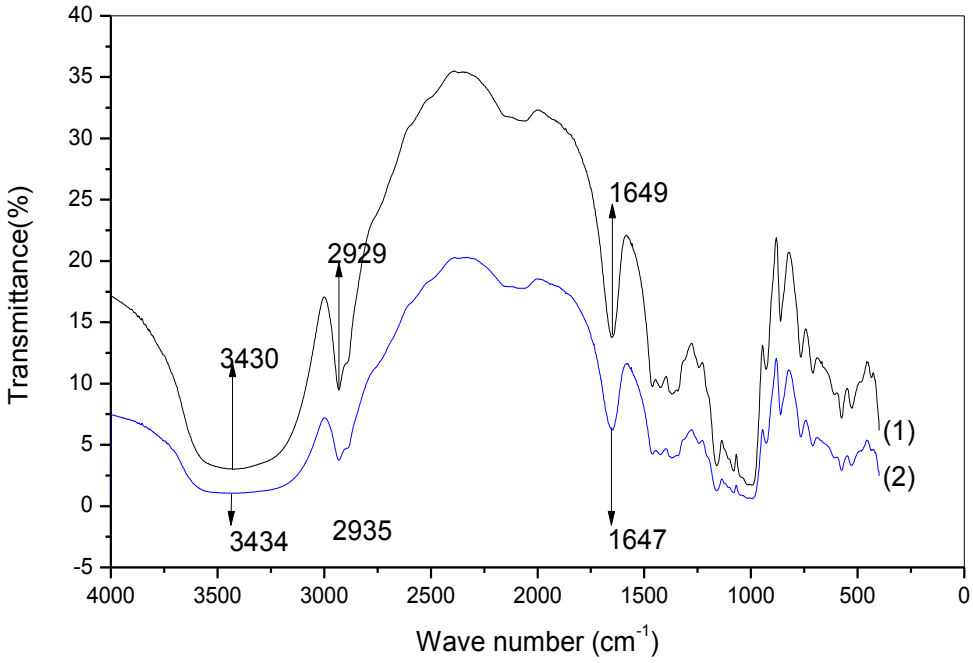

Figure 4.2; *FTIR spectra of sweet potato natural starch (1), and physical modified starch (2)*

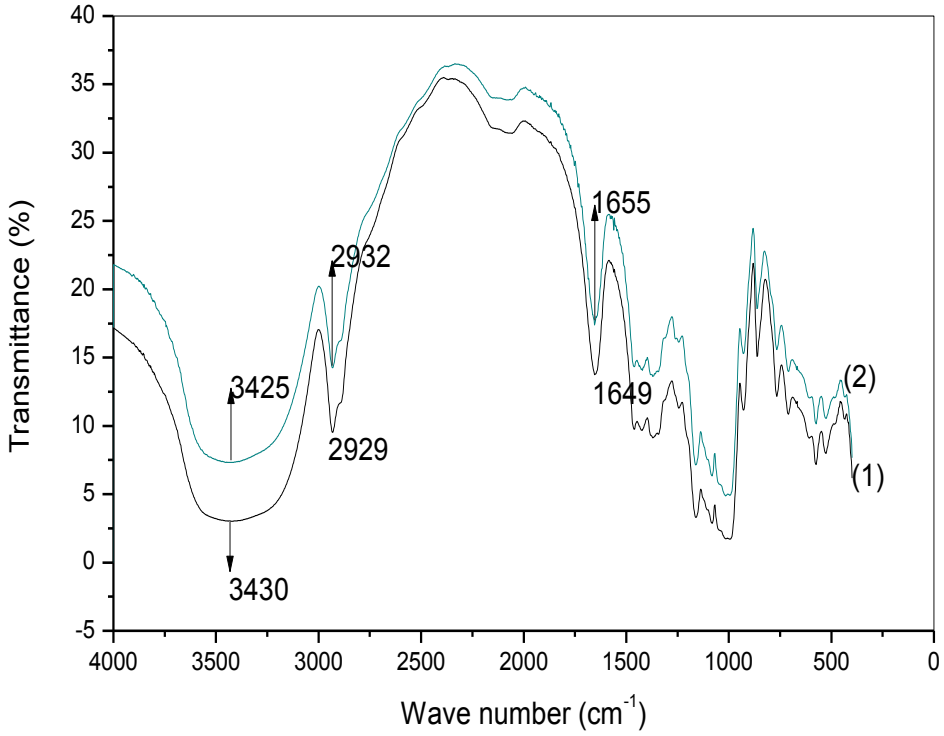

Figure 4.3*; FTIR spectra of sweet potato natural starch (1), and alkaline treated starch (2)*

4.2. Gravimetric Measurements

4.2.1 Mild Steel Corrosion

The corrosion rates of mild steel coupons in 0.25 M H_2SO_4 and 1 M HCL with and without the inhibitors (Alkaline treated starch (ASS), Acid treated starch (ATS), physically modified starch (PMS)) and native starch (NS) were studied using gravimetric techniques under aerated conditions.

4.2.1.1 Corrosion of Mild Steel in 0.25 M H_2SO_4

The calculated values of corrosion rate, inhibition efficiency and degree of surface coverage for mild steel corrosion in 0.25 M H_2SO_4 without and with different concentration of the four inhibitors as a function of time in days are presented in Table 4.2. The variation of corrosion rate against time (hrs) for mild steel corrosion in 0.25 M H_2SO4 without and with different concentration of the four inhibitors is presented graphically in Figure 4.4 a-d. Inspection of the Figures reveals that corrosion rates reduced in the presence of the inhibitors as compared to the free acid solution, indicating that the four inhibitors inhibited the dissolution of mild steel in 0.25 M H_2SO_4. Also the corrosion rate reduced with increase in time of immersion at all concentrations for the four inhibitors, but the rate of corrosion was least in ASS (Alkaline steeped starch) and highest in NS (Natural Starch) following this sequence ASS < ATS< PMS< NS. The lowest corrosion rate was exhibited by 0.5g/l of ASS. The high corrosion rate of NS

could be ascribed to its unfavorable characteristics such as poor solubility in cold water and tendency to retrograde (Shi et al. 2011).

The plot of Inhibition Efficiency as a function of time (h) is presented in Figures 4.5a to Figures 4.5d. The plots show that inhibition efficiency decreased with increasing time for the four inhibitors. ASS exhibited the best inhibition efficacy when compared to other inhibitors, following the trend ASS> ATS> PMS> NS at all concentration.

The inhibition of mild steel corrosion in the presence of the inhibitors could be attributed to the adsorption of starch molecules on to mild steel surface resulting in film formation, which blocks the metal and thus do not permit the corrosion process to take place. Starch adsorption is attributed to the interaction between the lone pair of electrons of the oxygen atom and the steel surface. The presence of d π vacant orbital of low energy in the iron atom, as observed in transition group metals, facilitates the adsorption process Mobin *et al.* (2011).

Furthermore, the plots revealed that increase in concentration increased inhibition efficiency with a maximum efficiency of 62.76% after 24hrs of immersion in 0.25M H_2SO_4 containing 0.5g/l of ASS (Alkaline steeped starch).

However for inhibitor ASS at concentration of 0.5g/l, the maximum inhibition efficiency was attained and further addition of the inhibitor did not significantly influence the inhibition efficiency

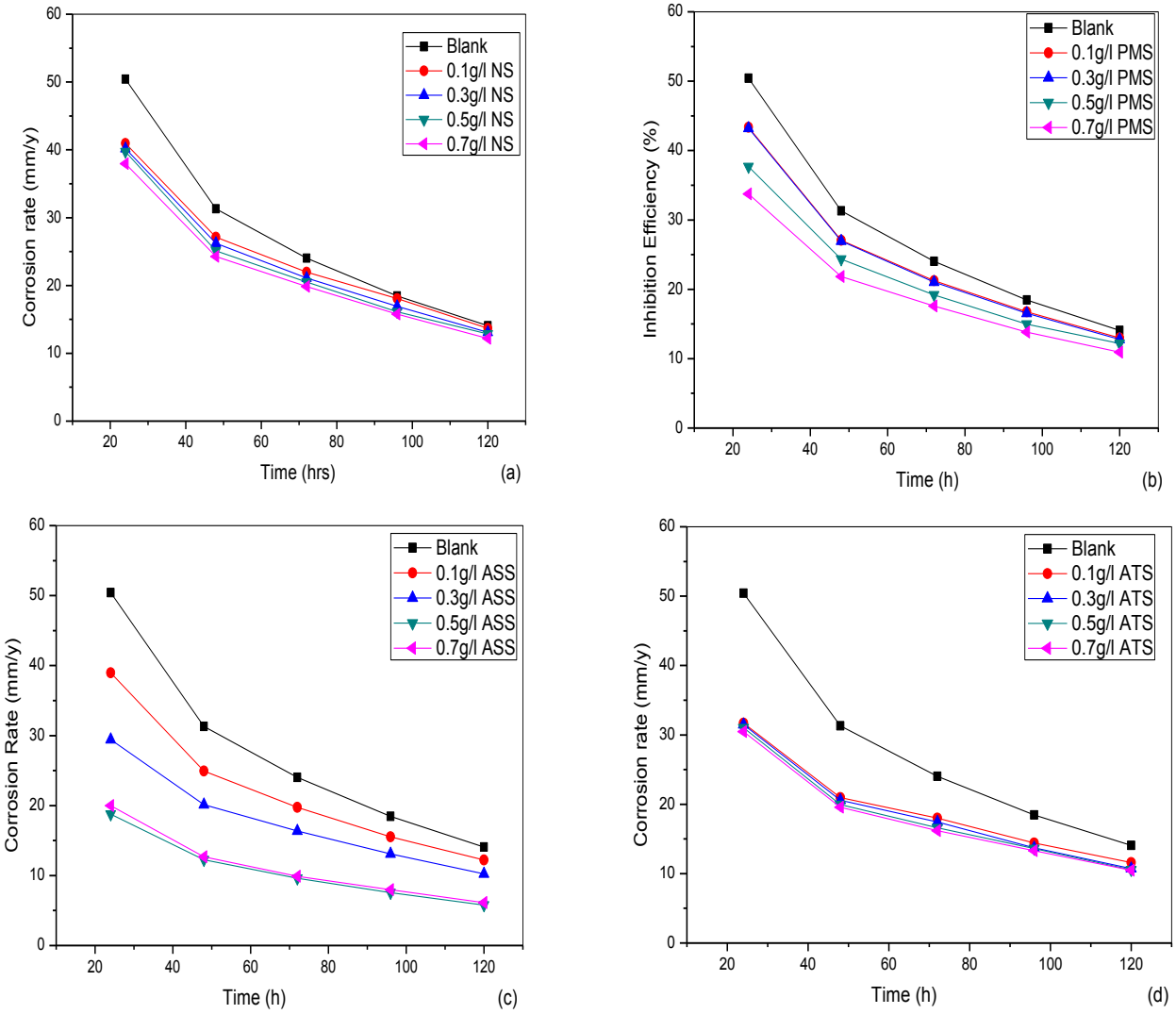

Figure 4.4: *Plots of Corrosion rate against Time for mild steel in 0.25 M H_2SO_4 in the presence and absence of (a)Natural Starch, (b)Physically modified starch, (c)Alkaline steeped starch and (d) Acid Treated starch under aerated conditions.*

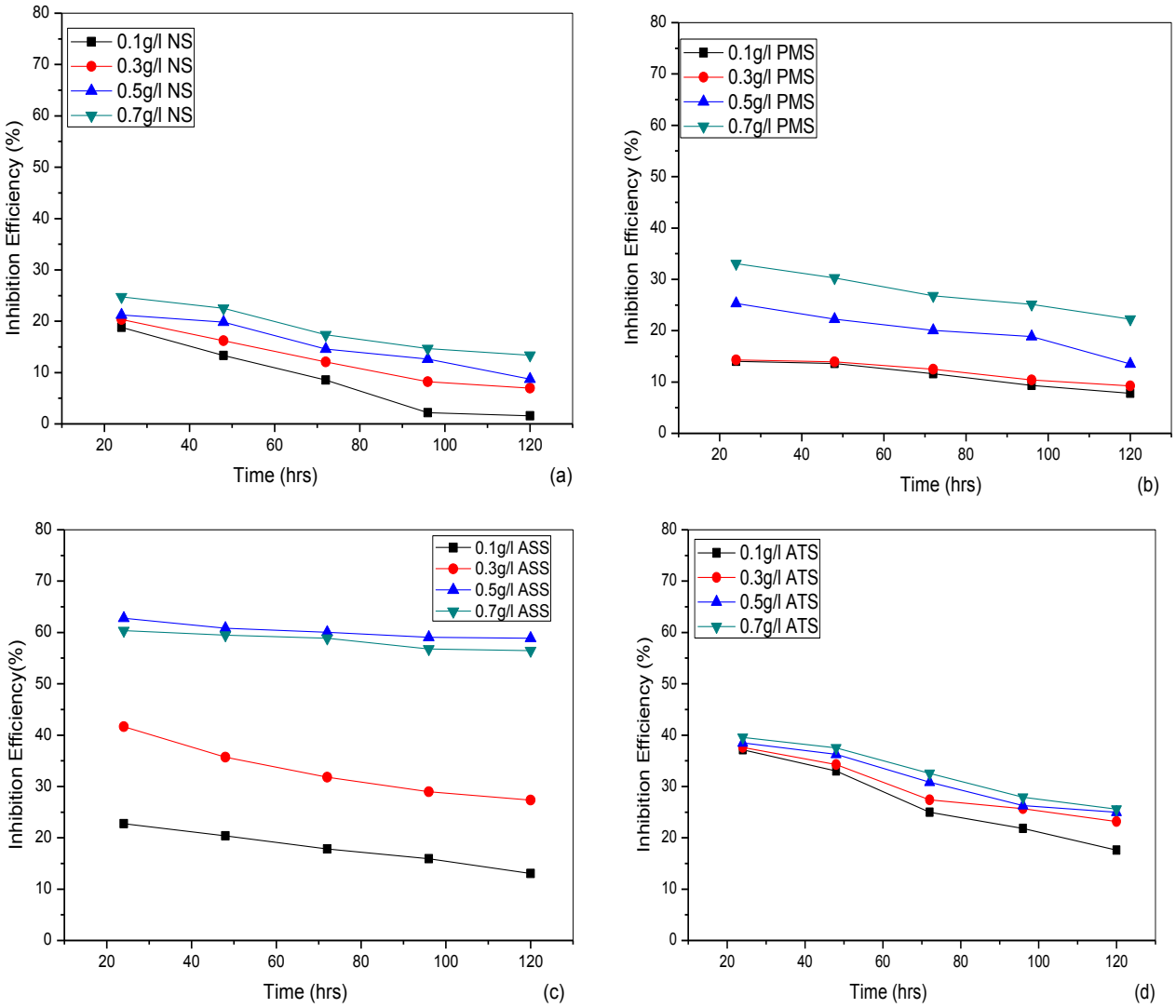

Figure 4.5: *Plots of Inhibition Efficiency against Time for mild steel in 0.25 M H_2SO_4 in the presence and absence of (a)Natural Starch, (b)Physically modified starch, (c)Alkaline steeped starch and (d) Acid Treated starch*

Table 4.2 Calculated values of Corrosion rate, Inhibition efficiency and degree of surface coverage of mild steel in 0.25 M H_2SO_4 in the presence and absence of NS, PMS, ASS and ATS corrosion inhibitors under aerated condition

	Corrosion Rate (mmy^{-1})					Inhibition Efficiency (%)					Degree of Surface Coverage(**Θ**)				
Time	24 h	48 h	72 h	96 h	120 h	24 h	48 h	72 h	96 h	120 h	24 h	48 h	72 h	96 h	120 h
InhibitorConc															
Blank	**50.43**	**31.31**	**24.02**	**18.46**	**14.08**	-	-	-	-	-	-	-	-	-	-
0.1g/l NS	**46.79**	**29.14**	**23.97**	**18.06**	**13.70**	**07.22**	**06.93**	**04.37**	**02.17**	**01.56**	**0.0722**	**0.0693**	**0.0437**	**0.0217**	**0.0156**
0.3g/l NS	**43.18**	**27.23**	**21.12**	**16.94**	**13.10**	**14.38**	**13.03**	**12.07**	**08.23**	**06.96**	**0.1438**	**0.1303**	**0.1207**	**0.0823**	**0.0696**
0.5g/l NS	**39.74**	**25.10**	**20.52**	**16.13**	**12.85**	**21.20**	**19.83**	**14.57**	**12.62**	**08.74**	**0.2212**	**0.1983**	**0.1457**	**0.1262**	**0.0874**
0.7g/l NS	**37.95**	**24.26**	**19.85**	**15.78**	**12.20**	**24.75**	**22.52**	**17.36**	**14.68**	**13.35**	**0.2475**	**0.2252**	**0.1736**	**0.1468**	**0.1335**
0.1g/l PMS	**45.35**	**28.05**	**22.23**	**17.74**	**13.58**	**10.09**	**09.13**	**07.45**	**03.90**	**03.55**	**0.1009**	**0.1361**	**0.1162**	**0.0932**	**0.0781**
0.3g/l PMS	**42.23**	**26.95**	**21.02**	**16.54**	**12.78**	**16.26**	**13.93**	**12.49**	**10.40**	**09.23**	**0.1626**	**0.1393**	**0.1249**	**0.1040**	**0.0923**
0.5g/l PMS	**37.67**	**24.35**	**19.20**	**14.98**	**12.18**	**25.30**	**22.23**	**20.07**	**18.85**	**13.49**	**0.2530**	**0.2223**	**0.2007**	**0.1885**	**0.1349**
0.7g/l PMS	**33.75**	**21.84**	**17.58**	**13.82**	**10.95**	**33.08**	**30.25**	**26.81**	**25.14**	**22.23**	**0.3308**	**0.3025**	**0.2681**	**0.2514**	**0.2223**
0.1g/l ASS	**33.95**	**24.93**	**19.74**	**15.52**	**12.24**	**32.68**	**20.38**	**17.82**	**15.92**	**13.07**	**0.3268**	**0.2038**	**0.1782**	**0.1592**	**0.1307**
0.3g/l ASS	**29.43**	**20.13**	**16.38**	**13.11**	**10.23**	**41.64**	**35.71**	**31.80**	**28.98**	**27.34**	**0.4164**	**0.3571**	**0.3180**	**0.2898**	**0.2734**
0.5g/l ASS	**18.78**	**12.26**	**9.60**	**7.56**	**5.79**	**62.76**	**60.84**	**60.03**	**59.05**	**58.88**	**0.6276**	**0.6084**	**0.6003**	**0.5905**	**0.5888**
0.7g/l ASS	**19.99**	**12.68**	**9.88**	**7.98**	**6.13**	**60.36**	**59.50**	**58.87**	**56.77**	**56.46**	**0.6036**	**0.5950**	**0.5887**	**0.5677**	**0.5646**
0.1g/l ATS	**35.69**	**25.28**	**20.02**	**16.43**	**12.90**	**29.23**	**19.26**	**16.65**	**10.99**	**08.38**	**0.2923**	**0.1926**	**0.1665**	**0.1099**	**0.0838**
0.3g/l ATS	**31.47**	**20.58**	**17.44**	**14.72**	**11.72**	**37.59**	**34.27**	**27.39**	**20.26**	**16.76**	**0.3759**	**0.3427**	**0.2739**	**0.2026**	**0.1676**
0.5g/l ATS	**31.02**	**19.95**	**16.62**	**13.61**	**10.56**	**38.49**	**36.28**	**30.81**	**26.27**	**25.00**	**0.3849**	**0.3628**	**0.3081**	**0.2627**	**0.2500**
0.7g/l ATS	**30.48**	**19.56**	**16.20**	**13.31**	**10.48**	**39.56**	**37.53**	**32.56**	**27.90**	**25.57**	**0.3956**	**0.3753**	**0.3256**	**0.2790**	**0.2557**

4.2.1.2 Corrosion of mild steel in 1 M HCl

Data of the corrosion rate, inhibition efficiency and degree of surface coverage for corrosion studies in 1 M HCl are presented in Table 4.3 and illustrated graphically In Figures 4.6a-d for corrosion rates and Figures 4.7a-d for inhibition efficiency. Figures 4.6a-d shows that corrosion rates reduced in the presence of the inhibitors as compared to the free acid solution. Corrosion rates decreased with increase in concentration indicating that more inhibitor molecules were adsorbed on the surface of the metal. The Alkaline steeped starch (ASS) exhibited the lowest corrosion rates at inhibitor concentration of 0.5g/l ASS. The corrosion rate of mild steel in the presence and absence of the four inhibitors in 1 M HCl were similar but lower than that of mild steel in 0.25 M H_2SO_4.

The maximum inhibition efficiency value attained was 55.65% at 30^oC by 0.5g/l ASS/1 M HCL system. The inhibition efficiency increased with increase in concentration but decreased with increase in time of immersion, indicating that adsorption of the inhibitor molecules was physical. Inhibition efficiency for the four inhibitors followed the trend ASS>ATS>MAS>NS.

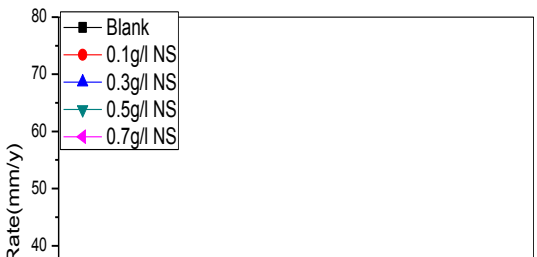

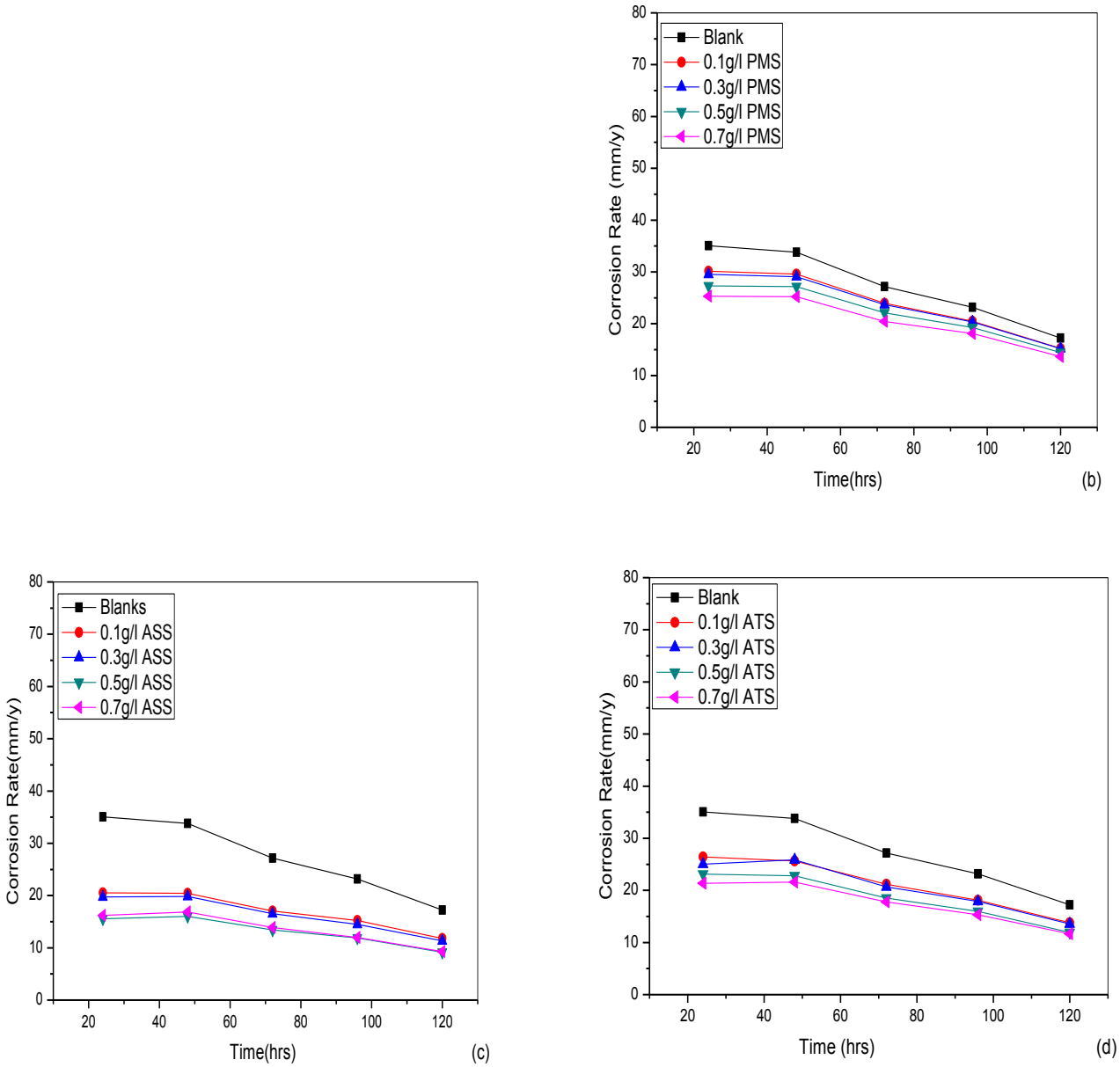

Figures 4.6: *Plots of Corrosion rate against Time for mild steel in 1 M HCL in the presence and absence of (a)Natural Starch, (b)Physically modified starch, (c)Alkaline steeped starch and (d) Acid Treated starch under aerated conditions.*

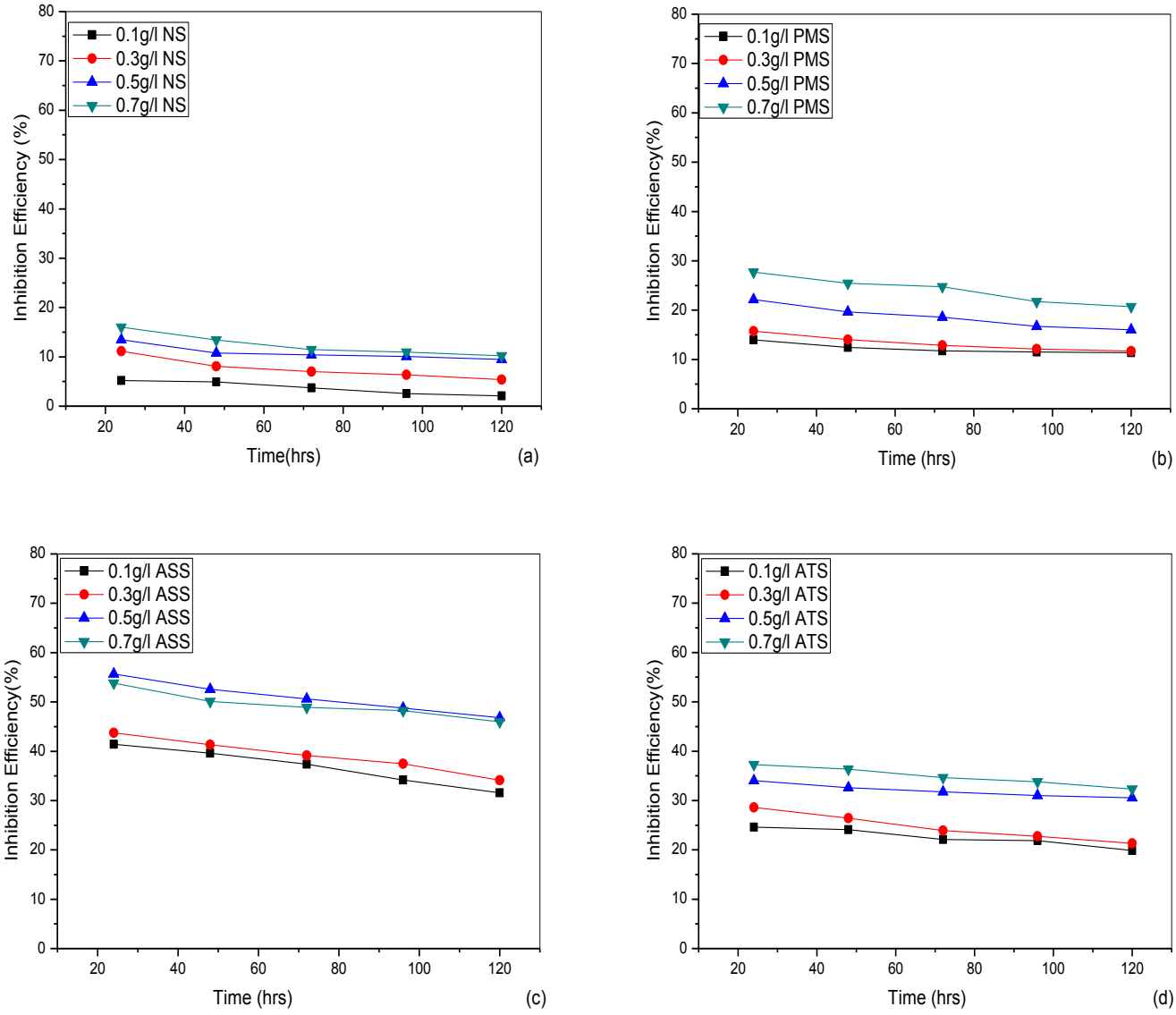

Figure 4.7: *Plots of Inhibition Efficiency against Time for mild steel in 1M HCL in the presence and absence of (a) Natural Starch, (b) Physically modified starch, (c)Alkaline steeped starch and (d) Acid Treated starch under aerated conditions.*

Table 4.3 Calculated values of Corrosion rate, Inhibition efficiency and degree of surface coverage of mild steel in 1 M HCl in the presence and absence of NS, PMS, ASS and ATS corrosion inhibitors under aerated condition

	Corrosion Rate (mmy^{-1})					Inhibition Efficiency(%)					Degree of Surface Coverage(Θ)				
Time	**24 h**	**48 h**	**72 h**	**96 h**	**120 h**	**24 h**	**48 h**	**72 h**	**96 h**	**120 h**	**24 h**	**48 h**	**72 h**	**96 h**	**120 h**
InhibitorConc															
Blank	**35.04**	**33.79**	**27.17**	**23.15**	**17.21**	**-**	**-**	**-**	**-**	**-**	**-**	**-**	**-**	**-**	**-**
0.1g/l NS	**33.22**	**32.13**	**26.16**	**22.56**	**16.85**	**05.19**	**04.91**	**03.72**	**02.55**	**02.09**	**0.0519**	**0.0491**	**0.0372**	**0.0255**	**0.0209**
0.3g/l NS	**31.14**	**31.05**	**25.26**	**21.68**	**16.28**	**11.13**	**08.10**	**07.03**	**06.35**	**05.40**	**0.1113**	**0.0810**	**0.0703**	**0.0635**	**0.0540**
0.5g/l NS	**28.32**	**29.74**	**24.35**	**20.82**	**15.58**	**19.18**	**11.99**	**10.38**	**10.07**	**09.47**	**0.1918**	**0.1199**	**0.1038**	**0.1007**	**0.0947**
0.7g/l NS	**27.03**	**28.25**	**24.06**	**20.61**	**15.45**	**22.86**	**16.40**	**11.45**	**10.97**	**10.23**	**0.2286**	**0.1640**	**0.1145**	**0.1097**	**0.1023**
0.1g/l PMS	**31.74**	**30.88**	**24.98**	**21.48**	**16.05**	**09.42**	**08.61**	**08.06**	**07.21**	**06.74**	**0.0942**	**0.0861**	**0.0806**	**0.0721**	**0.0674**
0.3g/l PMS	**29.52**	**29.05**	**23.67**	**20.34**	**15.20**	**15.75**	**14.03**	**12.88**	**12.14**	**11.68**	**0.1575**	**0.1403**	**0.1288**	**0.1214**	**0.1168**
0.5g/l PMS	**27.28**	**27.16**	**22.12**	**19.28**	**14.45**	**22.15**	**19.62**	**18.59**	**16.72**	**16.04**	**0.2215**	**0.1962**	**0.1859**	**0.1672**	**0.1604**
0.7g/l PMS	**25.32**	**25.19**	**20.45**	**18.12**	**13.65**	**27.74**	**25.45**	**24.73**	**21.73**	**20.69**	**0.2774**	**0.2545**	**0.2473**	**0.2173**	**0.2069**
0.1g/l ASS	**20.53**	**20.41**	**17.02**	**15.24**	**11.78**	**41.41**	**39.60**	**37.36**	**34.17**	**31.55**	**0.4141**	**0.3960**	**0.3736**	**0.3417**	**0.3155**
0.3g/l ASS	**19.72**	**19.82**	**16.54**	**14.48**	**11.34**	**43.72**	**41.34**	**39.12**	**37.45**	**34.11**	**0.4372**	**0.4134**	**0.3912**	**0.3745**	**0.3411**
0.5g/l ASS	**15.54**	**16.03**	**13.42**	**11.87**	**09.16**	**55.65**	**52.56**	**50.61**	**48.73**	**46.78**	**0.5565**	**0.5256**	**0.5061**	**0.4873**	**0.4678**
0.7g/l ASS	**16.19**	**16.86**	**13.88**	**11.98**	**09.30**	**53.79**	**50.10**	**48.91**	**48.25**	**45.96**	**0.5379**	**0.5010**	**0.4891**	**0.4825**	**0.4596**
0.1g/l ATS	**26.41**	**25.64**	**21.16**	**18.09**	**13.79**	**24.63**	**24.12**	**22.12**	**21.86**	**19.87**	**0.2463**	**0.2412**	**0.2212**	**0.2186**	**0.1987**
0.3g/l ATS	**25.02**	**25.87**	**20.68**	**17.88**	**13.54**	**28.60**	**26.40**	**23.89**	**22.76**	**21.32**	**0.2860**	**0.2640**	**0.2389**	**0.2276**	**0.2132**
0.5g/l ATS	**23.11**	**22.78**	**18.54**	**15.97**	**11.95**	**34.05**	**32.58**	**31.76**	**31.02**	**30.56**	**0.3405**	**0.3258**	**0.3176**	**0.3102**	**0.3056**
0.7g/l ATS	**21.35**	**21.58**	**17.76**	**15.32**	**11.65**	**37.30**	**36.35**	**34.63**	**33.82**	**32.31**	**0.3730**	**0.3635**	**0.3463**	**0.3382**	**0.3231**

4.2.1.3 Effect of Inhibitor Concentration.

The effect of inhibitor concentration on inhibition efficiency of the unmodified and modified starch samples on mild steel in 0.25 M H_2SO_4 and 1 M HCl are presented in Figures 4.5 and 4.6 respectively. The NS, PMS and ASS samples showed maximum inhibition efficiencies of 24.75%, 33.08% and 39.56% in 0.25M H_2SO_4 and 22.86%, 27.74% and 37.30% in 1 M HCl at an optimum concentration of 0.7g/l. The increased IE with increasing inhibitor concentration for inhibitors NS, PMS and ATS indicates that more inhibitor molecules were adsorbed on the steel surface leading to the formation of a protective film (Rao and Singall, 2009). However, ATS exhibited maximum inhibition efficiency of 62.76% and 55.65% in 0.25 M H_2SO_4 and 1 M HCl respectively at a concentration of 0.5g/l and further increase in concentration did not cause any significant change in the performance of the starch sample. The inhibition efficiency of the four inhibitors followed the same trend with ASS exhibiting the highest inhibition efficiency. Mobin and Parveen (2011) carried out weight loss tests on mild steel in 0.1 M H_2SO_4 in presence of starch and observed that starch inhibits the corrosion rates of mild steel to a considerable extent, with its efficiency increasing with increase in concentration. The values of inhibition efficiency (IE%) and corrosion rate (CR) obtained from gravimetric method at different concentrations of the four starch samples in 0.25 M H_2SO_4 and 1 M HCl respectively are summarized in Table 4.2 and 4.3.

4.2.1.4 Effect of Immersion Time

In order to assess the stability of inhibitive behaviour of the starch samples on a time scale, weight loss measurements were performed in 0.25 M H_2SO_4 and 1 M HCl, in the absence and presence of the starch samples at various concentrations for 24 to 120 h immersion time at room temperature. Inhibition efficiencies were plotted against immersion time as seen from Figure 4.5 for mild steel in 0.25 M H_2SO_4 and Figure 4.7 for mild steel in 1 M HCl. This figure shows that inhibition efficiency of the four starch samples followed the same trend, decreasing with increasing immersion time from 24 to 120 h. Decrease in inhibition efficiency with increasing time suggests possible peeling or dissolution of the protective starch layer from the metal surface at longer periods. This behaviour shows that the starch was physically adsorbed on the metal surface Oguzie (2004). This trend was observed by Ochoa *et al.* (2013) in the use of caboxymethylated starch as corrosion inhibitor for carbon steel XC35 in a 200 mgL^{-1} NaCl solution; they observed that after 24 hrs, inhibition efficacy of the modified starch decreased.

4.2.1.5 Effect of Acid

The data of inhibition efficiency in 0.25 M H_2SO_4 and 1 M HCl acid is presented in Tables 4.2 and 4.3 respectively. In acid medium, starch may be partially hydrolyzed into simpler carbohydrates but the products with higher hydrophilicity than starch is likely to go into the bulk water. As the hydrolysis is

quite slow, only negligible starch molecules are expected to hydrolyze and desorbs from the steel surface. Also, the starch in bulk water may occupy the steel surface as the molecules are in dynamic equilibrium. So, even after slow hydrolysis, inhibition by starch is effective.

As observed in the data presented, the inhibition efficacy for the starches in 0.25 M H_2SO_4 were slightly higher than that of the starches in 1 M HCl. This could be ascribed to the fact that 1 M HCl is more concentrated than 0.25 M H_2SO_4

$H_2SO_4 \rightarrow 2H^+ + SO_4^{2-}$

$HCl \rightarrow H^+ + Cl^-$

Hence 1 M HCl is equivalent to 0.5 M H_2SO_4, making 0.25 M H_2SO_4 less acidic when compared to 1 M HCl.

4.2.2 Galvanised Steel Corrosion

The corrosion studies of galvanised steel in 0.25 M H_2SO_4 and 1 M HCL with or without different concentrations of inhibitors under aerated conditions were carried out.

4.2.2.1 Corrosion of galvanised steel in 0.25 M H_2SO_4

Data of the corrosion of galvanised steel in the presence and absence of the four inhibitors in the free acid solution of 0.25 M H_2SO_4 is presented in Table 4.4. Graphical illustrations of these data are presented in Figure 4.8a to d for corrosion rates and Figures 4.9a to d for inhibition efficiency.

Plots of corrosion rate against time as presented in Figure 4.8a to d, shows that the corrosion rate of galvanised steel decreased with increase in inhibitor concentration for the four inhibitors which proves that the inhibitor molecules were adsorbed on the metal and retarded corrosion of the metal. The rate of corrosion was least in ASS (Alkaline steeped starch) and highest in NS (Natural Starch) following this sequence ASS < ATS< PMS< NS. The lowest corrosion rate was exhibited by 0.7g/l of ASS. This implies that increase in concentration of inhibitor increases the rate at which the inhibitor molecules are adsorbed on the galvanised steel surface hence reducing corrosion rate.

Plots of inhibition efficiency against time as presented in Figure 4.9a to d shows that inhibition efficiency decreased with increasing time of immersion, this trend was exhibited by the four inhibitors at all concentrations. However, increase in concentration of the inhibitor increased the inhibition efficiency with ASS exhibiting the maximum inhibition efficiency. The inhibition efficiency followed the sequence ASS>ATS>PMS>NS.

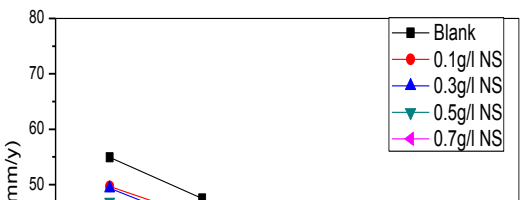

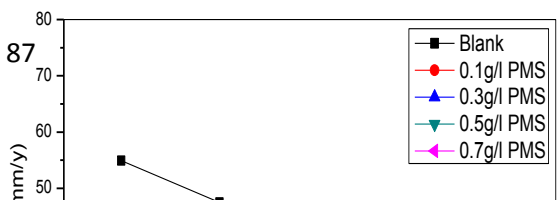

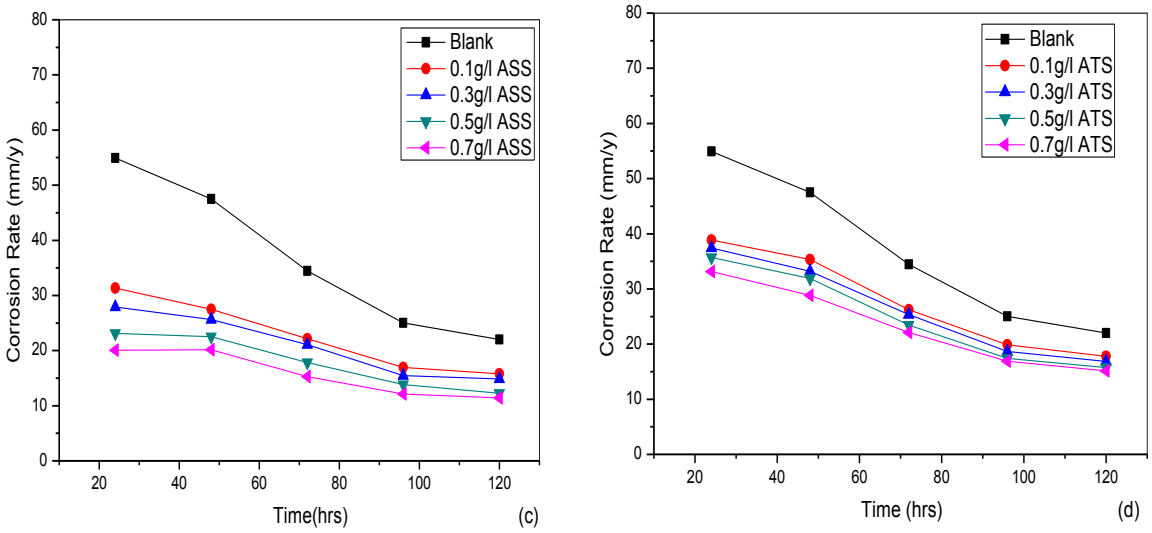

***Figure 4.8**: Plots of Corrosion rate against Time for galvanised steel in 0.25M H_2SO_4 in the presence and absence of (a)Natural Starch, (b)Physically modified starch, (c)Alkaline steeped starch and (d) Acid Treated starch under aerated conditio*

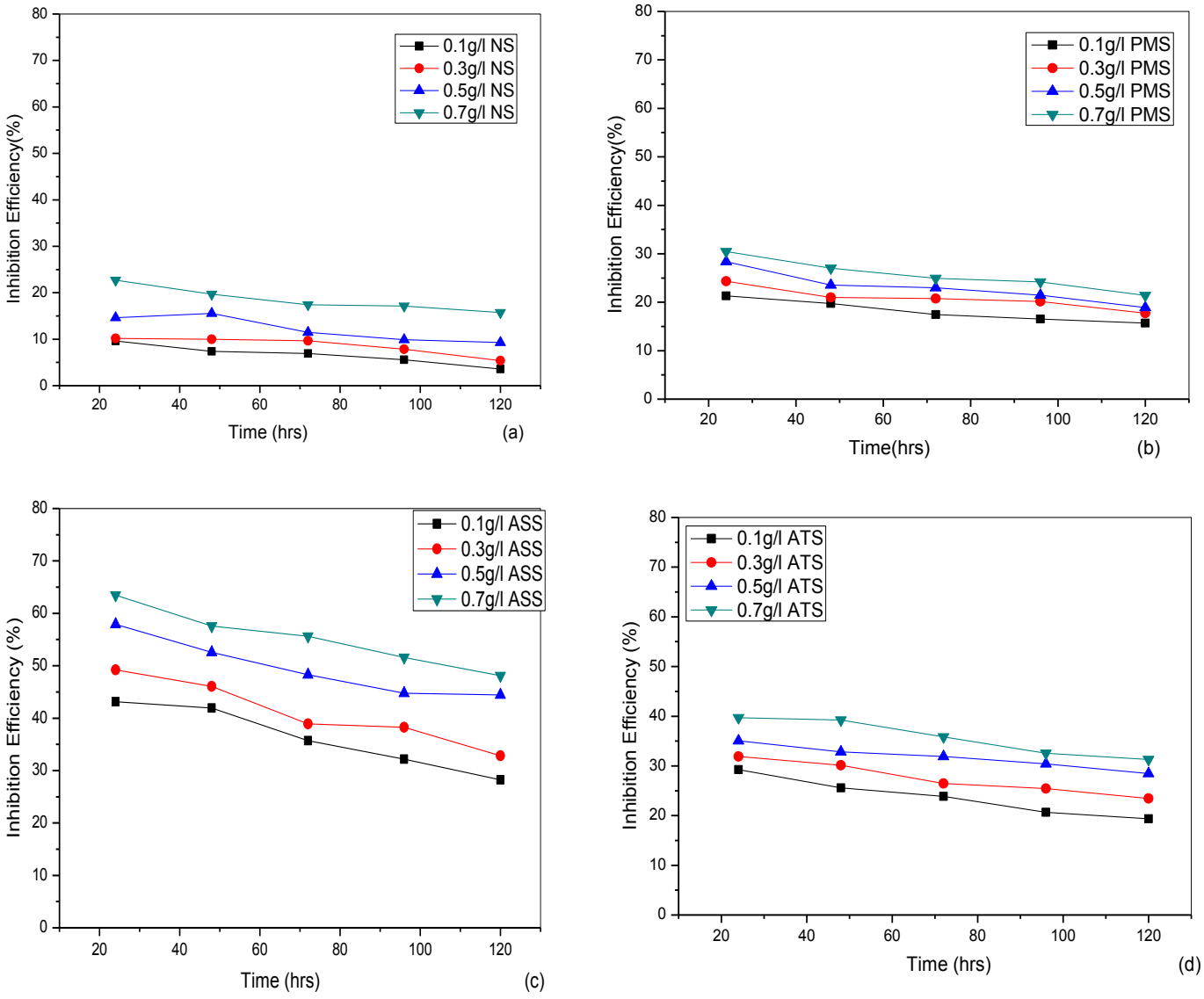

Figure 4.9: *Plots of Inhibition Efficiency against Time for galvanised steel in 0.25M H_2SO_4 in the presence and absence of (a)Natural Starch, (b)Physically modified starch, (c)Alkaline steeped starch and (d) Acid Treated starch*

Table 4.4 Calculated values of Corrosion rate, Inhibition efficiency and degree of surface coverage of galvanised steel in 0.25M H_2SO_4 in the presence and absence of NS, PMS, ASS and ATS corrosion under aerated condition

	Corrosion Rate (mmy^{-1})					Inhibition Efficiency (%)					Degree of Surface Coverage(**Θ**)				
Time	24 h	48 h	72 h	96 h	120 h	24 h	48 h	72 h	96 h	120 h	24 h	48 h	72 h	96 h	120 h
InhibitorConc															
Blank	**54.95**	**47.49**	**34.47**	**25.02**	**22.03**	-	-	-	-	-	-	-	-	--	-
0.1g/l NS	**50.67**	**43.98**	**32.09**	**23.62**	**21.24**	**07.79**	**7.39**	**6.90**	**5.59**	**3.59**	**0.0779**	**0.0739**	**0.0690**	**0.0559**	**0.0359**
0.3g/l NS	**48.35**	**42.75**	**31.14**	**23.06**	**20.84**	**12.01**	**9.98**	**9.66**	**7.83**	**5.40**	**0.12.01**	**0.0998**	**0.0966**	**0.0783**	**0.0540**
0.5g/l NS	**44.17**	**40.11**	**30.51**	**22.54**	**19.98**	**19.62**	**15.54**	**11.49**	**9.91**	**9.30**	**0.1962**	**0.1554**	**0.1149**	**0.0991**	**0.9300**
0.7g/l NS	**41.47**	**38.14**	**28.47**	**20.91**	**18.56**	**24.53**	**19.69**	**17.41**	**17.11**	**15.75**	**0.2453**	**0.1969**	**0.1741**	**0.1711**	**0.1575**
0.1g/l MS	**48.24**	**41.13**	**31.05**	**22.89**	**20.57**	**12.21**	**11.29**	**09.92**	**08.51**	**06.63**	**0.1221**	**0.1129**	**0.0992**	**0.0851**	**0.0663**
0.3g/l PMS	**44.58**	**39.53**	**29.32**	**21.98**	**19.42**	**18.87**	**16.76**	**14.94**	**12.15**	**11.85**	**0.1887**	**0.1676**	**0.1494**	**0.1215**	**0.1185**
0.5g/l PMS	**41.36**	**36.32**	**26.54**	**19.65**	**17.86**	**24.73**	**23.52**	**23.00**	**21.46**	**18.88**	**0.2473**	**0.2352**	**0.2300**	**0.2146**	**0.1888**
0.7g/l PMS	**38.22**	**34.65**	**25.87**	**18.97**	**17.31**	**30.45**	**27.04**	**24.95**	**24.18**	**21.42**	**0.3045**	**0.2704**	**0.2495**	**0.2418**	**0.2142**
0.1g/l ASS	**31.32**	**27.51**	**22.16**	**16.97**	**15.80**	**43.13**	**41.92**	**35.71**	**32.17**	**28.25**	**0.4313**	**0.4192**	**0.3571**	**0.3217**	**0.2825**
0.3g/l ASS	**27.91**	**25.62**	**21.06**	**15.45**	**14.85**	**49.21**	**46.05**	**38.90**	**38.25**	**32.82**	**0.4921**	**0.4605**	**0.3890**	**0.3825**	**0.3282**
0.5g/l ASS	**23.14**	**22.54**	**17.82**	**13.82**	**12.24**	**57.88**	**52.54**	**48.30**	**44.76**	**44.44**	**0.5788**	**0.5254**	**0.4830**	**0.4476**	**0.4444**
0.7g/l ASS	**20.07**	**20.14**	**15.29**	**12.11**	**11.43**	**63.48**	**57.59**	**55.64**	**51.60**	**48.12**	**0.6348**	**0.5759**	**0.5564**	**0.5160**	**0.4812**
0.1g/l ATS	**39.87**	**35.34**	**26.24**	**19.85**	**17.76**	**27.44**	**25.58**	**23.88**	**20.66**	**19.38**	**0.2744**	**0.2558**	**0.2388**	**0.2066**	**0.1938**
0.3g/l ATS	**37.43**	**33.18**	**25.35**	**18.65**	**16.86**	**31.88**	**30.13**	**26.48**	**25.46**	**23.47**	**0.3188**	**0.3013**	**0.2648**	**0.2546**	**0.2347**
0.5g/l ATS	**35.69**	**31.89**	**23.47**	**17.41**	**15.76**	**35.05**	**32.84**	**31.92**	**30.42**	**28.46**	**0.3505**	**0.3284**	**0.3192**	**0.3042**	**0.2846**
0.7g/l ATS	**30.13**	**28.85**	**22.12**	**16.88**	**15.14**	**45.17**	**39.25**	**35.83**	**32.53**	**31.28**	**0.4517**	**0.3925**	**0.3583**	**0.3253**	**0.3128**

4.2.2.2 Corrosion of Galvanised Steel in 1 M HCL

The calculated values of corrosion rate, inhibition efficiency, and degree of surface coverage for the corrosion of galvanised steel in 1 M HCL in the presence and absence of the four inhibitors is presented in Table 4.5. The corrosion rate data are illustrated graphically in Figures 4.10a to d. From graphical illustration, the corrosion rate of galvanised steel decreased with increase in the inhibitor concentration for all the four inhibitors. ASS exhibited the least corrosion rate at inhibitor concentration of 0.7g/l

Generally, the corrosion rate of galvanised steel with and without the four inhibitors decreased with increase in time of immersion following the trend ASS<ATS<PMS<NS.

The plots of the inhibition efficiency of the corrosion of galvanised steel in 1M HCl is presented in Figures 4.11 a to d. Close Inspection of the plots shows that increase in inhibitor concentration increased inhibition efficiency with ASS exhibiting the highest inhibition efficiency of 52.65% at 0.7g/l after 24 hours immersion in the acid inhibitor system. However, the inhibition efficiency for the four inhibitors decreased with increasing time of immersion at all concentration.

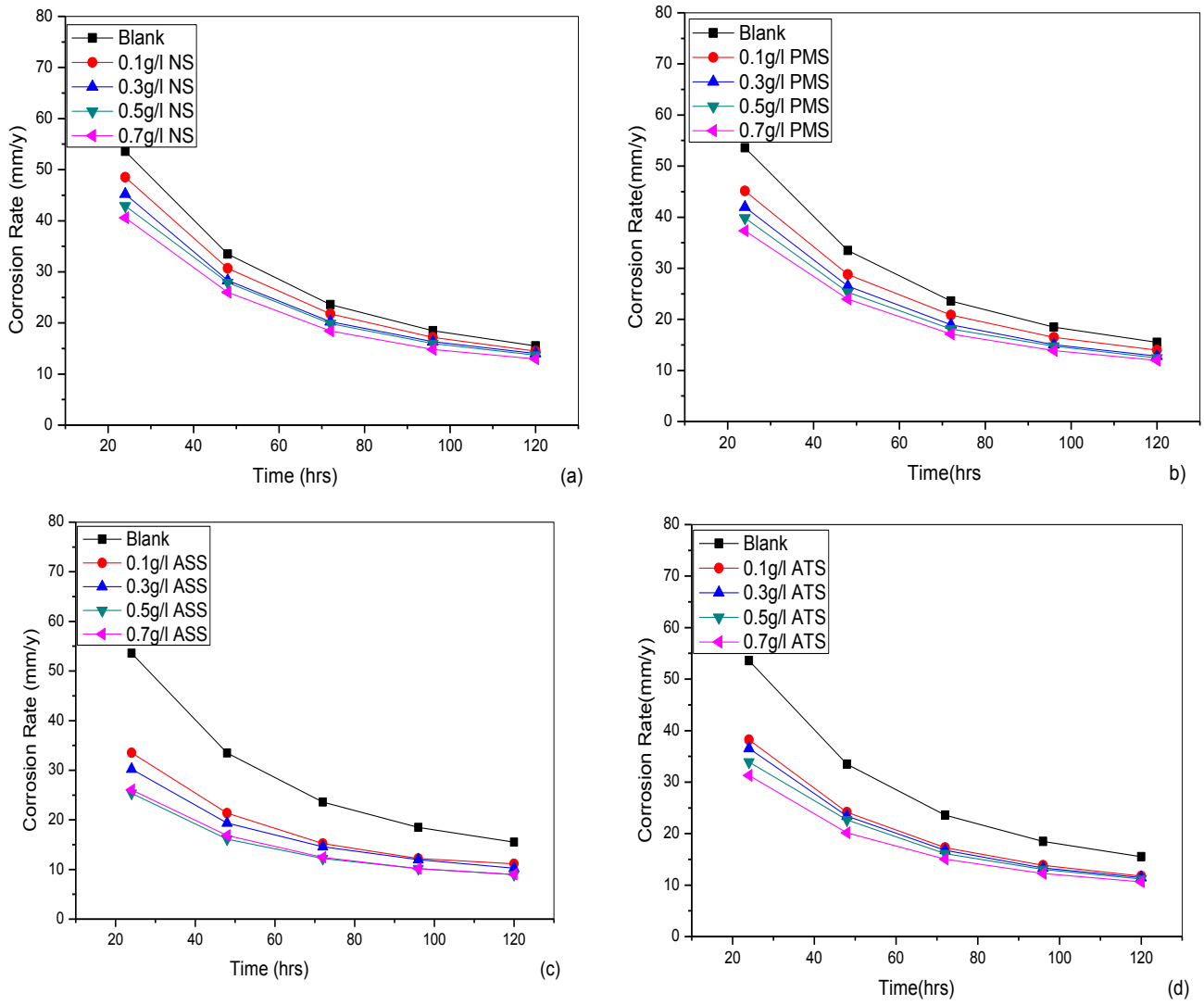

Figure 4.10: *Plots of Corrosion rate against Time for galvanised steel in 1M HCL in the presence and absence of (a)Natural Starch, (b)Physically modified starch, (c)Alkaline steeped starch and (d) Acid Treated starch under aerated conditions.*

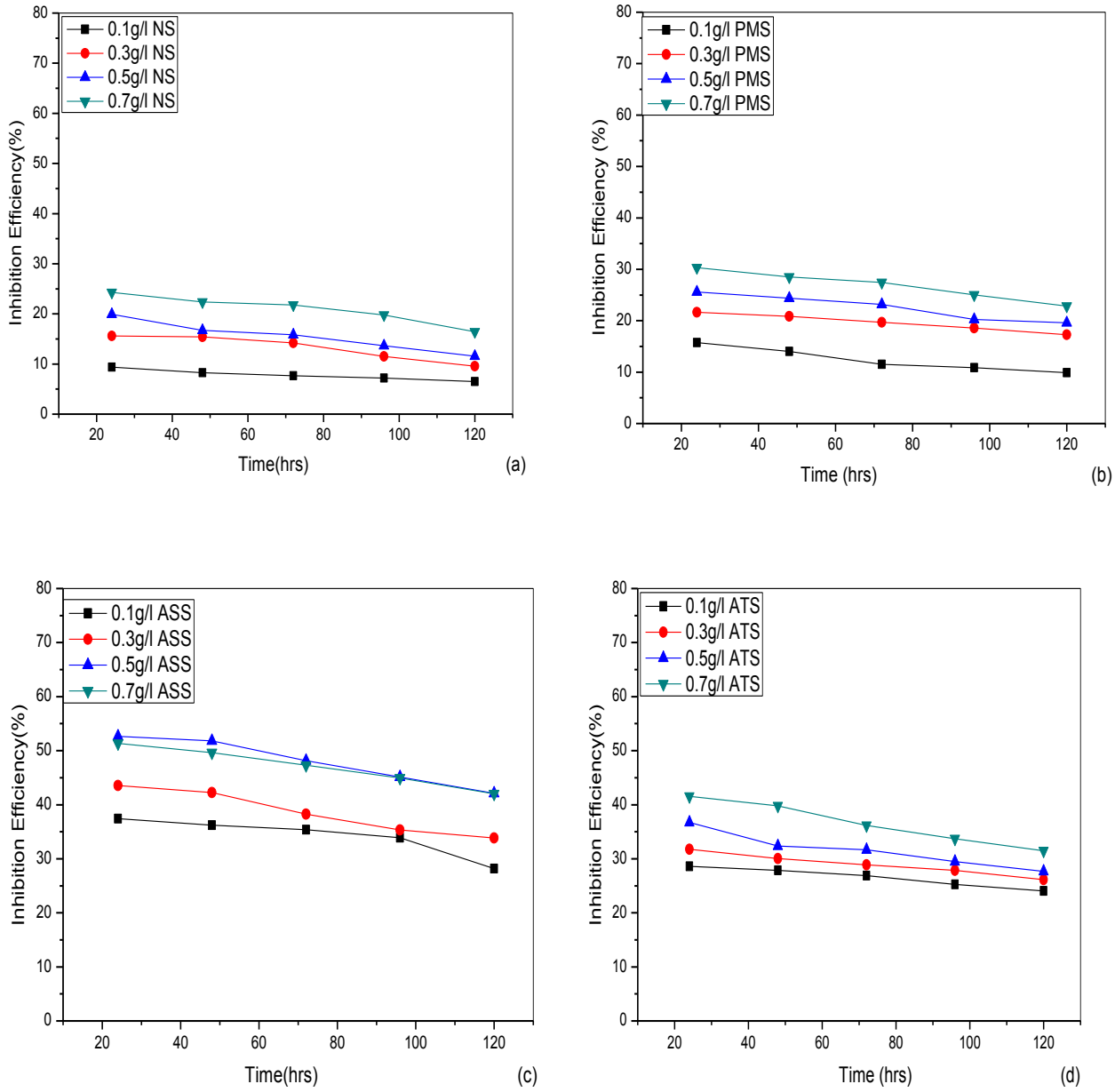

Figure 4.11: *Plots of Inhibition Efficiency against Time for galvanised steel in 1M HCL in the presence and absence of (a)Natural Starch, (b)Physically modified starch, (c)Alkaline steeped starch and (d) Acid Treated starch under aerated conditions.*

Table4.5: Calculated values of Corrosion rate, Inhibition efficiency and degree of surface coverage of galvanised steel in 1 M HCl in the presence and absence of NS, PMS, ASS and ATS corrosion inhibitors under aerated conditions

	Corrosion Rate (mmy^{-1})					Inhibition Efficiency(%)					Degree of Surface Coverage(**Θ**)				
Time	24 h	48 h	72 h	96 h	120 h	24 h	48 h	72 h	96 h	120 h	24 h	48 h	72 h	96 h	120 h
Inh. Conc															
Blank	**53.56**	**33.48**	**23.59**	**18.49**	**15.50**										
0.1g/l NS	**48.54**	**30.71**	**21.78**	**17.16**	**14.49**	**9.37**	**8.27**	**7.67**	**7.19**	**6.52**	**0.0937**	**0.0827**	**0.0767**	**0.0719**	**0.0652**
0.3g/l NS	**45.21**	**28.32**	**20.24**	**16.36**	**14.02**	**15.59**	**15.41**	**14.20**	**11.52**	**9.55**	**0.1559**	**0.1541**	**0.1420**	**0.1152**	**0.0955**
0.5g/l NS	**42.89**	**27.89**	**19.86**	**15.97**	**13.71**	**19.92**	**16.70**	**15.81**	**13.63**	**11.55**	**0.1992**	**0.1670**	**0.1581**	**0.1363**	**0.1155**
0.7g/l NS	**40.56**	**25.98**	**18.45**	**14.83**	**12.95**	**24.27**	**22.40**	**21.79**	**19.79**	**16.45**	**0.2427**	**0.2240**	**0.2179**	**0.1979**	**0.1645**
0.1g/l PMS	**45.12**	**28.79**	**20.87**	**16.48**	**13.97**	**15.75**	**14.00**	**11.53**	**10.87**	**9.87**	**0.1575**	**0.1400**	**0.1153**	**0.1087**	**0.0987**
0.3g/l PMS	**41.98**	**26.50**	**18.95**	**15.06**	**12.82**	**21.62**	**20.84**	**19.67**	**18.55**	**17.29**	**0.2162**	**0.2084**	**0.1967**	**0.1855**	**0.1729**
0.5g/l PMS	**39.86**	**25.32**	**18.12**	**14.75**	**12.46**	**25.58**	**24.37**	**23.19**	**20.23**	**19.61**	**0.2558**	**0.2437**	**0.2319**	**0.2023**	**0.1961**
0.7g/l PMS	**37.32**	**23.94**	**17.12**	**13.86**	**11.96**	**30.32**	**28.49**	**27.43**	**25.04**	**22.84**	**0.3032**	**0.2849**	**0.2743**	**0.2504**	**0.2284**
0.1g/l ASS	**33.52**	**21.35**	**15.24**	**12.22**	**11.13**	**37.42**	**36.23**	**35.40**	**33.91**	**28.19**	**0.3742**	**0.3623**	**0.3540**	**0.3391**	**0.2819**
0.3g/l ASS	**30.24**	**19.34**	**14.56**	**11.96**	**10.25**	**43.54**	**42.23**	**38.28**	**35.32**	**33.87**	**0.4354**	**0.4223**	**0.3828**	**0.3532**	**0.3387**
0.5g/l ASS	**25.36**	**16.13**	**12.23**	**10.15**	**8.97**	**52.65**	**51.82**	**48.16**	**45.11**	**42.13**	**0.5265**	**0.5182**	**0.4816**	**0.4511**	**0.4213**
0.7g/l ASS	**26.06**	**16.86**	**12.43**	**10.18**	**8.99**	**51.34**	**49.64**	**47.30**	**44.94**	**42.00**	**0.5134**	**0.4964**	**0.4730**	**0.4494**	**0.4200**
0.1g/l ATS	**38.23**	**24.16**	**17.25**	**13.82**	**11.77**	**28.62**	**27.84**	**26.88**	**25.26**	**24.06**	**0.2862**	**0.2784**	**0.2688**	**0.2526**	**0.2406**
0.3g/l ATS	**36.56**	**23.42**	**16.78**	**13.34**	**11.45**	**31.74**	**30.04**	**28.87**	**27.85**	**26.13**	**0.3174**	**0.3004**	**0.2887**	**0.2785**	**0.2613**
0.5g/l ATS	**33.89**	**22.65**	**16.12**	**13.05**	**11.21**	**36.73**	**32.35**	**31.67**	**29.48**	**27.68**	**0.3673**	**0.3235**	**0.3167**	**0.2948**	**0.2768**
0.7g/l ATS	**31.31**	**20.16**	**15.06**	**12.26**	**10.62**	**41.54**	**39.78**	**36.16**	**33.69**	**31.48**	**0.4154**	**0.3978**	**0.3616**	**0.3369**	**0.3148**

4.2.2.3 Effect of Inhibitor Concentration.

The effect of inhibitor concentration on the inhibition efficiency of the starch samples on galvanised steel in 0.25 M H_2SO_4 and 1 M HCl are presented in Figure 4.11a to d. The NS, PMS, ATS and ASS samples exhibited maximum inhibition efficiencies of 24.53%, 30.45%, 63.48% and 45.17% respectively in 0.25 M H_2SO_4 at an optimum concentration of 0.7g/l, while in 1M HCl acidic media the NS, PMS and ASS samples exhibited maximum inhibition efficiencies of 24.27%, 30.32% and 41.54% at an optimum concentration of 0.7g/l. The increased IE with increasing inhibitor concentration for inhibitors NS, PMS, ASS and ATS in 0.25 M H_2SO_4 as well as NS, PMS and ATS in 1M HCl indicates increase in adsorption of the starch molecules onto the surface of the metal. ASS exhibited a maximum inhibition efficiency of 52.65% in 1M HCl at a concentration of 0.5g/l and further increase in concentration did not result in any significant change in the performance of the starch sample. The results obtained were in agreement with works done by other authors (Mobin *et al.*; 2011, Ochoa *et al.*; 2013, Bello *et al.*; 2010 and Rosliza and Nik; 2010).

4.2.2.4 Effect of Immersion Time

In order to assess the stability of inhibitive behaviour of the starch samples on a time scale, weight loss measurements were performed in 0.25 M H_2SO_4 and 1M HCl, in the absence and presence of the starch samples at various concentrations for 24 to 120 h immersion time at room temperature. The calculated inhibition

efficiency values were plotted against immersion time as presented in Figure 4.11a to d. The inhibition efficiency of the four starch samples followed the same trend, decreasing with increasing immersion time from 24 to 120 h. Decrease in the inhibition efficiency with increasing time suggests possible desorption of some of the adsorbed starch molecules from the metal surface at longer periods. This behaviour shows that the starch was physically adsorbed on the metal surface Oguzie (2004). This trend was observed by Ochoa *et al.* (2013) in the use of caboxymethylated starch as corrosion inhibitor for carbon steel XC35 in a 200 mgL^{-1} NaCl solution, they observed that after 24 h, inhibition efficacy of the modified starch decreased.

4.2.2.5 Effect of Acid

The variation of inhibition efficiency in 0.25 M H_2SO_4 and 1 M HCl acid is presented in Tables 4.4 and 4.5. As observed in the data in given, the corrosion rates of the coupons immersed in the starches / 0.25 M H_2SO_4 system were higher than that in the starch/ 1 M HCl system which in turn affected their inhibition efficiencies in like manner as observed. This could be attributed to the fact that sulphuric acid is dibasic which makes it more aggressive and on the other hand hydrochloric acid dissociates in water and the Cl^- acts as a precursor to corrosion inhibition.

4.3 Synergism Considerations (Effect of Halides)

Synergism is an effective method used to improve inhibitive performance, reduce inhibitor content and to diversify the application of the inhibitor in corrosive media. The use of halides has been employed in the study of synergism (Feng *et al*.; 1999, Larabi *et al*.; 2004, Okafor and Zheng; 2009, Umoren *et al*.; 2006). Corrosion inhibition synergism is attributed to the stabilization of adsorbed halide ions by means of electrostatic interaction with the inhibitor which leads to greater surface coverage and greater inhibition. In addition the increased inhibition efficiency due to the synergistic use of KI can be ascribed to the formation of intermediate bridges or complex between the metal surface and the positive end of the inhibitor. It is noteworthy that halide ions when present in the test solutions have the tendency to be specifically adsorbed on metal surfaces, where they facilitate adsorption of protonated inhibitor species by forming intermediate bridges between the metal surfaces and the inhibitor (Oguzie 2004). The effect of potassium iodide (KI) on the corrosion rate and inhibition efficiency for the four inhibitors studied were calculated from the gravimetric data under ambient conditions for 120 hours, and the results are presented in Tables 4.6 and 4.7 for mild steel and galvanised steel respectively.

From the result obtained for mild steel corrosion, the inhibition efficiency of 0.4g/l halide alone in sulphuric acid media, increased with increase in time and this is attributed to the inhibitive effect of I^- (iodine ion). The inhibition efficiency

of NS and ATS in combination with 0.4g/l KI exhibited the same trend, increasing with increase in time upto 72 hrs after which the inhibition efficiency decreased with increase in time. Maximum inhibition efficiency obtained by NS and ATS in the absence of KI are 24.75% and 39.56 % respectively as presented in Table 4.2, but in synergy with KI 85.59 % and 87.72 % respectively. The inhibition efficiency of ASS in combination with KI increased with increase in time up to 96 hours at 83.64 % after which it followed a downward trend. The inhibition efficiency of PMS in combination with KI followed an upward trend of increasing with increase in time, its maximum efficiency was 85.05 %.

For galvanised steel, PMS and ATS in synergy with 0.4g/l KI increased with increase in time up to 48 hours after which it followed a downward trend. Maximum inhibition efficiency obtained was 95.62 % and 93.94 % respectively. NS in synergy with KI increased in efficiency with maximum efficiency of 92.60 %, while the inhibition efficiency of ASS in synergy with KI decreased with increase in time exhibiting a maximum inhibition efficiency of 93.67 %.

The synergistic inhibition brought about by the combination of each of the four corrosion inhibitors (NS, PMS, ASS, ATS) with iodide ions for the corrosion of mild steel and galvanised steel in 0.25 M H_2SO_4 can be explained on the basis that halide ions have a greater tendency to be adsorbed on the surface in attraction with organic cations. The protonated inhibitor is then adsorbed by coulombic attraction at the steel surface, where iodide ions are already adsorbed by

chemisorptions. Greater surface coverage from the stabilization of adsorbed iodide ions by means of electrostatic interaction with protonated inhibitor facilitates corrosion inhibition synergism. I^- alone polarizes both the anodic and cathodic reaction of iron over a wide potential range. It is apparent then that the effects of I^- are not due to electrostatic effects alone, but some covalent bonding to the metal must be involved. The large size and ease of polarizability of I^- facilitates electron pair bonding. The halide ions are first adsorbed on the metal surface and the inhibitor is then drawn in to the double layer by the adsorbed halide ion, such that the ion pair formation occurs directly on the metal surface:

$$A_s \rightarrow A_{ads} \quad (4.1)$$

$$C_s + A_{ads} \rightarrow (CA)_{ads} \quad (4.2)$$

Where C_s and A_s represent inhibitor and halide ion respectively, in the bulk solution, while A_{ads} and CA_{ads} refers to halide ion and ion-pair, respectively, in the adsorbed state.

In the case where the corrosion inhibitor exist as molecular specie, antagonistic behaviour prevails which may be attributed to competitive adsorption.

Mobin and Parveen (2011) who carried out weight loss tests on mild steel in 0.1 M H_2SO_4 in presence of starch observed that starch inhibits the corrosion rates of mild steel to a considerable extent; the maximum inhibition efficiency (%IE) they obtained 66.21% at 30^{o}C in presence of starch concentration of 200 ppm. The

effect of the addition of very small concentration of sodium dodecyl sulfate and cetyl trimethyl ammonium bromide on the corrosion inhibition behaviour of starch was also studied. The IE of starch significantly improved in presence of both the surfactants. The effect of surfactants on the corrosion inhibition behavior of starch was synergistic with maximum IE of 69.43% for SDS and 70.28% for CTAB. Results obtained were in agreement with the result obtained by .Parveen and Mobin (2013), and Umoren and Solomon (2010).

Table 4.6: Calculated Values of Corrosion Rate (mm/y), Inhibition Efficiency (%IE) and Degree of Surface Coverage(Ɵ) for Mild Steel in 0.25 M H_2SO_4 in the Absence and Presence of Unmodified and Modified Starch Samples with Pottasium Iodide (KI) from Gravimetric Studies

	Corrosion Rate(mmy^{-1})					Inhibition Efficiency(%)					Degree of Surface Coverage(Ɵ)				
Time	24 h	48 h	72 h	96 h	120 h	24 h	48 h	72 h	96 h	120 h	24 h	48 h	72 h	96 h	120 h
Inh. Conc															
Blank	50.43	31.31	24.02	18.46	14.08	---	-	-	-	-	-	-	=	-	-
Blank +KI	31.16	16.32	11.21	8.16	6.73	38.21	47.88	53.33	55.8	52.20	0.3821	0.4788	0.5333	0.558	0.5220
0.7g/l NS+KI	10.14	5.83	3.46	2.92	2.38	79.89	81.38	85.59	84.18	83.09	0.7989	0.8138	0.8559	0.8418	0.8309
0.7g/l PMS+KI	8.65	5.13	3.67	2.76	2.10	82.85	83.62	84.72	85.05	85.09	0.8285	0.8362	0.8472	0.8505	0.8509
0.7g/l ASS+KI	8.47	5.90	4.02	3.02	2.36	83.20	83.22	83.26	83.64	83.24	0.8320	0.8322	0.8326	0.8364	0.8324
0.7g/l ATS+KI	8.34	4.43	2.95	2.35	2.03	83.46	85.85	87.72	87.27	85.58	0.8346	0.8585	0.8772	0.8727	0.8558

Table 4.7: Calculated Values of Corrosion Rate (mm/y), Inhibition Efficiency (%IE) and Degree of Surface Coverage(Ɵ) for Galvanised Steel in 0.25 M H_2SO_4 in the Absence and Presence of Unmodified and Modified Starch Samples with Pottasium Iodide (KI) from Gravimetric Studies

	Corrosion Rate(mmy^{-1})					Inhibition Efficiency(%)					Degree of Surface Coverage(Ɵ)				
Time	24 h	48 h	72 h	96 h	120 h	24 h	48 h	72 h	96 h	120 h	24h	48 h	72 h	96 h	120 h
InhibitorConc															
Blank	54.95	47.49	34.47	25.02	22.03	-	-	-	-	-	-	-	-	-	-
Blank +KI	39.29	32.28	23.62	16.63	13.96	28.50	32.03	31.48	33.53	36.31	0.2850	0.3203	0.3148	0.3353	0.3631
0.7g/l NS+KI	2.83	5.66	2.83	2.03	1.63	84.85	88.08	91.79	91.88	92.60	0.8485	0.8808	0.9179	0.9188	0.9260
0.7g/l PMS+KI	3.47	2.08	1.74	1.30	1.18	93.69	95.62	94.95	94.80	94.64	0.9369	0.9562	0.9495	0.9480	0.9464
0.7g/l ASS+KI	3.48	4.18	4.06	3.39	2.99	93.67	91.20	88.22	86.45	86.42	0.9367	0.9120	0.8822	0.8645	0.8642
0.7g/l ATS+KI	4.75	2.88	2.15	1.61	1.49	91.36	93.94	93.76	93.57	93.24	0.9136	0.9394	0.9509	0.9357	0.9324

4.4 Potentiodynamic Polarization Measurements

4.4.1 Mild Steel Corrosion

The kinetics of the anodic and cathodic reactions occurring on mild steel electrodes in 0.25 M H_2SO_4 solutions in the presence of the four inhibitors (NS, PMS, ASS, ATS) with and without KI was studied using polarization measurements. The potentiodynamic polarization curves for the corrosion of mild steel in 0.25 M H_2SO_4 in the absence and presence of varying concentration of the four inhibitors (NS, PMS, ASS, ATS) and the inhibitors in combination with 0.4g/l of KI are presented in Figures 4.12 to 4.15. The values of electrochemical parameters as deduced from these curves, e.g., corrosion potential (Ecorr) corrosion current density (Icorr) and Inhibition efficiency are presented in Table 4.8.

The IE was calculated from the measured Icorr values using the relationship:

$$\%IE = \frac{i^o_{corr} - i_{corr}}{i^o_{corr}} \times 100 \qquad (4.9)$$

where, i^o_{corr} is corrosion current density in the absence of inhibitor and i_{corr} is corrosion current density in the presence of inhibitor.

The plots for NS is presented Figure 4.12, from the plots we observe that the anodic and cathodic reactions in blank acid follow Tafel's law. The inhibited solution containing 0.1g/l NS shifted the Ecorr slightly to the cathodic direction with the cathodic and anodic branches shifted to lower values of corrosion

current. The solution containing 0.7g/l of NS shifted the E_{corr} slightly further to the cathodic direction with its anodic branch slightly higher than that of the blank's Ecorr and the cathodic branch lower. This shows that NS exhibited both cathodic and anodic inhibition effect. On the other hand, the inhibited solution containing 0.7g/l +0.4g/l KI shifted the Ecorr in the anodic direction and a high inhibiting effect is observed on the anodic reaction while cathodic effect was not notably affected.

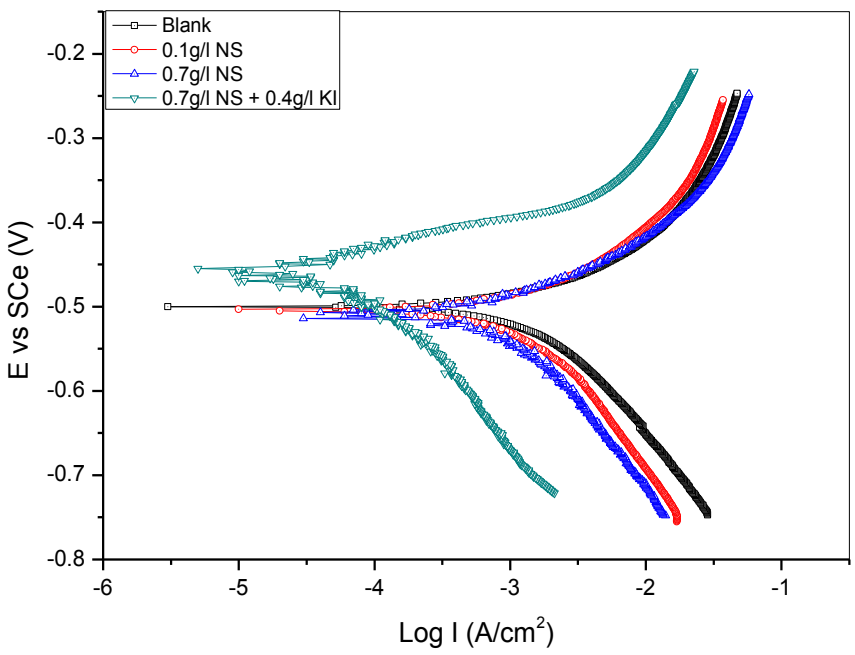

Figure 4.12: *Polarization Curves for mild steel corrosion in 0.25M H_2SO_4 using NS in the absence and presence of KI*

Figure 4.13 shows the anodic and cathodic polarization curves of mild steel dissolution in 0.25M H_2SO_4 in the presence of PMS with and without KI. Ecorr of solutions with only the PMS inhibitor was slightly lower both at the cathodic and anodic branches. The Ecorr of the 0.7g/l +0.4g/l KI was shifted towards the anodic direction with a profound lower cathodic branch.

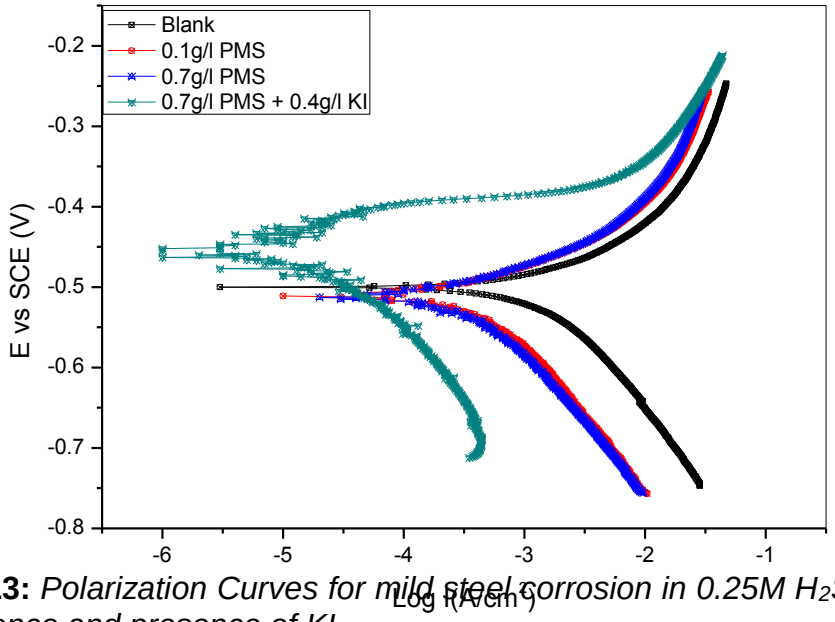

Figure 4.13: *Polarization Curves for mild steel corrosion in 0.25M H_2SO_4 using PMS in the absence and presence of KI*

Figure 4.14 represents the potentiodynamic polarization curves for the corrosion of mild steel in 0.25M H_2SO_4 in the presence of ASS with and without KI. The Ecorr of the solutions containing both 0.1g/l and 0.7g/l of ASS shifted slightly towards the cathodic direction with their cathodic branches profoundly lower indicating lower values of corrosion current. The Ecorr of the 0.7g/l +0.4g/l KI shifted towards the anodic direction.

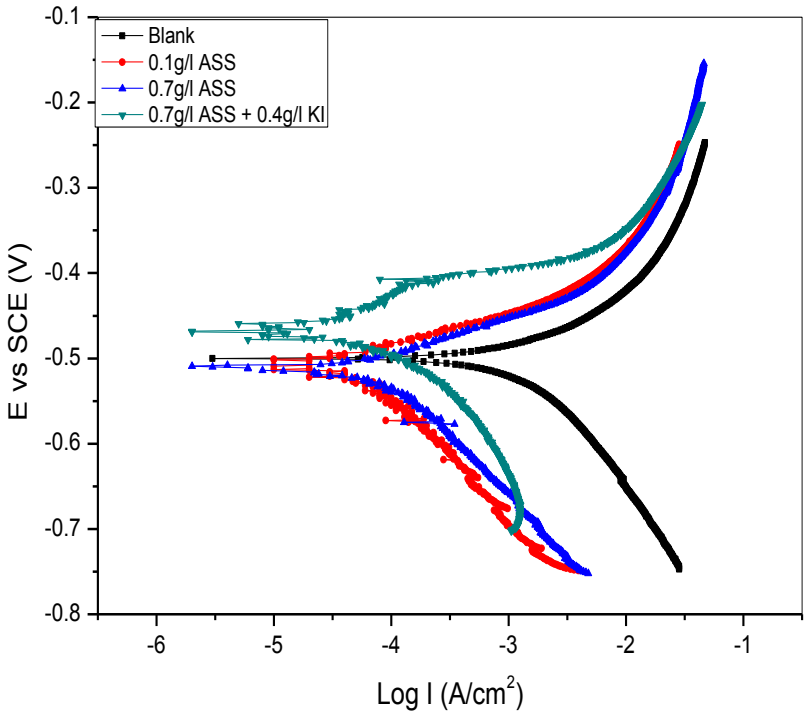

Figure 4.14: *Polarization Curves for mild steel corrosion in 0.25M H_2SO_4 using ASS in the absence and presence of KI*

Figure 4.15 represents the potentiodynamic polarization curves for the corrosion of mild steel in 0.25M H_2SO_4 in the presence of ATS with and without KI. The Ecorr of the solutions containing both 0.1g/l slightly shifts towards the cathodic directions with its branches lower while the Ecorr of solutions containing 0.7g/l of ASS shifted slightly towards the anodic direction with both branches lower indicating lower values of corrosion current. The Ecorr of the 0.7g/l +0.4g/l KI shifted towards the anodic direction with its cathodic branch profoundly lower.

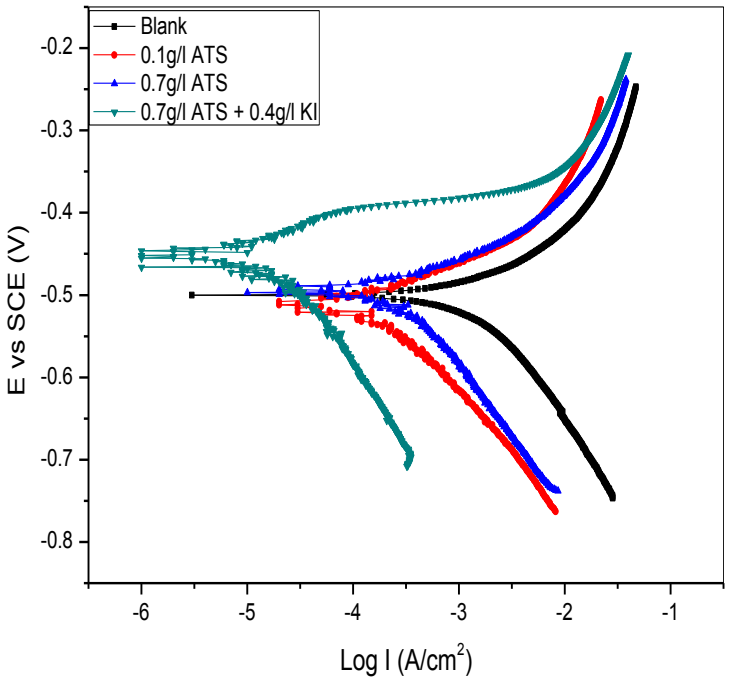

Figure 4.15: *Polarization Curves for mild steel corrosion in 0.25M H_2SO_4 using ATS in the absence and presence of KI*

Table 4.8 Potentiodynamic Polarization parameters for corrosion of mild steel in the presence and absence of the four inhibitors and KI

Inhibitor Concentration (g/l)	Ecorr(V/SCE)	Icorr(A/cm2)	Inhibition Efficiency(%)
Blank	500.05	2940	-
0.1g/l NS	504.00	1975	32.82
0.7g/l NS	508.79	1476	49.79
0.7g/l NS + 0.4g/l KI	457.89	69.57	97.63
0.1g/l PMS	510.29	745.3	74.65
0.7g/l PMS	512.70	720.5	75.49
0.7g/l PMS + 0.4g/l KI	454.54	131.9	95.51
0.1g/l ASS	505.70	216.7	92.62
0.7g/l ASS	509.49	103.9	96.47
0.7g/l ASS + 0.4g/l KI	467.55	46.48	98.42
0.1g/l ATS	510.67	286.4	90.26
0.7g/l ATS	495.60	259.4	91.17
0.7g/l ATS + 0.4g/l KI	449.02	8.57	99.70

4.4.2 Mild Steel Corrosion in 1 M HCl

Polarization curves for mild steel at various concentrations of the four starch samples in aerated solutions are shown in Figure 4.16 to 4.19. The extrapolation of Tafel straight line allows for the calculation of the corrosion current density (Icorr). The values of Icorr, the corrosion potential (Ecorr), and inhibition efficiency (IE %) are presented in Table 4.9

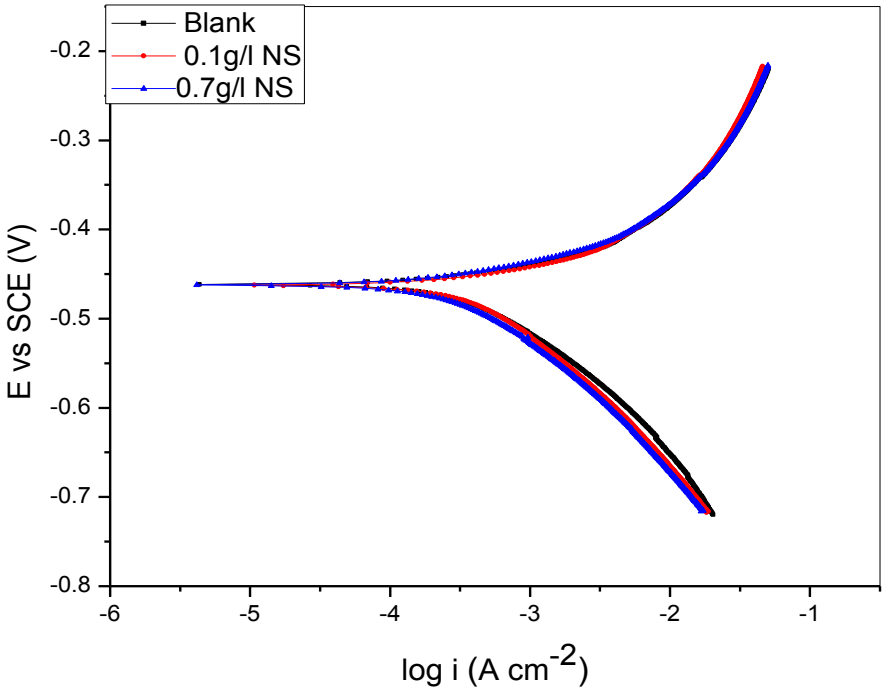

Figure 4.16: *Polarization Curves for mild steel corrosion in 1M HCL in the absence and presence of NS*

Figure 4.16 represents the graphical illustration of the inhibitory effect of NS on the corrosion of galvanised steel in 1 M HCl. The plots clearly show that, the addition of the unmodified starch sample shifts the corrosion potential (Ecorr) slightly in the positive direction and reduces both the anodic and cathodic current

densities slightly. The cathodic current, was however reduced more than the anodic current.

This means that the unmodified starch have slight effects on retarding the cathodic hydrogen evolution reaction and inhibiting the anodic dissolution of mild steel.

Figure 4.17 represents the polarisation curves for mild steel corrosion in the presence and absence of PMS. The curve clearly shows that, the addition of the PMS sample shifts the corrosion potential (Ecorr) slightly in the positive direction and reduces both the anodic and cathodic current densities. The anodic current, was however reduced more than the cathodic current.

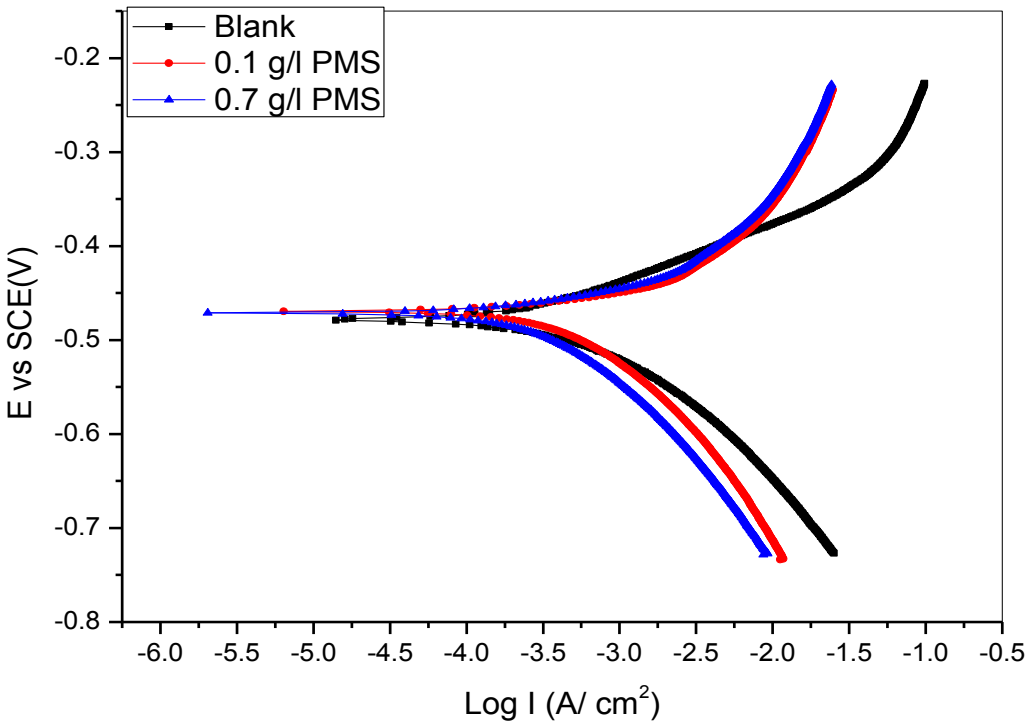

Figure 4.17 *Polarization Curves for mild steel corrosion in 1M HCL in the absence and presence of PMS*

The polarization curves for mild steel corrosion in 1M HCL in the absence and presence of ASS is presented in Figure 4.18. The curve clearly shows that, the addition of the ASS sample shifts the corrosion potential (Ecorr) slightly in the positive direction and reduces both the anodic and cathodic current densities significantly. The cathodic current, was however reduced more than the anodic current.

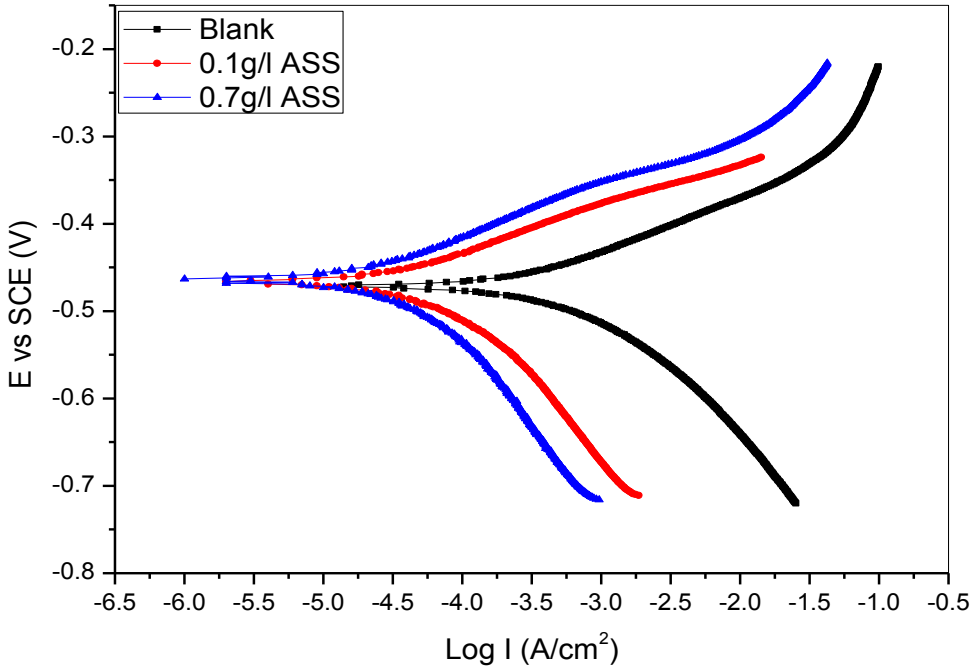

Figure 4.18 *Polarization Curves for mild steel corrosion in 1M HCL in the absence and presence of ASS*

The polarization curves for mild steel corrosion in 1 M HCL in the absence and presence of ATS is presented in Figure 4.19. Close study of the curve reveals that, the addition of the ATS sample shifts the corrosion potential (Ecorr) slightly to the positive direction and reduces both the anodic and cathodic current densities significantly with the cathodic current reduced more than the anodic current.

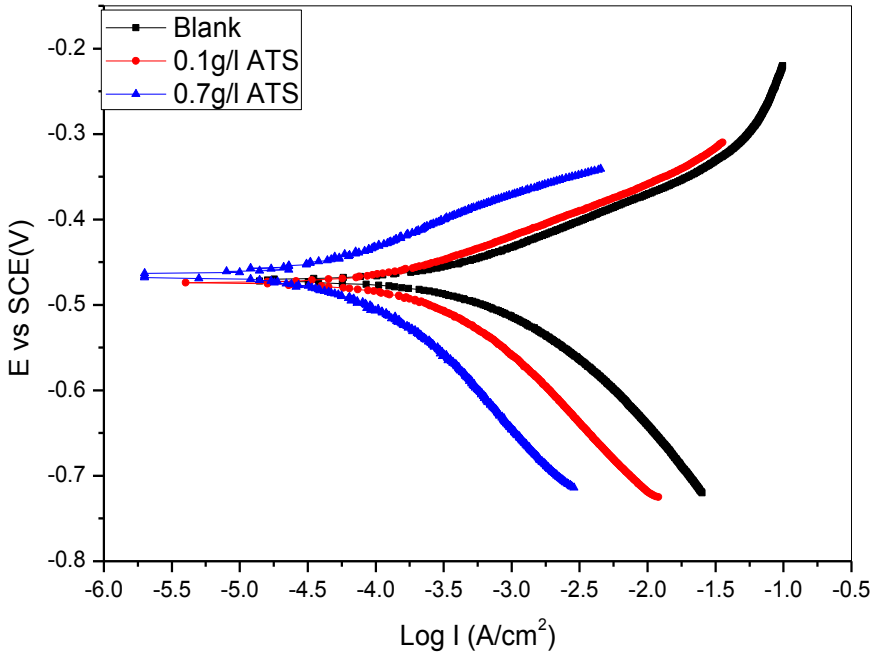

Figure 4.19: *Polarization Curves for mild steel corrosion in 1 M HCL using ATS in the absence and presence of ATS*

Table 4.9 Potentiodynamic Polarization parameters for corrosion of mild steel in 1 M HCl the presence and absence of the four inhibitors

Inhibitor Concentration (g/l)	Ecorr(V/SCE)	Icorr(A/cm2)	Inhibition Efficiency(%)

Blank	471.32	649.40	-
0.1g/l NS	475.00	459.12	29.30
0.7g/l NS	471.79	377.6	41.85
0.1g/l PMS	474.29	245.3	62.22
0.7g/l PMS	465.44	156.05	75.97
0.1g/l ASS	474.34	189.60	70.80
0.7g/l ASS	463.99	99.10	84.74
0.1g/l ATS	474.25	225.7	65.24
0.7g/l ATS	467.99	101.74	84.33

4.4.3 GALVANISED STEEL CORROSION

The potentiodynamic polarization curves for the corrosion of galvanised steel in 0.25 M H_2SO_4 in the absence and presence of varying concentration of the four inhibitors (NS, PMS, ASS, ATS) and the inhibitors in combination with 0.4g/l of KI are presented in Figures 4.20 to 4.23.

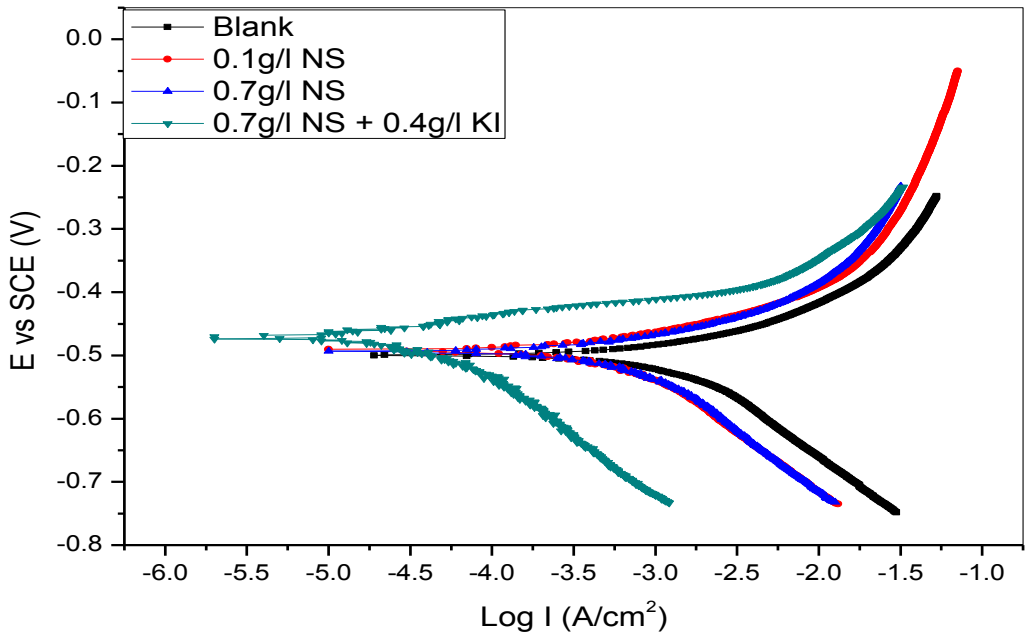

Figure 4.20: *Polarization Curves for galvanised steel corrosion in 0.25M H_2SO_4 using NS in the absence and presence of KI*

Figure 4.20 represents the potentiodynamic polarization curves for the corrosion of galvanised steel in 0.25 M H_2SO_4 in the presence of NS with and without KI. The Ecorr of the solution containing both 0.1g/l and 0.7g/l of NS slightly shifted towards the cathodic directions with both branches lower, exhibiting the character

of a mixed inhibitor. The Ecorr of the solution containing 0.7g/l +0.4g/l KI shifted towards the anodic direction with its cathodic branch profoundly lower.

Plots of the kinetics of anodic and cathodic reactions of PMS at varying concentrations with and without KI are presented in Figure 4.21. The plots reveals that the Ecorr of the three different solution shifted slightly towards the anodic direction with the 0.7g/l +KI shifted more towards the anodic direction and with both branches (anodic and cathodic) exhibiting lower Icorr values as indicated in the plot

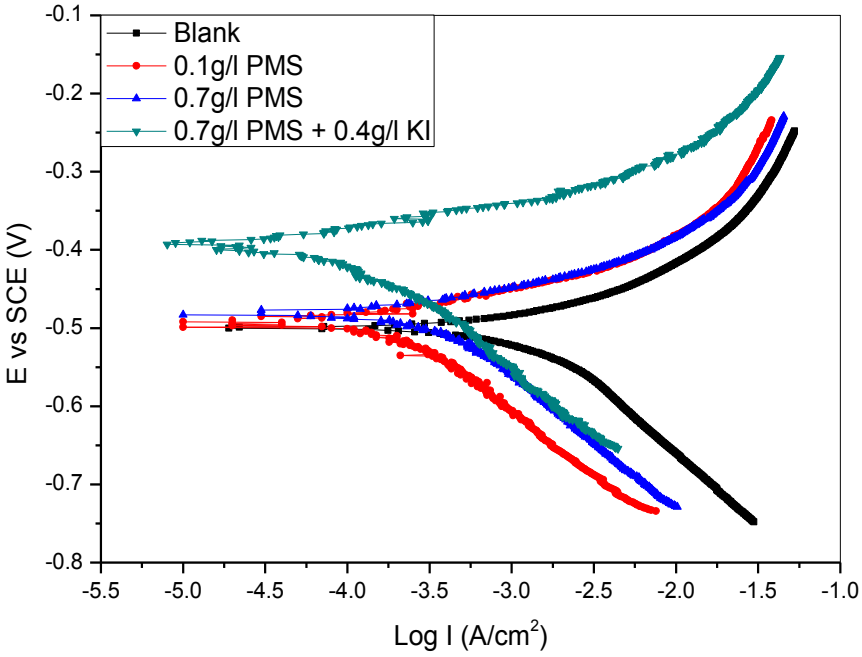

Figure 4.21: *Polarization Curves for galvanised steel corrosion in 0.25M H_2SO_4 using PMS in the absence and presence of KI*

Graphical Representation of the kinetics of anodic and cathodic reactions of ASS at varying concentration with and without KI is presented in Figure 4.22. The

plots reveals that the Ecorr of the three different solution shifted slightly towards the anodic direction with the 0.7g/l +KI more anodic and with both branches (anodic and cathodic) exhibiting lower Icorr values as indicated in the plot**.** However, it was observed that the 0.7g/l +KI was less anodic compared to NS, PMS and ATS with KI this corroborates the result obtained from the synergistic studies.

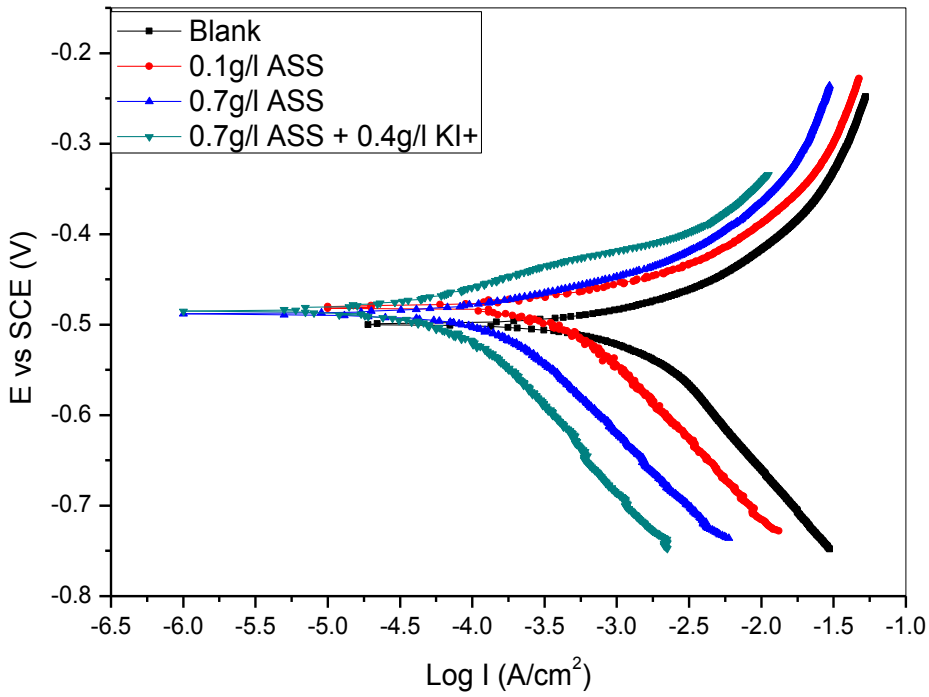

Figure 4.22: *Polarization Curves for galvanised steel corrosion in 0.25M H_2SO_4 using ASS in the absence and presence of KI*

Figure 4.23 presents the plots of the kinetics of the anodic and cathodic reactions of ATS at varying concentration with and without KI. Close observation of the plot reveals the slight shift of the Eccorr of 0.7g/l ATS+0.4g/l KI towards the

anodic direction with both branches exhibiting the lowest values of Icorr as indicated in the plot. Ecorr of 0.1g/l and 0.7g/l where slightly shifted towards the anodic directions.

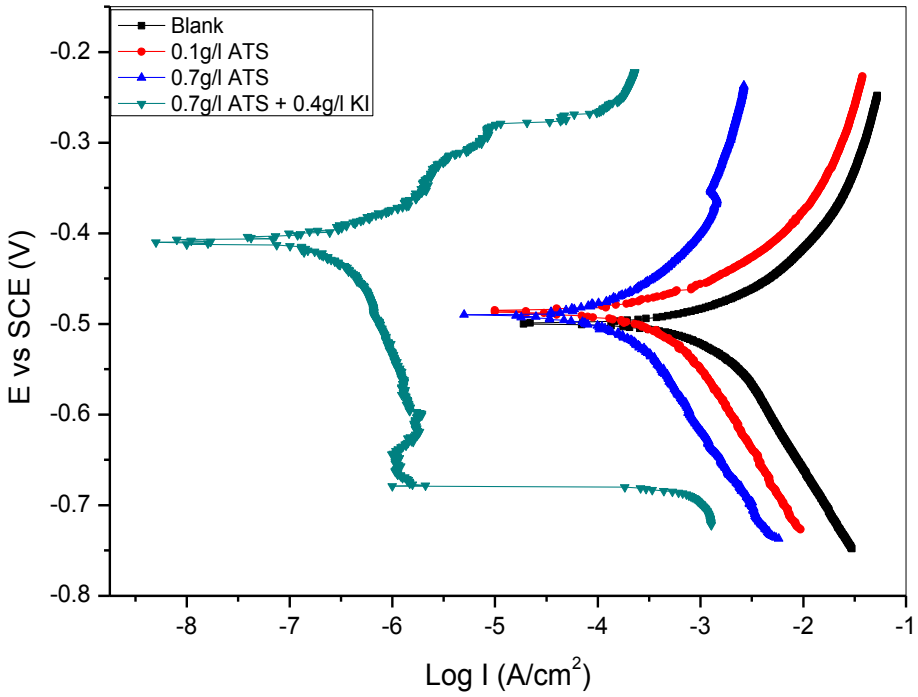

Figure 4.23: *Polarization Curves for galvanised steel corrosion in 0.25M H_2SO_4 using ASS in the absence and presence of KI*

Table 4.10 Potentiodynamic Polarization parameters for corrosion of galvanised steel in the presence and absence of the four inhibitors and KI

Inhibitor Concentration (g/l)	Ecorr(V/SCE)	Icorr(A/cm2)	Inhibition Efficiency %
Blank	499.61	2592	-

0.1g/l NS	492.00	1970	23.99
0.7g/l NS	493.48	1447	44.17
0.7g/l NS + 0.4g/l KI	471.23	42.05	98.38
0.1g/l PMS	491.41	357.5	86.21
0.7g/l PMS	481.58	304.5	88.25
0.7g/l PMS +0.4g/l KI	392.00	256.5	90.10
0.1g/l ASS	480.48	316.6	87.78
0.7g/l ASS	488.17	274.4	89.41
0.7g/l ASS + 0.4g/l KI	482.00	42.28	98.37
0.1g/l ATS	486.41	788.4	69.58
0.7g/l ATS	480.67	488.8	81.14
0.7g/l ATS + 0.4g/l KI	408.72	59.00	97.72

Potentiodynamic polarization curves obtained after immersion in the acid solution (0.25 M H_2SO_4 and 1 M HCl) containing NS, PMS, ASS and ATS at different concentrations and for both metals as presented in Figure 4.12 to 4.23 were compared with the current-voltage curve obtained without inhibitor. In the

presence of the inhibitors, it may be observed that the anodic and cathodic kinetics depend on inhibitor concentration. The anodic and the cathodic branches describe the iron dissolution and the oxygen reduction reaction, respectively. From the shape of the polarization curves (Fig. 4.20 To 4.31) it is obvious that both anodic and cathodic reactions are inhibited. Furthermore, the shape of the polarization curves suggests that both kinetics are under mixed control. The potentiodynamic polarization parameters summarized in Tables 4.8 to 4.10 show that the corrosion current density is markedly reduced as the concentration of inhibitor increases, which indicates that NS, PMS, ASS and ATS have pronounced corrosion inhibition effect on mild steel and galvanised steel in acidic media. It is evident from the data shown in Tables 4.8 to 4.10 that as the concentration of the inhibitor increases, the corrosion potential (*Ecorr*) is not changing significantly and lower corrosion current density (*Icorr*) values are obtained. The increase in inhibition efficiency due to the increase in concentration could be ascribed to the starch molecules, displacing water molecules originally adsorbed onto the mild steel surface. Also, Rosliza and Wan Nik (2013) observed that R_p values obtained from Linear polarisation tests carried out on the use of tapioca starch as corrosion inhibitor increased with increase in inhibitor concentration and the capacitance, C_{dl} values decreased indicating the formation of a surface film. The surface not covered by adsorbed starch molecules is proportional to the C_{dl}. Thus, effective corrosion resistance is associated with high R_p and low C_{dl} values (Rosliza *et al*; 2008). They observed that Increase in R_p values and decrease in C_{dl} values by

inhibitors are related to the increased degree of protection of metals in corrosive media. Singh et al 2010 observed the same behaviour on the study on the aqueous extract of Kalmegh (*Andrographis paniculata*) leaves as green inhibitor for mild steel in 1 M HCl. They observed that increasing the inhibitor concentration, decreases the C_{dl} values which results in increased inhibition efficiency. They attributed the decrease in C_{dl} values to be a decrease in local dielectric constant and/or an increase in the thickness of the electrical double layer, suggesting that Kalmegh **(***Andrographis paniculata*) leaves extract acted by adsorption at the mild steel/solution interface. On the other hand, the decrease in the values of C_{dl} with an increase in the inhibitor concentration is as a result of increase in the surface coverage by the inhibitor, which leads to an increase in the inhibition efficiency. The capacitance decreases as the corrosion inhibitors coverage increases since the capacitance is inversely proportional to the distance between the charges.

Moreover, the use of KI significantly reduced the corrosion current density values for the four inhibitors. The values of inhibition efficiency obtained from electrochemical and weight loss methods remain different, this may be due to the fact that Inhibition efficiency obtained from electrochemical method is an instantaneous value while, inhibition efficiency calculated from weight loss method is an average value. However, the electrochemical results on a whole are in good agreement with weight loss results.

4.5 Fourier Transform Infrared Spectroscopy (FTIR) Analysis of Adsorbed Surface

FTIR analysis was carried out on the metal surfaces to predict whether the ASS starch samples were adsorbed or not adsorbed. In the present study, FTIR spectra were used to support the fact that corrosion inhibition of mild steel and galvanised

steel in acid media is due to the adsorption of inhibitor molecules on the mild steel surface.

4.5.1 FTIR for Adsorbed film on Mild Steel

Presented in Figure 4.24 Is the FTIR spectra for the ASS starch sample and ASS-mild steel complex in 1 M HCl and 0.25 M H_2SO_4.

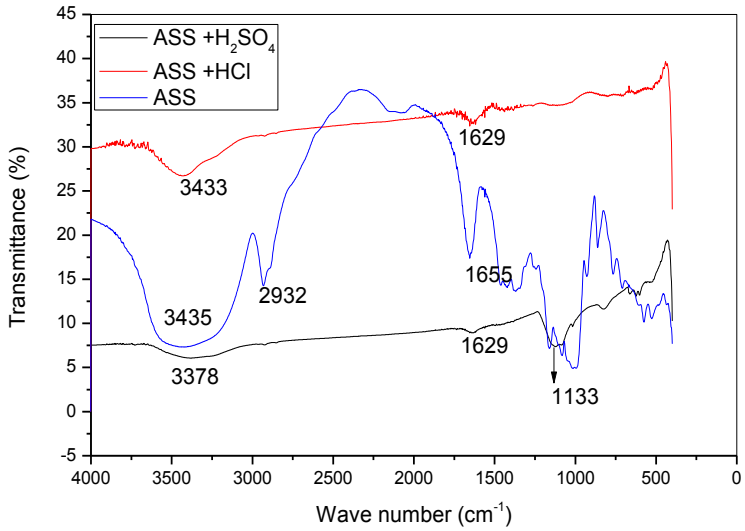

Figure 4.24*; FTIR spectra for ASS and ASS-mild steel complex in 1.0 M HCl, and 0.25 M H_2SO_4 solution.*

Fig. 4.24 shows the FT-IR spectra of ASS and ASS-mild steel complex in 1.0 M HCl and 0.25 M H_2SO_4. As can be seen from the FT-IR shown in Fig. 4.24, the spectrum exhibits very clear and strong features assigned to the polysaccharide molecules of ASS. The major and strongest vibrational modes in the ASS spectrum are those located at 1016, 1026, 1158, 1371, 1422, 1655, 2932, and a broad absorption band at 3000-3600 cm^{-1}. The strong vibrational mode located at 3000-3600 cm^{-1} is assigned to the stretching vibrations of the O-H bond, the other

strong vibrational mode located at 1016 cm^{-1} is assigned to the stretching vibrations of the C-O bond of carboxylate group associated with the ASS molecules, the two vibrational modes located at 1158, 1371 and 1422 cm^{-1}, with relatively low intensity, are assigned to the stretching vibrations of the C-O bond, and the weak vibrational mode located at 2932 cm^{-1} is assigned to the stretching vibrations of the C-H bond. The absorption band located at 1655 cm^{-1}, with relatively low intensity, may be assigned to the stretching mode of carbonyl (C=O) group (Banerji and Chen 2007).

In order to address the adsorption of ASS onto the surface of mild steel and the possible formation of ASS-mild steel complex, it is most instructive to compare the relative intensities of the major vibrational modes of plain ASS spectrum to those of the of ASS- mild steel complexes spectrum. Close inspection of Fig. 4.24, shows the FTIR spectra of ASS and ASS-mild steel complex in 1.0 M aqueous solutions of hydrochloric acid and 0.25 M aqueous solution of sulfuric acid, reveals the presence of very interesting features. The weak vibrational mode located at 2932 cm^{-1}(C-H stretch) is vanished completely in the ASS -mild steel complex spectra in acidic media. At the major bands concerning the stretching vibrations of the O-H bond at 3000-3600 cm^{-1}, there is a disappearance for ASS-mild steel complex spectra in 0.25 M H_2SO_4 and a vanishing band for ASS-mild steel complex spectra in 1 M HCl. The stretching vibrations of the C-O bond of carboxylate group associated with the ASS molecule at 1016 cm^{-1} vanished completely for both ASS-mild steel complex spectra in 1 M HCl and ASS-mild

steel complex spectra in 0.25 M H_2SO_4. However, there was a reduction of intensity and broadening of the band at 1035-1220 cm^{-1} for the ASS-mild steel complex spectra in sulphuric acid and this could be attributed to the bond formation by ASS in 0.25 M H_2SO_4 and mild steel. At 1655cm^{-1}, a very weak intensity that was shifted to a lower wave number was observed in the ASS-steel complex spectra in 1 M HCl while it was barely noticed in the ASS-mild steel complex spectra in 0.25 M H_2SO_4. Furthermore, a disappearance of almost all the intensities of the major bands in sulphuric acid is much more than those in hydrochloric acid. Also the transmittance of ASS-mild steel complex spectra in hydrochloric acid is higher than that of ASS-mild steel complex spectra in sulphuric acid, and this could be as a result of the effect of chloride ions on mild steel. These disappearance of peaks observed for for both ASS-mild steel complex spectra in 1 M HCl and ASS-mild steel complex spectra in 0.25 M H_2SO_4 means increased frequency indicating the formation of stronger bonds between ASS and mild steel in the acidic media.

4.5.2 FTIR for Galvanised Steel

Figure 4.25 presents the spectrum of ASS, ASS on galvanised steel surface in 0.25 M H_2SO_4 and ASS on galvanised steel surface in 1.0 M HCl.

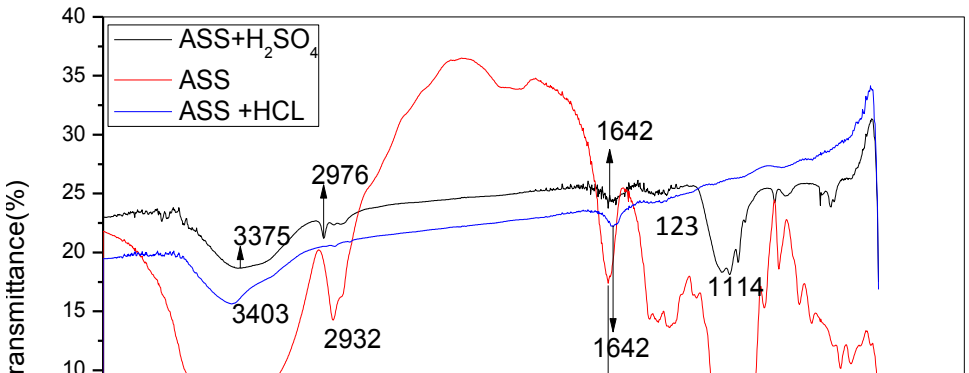

Figure 4.25: *FTIR spectra for ASS and ASS-galvanised steel complex in 1.0 M HCl, and 0.25 M H_2SO_4 solution.*

The weak vibrational mode located at 2932 cm^{-1}(C-H stretch) vanished completely in the ASS -galvanised steel complex spectra in 1.0 M HCl media while for the ASS on galvanised steel surface in 0.25 M H_2SO_4, the peak shifted to 2974cm^{-1}. At the major bands concerning the stretching vibrations of the O-H bond at 3000-3600 cm^{-1}, there is a reduction of their intensities for both ASS-mild steel complex spectra in 0.25 M H_2SO_4 and ASS-mild steel complex spectra in 1 M HCl. The stretching vibrations of the C-O bond of carboxylate group associated with the ASS molecule at 1016 cm^{-1} vanished completely for ASS-galvanised steel complex spectra in 1 M HCl while there was a slight reduction of the intensity for ASS-galvanised steel complex spectra in 0.25 M H_2SO_4. At 1655cm^{-1}, a very weak intensity that was shifted to a lower wave number was observed for both ASS-steel complex spectra in 1 M HCl and ASS-mild steel complex spectra in 0.25 M H_2SO_4. Furthermore, a disappearance of almost all the intensities of the major bands was observed more in hydrochloric acid than in

sulphuric acid for galvanised steel and this could be attributed to the synergistic effect of chloride ions on galvanised steel. These disappearances of peaks observed for both ASS-galvanised steel complex spectra in 1 M HCl and ASS-galvanised steel complex spectra in 0.25 M H_2SO_4 means increased frequency indicating the formation of stronger bonds between ASS and mild steel in the acidic media.

The overall features of the FT-IR spectra shown in Fig. 4.24 and 4.25 suggested that there is a strong adsorption of ASS onto the surface of the steel, which is more pronounced in hydrochloric acid than sulphuric acid, due to the electrostatic binding of the carboxylate groups of the ASS molecule to sites along oxide surfaces of steel (Williams *et al.* 2006). This conclusion was interpreted from the large reduction of the intensities of all prominent bands and the shift in position of the stretching vibrations bands of the C-O bond in ASS-steel complex spectra relative to plain ASS spectrum. All these significant changes in peaks show that the inhibitors interacted on the metal surface (Saravanamoorthy and Velmathi, 2013). The result obtained from FT-IR spectra provides a strong interaction between inhibitor molecules and the mild Steel and galvanised steel surface.

4.6 Morphological Studies of Mild Steel and Galvanised Steel

The three dimensional and two dimensional surface images of the mild steel and galvanised steel surface exposed to uninhibited and inhibited acid solution are shown in Figure 4.26 to Figure 4.33.

Fig 4.26 displayed the three dimensional AFM image of mild steel surface immersed in 0.25 M H_2SO_4 solution without and with the addition of 0.5 g/l ASS. From the Figure above it can be seen that the corrosion pattern of mild steel in uninhibited 0.25 M H_2SO_4 solution appears non uniform with some parts showing deep ridges. By contrast, the corrosion morphology of mild steel in inhibited 0.25 M H_2SO_4 solution containing the inhibitor had less sharp ridges and some degree of smoothness. This is observed in Figure 4.27 which shows the two dimensional topographs of the metals after immersion. This could be ascribed to the adsorbed starch molecules which prevented the corrosion of mild steel.

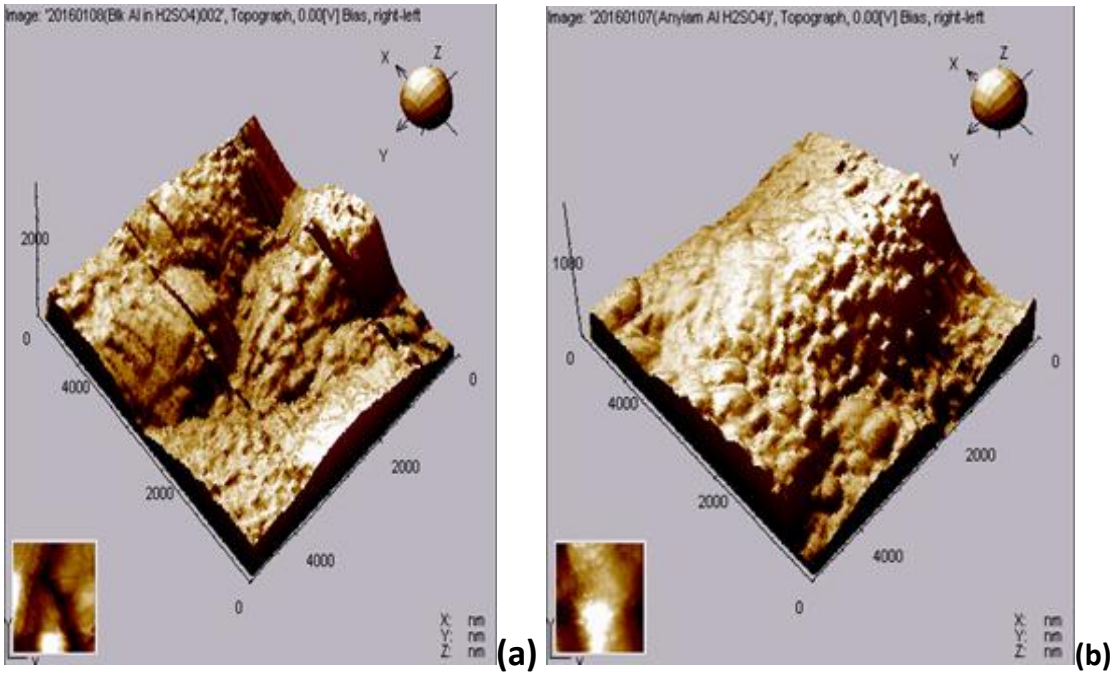

Figure 4.26*: AFM three dimensional images for the mild steel surface in 0.25M H_2SO_4 solution (a) Blank 0.25 M H_2SO_4 (b) 0.25 M H_2SO_4 + 0.5g/ l ASS*

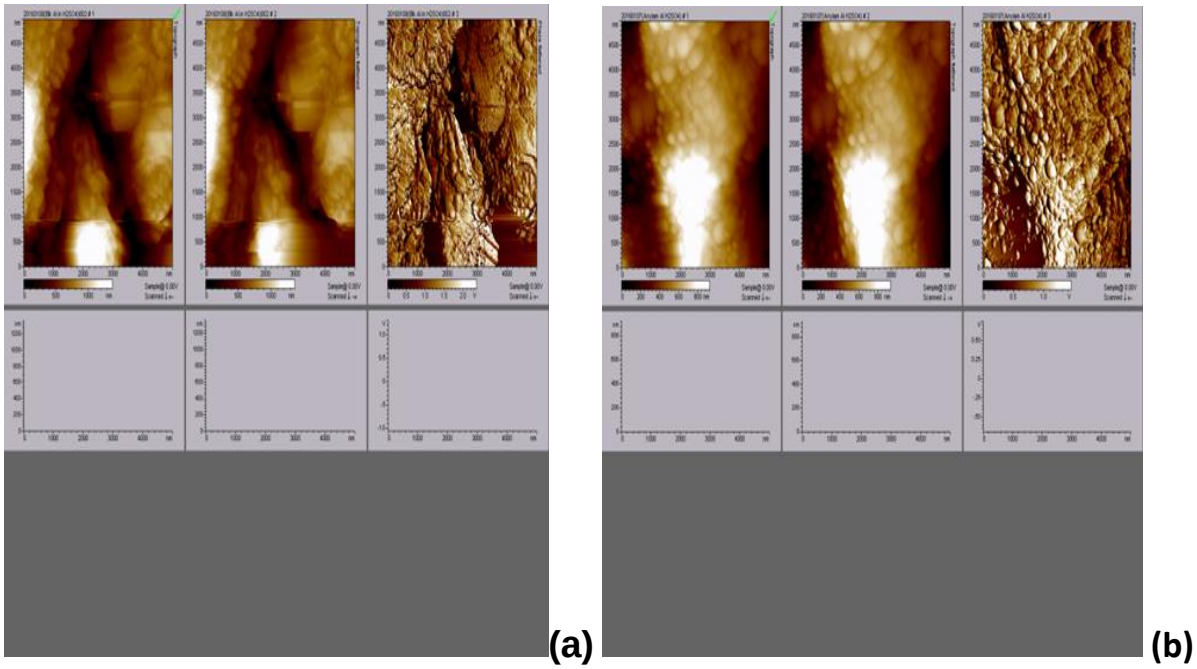

Figure 4.27; *AFM two dimensional images for the mild steel surface in 0.25M H_2SO_4 solution (a) Blank 0.25 M H_2SO_4 (b) 0.25 M H_2SO_4 + 0.5g/ l ASS*

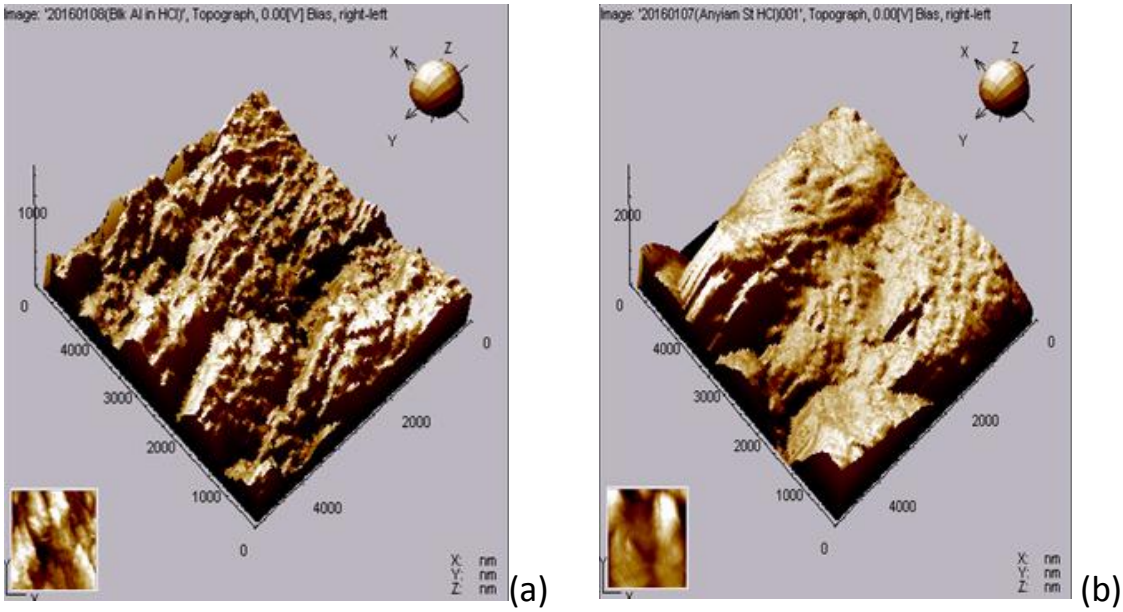

Figure 4.28*: AFM three dimensional images for the mild steel surface in 1 M HCl solution (a) Blank 1 M HCl (b) 1 M HCl + 0.5g/ l ASS*

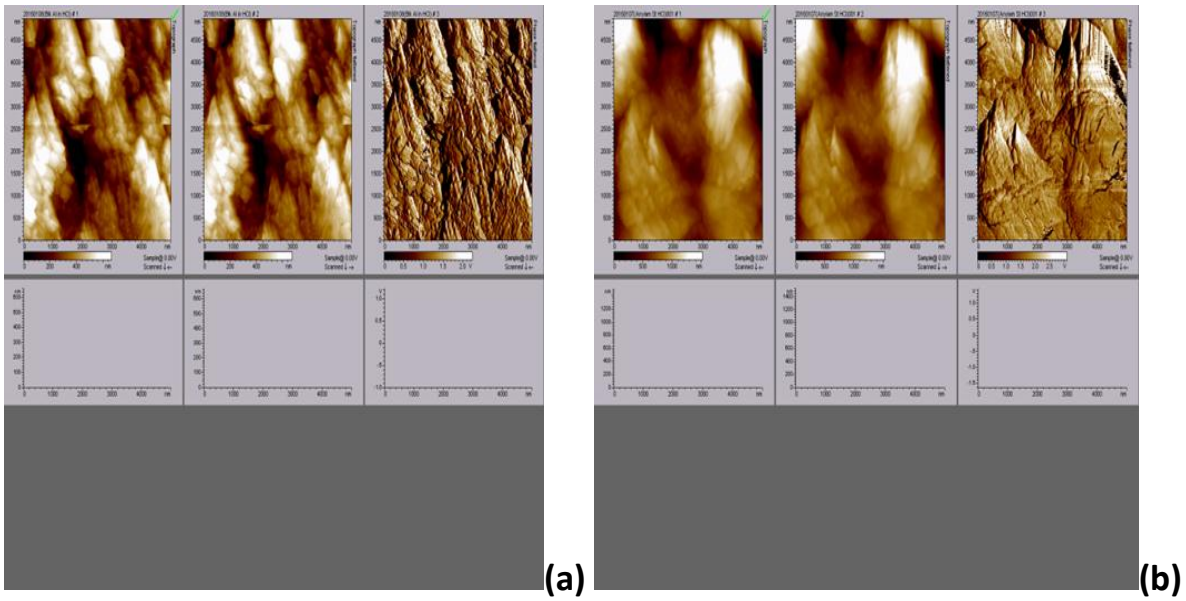

Figure 4.29*: AFM two dimensional images for the mild steel surface in 1 M HCl solution (a) Blank 1 M HCl (b) 1 M HCl + 0.5g/ l ASS*

Figure 4.28 and 4.29 presents the three dimensional and two dimensional surface images of the mild steel after immersion in uninhibited and inhibited hydrochloric acid media. The mild steel surface exposed to inhibited acid solution was found to be smoother than the one exposed to uninhibited acid solution. This is due to the adsorbed starch molecules which prevented the corrosion of mild steel.

Figures 4.30 and 4.31 presents the three dimensional and two dimensional surface images of the mild steel after immersion in uninhibited and inhibited solution of 0.25 M H_2SO_4. The mild steel surface exposed to inhibited acid solution was found to be smoother than the one exposed to uninhibited acid solution. This is due to the adsorbed starch molecules which inhibited the corrosion of galvanised steel in the acidic media. This confirms the active role of the modified starch in corrosion inhibition.

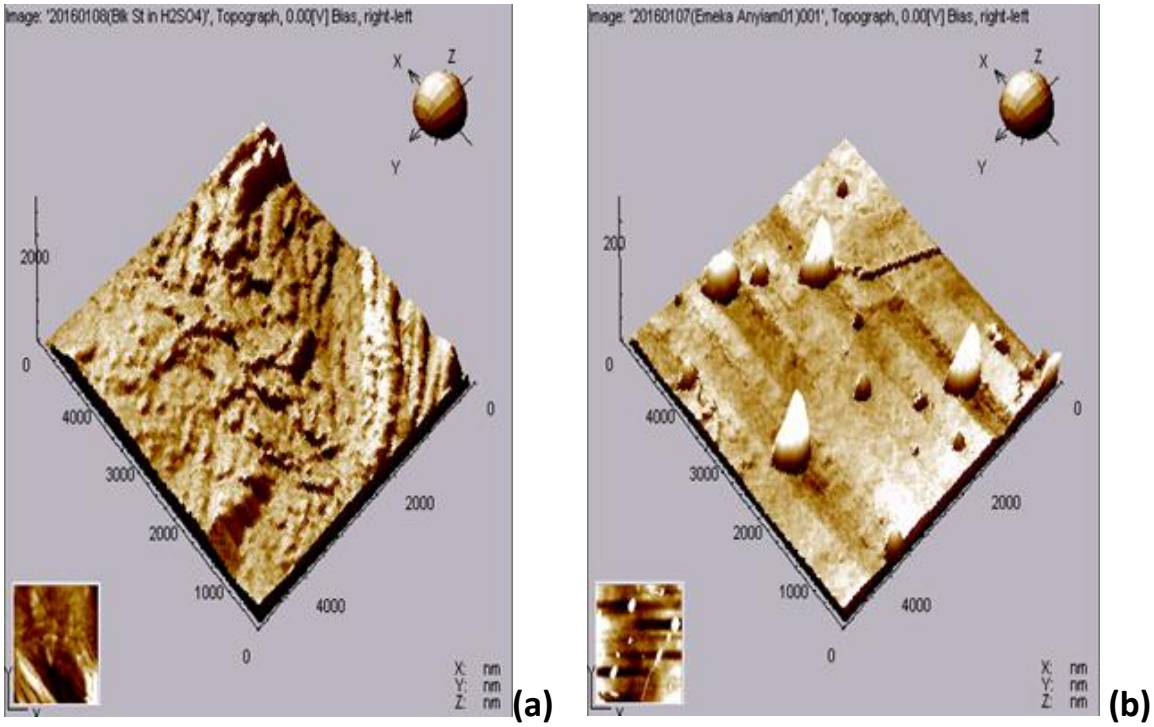

Figure 4.30*: AFM three dimensional images for the galvanised steel surface in 0.25M H_2SO_4 solution (a) Blank 0.25 M H_2SO_4 (b) 0.25 M H_2SO_4 + 0.5g/ l ASS*

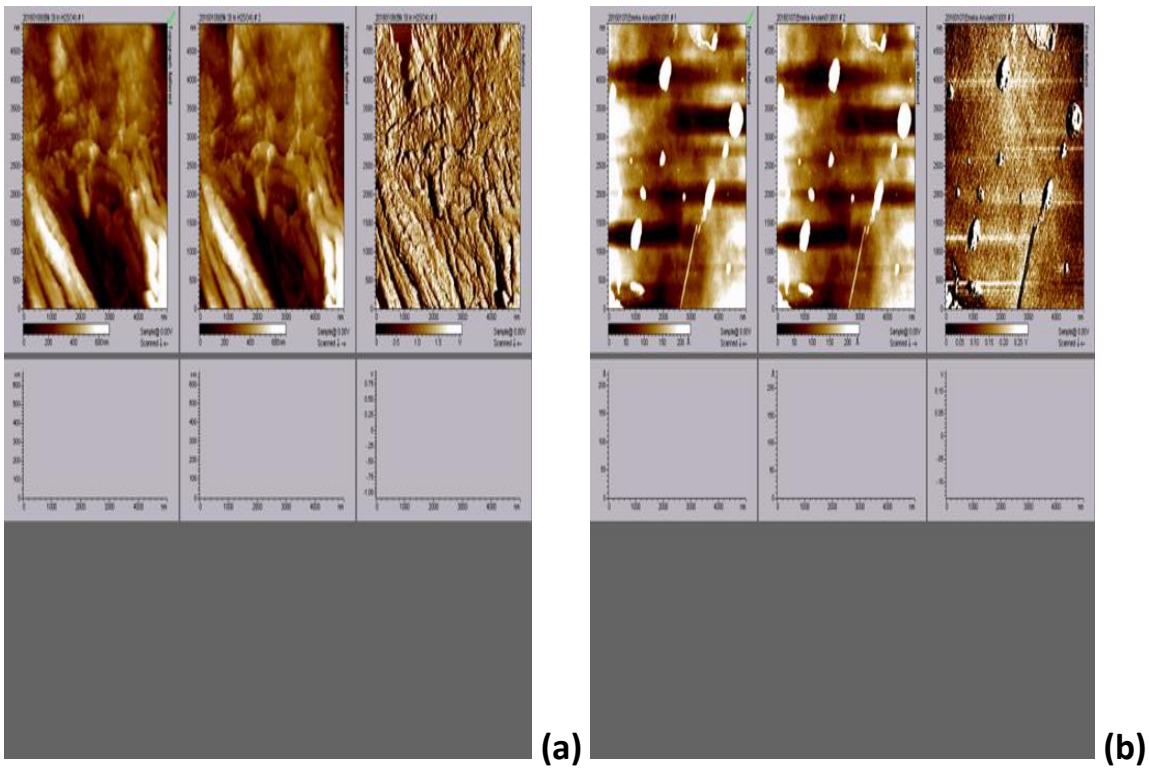

Figure 4.31*: AFM two dimensional images for the galvanised steel surface in 0.25M H_2SO_4 solution (a) Blank 0.25 M H_2SO_4 (b) 0.25 M H_2SO_4 + 0.5g/ l ASS*

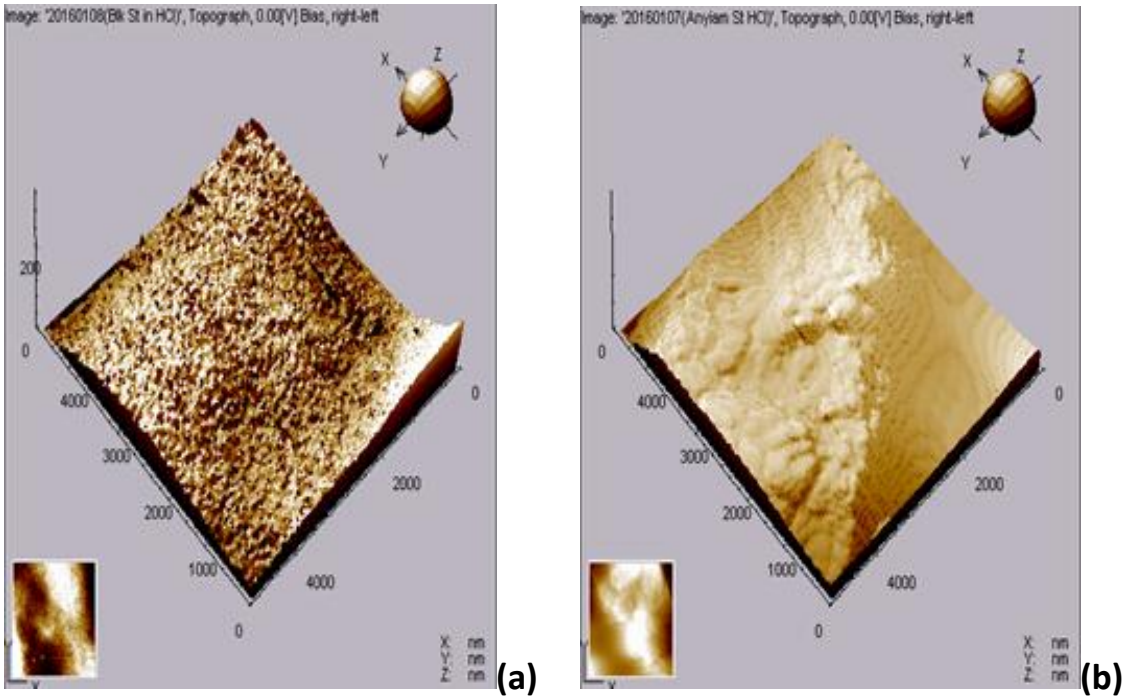

Figure 4.32*: AFM three dimensional images for the mild steel surface in 1 M HCl solution (a) Blank 1 M HCl (b) 1 M HCl + 0.5g/ l ASS*

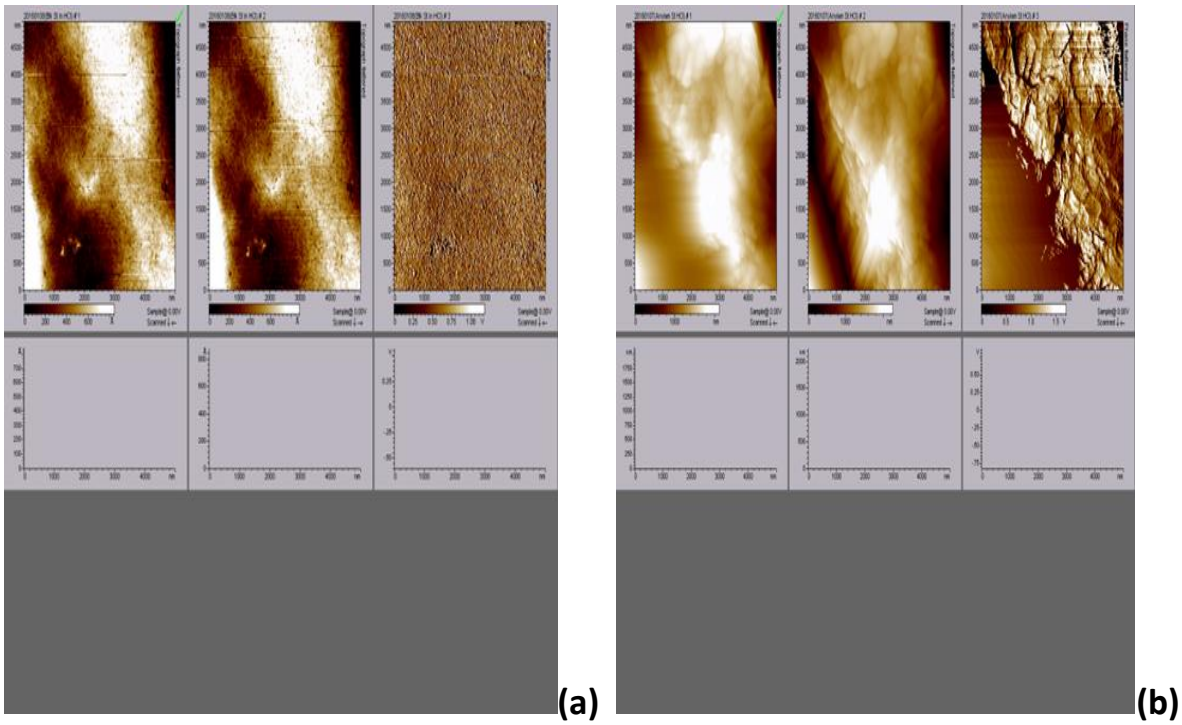

Figure 4.33*: AFM two dimensional images for the mild steel surface in 1 M HCl solution (a) Blank 1 M HCl (b) 1 M HCl + 0.5g/ l ASS*

Figures 4.32 and 4.33 present the three dimensional and two dimensional surface images of the galvanised steel after immersion in uninhibited and inhibited solutions of 1 M HCl. The galvanised steel surface exposed to inhibited acid solution had some degree of smoothness in comparison to the one exposed to the uninhibited acid solution. This is due to the adsorbed starch molecules which inhibited the corrosion of galvanised steel in the acidic media. The surface images presented in Figures 4.32 to Figures 4.33, confirms the active role of the modified starch in the corrosion inhibition of the metals in acidic media.

4.7 Adsorption considerations

The adsorption of organic compounds on metal surfaces can be described by two main types of interactions namely, physical adsorption and chemical adsorption. These adsorptions are dependent on the electronic structure of the metal, the nature of the electrolyte and the chemical structure of the organic compounds. The character of adsorption of the four inhibitors was elucidated from the values of degree of surface coverage (Ɵ) calculated from the weight loss data for the different concentration of the four inhibitors. Classical adsorptions isotherms of Freundlich, Temkin, Frumkin and Langmuir as well as substitutional adsorption isotherms off Flory-Huggins, Dhar Flory=Huggins and Bockris-Swinkles have been used to represent the adsorption behaviour of organic compounds on metal surfaces (Martinez & Stern (2001); Martinez (2002)). Attempts were made to fit the Ɵ values to Langmuir's, Freundlich's and Temkin's adsorption isotherms.

4.7.1 Langmuir Isotherm

Langmuir plot describes the relationship between the surface coverage and inhibition concentration of a material. The plots of C/Ɵ against C are drawn which is characteristics of Langmuir adsorption isotherm given by equation:

$$\frac{C}{\theta} = \frac{1}{K} + C \qquad (4.3)$$

Where Ɵ is the degree of surface coverage, K is the equilibrium constant of the adsorption process and C is the starch concentration. The plots of C/Ɵ versus C

for mild steel and galvanised steel corrosion in both 0.25M H_2SO_4 and 1M HCl for the four inhibitors are shown in Figures 4.34 –4.37. The plots yield a straight line with slope and regression coefficient, R^2, almost equal to unity. This suggests that the four inhibitors being studied obeyed the Langmuir isotherm and there was negligible interaction between the adsorbed molecules. Data obtained from the plot of Langmuir's isotherm are presented in Table 4.20. Correlation coefficients of the linear regression (R^2) plots of > 0.5998 were obtained from Langmuir's isotherm which gave the best fit.

Data obtained from Langmuir isotherm plots indicates that the value of K_{ads} for the four inhibitors followed the trend ASS>ATS>PMS>NS for the metals in the acidic media.

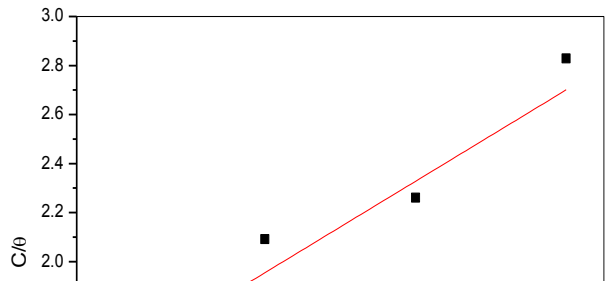

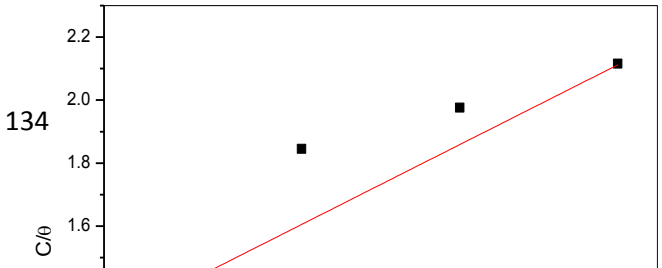

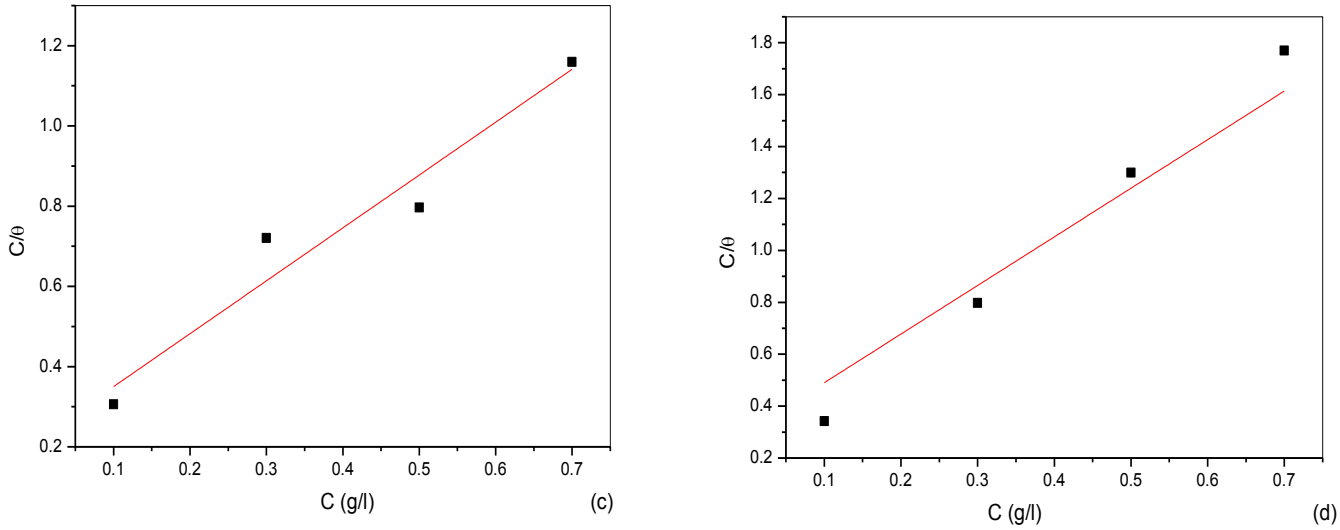

***Figure 4.34**: Langmuir Isotherm Plots of the Corrosion of Mild Steel in 0.25M H_2SO_4 in the Presence of (a) Natural starch, (b) Physical modified starch, (c) Alkaline treated starch and (d) Acid treated starch.*

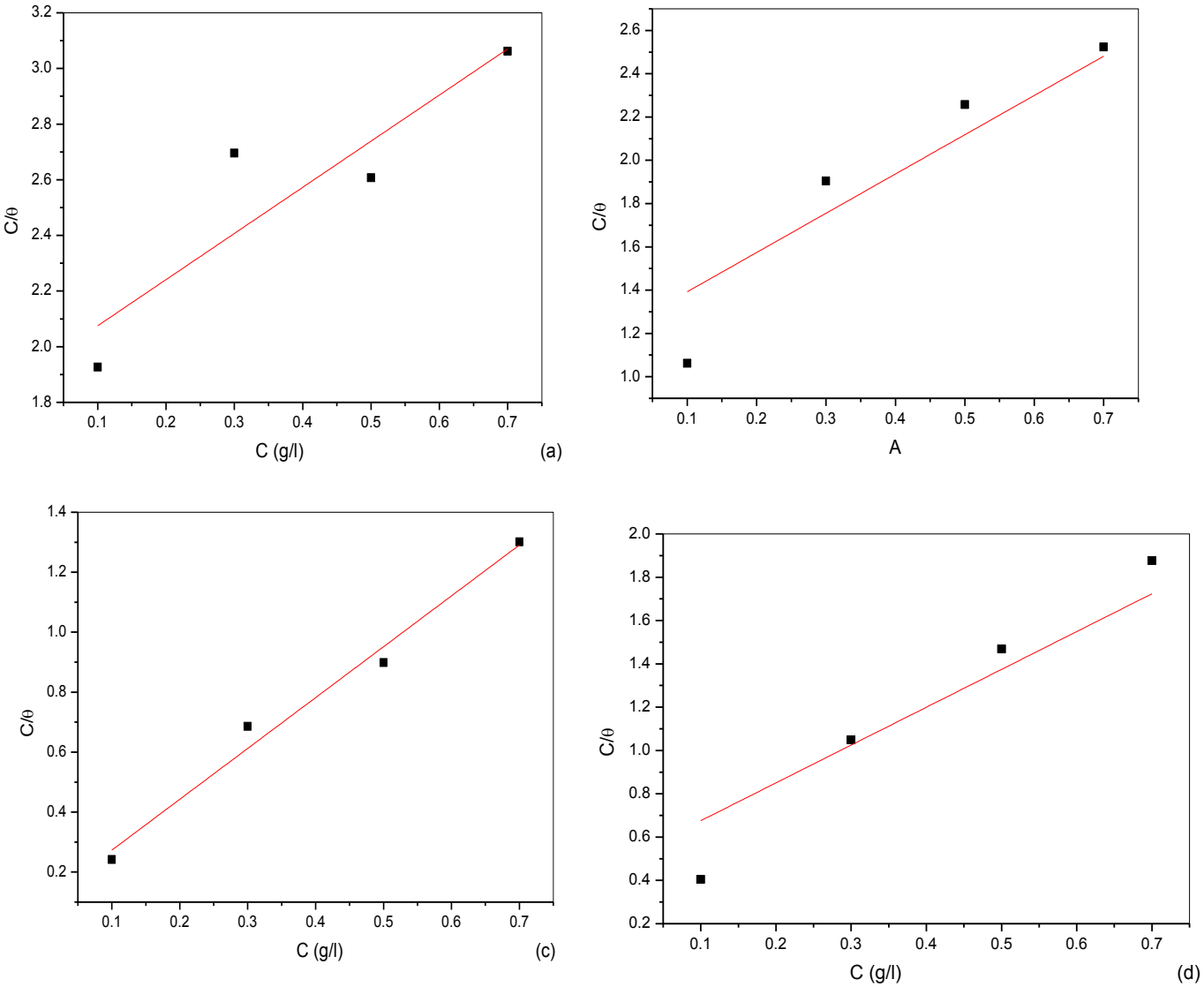

Figure 4.35: *Langmuir Isotherm Plots of the Corrosion of Mild Steel in 1M HCL in the Presence of (a) Natural starch, (b) Physical modified starch, (c) Alkaline treated starch and (d) Acid treated starch.*

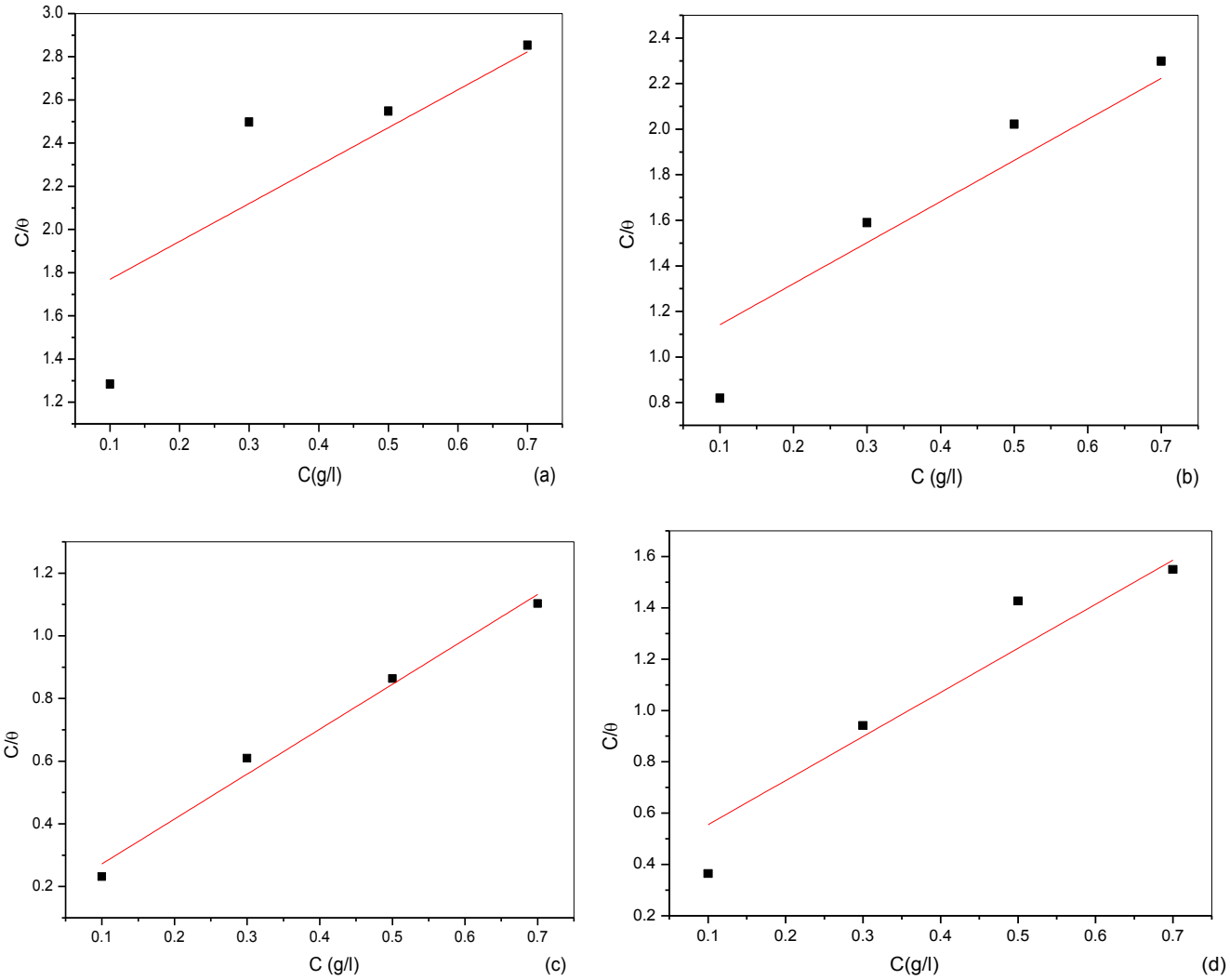

Figure 4.36: *Langmuir Isotherm Plots of the Corrosion of Galvanised Steel in 0.25M H_2SO_4 in the Presence of (a) Natural starch, (b) Physical modified starch, (c) Alkaline treated starch and (d) Acid treated starch.*

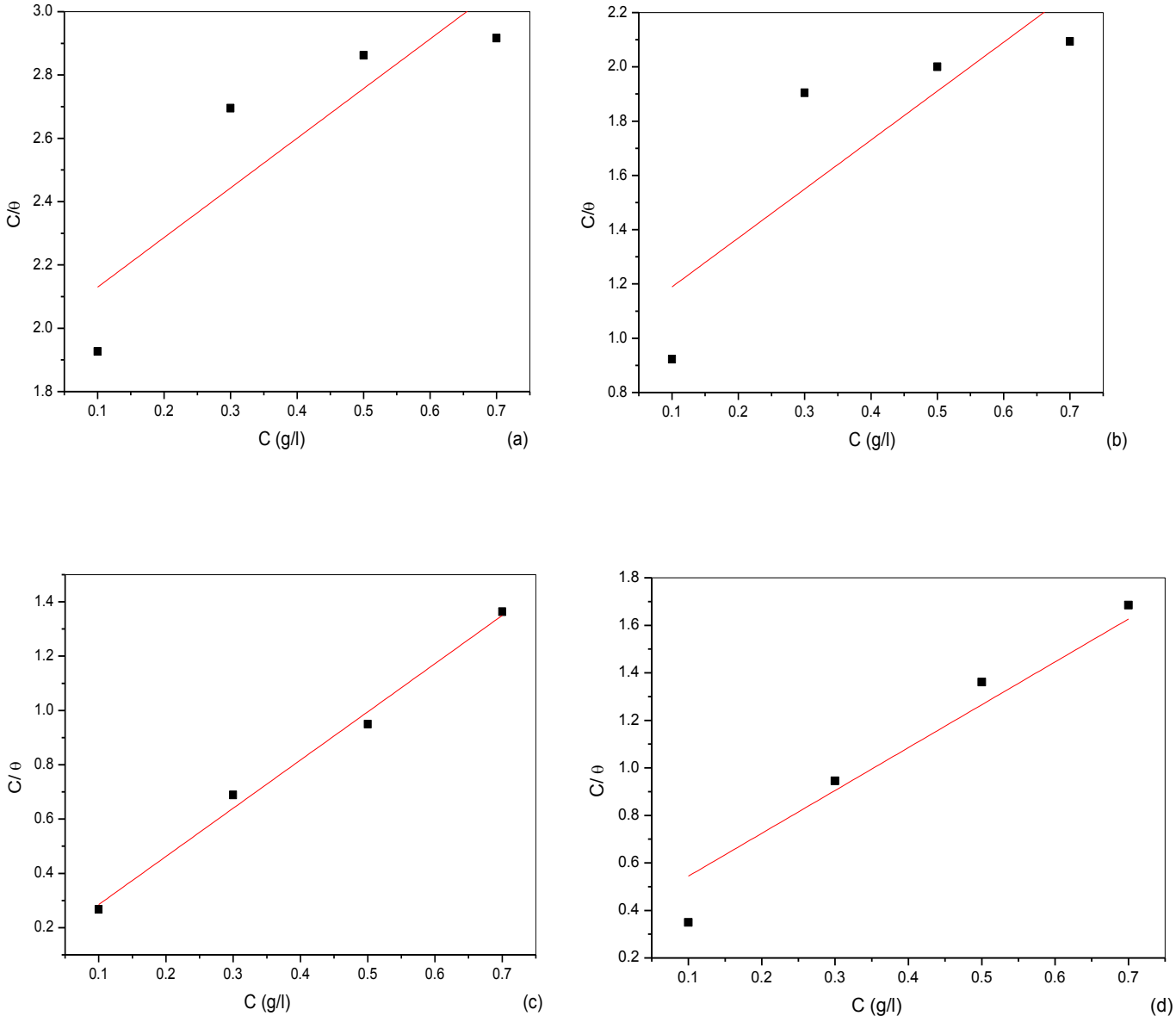

***Figure 4.37**: Langmuir Isotherm Plots of the Corrosion of Galvanised Steel in 1 M HCl in the Presence of (a) Natural starch, (b) Physical modified starch, (c) Alkaline treated starch and (d) Acid treated starch.*

4.7.2 Freundlich Isotherm

The adsorption isotherm of Freundlich was also tested for its fit to the experimental data obtained from the gravimetric studies. Freundlich adsorption isotherm is given by Equation 4.4 and the linearized version by Equation 4.5. Values of lnθ were plotted against lnC as presented in Figures 4.38 – 4.40.

$$\theta = KC^n \quad (4.4)$$

Where 0<n<1

$$\ln\theta = \ln K + n\ln C \quad (4.5)$$

Where n is the lateral interaction term describing the molecular interactions in the adsorption layer and the heterogeneity of the metal surface; θ is the degree of surface coverage; K_{ads} is the equilibrium constant of adsorption process; C is the concentration of the inhibitor.

Plots of the logarithm of surface coverage (In θ) against logarithm of the concentration of the extract (ln C) for the different concentrations of the four inhibitors at room temperature are shown in Figures 4.46 – 4.49. Correlation coefficients of the linear regression (R^2) plots of >0.5761 were obtained as presented in Table 4.20, implying some degree of agreement of the data to the Freundlich adsorption isotherm model. It is observed from the data obtained from Figures 4.38 – 4.41, the Freundlich adsorption isotherm model gave a better fit

than Temkin model. The K_{ads} value obtained for the Freundlich's isotherm follows the trend ASS>ATS>PMS>NS.

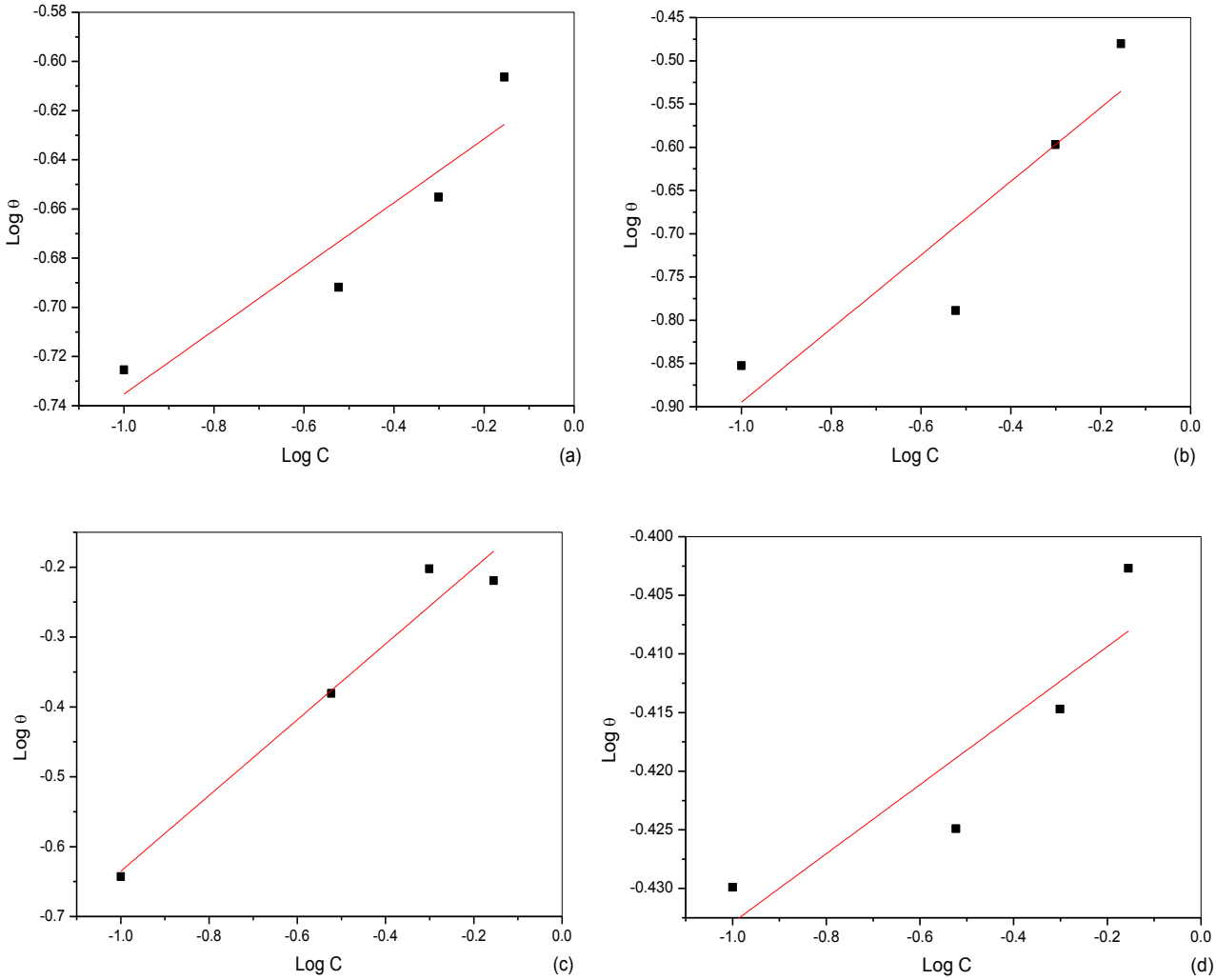

Figure 4.38: Freundlich Isotherm Plots of the Corrosion of Mild Steel in 0.25M H_2SO_4 in the Presence of (a) Natural starch, (b) Physical modified starch, (c) Alkaline treated starch and (d) Acid treated starch.

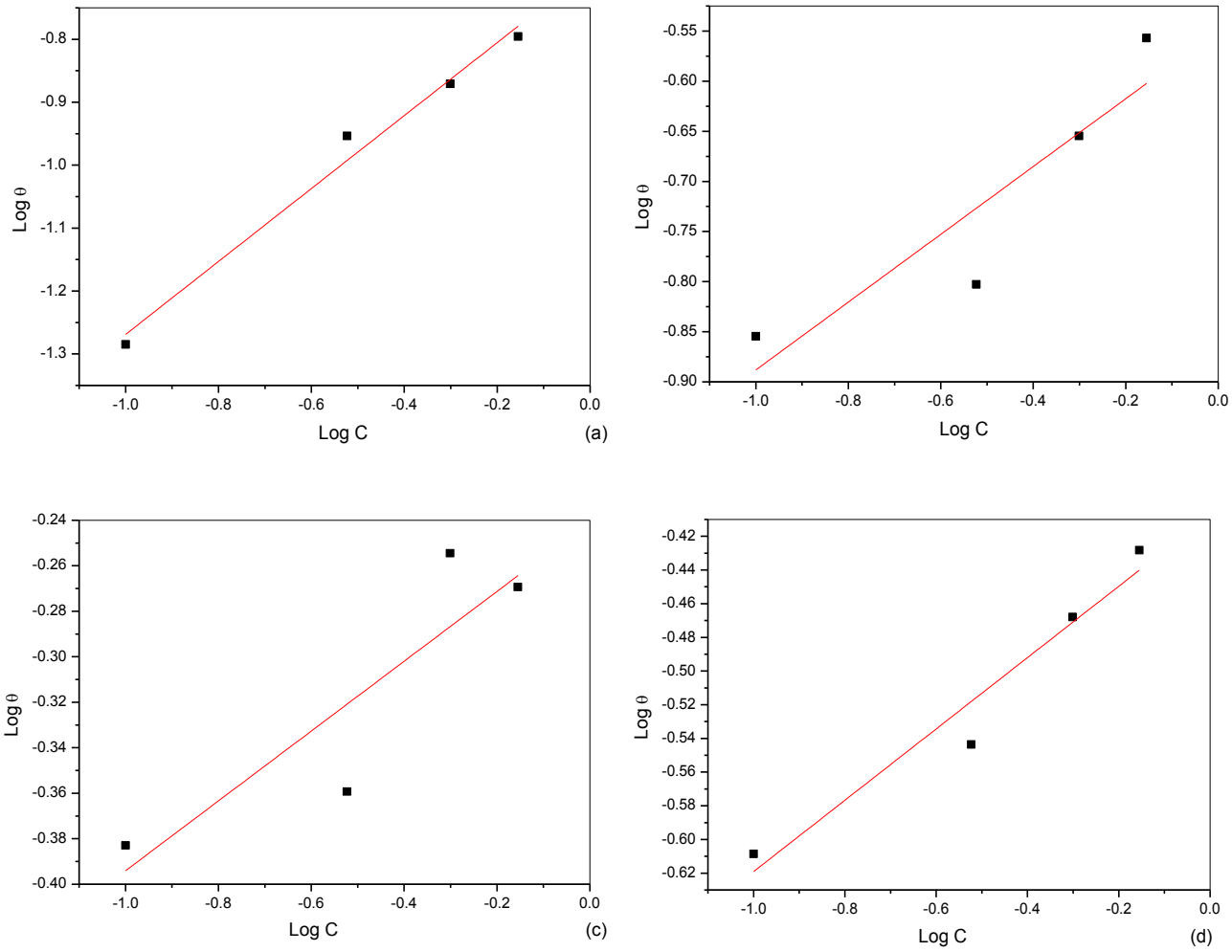

***Figure 4.39**: Freundlich Isotherm Plots of the Corrosion of Mild Steel in 1M HCL in the Presence of (a) Natural starch, (b) Physical modified starch, (c) Alkaline treated starch and (d) Acid treated starch.*

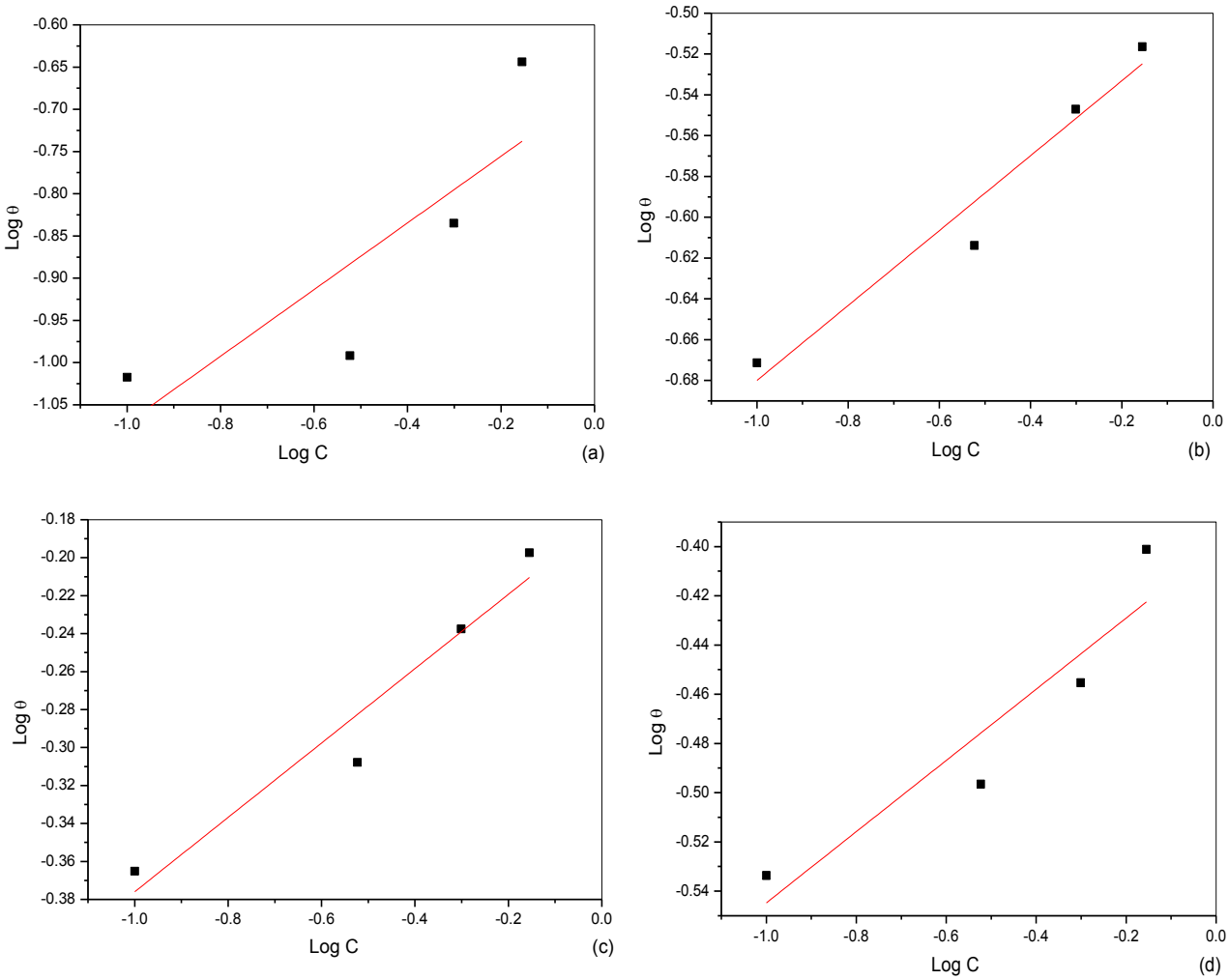

***Figure 4.40**: Freundlich Isotherm Plots of the Corrosion of Galvanised Steel in 0.25M H_2SO_4 in the Presence of (a) Natural starch, (b) Physical modified starch, (c) Alkaline treated starch and (d) Acid treated starch.*

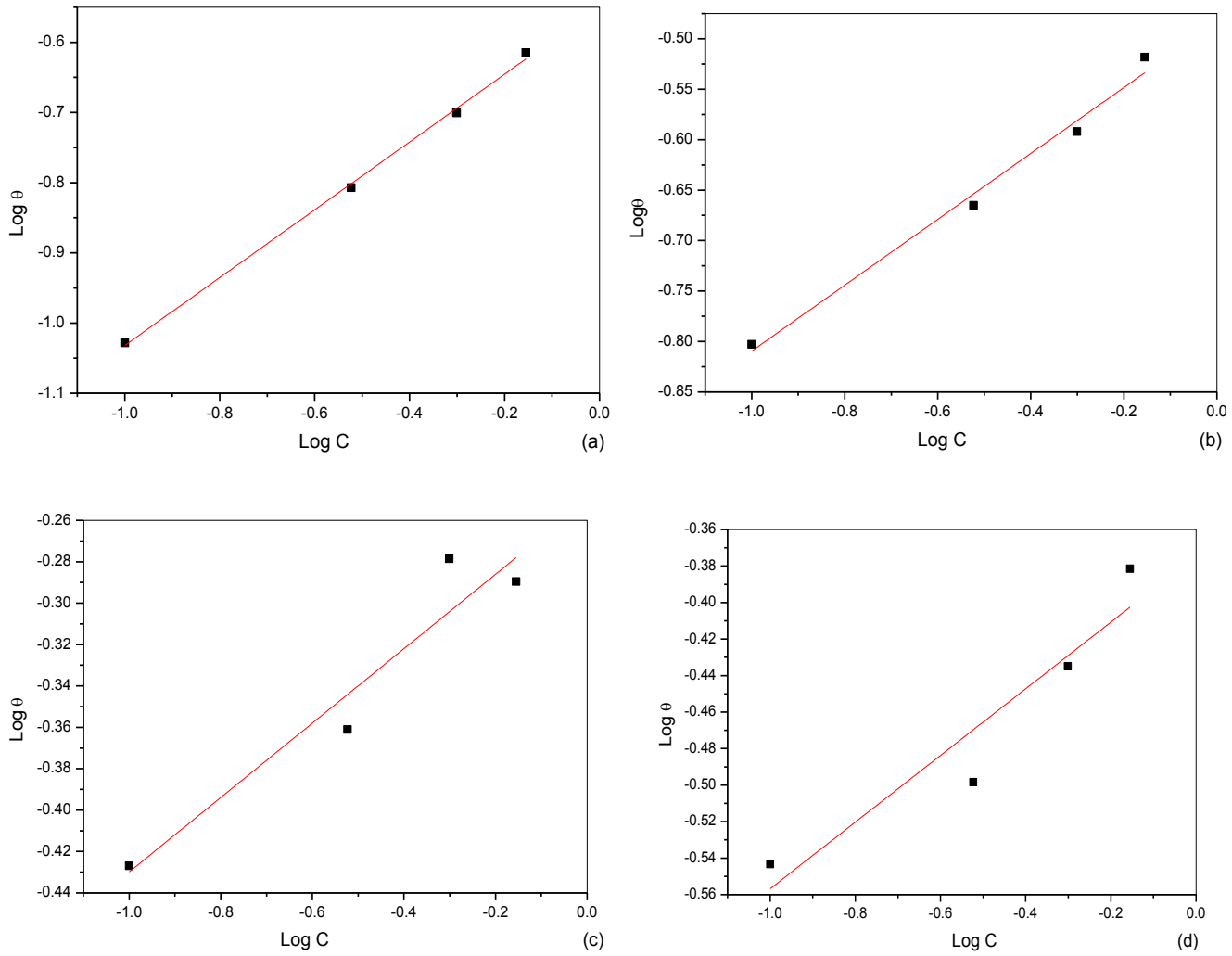

Figure 4.41: *Freundlich Isotherm Plots of the Corrosion of Galvanised Steel in 1M HCL in the Presence of (a) Natural starch, (b) Physical modified starch, (c) Alkaline treated starch and (d) Acid treated starch.*

4.7.3 Temkin Isotherm

The adsorption isotherm of Temkin was also tested for its fit to the experimental data obtained from the gravimetric studies. Temkin adsorption isotherm assumes a uniform distribution of adsorption energy which increases with increase of the surface coverage is given by the equation below (Mu et al., 2005).

$$exp(-2a\theta) = K_{ads}C \qquad (4.6)$$

Where a is the lateral interaction term describing the molecular interactions in the adsorption layer and the heterogeneity of the metal surface; θ is the degree of surface coverage; K_{ads} is the equilibrium constant of adsorption process; C is the concentration of the inhibitor.

Graphical representation of the surface coverage (θ) against logarithm of the concentration of the four inhibitors (ln C) at room temperature, are presented in Figures 4.42 – 4.45 and the adsorption parameters K and R^2 are presented in Table 4.20. Correlation coefficients of the linear regression (R^2) plots of > 0.4770 were obtained, implying some degree of agreement of the data to the Temkin adsorption isotherm model, especially for the adsorption of the inhibitors on both galvanised and mild steel. K_{ads} value obtained for the four inhibitors followed the trend ATS>ASS>NS>PMS for both mild steel and galvanised steel in H_2SO_4 and ASS>ATS>PMS>PMS for both metals in HCL.

Table 4.11 Langmuir Isotherm data for NS, PMS, ASS and ATS on mild steel surface from 0.25M H_2SO_4 solution

	NS		PMS		ASS		ATS	
C(g/l)	Θ	C/Θ	Θ	C/Θ	Θ	C/Θ	Θ	C/Θ
0.1000	0.0722	1.3850	0.1009	0.9912	0.3268	0.3060	0.2923	0.3421
0.3000	0.1438	2.0920	0.1626	1.8450	0.4164	0.7205	0.3759	0.7980
0.5000	0.2212	2.2604	0.2530	1.9763	0.6276	0.7967	0.3849	1.2990
0.7000	0.2475	2.8283	0.3308	2.1160	0.6036	1.1597	0.3956	1.7695

Table 4.12 Langmuir Isotherm data for NS, PMS, ASS and ATS on mild steel surface from 1M HCL solution

	NS		PMS		ASS		ATS	
C(g/l)	Θ	C/Θ	Θ	C/Θ	Θ	C/Θ	Θ	C/Θ
0.1000S	0.0519	1.9268	0.0942	1.0616	0.4141	0.2415	0.2463	0.4050
0.3000	0.1113	2.6954	0.1575	1.9048	0.4372	0.6862	0.2860	1.0489
0.5000	0.1918	2.6069	0.2215	2.2573	0.5565	0.8985	0.3405	1.4684
0.7000	0.2286	3.0621	0.2774	2.5234	0.5379	1.3014	0.3730	1.8767

Table 4.13 Langmuir Isotherm data for adsorption of NS, PMS, ASS and ATS on galvanised steel surface from 0.25M H_2SO_4 solution

	NS		PMS		ASS		ATS	
C(g/l)	Θ	C/Θ	Θ	C/Θ	Θ	C/Θ	Θ	C/Θ
0.1000	0.0779	1.2837	0.1221	0.8190	0.4313	0.2319	0.2744	0.3644
0.3000	0.1201	2.4979	0.1887	1.5898	0.4921	0.6096	0.3188	0.9410
0.5000	0.1962	2.5484	0.2473	2.0218	0.5788	0.8639	0.3505	1.4265
0.7000	0.2453	2.8536	0.3045	2.2989	0.6348	1.1027	0.4517	1.5497

Table 4.14 Langmuir Isotherm data for adsorption of NS, PMS, ASS and ATS on galvanised steel surface from 1M HCL solution

	NS		PMS		ASS		ATS	
C(g/l)	Θ	C/Θ	Θ	C/Θ	Θ	C/Θ	Θ	C/Θ
0.1000	0.0519	1.9268	0.1084	0.9225	0.3742	0.2673	0.2862	0.3494
0.3000	0.1113	2.6954	0.1575	1.9048	0.4354	0.6890	0.3174	0.9452
0.5000	0.1747	2.8620	0.2500	2.0000	0.5265	0.9497	0.3673	1.3613
0.7000	0.2400	2.9167	0.3344	2.0933	0.5134	1.3635	0.4154	1.6851

Table4.15 Freudlich/Temkin Isotherm data for adsorption of NS, PMS, ASS and ATS on mild steel surface from 0.25 H_2SO_4 solution

Inhibitor Conc		NS		PMS		ASS		ATS	
C(g/l)	Log C	Θ	Log Θ	Θ	Log Θ	Θ	Log Θ	Θ	Log Θ
0.1000	-1	0.1882	-0.7254	0.1404	-0.8526	0.2276	-0.6428	0.3716	-0.4299
0.3000	-0.5229	0.2033	-0.6918	0.1626	-0.7888	0.4164	-0.3805	0.3759	-0.4249
0.5000	-0.301	0.2212	-0.6552	0.2530	-0.5969	0.6276	-0.2023	0.3849	-0.4147
0.7000	-0.1549	0.2475	-0.6064	0.3308	-0.4804	0.6036	-0.2193	0.3956	-0.4027

Table4.16 Freudlich/Temkin Isotherm data for adsorption of NS, PMS, ASS and ATS on mild steel surface from 1M HCL solution

Inhibitor Conc		NS		PMS		ASS		ATS	
C(g/l)	Log C	Θ	Log Θ	Θ	Log Θ	Θ	Log Θ	Θ	Log Θ
0.1000	-1	0.0519	-1.2848	0.1398	-0.8545	0.4141	-0.3829	0.2463	-0.6085
0.3000	-0.5229	0.1113	-0.9535	0.1575	-0.8027	0.4372	-0.3593	0.2860	-0.5436
0.5000	-0.301	0.1347	-0.8706	0.2215	-0.6546	0.5565	-0.2545	0.3405	-0.4679
0.7000	-0.1549	0.1601	-0.7956	0.2774	-0.5569	0.5379	-0.2693	0.3730	-0.4283

Table4.17 Freudlich/Temkin Isotherm data for adsorption of NS, PMS, ASS and ATS on galvanised steel surface from 0.25 H_2SO_4 solution

Inhibitor Conc		NS		PMS		ASS		ATS	
C(g/l)	Log C	Θ	Log Θ	Θ	Log Θ	Θ	Log Θ	Θ	Log Θ
0.1000	-1	0.0961	-1.0173	0.2131	-0.6714	0.4313	-0.3652	0.2926	-0.5337
0.3000	-0.5229	0.1019	-0.9918	0.2433	-0.6139	0.4921	-0.3079	0.3188	-0.4965
0.5000	-0.301	0.1463	-0.8348	0.2837	-0.5471	0.5788	-0.2375	0.3505	-0.4553
0.7000	-0.1549	0.2271	-0.6438	0.3045	-0.5164	0.6348	-0.1974	0.3971	-0.4011

Table4.18 Freudlich/Temkin Isotherm data for adsorption of NS, PMS, ASS and ATS on galvanised steel surface from 1M HCL solution

Inhibitor Conc		NS		PMS		ASS		ATS	
C(g/l)	Log C	Θ	Log Θ	Θ	Log Θ	Θ	Log Θ	Θ	Log Θ
0.1000	-1	0.0937	-1.0283	0.1575	-0.8027	0.3742	-0.4269	0.2862	-0.5433
0.3000	-0.5229	0.1559	-0.8072	0.2162	-0.6651	0.4354	-0.3611	0.3174	-0.4984
0.5000	-0.301	0.1992	-0.7007	0.2558	-0.5921	0.5265	-0.2786	0.3673	-0.4349
0.7000	-0.1549	0.2427	-0.6149	0.3032	-0.5183	0.5134	-0.2895	0.4154	-0.3815

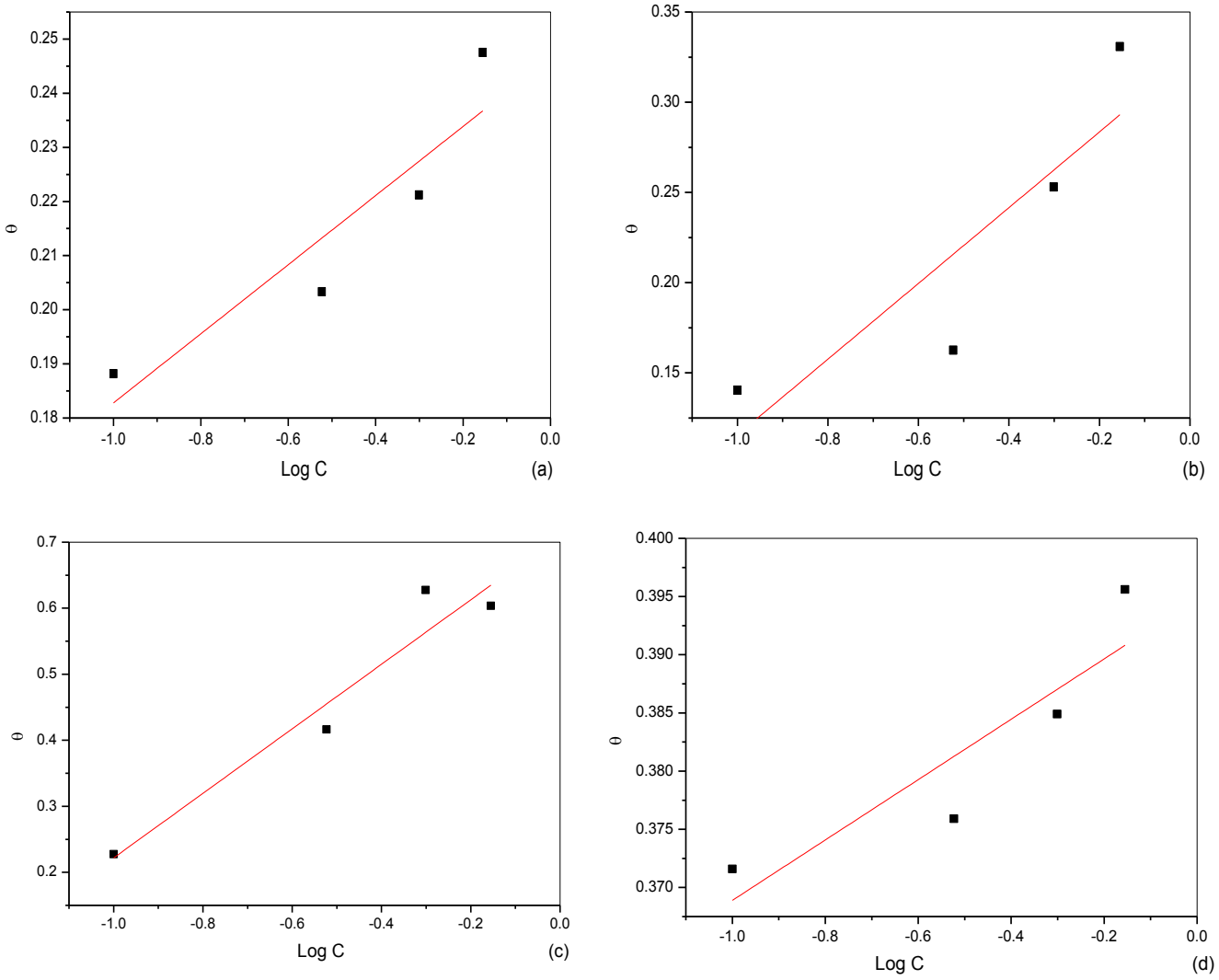

Figure 4.42: *Temkin Isotherm Plots of the Corrosion of Mild Steel in 0.25M H_2SO_4 in the Presence of (a) Natural starch, (b) Physical modified starch, (c) Alkaline treated starch and (d) Acid treated starch.*

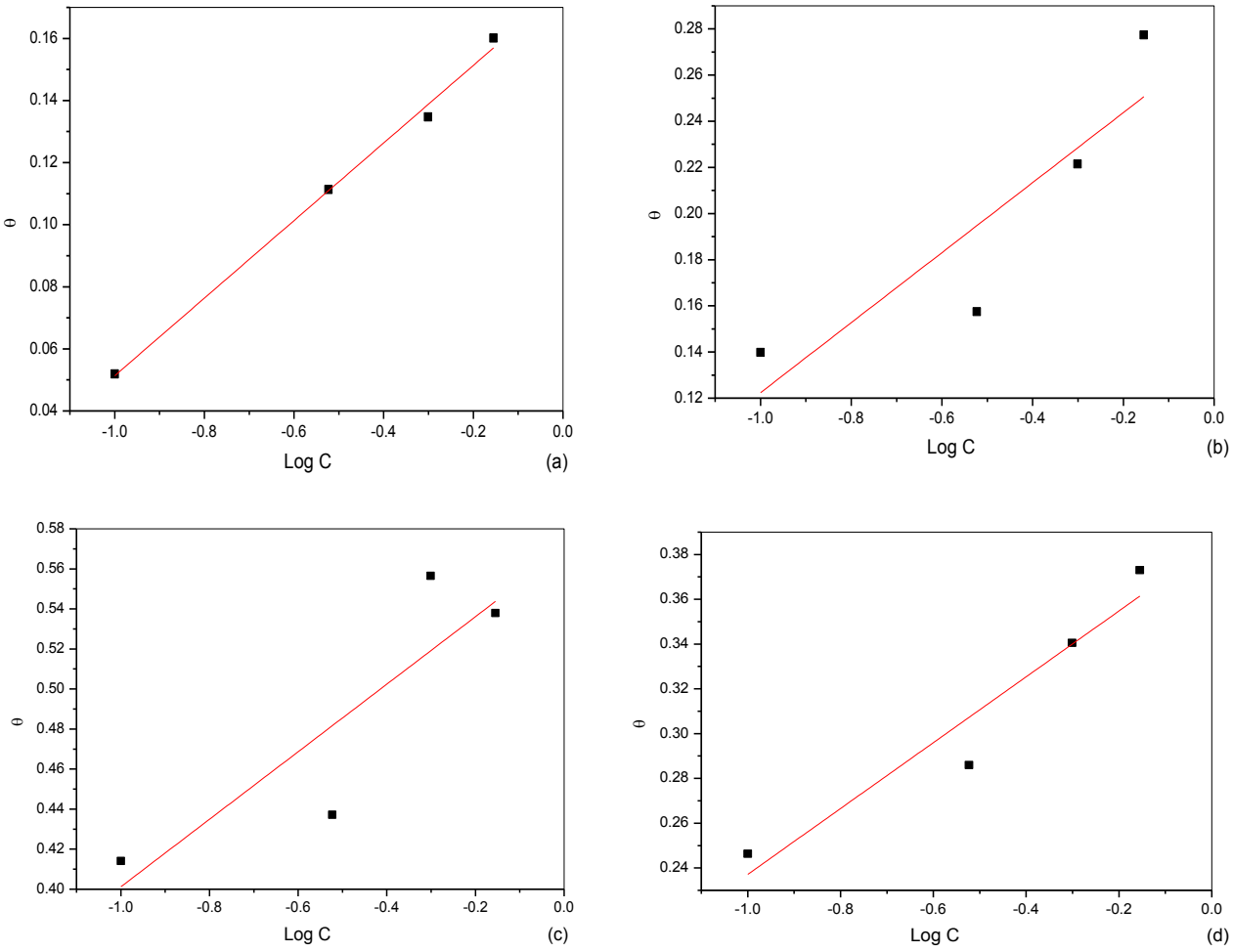

Figure 4.43: *Temkin Isotherm Plots of the Corrosion of Mild Steel in 1M HCL in the Presence of (a) Natural starch, (b) Physical modified starch, (c) Alkaline treated starch and (d) Acid treated starch.*

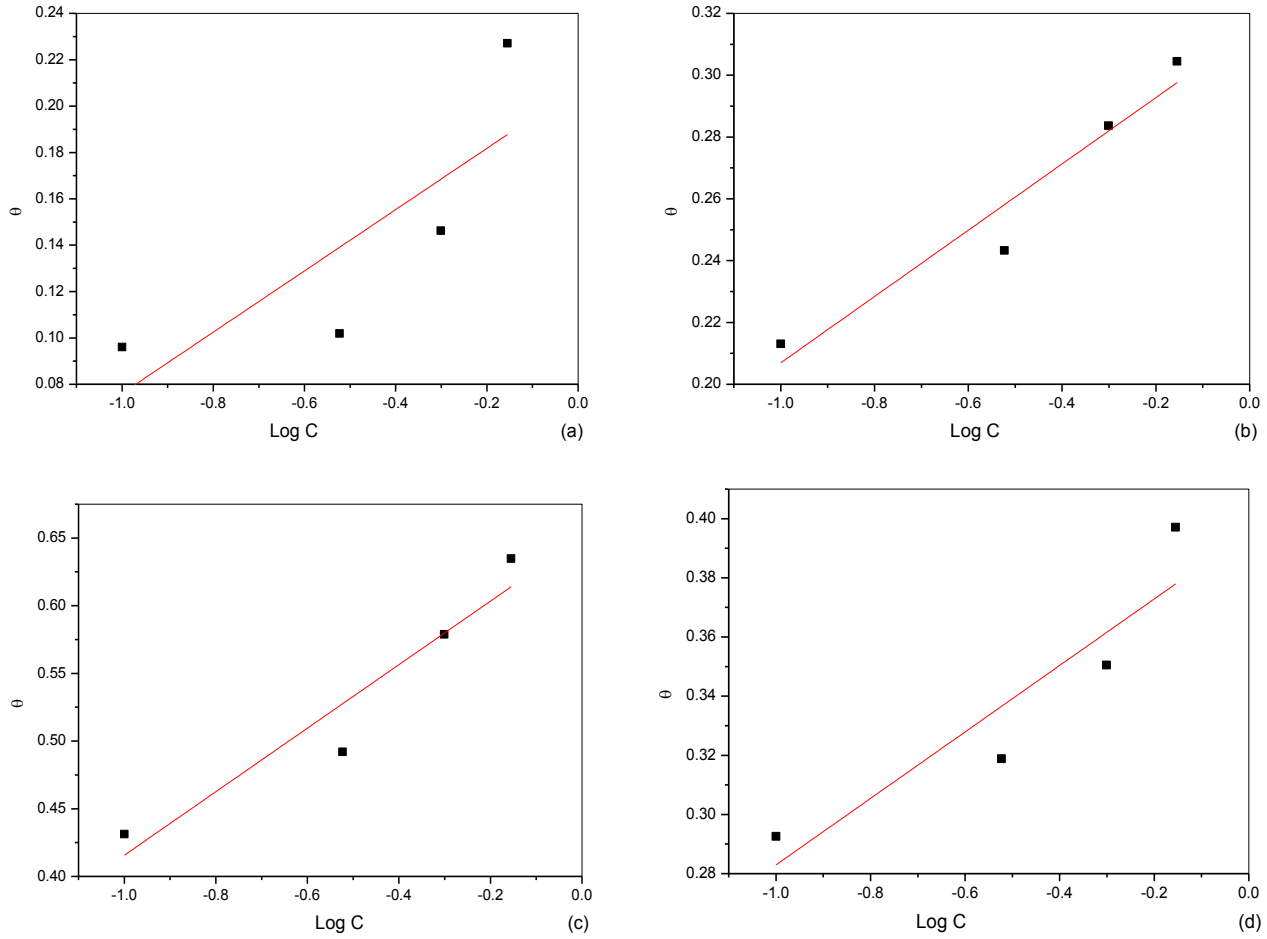

Figure 4.44: *Temkin Isotherm Plots of the Corrosion of Galvanised Steel in 0.25M H_2SO_4 in the Presence of (a) Natural starch, (b) Physical modified starch, (c) Alkaline treated starch and (d) Acid treated starch.*

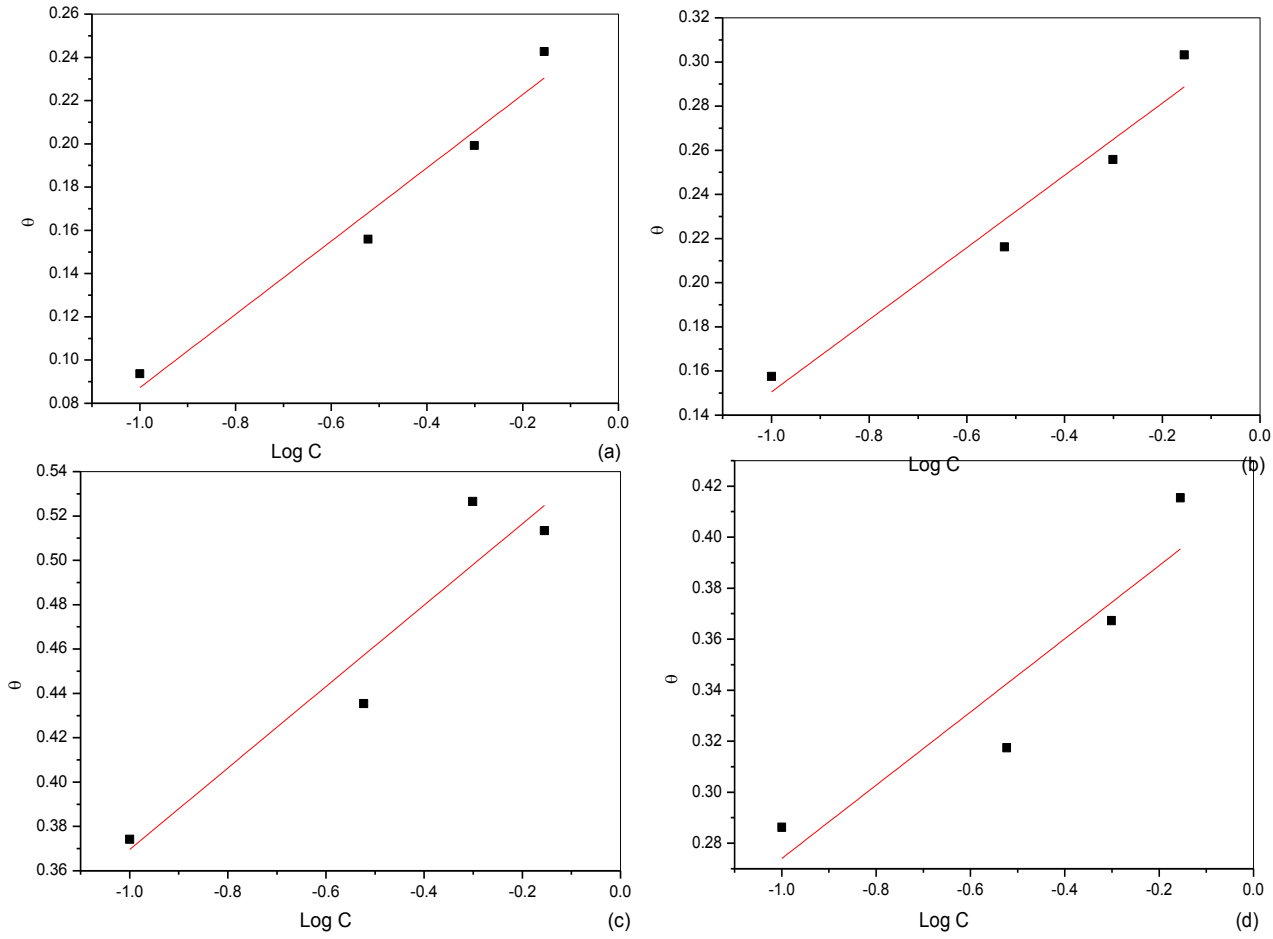

Figure 4.45: *Temkin Isotherm Plots of the Corrosion of Galvanised Steel in 1M HCL in the Presence of (a) Natural starch, (b) Physical modified starch, (c) Alkaline treated starch and (d) Acid treated starch.*

Table 4.19: Linear regression parameters for Langmuir, Freundlich and Temkin

Metal/ System	Inh.	Langmuir			Freundlich			Temkin		
		K	Slope	R^2	K	Slope	R^2	K	Slope	R^2
Mild Steel /H_2SO_4	NS	0.7167	1.8650	0.9262	0.2480	0.1298	0.8234	4.749	0.0638	0.7826
	PMS	0.8161	1.2670	0.7380	0.3396	0.4258	0.7590	4.7172	0.2099	0.6766
	ASS	4.5809	1.3187	0.9177	0.8704	0.5422	0.9428	4.2805	0.4887	0.9049
	ATS	3.3009	1.8731	0.9527	0.3949	0.0294	0.7253	$4.17x\ 10^6$	0.0259	0.7185
Mild steel / HCL	NS	0.5238	1.6587	0.7266	0.2045	0.5796	0.9776	4.1022	0.1249	0.9939
	PMS	0.8258	1.8145	0.8740	0.2820	0.3383	0.7587	6.0840	0.1518	0.5896
	ASS	9.6618	1.6960	0.9759	0.5746	0.1535	0.6747	29.318	0.1687	0.6473
	ATS	1.9964	1.7469	0.9105	0.3915	0.2118	0.9288	13.624	0.1471	0.8942
Galvanised steel/H_2SO_4	NS	0.6276	1.7562	0.7327	0.2106	0.3949	0.5761	4.8302	0.1322	0.4770
	PMS	1.0405	1.8031	0.8858	0.3189	0.1836	0.9347	2.9282	0.1073	0.9078
	ASS	7.7700	1.4334	0.9805	0.6605	0.1959	0.9159	15.971	0.2347	0.8810
	ATS	2.6103	1.7182	0.9158	0.3981	0.1447	0.8228	33.710	0.1124	0.7780
Galvanised steel/HCL	NS	0.7477	1.8975	0.8353	0.2827	0.4832	0.9974	4.5510	0.1694	0.9527
	PMS	0.9914	1.8038	0.5998	0.3289	0.3265	0.9821	6.8743	0.1635	0.9354
	ASS	9.3023	1.7747	0.9883	0.5623	0.1798	0.8860	20.383	0.1835	0.8579
	ATS	2.7495	1.8039	0.9477	0.4225	0.1826	0.8532	18.322	0.1436	0.8089

The Free energy of adsorption was calculated using the relation in equation 4.6 (Khamis, 1990).

$$\Delta G^{o}_{ads} = -RT(In\ 55.5\ K_{ads}) \quad \textbf{(4.7)}$$

Table 4.20 Calculated values of free energy of adsorption

Metal/ System	Inh.	Langmuir		
		K_{ads}	R^2	ΔG_{ads}(kJmol^{-1})
Mild Steel /H_2SO_4	NS	0.7167	0.9262	-9.43
	PMS	0.8161	0.7380	-9.77
	ASS	4.5809	0.9177	-14.18
	ATS	3.3009	0.9527	-13.34
Mild steel / HCL	NS	0.5238	0.7266	-8.63
	PMS	0.8258	0.8740	-9.80
	ASS	9.6618	0.9759	-16.09
	ATS	1.9964	0.9105	-12.06
Galvanised steel/H_2SO_4	NS	0.6276	0.7327	-9.09
	PMS	1.0405	0.8858	-10.39
	ASS	7.7700	0.9805	-15.54
	ATS	2.6103	0.9158	-12.74
Galvanised steel/HCL	NS	0.7477	0.8353	-9.54
	PMS	0.9914	0.5998	-10.26
	ASS	9.3023	0.9883	-15.99
	ATS	2.7495	0.9477	-12.88

From Table 4.20 the calculated ΔGads for all the inhibitor-acid system is negative. The negative value indicates that the adsorption of the inhibitor molecule on to the steel surface is a spontaneous process and that the layer adsorbed were stable (Bouklah, 2006). Generally, values of up to −20 kJ mol−1 are consistent with physisorption, while those around −40 kJ mol−1 or higher

values are associated with chemisorption as a result of the sharing or transfer of electrons from organic molecules to the metal surface to form a coordinate type of metal bonds [Hosseini *et al.;* 2003]. In the present study, the calculated values range between -7.93 and $-15.84\,\text{kJ mol}^{-1}$ (Table 4.20), indicating that the adsorption mechanism of the four inhibitors (NS, PMS, ASS and ATS) on mild steel in 0.25 M H_2SO_4 and 1 M HCL solutions at the studied temperatures is by physisorption.

4.8 Temperature Studies

Gravimetric studies under varying temperature (30-60^{o}C) for the corrosion of mild steel and galvanised steel in the presence and absence of the four inhibitors were investigated. Analysis of the temperature dependence of inhibition efficiency as well as comparison of corrosion apparent activation energies in absence and presence of inhibitor gives some insight into the possible mechanism of inhibitor adsorption. A decrease in inhibition efficiency with the rise in temperature with analogous increase in corrosion activation energy in the presence of inhibitor compared to its absence is frequently interpreted as being suggestive of formation of an adsorption film of physical (electrostatic) nature. The reverse effect, corresponding to an increase in inhibition efficiency with rise in temperature and lower activation energy in the presence of inhibitor, suggests a chemisorption mechanism [Popova et al 2003, Oguzie et al 2004, Ebenso 2003]. The effect of temperature on the inhibited acid-metal reaction is highly complex because many changes occur on the metal surface, such as rapid etching, desorption of inhibitor and the inhibitor itself may undergo decomposition and/or rearrangement (Noor and AL-Moubaraki 2008; Hassan 2007).

4.8.1 Corrosion of mild steel in 0.25M H_2SO_4

The calculated value of corrosion rates and inhibition efficiency for the four inhibitors at different concentrations and temperatures for mild steel is presented in Table 4.21. Plots of corrosion rate against varying temperature are presented in Figures 4.46 a – d. From the plots, it is observed that corrosion rate is reduced in the presence of the four inhibitors as compared to the free acid solution. Also the corrosion rate increased with increase in temperature at all concentrations for the four inhibitors with ASS exhibiting the least corrosion rate. The trend for the corrosion rates of the four inhibitors is ASS<ATS<PMS<NS.

The plot of inhibition efficiency as a function of temperature at 30–60^{o}C is presented in Figures 4.47a to d. The plots reveal that inhibition efficiency increased with increase in inhibitor concentration showing a maximum efficiency of 82.40% at 30^{o}C temperature in the presence of alkaline treated starch concentration of 0.7g/l. This behaviour illustrates that increased concentration increases the rate at which the inhibitor molecules are adsorbed on the surface of the coupon, leading to the formation of a protective film. Acid treated starch exhibited a maximum IE of 62.02%, physically modified starch exhibited an IE of 56.54 % while the unmodified starch had a maximum IE of 39.45 % at highest concentration of 0.7g/l.

On the other hand, a decrease in inhibition efficiency was observed with increasing temperature. This suggests possible desorption of some of the adsorbed starch molecules from the metal surface at higher temperatures. This

behaviour shows that the inhibitor was physically adsorbed on the metal surface. As the temperature increases, the quantity of equilibrium of adsorption decreases (Ebenso et al 1999) and as a result, the plot of higher temperatures is below the lower ones. This is clearly demonstrated in Figure 4.47, which shows that the four inhibitors are physically adsorbed on the steel surface since the plots of higher temperatures are under that of lower ones. The decrease in inhibition efficiency with increasing temperature may also be due to the fact that most of the effects at elevated temperatures are adverse to corrosion inhibition by increasing the corrosion rate and decreasing the tendency of the inhibitors to be adsorbed on the steel surface.

Mobin *et al.* 2011 studied the corrosion inhibition of mild steel in 0.1 M H_2SO_4 in presence of starch (polysaccharide) using weight loss and potentiodynamic polarization measurements in the temperature range of 30–60°C. Starch inhibited the corrosion rates of mild steel to a considerable extent; the maximum inhibition efficiency (%IE) being 66.21% at 30^{o}C in presence of starch concentration of 200 ppm and, inhibition efficiency decreased with increase in temperature.

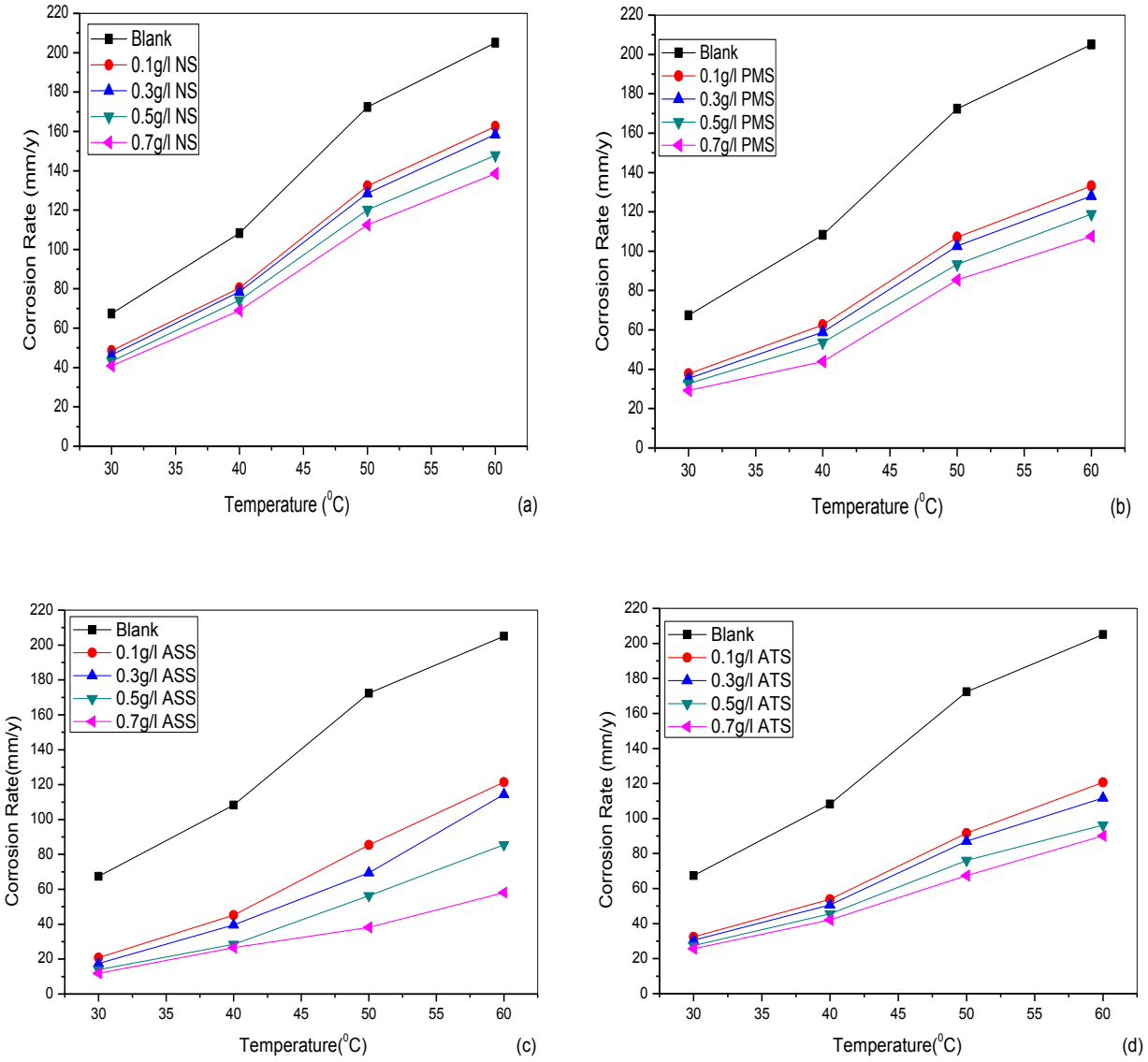

Figure 4.46: *Plots of Corrosion rate against Temperature for mild steel in 0.25M H_2SO_4 in the presence and absence of (a)Natural Starch, (b)Physically modified starch, (c)Alkaline steeped starch and (d) Acid Treated starch.*

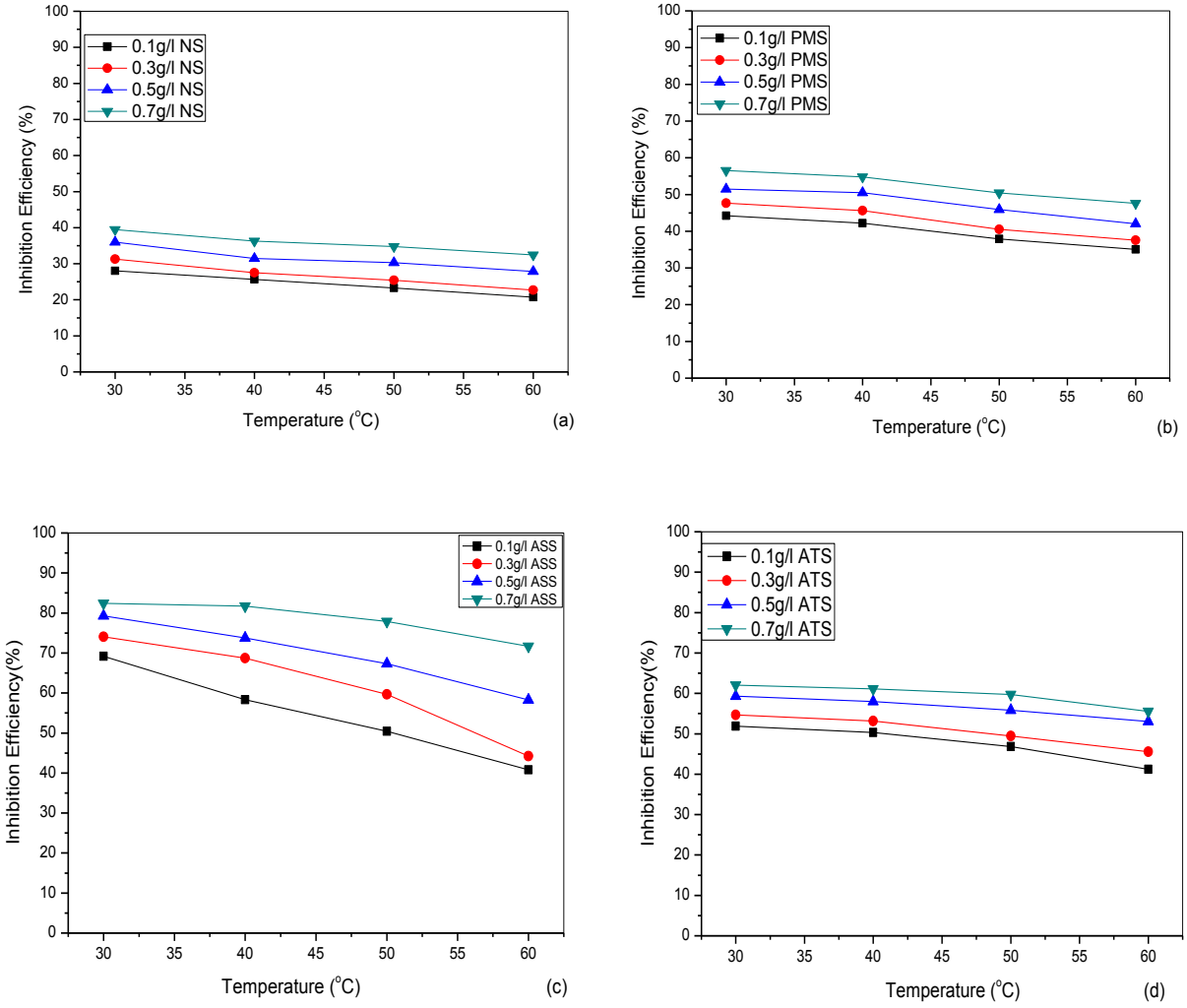

Figure 4.47: *Plots of Inhibition Efficiency against Temperature for mild steel in 0.25M H_2SO_4 in the presence and absence of (a)Natural Starch, (b)Physically modified starch, (c)Alkaline steeped starch and (d) Acid Treated starch*

Table 4.21 Calculated values of Corrosion rate, Inhibition efficiency and degree of surface coverage of mild steel in 0.25M H_2SO_4 in the presence and absence of NS, PMS, ASS and ATS corrosion inhibitors

	Corrosion Rate(mmy^{-1})				Inhibition Efficiency(%)				Degree of Surface Coverage(**Θ**)			
Temperature	30°C	40°C	50°C	60°C	30°C	40°C	50°C	60°C	30°C	40°C	50°C	60°C
InhibitorConc												
Blank	**67.42**	**108.3**	**172.4**	**205.1**	-	-	-	-	-	-	-	-
0.1g/l NS	**48.51**	**80.50**	**132.3**	**162.6**	**28.05**	**25.67**	**23.26**	**20.72**	**0.2805**	**0.2567**	**0.2326**	**0.2072**
0.3g/l NS	**46.32**	**78.51**	**128.6**	**158.5**	**31.30**	**27.51**	**25.41**	**22.72**	**0.3130**	**0.2751**	**0.2541**	**0.2272**
0.5g/l NS	**43.17**	**74.22**	**120.2**	**147.9**	**35.97**	**31.47**	**30.28**	**27.88**	**0.3597**	**0.3147**	**0.3028**	**0.2788**
0.7g/l NS	**40.82**	**69.00**	**112.5**	**138.5**	**39.45**	**36.29**	**34.75**	**32.47**	**0.3945**	**0.3629**	**0.3475**	**0.3247**
0.1g/l PMS	**37.61**	**62.61**	**107.1**	**133.2**	**44.22**	**42.19**	**37.88**	**35.06**	**0.4422**	**0.4219**	**0.3788**	**0.3506**
0.3g/l PMS	**35.31**	**58.91**	**102.6**	**128.1**	**47.63**	**45.61**	**40.49**	**37.54**	**0.4763**	**0.4561**	**0.4049**	**0.3754**
0.5g/l PMS	**32.71**	**53.61**	**93.31**	**118.9**	**51.48**	**50.50**	**45.88**	**42.03**	**0.5148**	**0.5050**	**0.4588**	**0.4203**
0.7g/l PMS	**29.30**	**43.96**	**85.41**	**107.5**	**56.54**	**54.80**	**50.46**	**47.59**	**0.5654**	**0.5480**	**0.5056**	**0.4759**
0.1g/l ASS	**20.76**	**45.14**	**85.40**	**121.4**	**69.21**	**58.33**	**50.46**	**40.79**	**0.6921**	**0.5833**	**0.5046**	**0.4079**
0.3g/l ASS	**17.50**	**39.61**	**69.51**	**114.4**	**74.04**	**68.71**	**59.68**	**44.21**	**0.7404**	**0.6871**	**0.5968**	**0.4421**
0.5g/l ASS	**13.98**	**28.41**	**56.32**	**85.54**	**79.26**	**73.77**	**67.33**	**58.29**	**0.7926**	**0.7377**	**0.6733**	**0.5829**
0.7g/l ASS	**11.88**	**26.61**	**38.14**	**58.10**	**82.40**	**81.71**	**77.88**	**71.67**	**0.8240**	**0.8171**	**0.7788**	**0.7167**
0.1g/l ATS	**32.42**	**53.84**	**91.70**	**120.6**	**51.91**	**50.30**	**46.81**	**41.20**	**0.5191**	**0.5030**	**0.4681**	**0.4120**
0.3g/l ATS	**30.54**	**50.75**	**87.14**	**111.7**	**54.70**	**53.16**	**49.45**	**45.54**	**0.5470**	**0.5316**	**0.4945**	**0.4554**
0.5g/l ATS	**27.41**	**45.52**	**76.11**	**96.32**	**59.34**	**57.97**	**55.85**	**53.03**	**0.5934**	**0.5797**	**0.5585**	**0.5303**
0.7g/l ATS	**25.61**	**42.09**	**67.41**	**90.14**	**62.02**	**61.14**	**59.73**	**55.56**	**0.6202**	**0.6114**	**0.5973**	**0.5556**

4.8.2 Corrosion of mild steel in 1M HCL

Data on the calculated values of the corrosion rates, inhibition efficiency and degree of surface coverage of mild steel corrosion in the presence and the absence of the four inhibitors in 1 M HCL is presented in Table 4.22. Graphical illustrations of these data are presented in Figures 4.48a-d and Figures 4.49a-d.

From Figures 4.47a-d, it was observed that corrosion rates decreased with increase in concentration of the inhibitor and increased with increase in temperature for the four inhibitors. Following this trend, for the corrosion rates ASS recorded the least corrosion rate values at all concentration.

Plots of inhibition efficiency against temperature for the four inhibitors at varying concentration are presented in Figure 4.48a-d which shows that inhibition efficiency increased with increasing concentration of the inhibitor. NS exhibited the least inhibition efficiency and ASS exhibited the maximum inhibition efficiency of 65.10% at inhibitor concentration of 0.7g/l.

Secondly, inhibition efficiency decreased with increase in temperature. For ASS inhibitor, the decrease in the inhibition efficiency at all concentration was slight as compared to the other three inhibitors with profound decrease in inhibition efficiency.

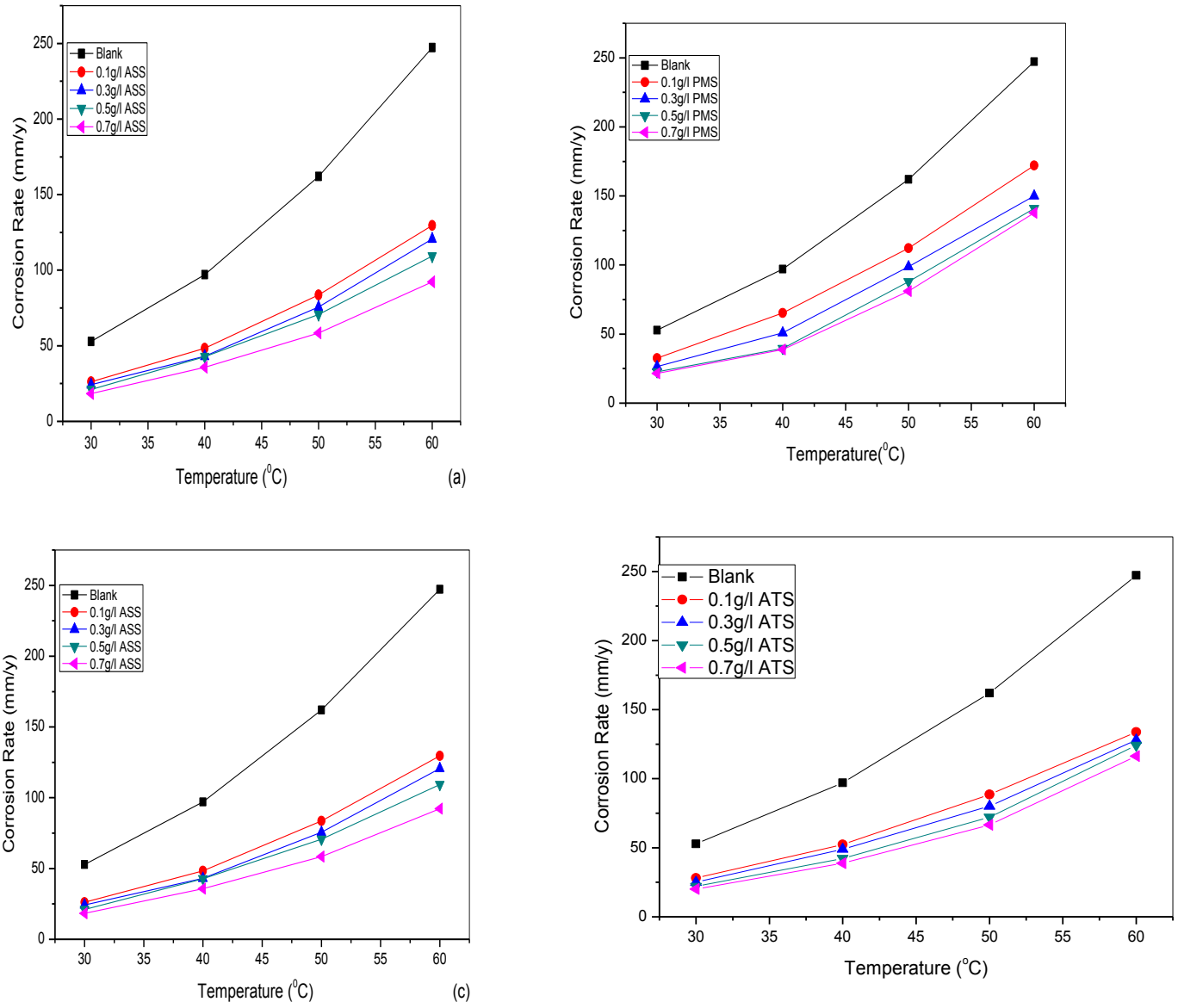

Figure 4.48: *Plots of Corrosion rate against Temperature for mild steel in 1MHCl in the presence and absence of (a) Natural Starch, (b)Physically modified starch, (c)Alkaline steeped starch and (d)Acid Treated starch.*

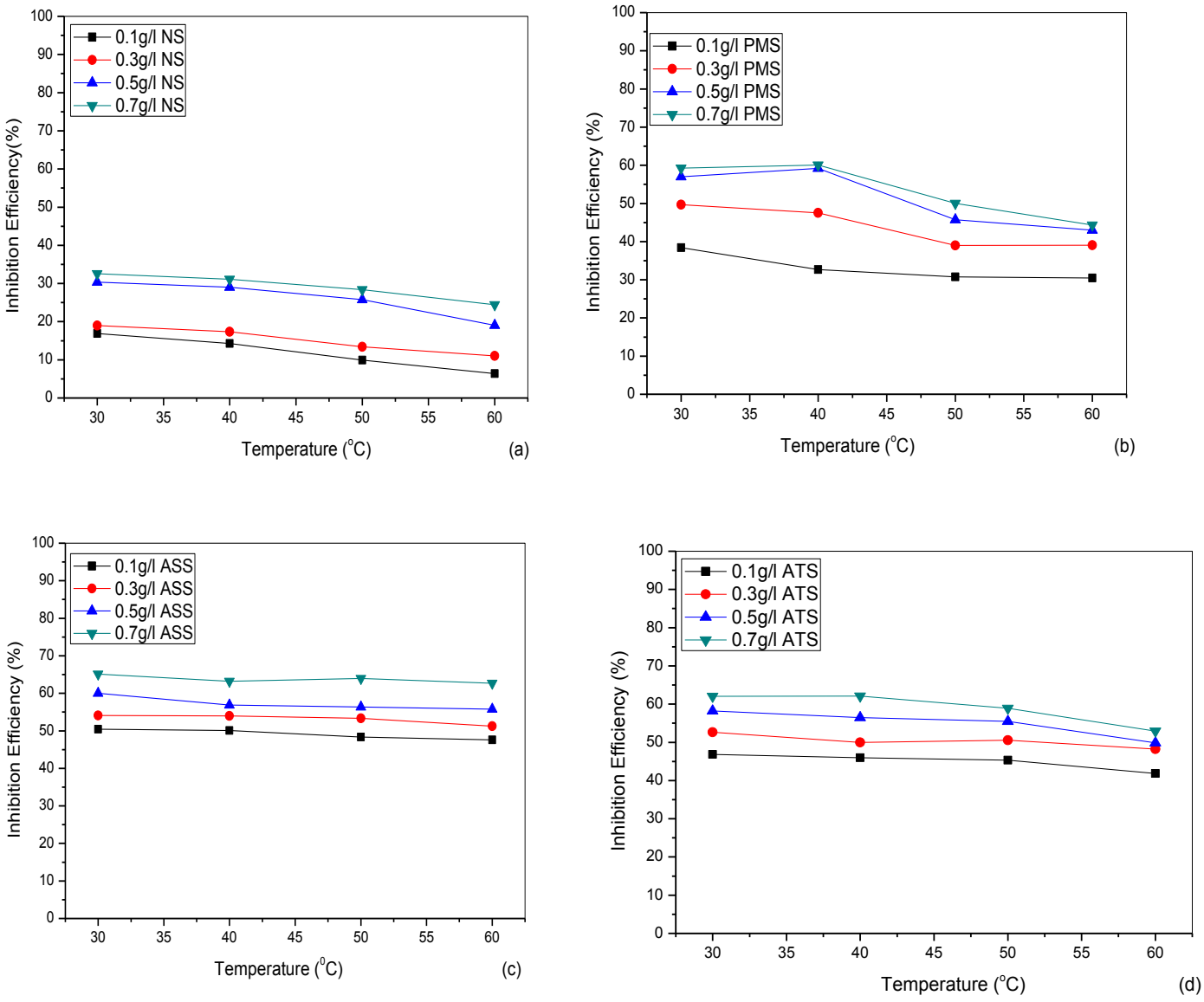

Figure 4.49: *Plots of Inhibition Efficiency against Temperature for mild steel in 1MHCl in the presence and absence of (a) Natural starch, (b) Physically modified starch, (c) Alkaline steeped starch and (d) Acid treated starch*

Table 4.22: Calculated values of Corrosion rate, Inhibition efficiency and degree of surface coverage of mild steel in 1 M HCl in the presence and absence of NS, PMS, ASS and ATS corrosion inhibitors

	Corrosion Rate(mmy^{-1})				Inhibition Efficiency(%)				Degree of Surface Coverage(Θ)			
Temperature	30ºC	40ºC	50ºC	60ºC	30ºC	40ºC	50ºC	60ºC	30ºC	40ºC	50ºC	60ºC
InhibitorConc												
Blank	**52.79**	**97.02**	**162.0**	**247.3**	-	-	-	-	-	-	-	-
0.1g/l NS	**43.87**	**83.19**	**145.9**	**231.5**	**16.90**	**14.26**	**9.94**	**6.39**	**0.1690**	**0.1496**	**0.0994**	**0.0639**
0.3g/l NS	**42.78**	**80.21**	**140.3**	**220.1**	**18.96**	**17.33**	**13.40**	**11.00**	**0.1896**	**0.1733**	**0.1340**	**0.1100**
0.5g/l NS	**36.76**	**68.86**	**120.3**	**200.2**	**30.37**	**29.02**	**25.74**	**19.05**	**0.3037**	**0.2902**	**0.2574**	**0.1905**
0.7g/l NS	**35.59**	**66.86**	**116.0**	**186.8**	**32.58**	**31.09**	**28.40**	**24.46**	**0.3258**	**0.3109**	**0.2840**	**0.2446**
0.1g/l PMS	**32.49**	**65.31**	**112.2**	**172.0**	**38.45**	**32.68**	**30.76**	**30.47**	**0.3845**	**0.3268**	**0.3076**	**0.3047**
0.3g/l PMS	**26.56**	**50.91**	**98.80**	**150.1**	**49.69**	**47.53**	**39.00**	**39.06**	**0.4969**	**0.4753**	**0.3900**	**0.3906**
0.5g/l PMS	**22.69**	**39.57**	**88.00**	**141.0**	**57.02**	**59.21**	**45.72**	**43.00**	**0.5702**	**0.5921**	**0.4572**	**0.4300**
0.7g/l PMS	**21.51**	**38.72**	**81.00**	**137.7**	**59.25**	**60.09**	**50.04**	**44.33**	**0.5925**	**0.6009**	**0.5004**	**0.4433**
0.1g/l ASS	**26.18**	**48.41**	**83.70**	**129.6**	**50.41**	**50.10**	**48.34**	**47.58**	**0.5041**	**0.501**	**0.4834**	**0.4758**
0.3g/l ASS	**24.23**	**43.07**	**75.60**	**120.6**	**54.10**	**53.95**	**53.35**	**51.25**	**0.5410**	**0.5395**	**0.5335**	**0.5125**
0.5g/l ASS	**21.12**	**42.85**	**70.70**	**109.4**	**59.99**	**56.86**	**56.38**	**55.78**	**0.5999**	**0.5686**	**0.5638**	**0.5578**
0.7g/l ASS	**18.42**	**35.71**	**58.40**	**92.30**	**65.10**	**63.19**	**63.97**	**62.70**	**0.6510**	**0.6319**	**0.6397**	**0.6270**
0.1g/l ATS	**28.05**	**52.41**	**88.60**	**133.8**	**46.86**	**45.98**	**45.30**	**41.83**	**0.4686**	**0.4598**	**0.453**	**0.4183**
0.3g/l ATS	**25.00**	**48.94**	**80.10**	**128.0**	**52.64**	**49.96**	**50.58**	**48.25**	**0.5264**	**0.4995**	**0.5058**	**0.4825**
0.5g/l ATS	**22.07**	**42.25**	**72.10**	**124.1**	**58.19**	**56.45**	**55.49**	**49.84**	**0.5819**	**0.5645**	**0.5549**	**0.4984**
0.7g/l ATS	**20.05**	**38.78**	**66.6**	**116.4**	**62.02**	**62.09**	**58.91**	**52.93**	**0.6202**	**0.6209**	**0.5891**	**0.5293**

4.8.3 Corrosion of galvanised steel in 0.25M H_2SO_4

Data of the calculated corrosion rates, inhibition efficiency and degree of surface coverage are presented in Table 4.23. Plots of corrosion rate against temperature for the four inhibitors, is presented in Figures 4.50a-d. From the plots, it is observed that corrosion rate decreased with increasing inhibitor concentration and increased with increasing temperature. This indicates that there is adsorption of the inhibitor molecules on the surface of the metal which retards corrosion rate. However, increase in temperature results in desorption of some of the inhibitor molecules on the metal surface and this results in increased corrosion rate at higher temperature.

Graphical illustration of the inhibition efficiency of the four inhibitors in the corrosion studies of galvanised steel in 0.25 M H_2SO_4 is presented in Figures 4.51a-d. From the plots, it is observed that inhibition efficiency increased with increase in inhibitor concentration and decreased with increase in temperature. NS exhibited the minimum inhibition efficiency at all concentration while the maximum inhibition efficiency of 84.07% was attained by ASS at concentration of 0.7g/l.

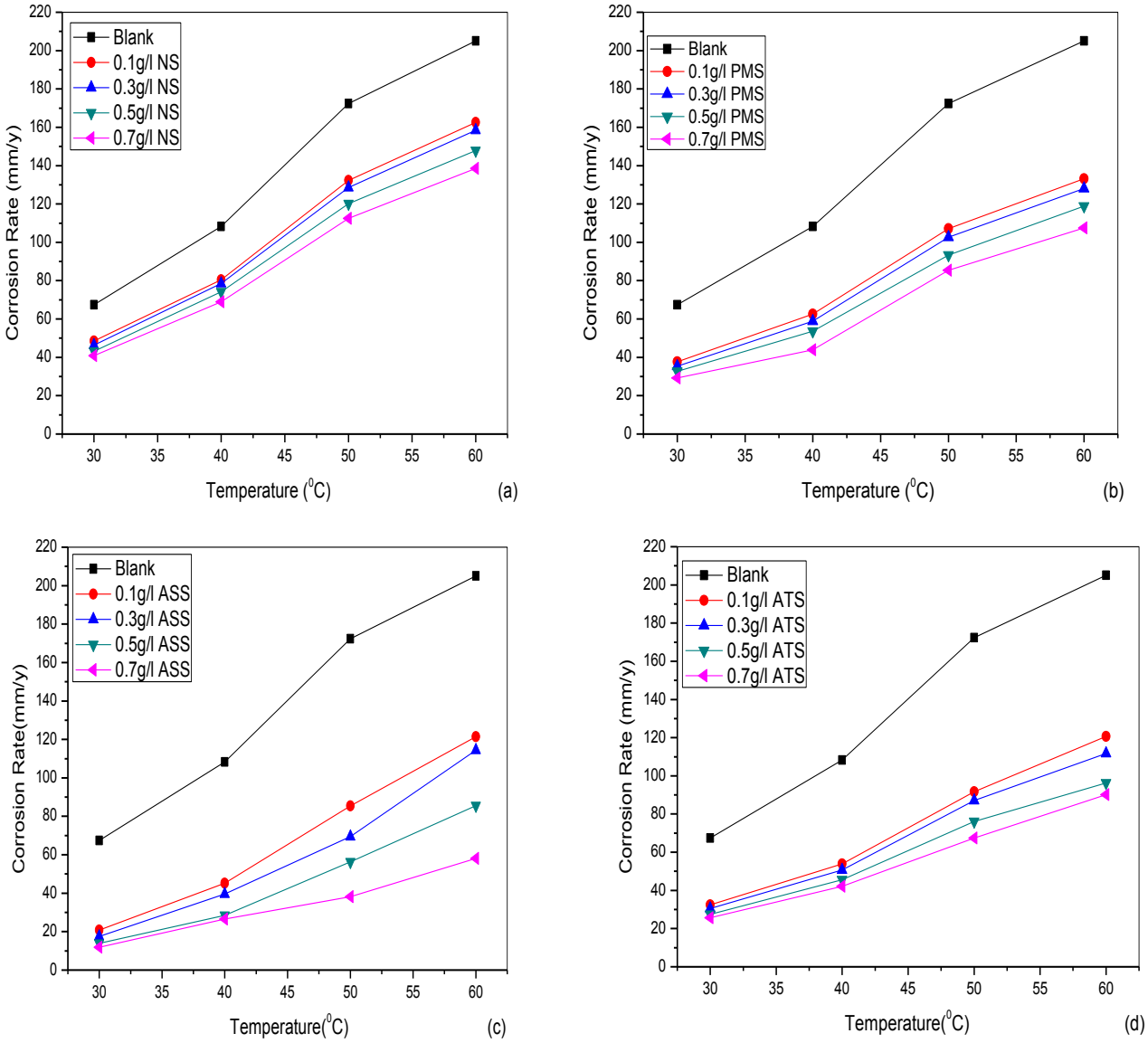

Figures 4.50: *Plots of Corrosion rate against Temperature for mild steel in 0.25M H_2SO_4 in the presence and absence of (a)Natural Starch, (b)Physically modified starch, (c)Alkaline steeped starch and (d) Acid Treated starch.*

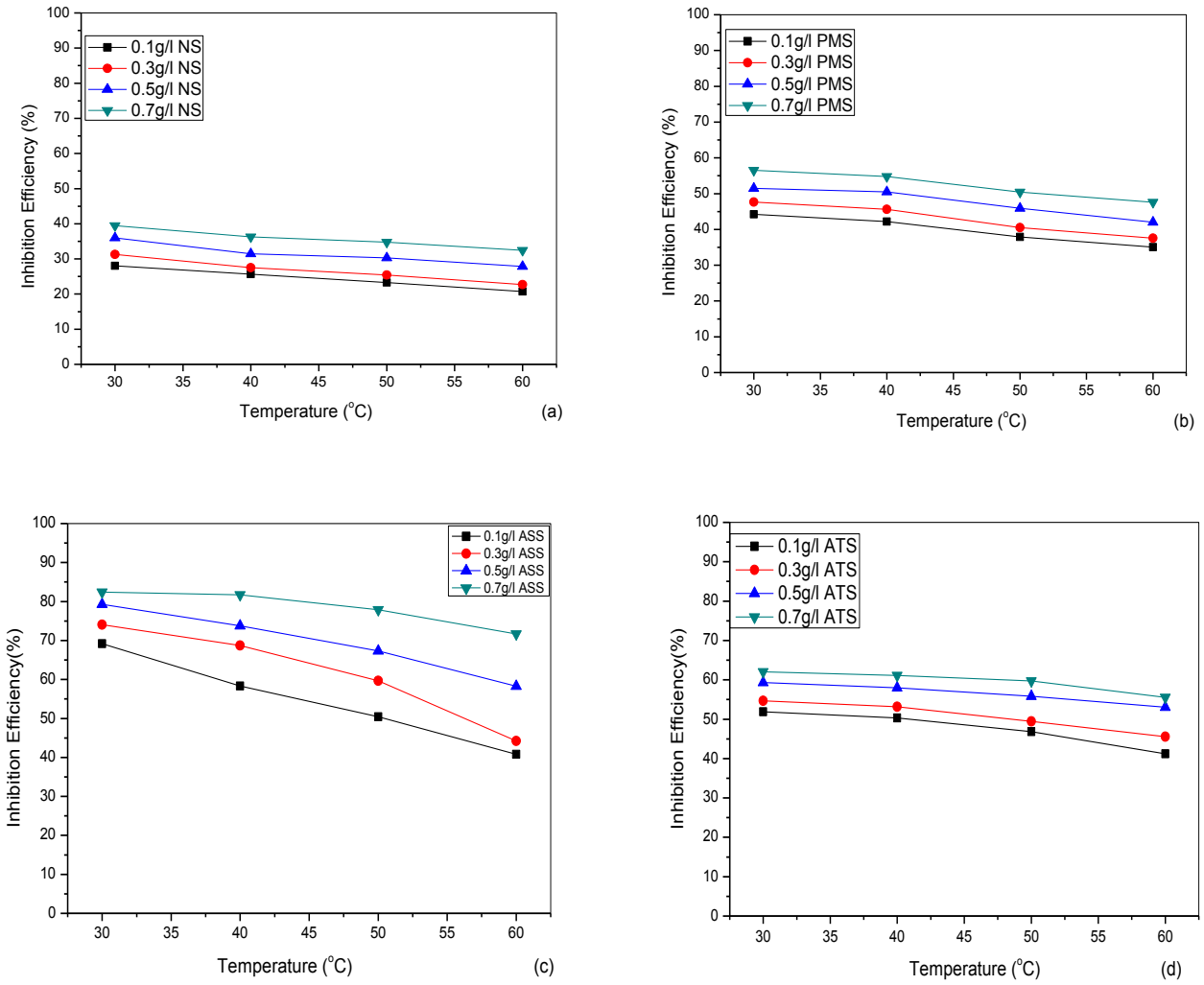

Figures 4.51: *Plots of Inhibition Efficiency against Temperature for mild steel in 0.25M H_2SO_4 in the presence and absence of (a)Natural Starch, (b)Physically modified starch, (c)Alkaline steeped starch and (d) Acid Treated starch*

Table 4.23 Calculated values of Corrosion rate, Inhibition efficiency and degree of surface coverage of galvanised steel in 0.25 M H_2SO_4 in the presence and absence of NS, PMS, ASS and ATS corrosion

	Corrosion Rate(mmy^{-1})				Inhibition Efficiency(%)				Degree of Surface Coverage(Θ)			
Temperature	30°C	40°C	50°C	60°C	30°C	40°C	50°C	60°C	30°C	40°C	50°C	60°C
InhibitorConc												
Blank	**87.53**	**161.32**	**207.32**	**289.71**	-	-	-	-	-	-	-	-
0.1g/l NS	**76.42**	**143.61**	**188.43**	**265.52**	**12.69**	**10.97**	**9.12**	**8.35**	**0.1269**	**0.1097**	**0.0912**	**0.0835**
0.3g/l NS	**75.63**	**142.51**	**186.21**	**261.22**	**13.60**	**11.76**	**10.18**	**9.84**	**0.1360**	**0.1176**	**0.1018**	**0.0984**
0.5g/lNS	**67.31**	**126.78**	**168.71**	**242.81**	**23.10**	**21.39**	**18.62**	**16.19**	**0.2310**	**0.2139**	**0.1862**	**0.1619**
0.7g/l NS	**59.92**	**113.24**	**150.92**	**219.92**	**31.54**	**29.16**	**27.20**	**24.09**	**0.3154**	**0.2916**	**0.2720**	**0.2409**
0.1g/l PMS	**55.12**	**103.41**	**139.51**	**209.46**	**37.03**	**35.90**	**32.71**	**27.70**	**0.3703**	**0.3590**	**0.3271**	**0.2770**
0.3g/l PMS	**51.64**	**98.87**	**132.21**	**198.32**	**41.00**	**38.72**	**36.22**	**31.55**	**0.4100**	**0.3872**	**0.3622**	**0.3155**
0.5g/l PMS	**47.54**	**92.91**	**124.54**	**187.88**	**45.69**	**42.41**	**39.93**	**35.15**	**0.4569**	**0.4241**	**0.3993**	**0.3515**
0.7g/l PMS	**42.61**	**85.31**	**116.23**	**174.44**	**51.39**	**47.12**	**43.94**	**39.79**	**0.5139**	**0.4712**	**0.4394**	**0.3979**
0.1g/l ASS	**26.70**	**58.41**	**98.34**	**155.30**	**69.50**	**63.79**	**52.57**	**46.40**	**0.6950**	**0.6379**	**0.5257**	**0.4640**
0.3g/l ASS	**22.30**	**50.31**	**85.44**	**142.39**	**74.52**	**68.81**	**58.79**	**50.85**	**0.7452**	**0.6881**	**0.5879**	**0.5085**
0.5g/l ASS	**16.08**	**38.45**	**68.32**	**119.93**	**81.63**	**76.17**	**67.05**	**58.60**	**0.8163**	**0.7617**	**0.6705**	**0.6705**
0.7g/l ASS	**13.94**	**30.11**	**55.45**	**102.00**	**84.07**	**81.34**	**73.25**	**64.79**	**0.8407**	**0.8134**	**0.7325**	**0.6479**
0.1g/l ATS	**48.61**	**91.05**	**120.63**	**176.62**	**44.46**	**43.56**	**41.81**	**39.04**	**0.4446**	**0.4356**	**0.4181**	**0.3904**
0.3g/l ATS	**45.75**	**88.93**	**118.45**	**170.22**	**47.73**	**44.87**	**42.87**	**41.24**	**0.4773**	**0.4487**	**0.4287**	**0.4124**
0.5g/l ATS	**43.90**	**78.53**	**108.11**	**162.44**	**53.27**	**51.32**	**47.85**	**43.93**	**0.5327**	**0.5132**	**0.4785**	**0.4393**
0.7g/l ATS	**37.19**	**70.35**	**100.46**	**154.75**	**57.51**	**56.39**	**51.51**	**46.58**	**0.5751**	**0.5639**	**0.5151**	**0.4658**

4.8.4 Corrosion of galvanised steel in 1M HCL

Data on the calculated values of the corrosion rates, inhibition efficiency and degree of surface coverage of galvanised steel corrosion in the presence and the absence of the four inhibitors in 1M HCL is presented in Table 4.24. Graphical illustrations of these data are presented in Figures 4.52a-d and Figures 4.53a-d.

From Figures 4.52a-d, corrosion rates decreased with increase in concentration of the inhibitor and increased with increase in temperature for the four inhibitors. ASS recorded the least corrosion rate values at all concentration while NS had the highest corrosion rate values.

Plots of inhibition efficiency against temperature for the four inhibitors at varying concentration are presented in Figure 4.53 a-d. Figure 4.53 shows that inhibition efficiency increased with increasing concentration of the inhibitor. NS exhibited the least inhibition efficiency and ASS exhibited the maximum inhibition efficiency of 62.81% at inhibitor concentration of 0.7g/l. However, inhibition efficiency decreased with increase in temperature.

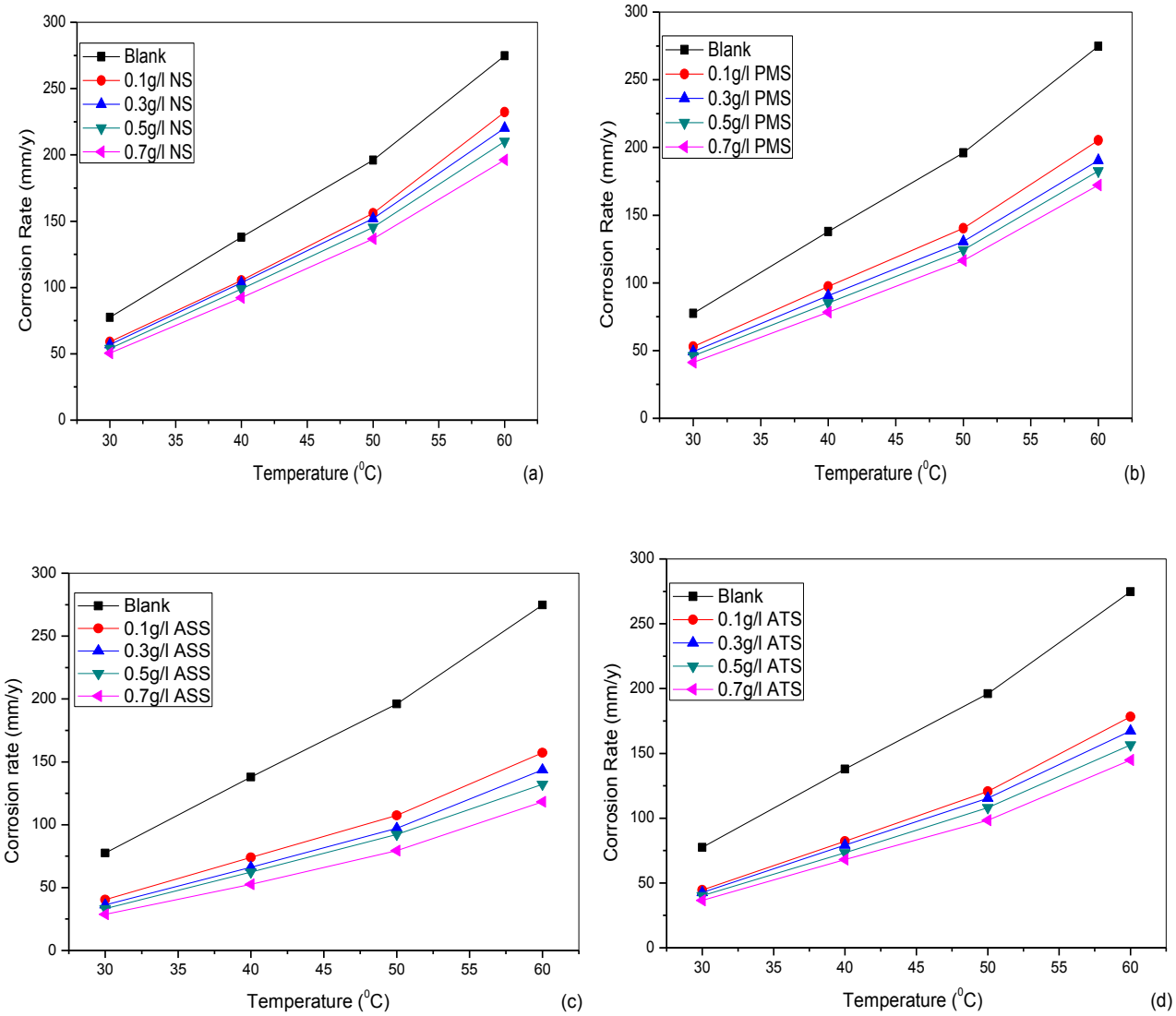

Figures 4.52: *Plots of Corrosion rate against Temperature for galvanised steel in 1M HCL in the presence and absence of (a) Natural Starch, (b) Physically modified starch, (c) Alkaline steeped starch and (d) Acid treated starch.*

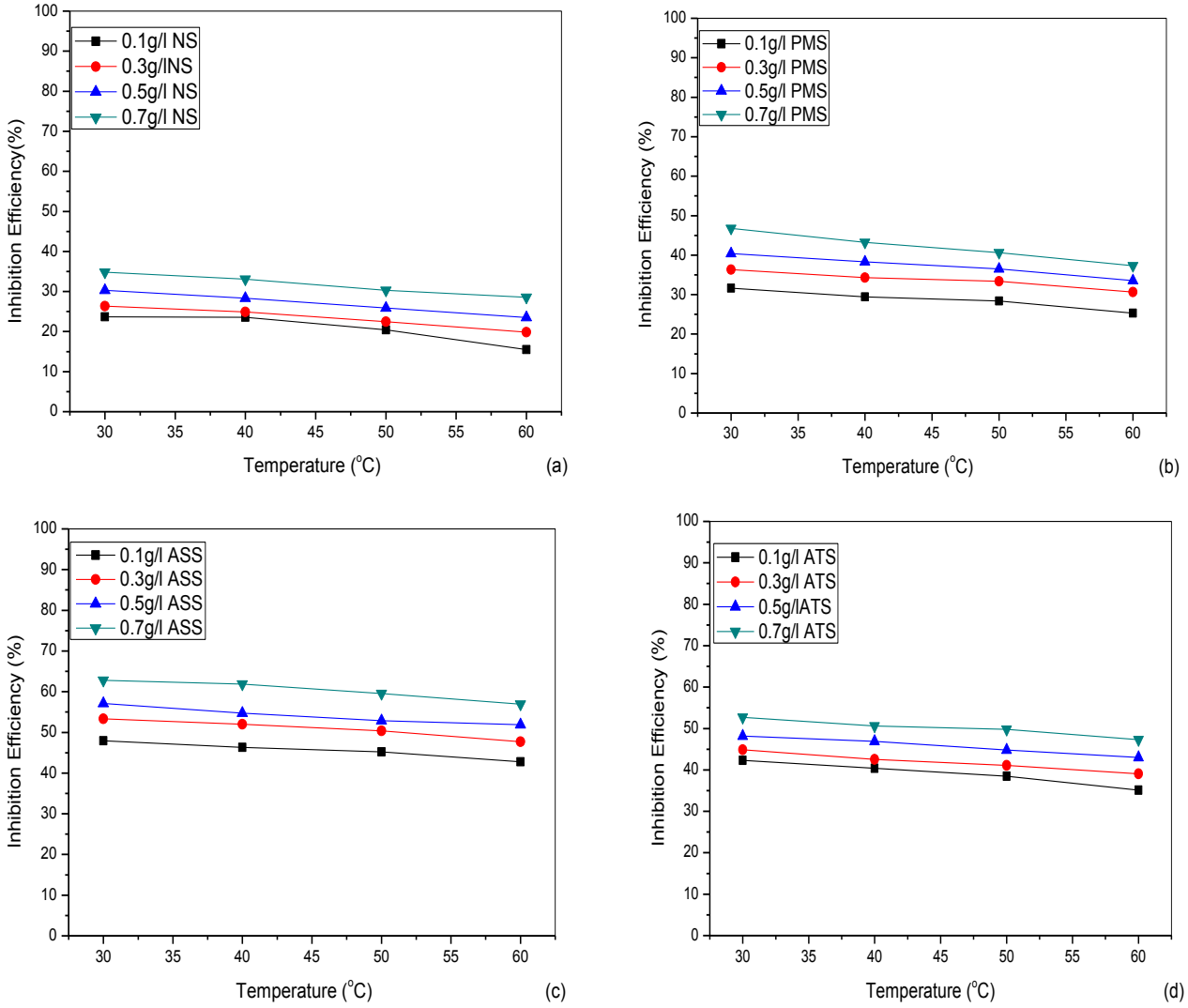

***Figures 4.53**: Plots of Inhibition Efficiency against Concentration for galvanised steel in 1M HCL in the presence and absence of (a) Natural Starch, (b) Physically modified starch, (c) Alkaline steeped starch and (d) Acid treated starch.*

Table 4.24: Calculated values of Corrosion rate, Inhibition efficiency and degree of surface coverage of galvanised steel in 1 M HCl in the presence and absence of NS, PMS, ASS and ATS corrosion inhibitors

	Corrosion Rate(mmy^{-1})				Inhibition Efficiency(%)				Degree of Surface Coverage(**Θ**)			
Temperature	30°C	40°C	50°C	60°C	30°C	40°C	50°C	60°C	30°C	40°C	50°C	60°C
InhibitorConc												
Blank	**77.44**	**137.9**	**196.0**	**274.7**	-	-	-	-	-	-	-	-
0.1g/l NS	**59.10**	**105.4**	**156.0**	**232.2**	**23.68**	**23.57**	**20.41**	**15.47**	**0.2368**	**0.2357**	**0.2041**	**0.1547**
0.3g/l NS	**57.02**	**103.6**	**152.0**	**220.2**	**26.37**	**24.87**	**22.45**	**19.84**	**0.2637**	**0.2487**	**0.2245**	**0.1984**
0.5g/l NS	**53.96**	**98.88**	**145.3**	**210.1**	**30.32**	**28.30**	**25.87**	**23.52**	**0.3032**	**0.2830**	**0.2587**	**0.2352**
0.7g/l NS	**50.49**	**92.30**	**136.6**	**196.2**	**34.80**	**33.07**	**30.30**	**28.58**	**0.3480**	**0.3307**	**0.3030**	**0.2858**
0.1g/l PMS	**52.94**	**97.32**	**140.4**	**205.2**	**31.64**	**29.43**	**28.37**	**25.30**	**0.3164**	**0.2943**	**0.2837**	**0.2530**
0.3g/l PMS	**49.31**	**90.62**	**130.6**	**190.5**	**36.32**	**34.29**	**33.37**	**30.65**	**0.3632**	**0.3429**	**0.3337**	**0.3065**
0.5g/l PMS	**46.18**	**85.10**	**124.4**	**182.6**	**40.37**	**38.29**	**36.53**	**33.53**	**0.4037**	**0.3829**	**0.3653**	**0.3353**
0.7g/l PMS	**41.23**	**78.32**	**116.4**	**172.2**	**46.78**	**43.21**	**40.61**	**37.31**	**0.4678**	**0.4321**	**0.4061**	**0.3731**
0.1g/l ASS	**40.32**	**74.02**	**107.4**	**157.2**	**47.93**	**46.32**	**45.20**	**42.77**	**0.4793**	**0.4632**	**0.4520**	**0.4277**
0.3g/l ASS	**36.14**	**66.21**	**97.24**	**143.6**	**53.33**	**51.99**	**50.39**	**47.73**	**0.5333**	**0.5199**	**0.5039**	**0.4773**
0.5g/l ASS	**33.21**	**62.42**	**92.32**	**132.2**	**57.12**	**54.74**	**52.90**	**51.87**	**0.5712**	**0.5474**	**0.5290**	**0.5187**
0.7g/l ASS	**28.80**	**52.61**	**79.32**	**118.3**	**62.81**	**61.85**	**59.53**	**56.93**	**0.6281**	**0.6185**	**0.5953**	**0.5693**
0.1g/l ATS	**44.66**	**82.20**	**120.6**	**178.3**	**42.33**	**40.39**	**38.47**	**35.09**	**0.4233**	**0.4039**	**0.3847**	**0.3509**
0.3g/l ATS	**42.72**	**79.20**	**115.4**	**167.4**	**44.84**	**42.57**	**41.12**	**39.06**	**0.4484**	**0.4257**	**0.4112**	**0.3906**
0.5g/l ATS	**40.15**	**73.25**	**108.2**	**156.6**	**48.15**	**46.88**	**44.80**	**42.99**	**0.4815**	**0.4688**	**0.4480**	**0.4299**
0.7g/l ATS	**36.61**	**68.13**	**98.36**	**144.8**	**52.72**	**50.59**	**49.82**	**47.29**	**0.5272**	**0.5059**	**0.4982**	**0.4729**

4.9 Thermodynamics Studies

Analysis of the temperature dependence of inhibition efficiency as well as comparison of corrosion apparent activation energies in absence and presence of inhibitor gives some insight into the possible mechanism of inhibitor adsorption. A decrease in inhibition efficiency with the rise in temperature with analogous increase in corrosion activation energy in the presence of inhibitor compared to

its absence is frequently interpreted as being suggestive of formation of an adsorption film of physical (electrostatic) nature. The reverse effect, corresponding to an increase in inhibition efficiency with rise in temperature and lower activation energy in the presence of inhibitor, suggests a chemisorptions mechanism [Ebenso; 2003, Oguzie *et al*.; 2004 & Popova *et al*.; 2003].

In examining the effect of temperature in the corrosion process in the presence of Inhibitors, parameters such as Activation energy (Ea), Enthalpy change, Entropy change and are deduced by applying the appropriate equations or plotting the appropriate graphs.

Plots of the logarithm of corrosion rate (log CR) versus reciprocal of absolute temperature (1/T) for the corrosion of mild steel and galvanised steel in the presence and absence of the four inhibitors in both 0.25 M H_2SO_4 and 1 M HCL media, are presented in Figure 4.54 - 4.57. Linear plots were obtained which indicates that it follows Arrhenius equation given as:

$$\log CR = \log A - \frac{E_a}{2.303RT} \qquad (4.8)$$

where CR is the corrosion rate, A is the Arrhenius constant, Ea is the apparent activation energy, R is the molar gas constant and T is the absolute temperature. The values of Ea obtained from the slope of the linear plot are presented in Table4.25 - 4.28. The increases in Ea values in the presence of the four inhibitors compared to the blank indicate the decrease in adsorption process of the inhibitor

on the metal surfaces with rise in temperature and a corresponding increase in reaction rate of greater area of metal that is exposed to acid [Quarashi & Sharma (2005)]. This shows physical adsorption [Martinez & Stern 2001].

Comparison of the data obtained for the activation energy of mild steel and galvanised steel shows that the highest value of Ea was attained by the corrosion of galvanised steel in ASS/ 0.25M H_2SO_4 system.

Plots of logarithm of corrosion rate/absolute temperature (log CR/T) versus reciprocal of absolute temperature (1/T) for the corrosion of mild steel and galvanised steel in the presence and absence of the four inhibitors in both 0.25 M H_2SO_4 and 1M HCL media, are presented in Figure 4.58 - 4.61. Enthalpy of adsorption, ΔH and entropy of adsorption, ΔS for the corrosion of the metals were obtained by the equation:

$$CR = \frac{RT}{Nh} exp\left(\frac{\Delta S}{R}\right) exp\left(-\frac{\Delta H}{RT}\right) \qquad (4.9)$$

where N is the Avogadro's number, h is the Planck's constant, R is the molar gas constant, and T is the absolute temperature

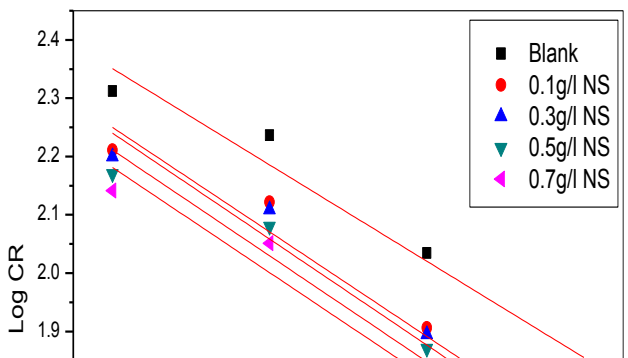

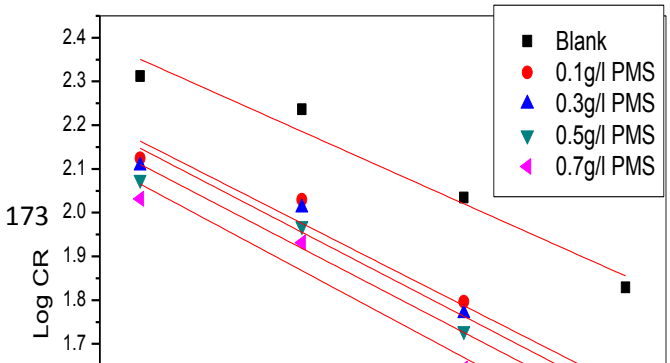

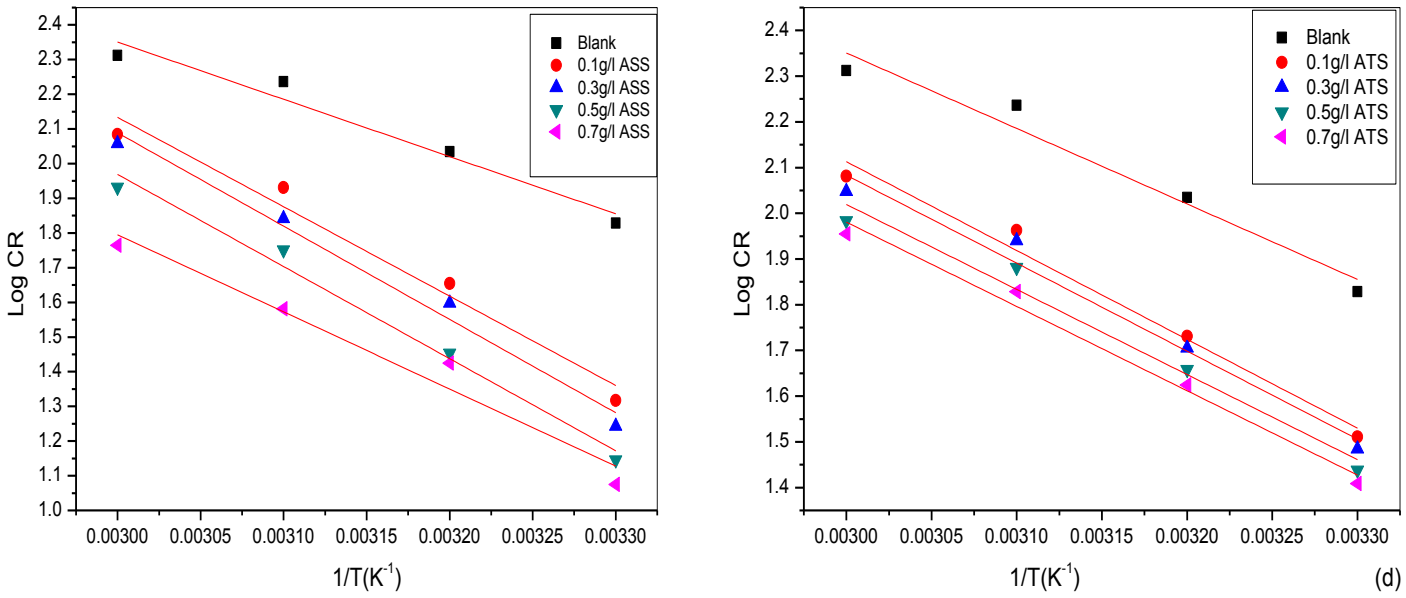

***Figure 4.54**: Plots of log CR versus 1/T for the corrosion of mild steel in 0.25M H_2SO_4 in the absence and presence of (a) Natural starch, (b) Physical modified starch, (c) Alkaline treated starch and (d) Acid treated starch.*

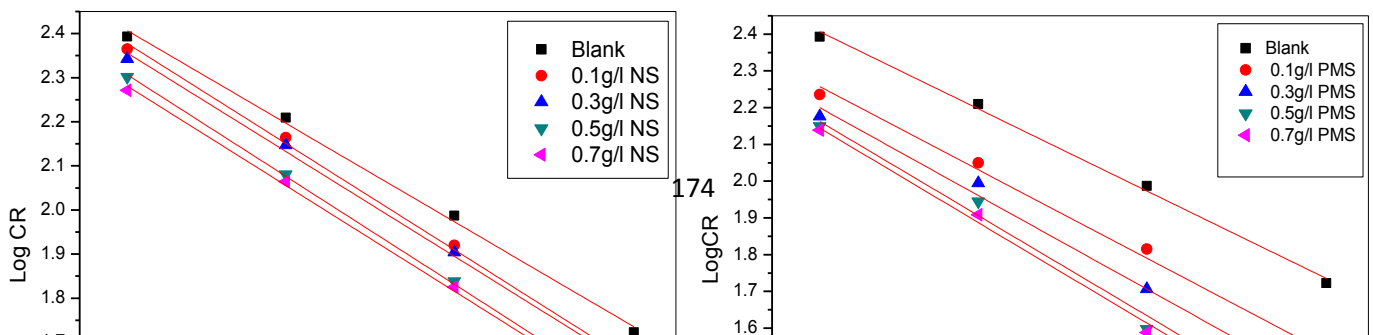

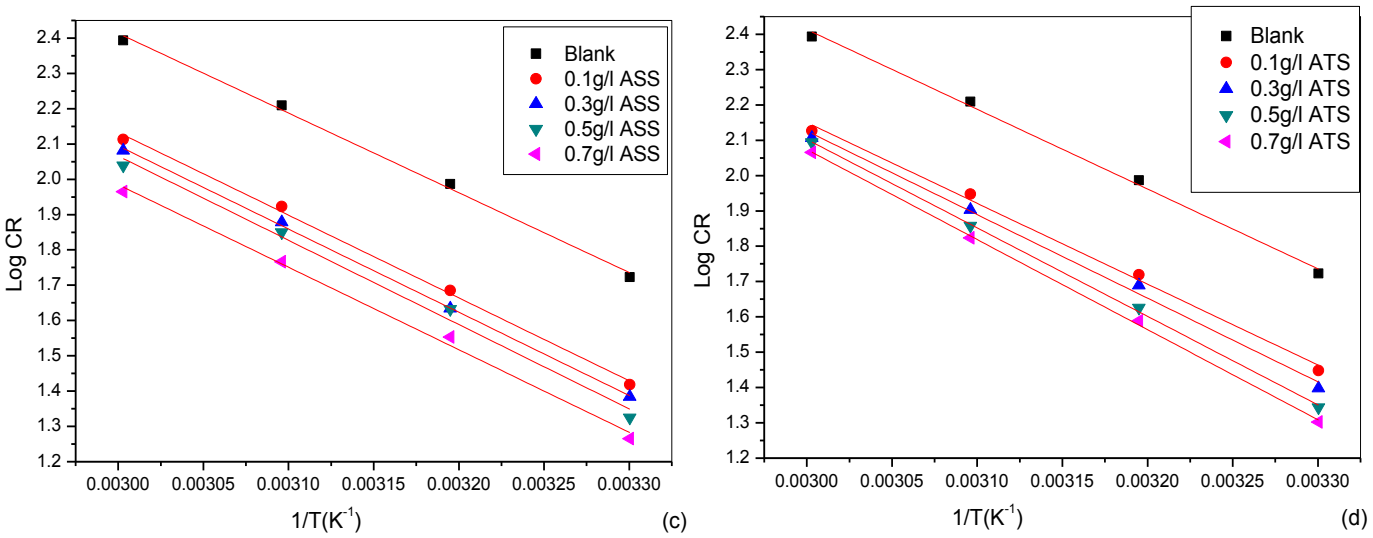

***Figure 4.55**: Plots of log CR versus 1/T for the corrosion of mild steel in 1M HCL in the absence and presence of (a) Natural starch, (b) Physical modified tarch, (c) Alkaline treated starch and (d) Acid treated starch.*

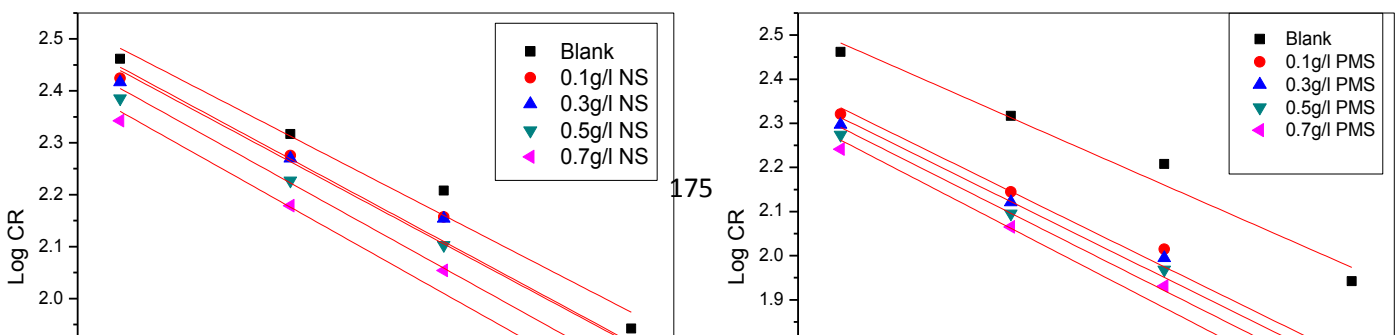

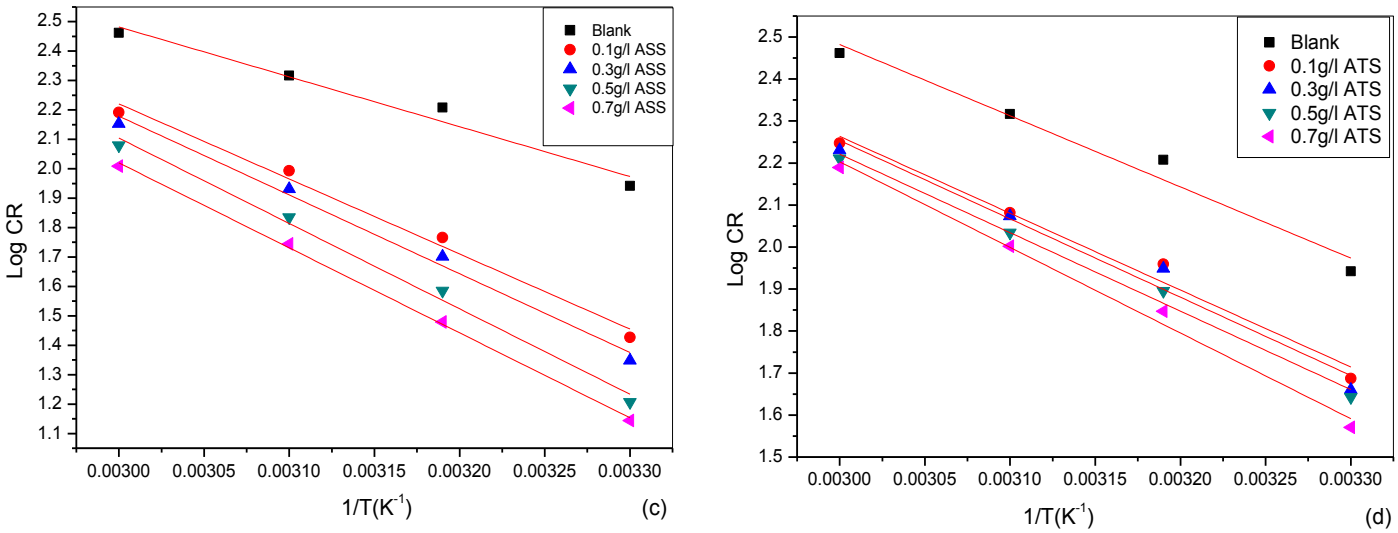

***Figure 4.56**: Plots of log CR versus 1/T for the corrosion of galvanised steel in 0.25M H_2SO_4 in the absence and presence of (a) Natural starch, (b) Physical modified starch, (c) Alkaline treated starch and (d) Acid treated starch.*

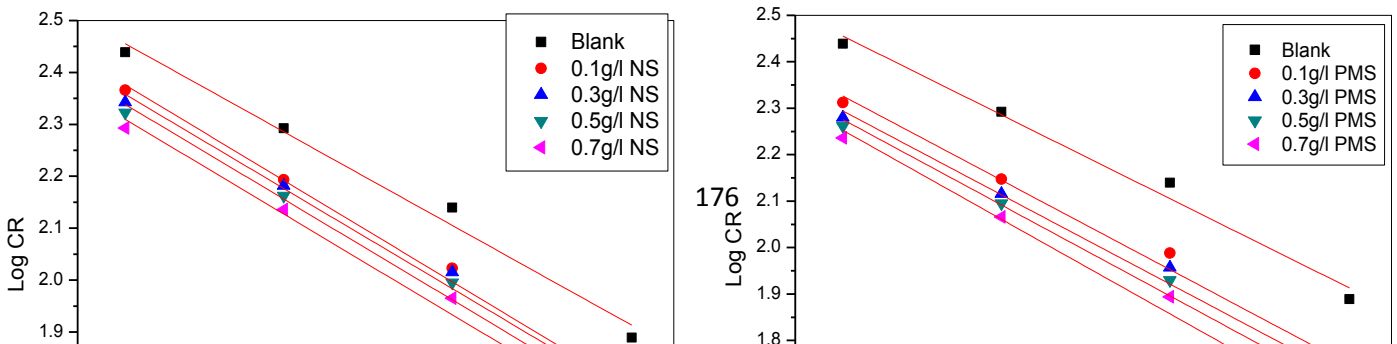

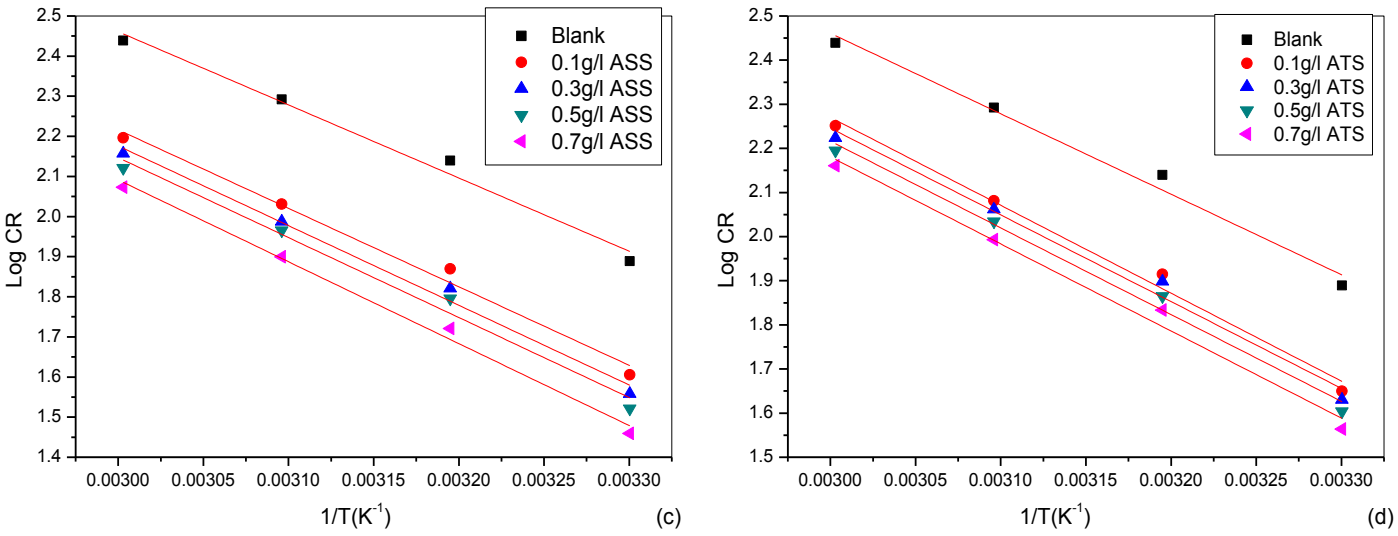

***Figure 4.57**: Plots of log CR versus 1/T for the corrosion of galvanised steel in 1M HCL in the absence and presence of (a) Natural starch, (b) Physical modified starch, (c) Alkaline treated starch and (d) Acid treated starch.*

Linear plot were obtained, from the slope $\left(-\frac{\Delta H}{2.303\ R}\right)$ the values of ΔH was calculated and from the intercept $\left[\log\left(\frac{R}{Nh}\right)+\left(\frac{\Delta S}{2.303R}\right)\right]$ of the linear plot, the values of ΔS was obtained. The calculated values are presented in Table 4.25 - 4.28, the result obtained indicates that IE % decreases when the temperature

increases. Such behaviour can be interpreted on the basis that increasing the temperature resulted in desorption of the adsorbed inhibitor molecules from the metal surface. The enthalpy value for the four inhibitors increased in presence of the inhibitors compared to the free acid solution with the corrosion of galvanised steel in 0.5g/l of ASS/ 0.25M H_2SO_4 system, recording the highest value of ΔH. The calculated values of ΔS is presented in Table 4.25-4.28, ΔS increased with the addition of the inhibitor, reflecting the fact that the adsorption process was accompanied by an increase in entropy, which is the driving force for the adsorption of the inhibitor onto the steel surface. ΔS values were positive for all inhibitors which indicate a decrease in the system order in the presence of additives [Refaey *et al.*; 2004].

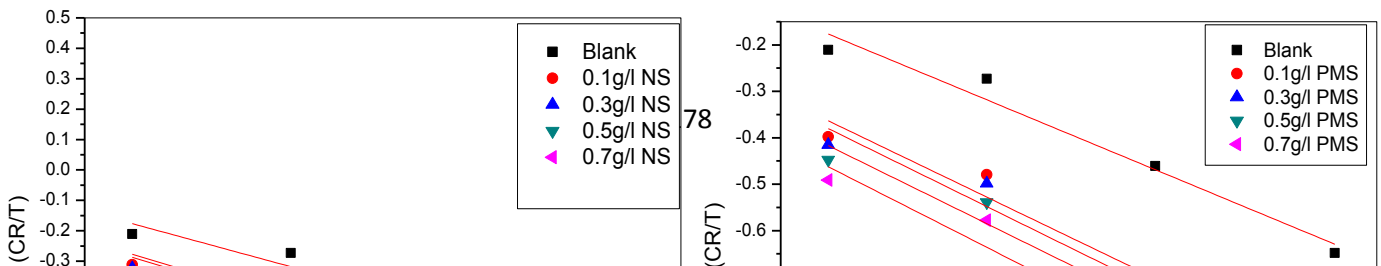

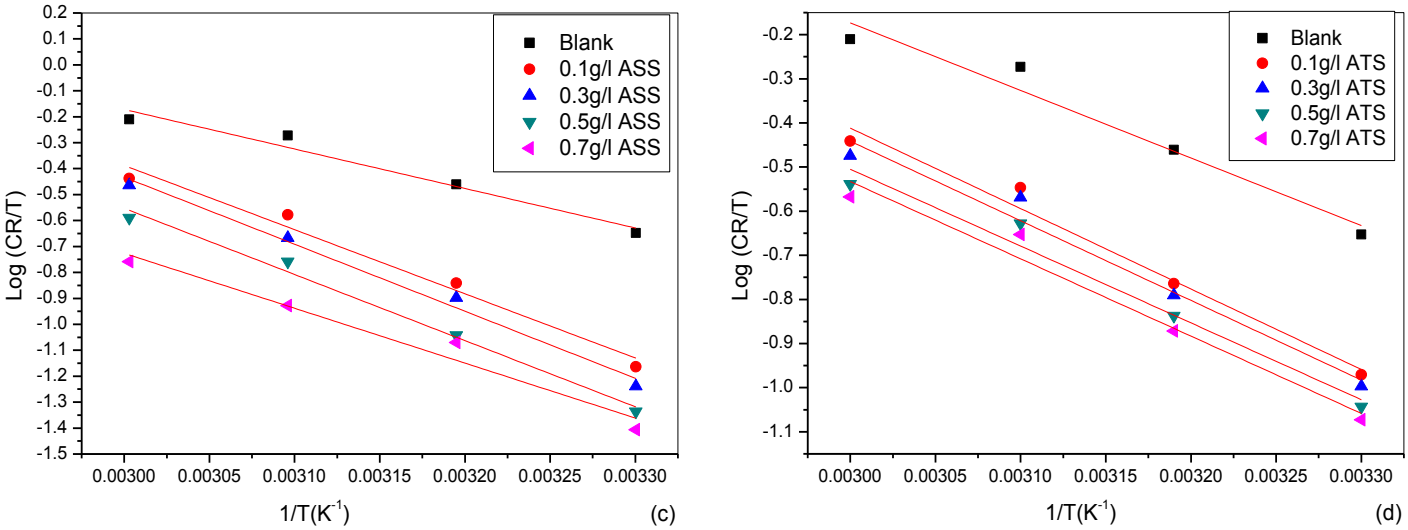

Figure 4.58:*Plot of Log CR/T versus 1/T for the corrosion of mild steel in 0.25M H_2SO_4 in the absence and presence of (a) Natural starch, (b) Physical modified starch, (c) Alkaline treated starch and (d) Acid treated starch.*

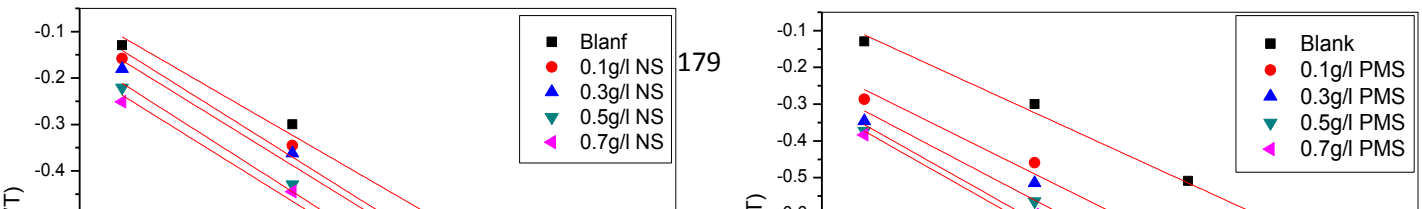

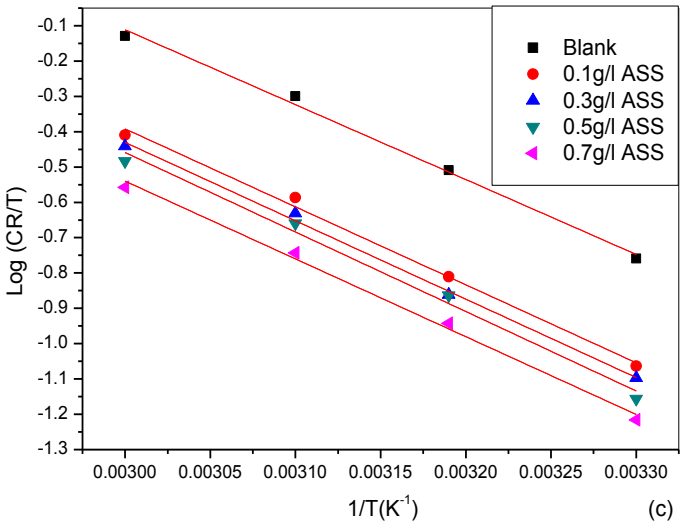

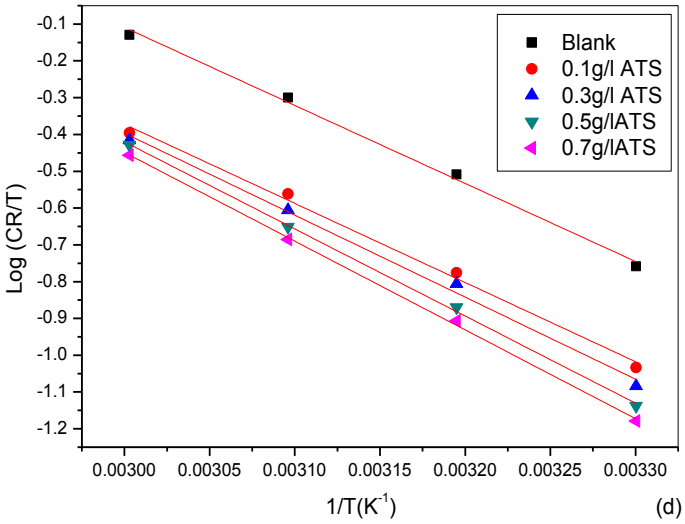

Figure 4.59: *Plot of Log CR/T versus 1/T for the corrosion of mild steel in 1M HCL in the absence and presence of (a) Natural starch, (b) Physical modified starch, (c) Alkaline treated starch and (d) Acid treated starch.*

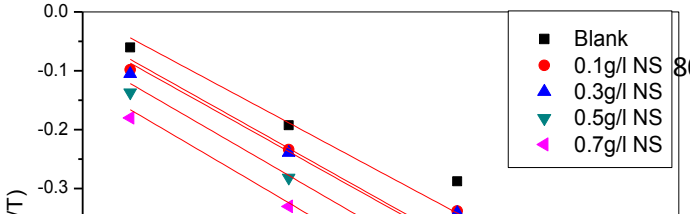

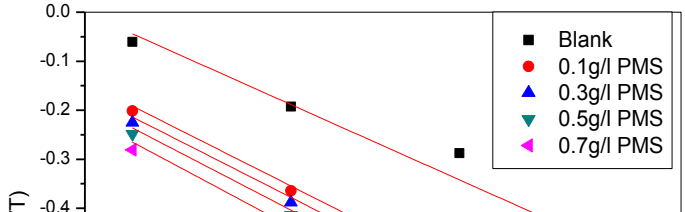

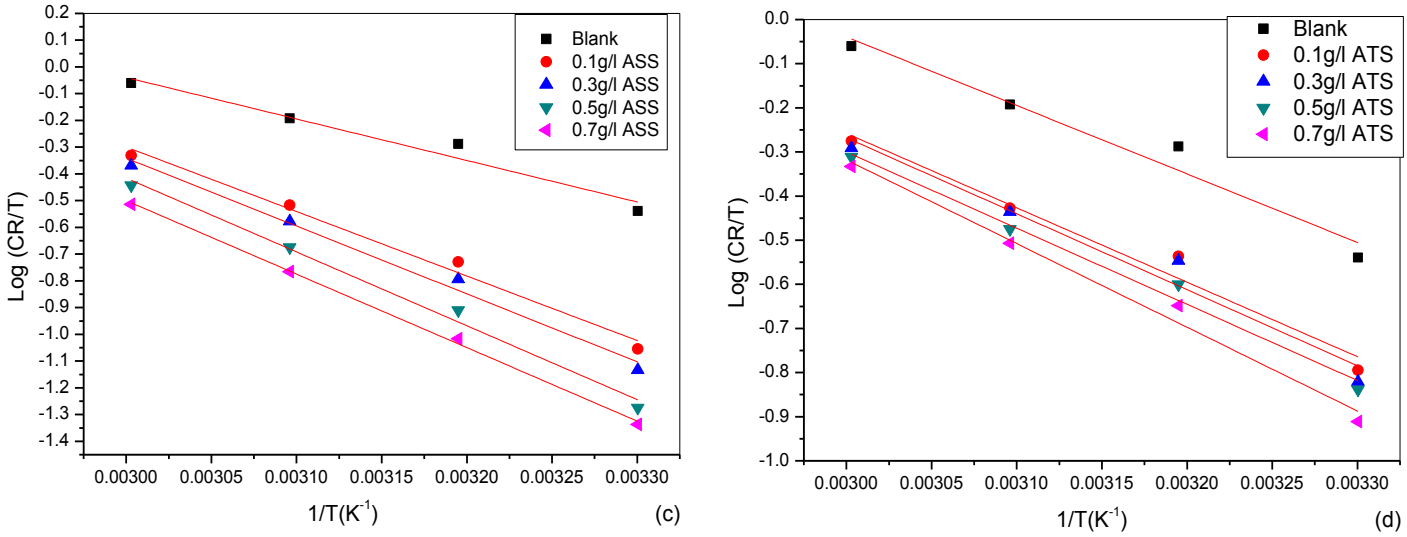

Figure 4.60:*Plot of Log CR/T versus 1/T for the corrosion of galvanised steel in 0.25M H_2SO_4 in the absence and presence of (a) Natural starch, (b) Physical modified starch, (c) Alkaline treated starch and (d) Acid treated starch.*

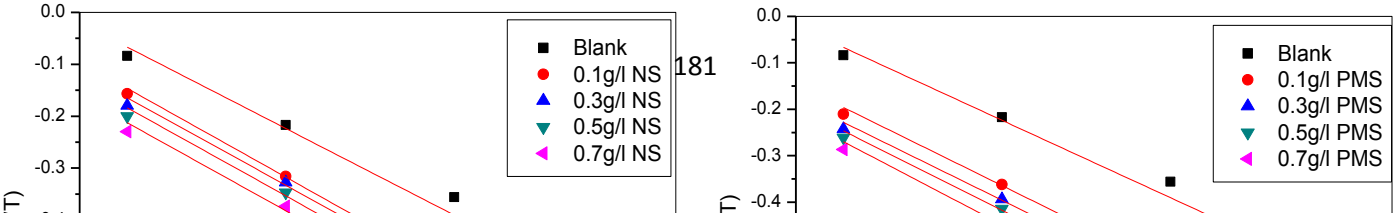

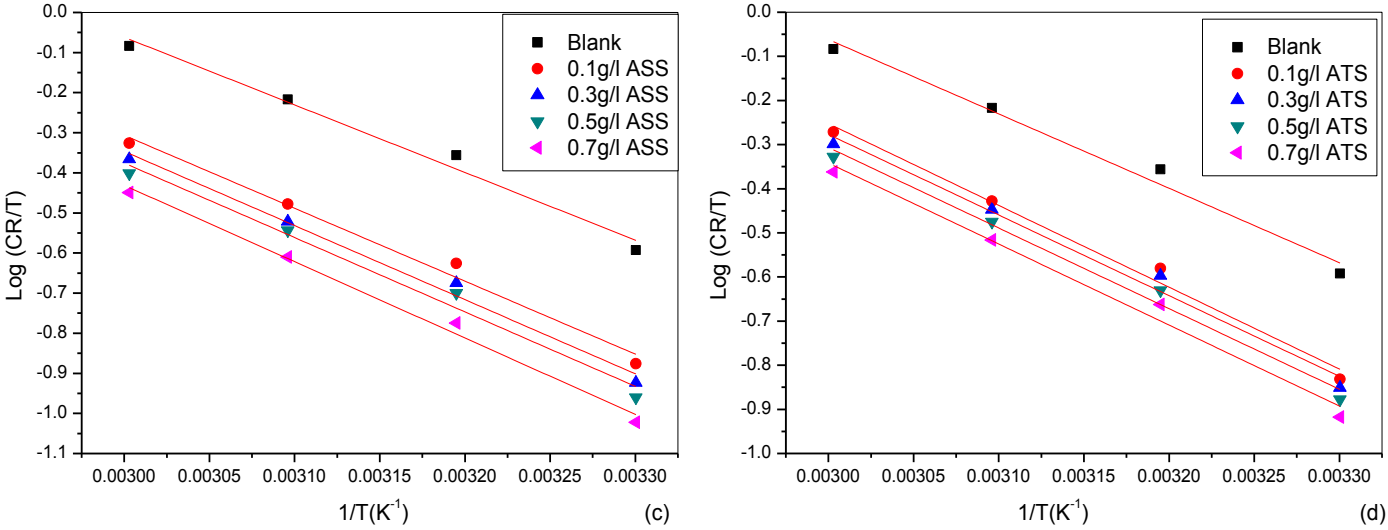

Figure 4.61: *Plot of Log CR/T versus 1/T for the corrosion of galvanised steel in 1M HCL in the absence and presence of (a) Natural starch, (b) Physical modified starch, (c) Alkaline treated starch and (d) Acid treated starch.*

Calculated values of Q_{ads} for the four inhibitors are presented in Table 4.25 t0 4.28. The negative value obtained signifies that the adsorption of NS, PMS, ASS, and ATS on both mild steel and galvanised surface is exothermic (Bhajiwala & Vashi; 2001). The negative value also shows that the degree of surface coverage decreased with rise in temperature. Such behaviour is often interpreted as being indicative of physical adsorption. Q_{ads} values were higher in Sulphuric acid than hydrochloric acid for both metals.

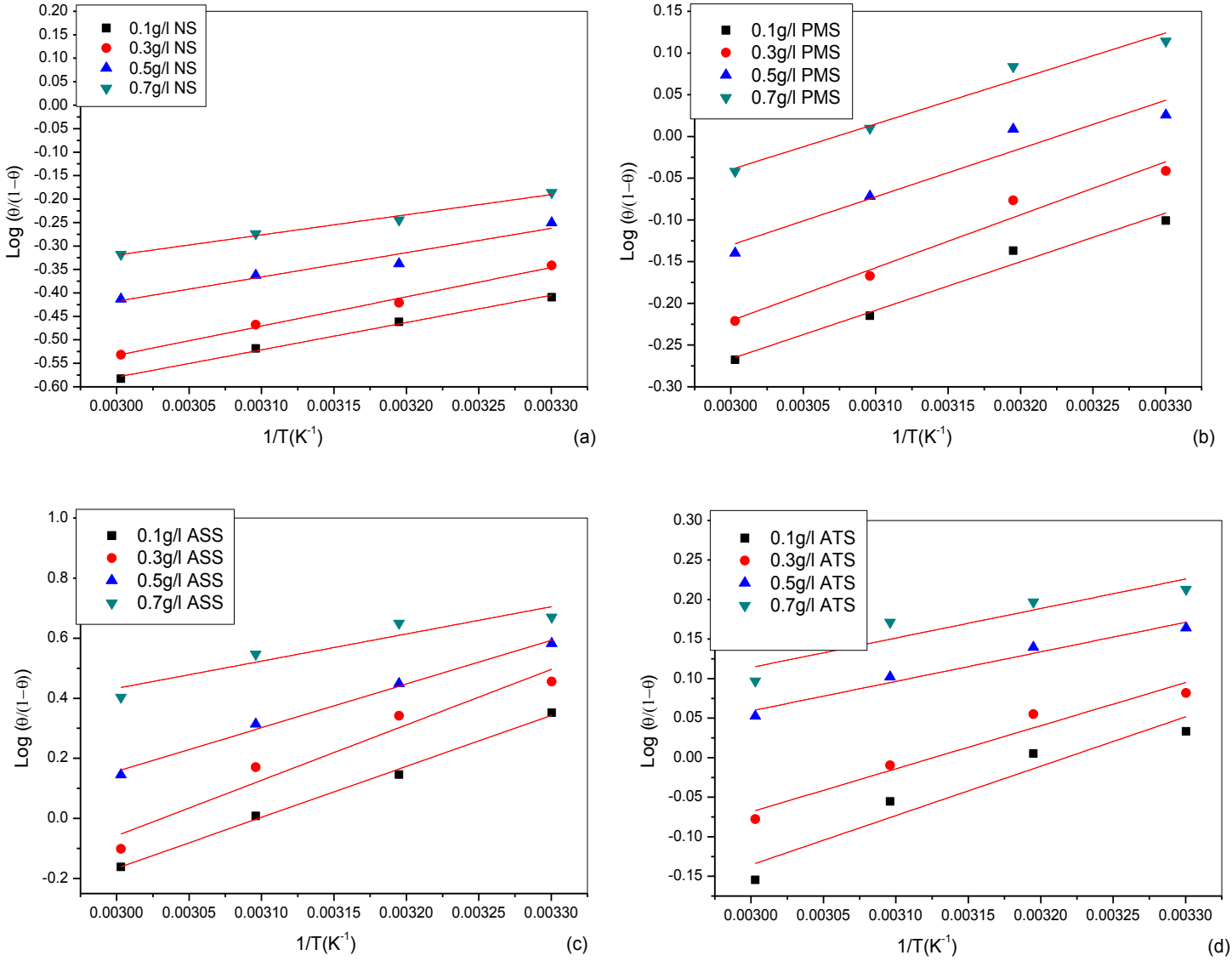

***Figure 4.62**: Adsorption isotherm plot for log (Θ/1-Θ) versus1/T for the corrosion of mild steel in 0.25M H_2SO_4 in the absence and presence of (a) Natural starch, (b) Physical modified starch, (c) Alkaline treated starch and (d) Acid treated starch.*

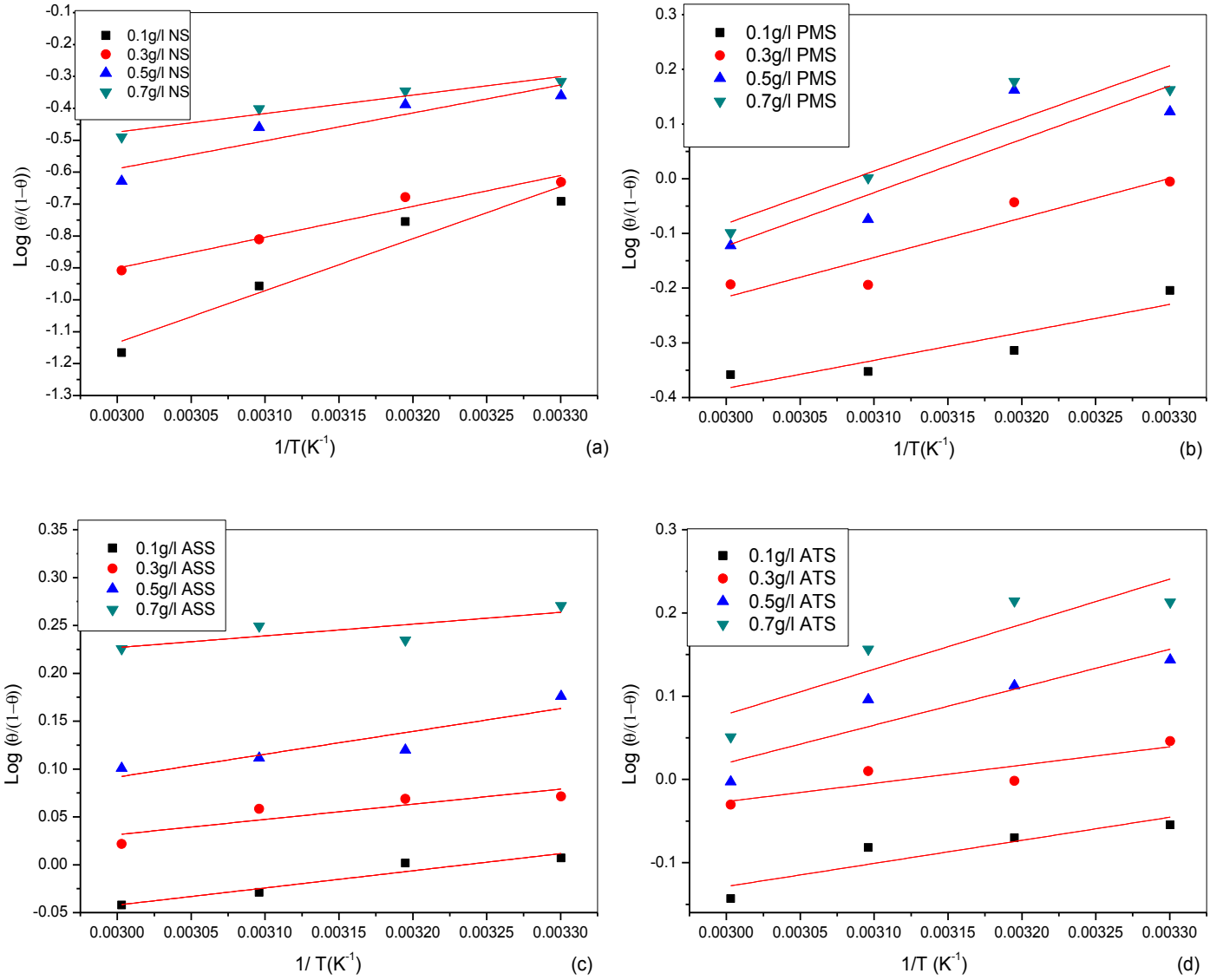

***Figure 4.63**: Adsorption isotherm plot for log (Θ/1-Θ) versus1/T for the corrosion of mild steel in 1M HCL in the absence and presence of (a) Natural starch, (b) Physical modified starch, (c) Alkaline treated starch and (d) Acid treated starch.*

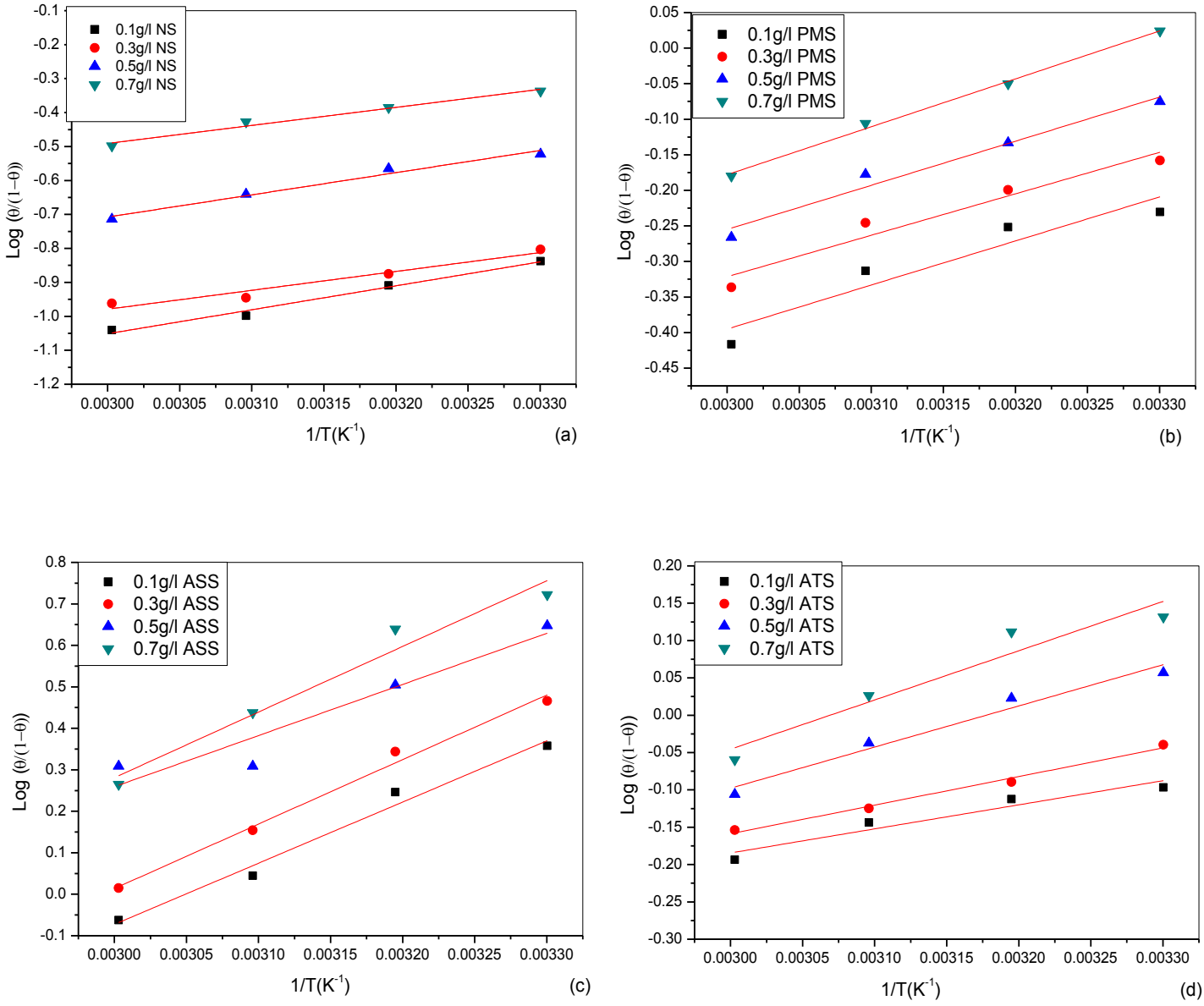

***Figure 4.64**: Adsorption isotherm plot for log (Θ/1-Θ) versus1/T for the corrosion of galvanised steel in 0.25M H_2SO_4 in the absence and presence of (a) Natural starch, (b) Physical modified starch, (c) Alkaline treated starch and (d) Acid treated starch.*

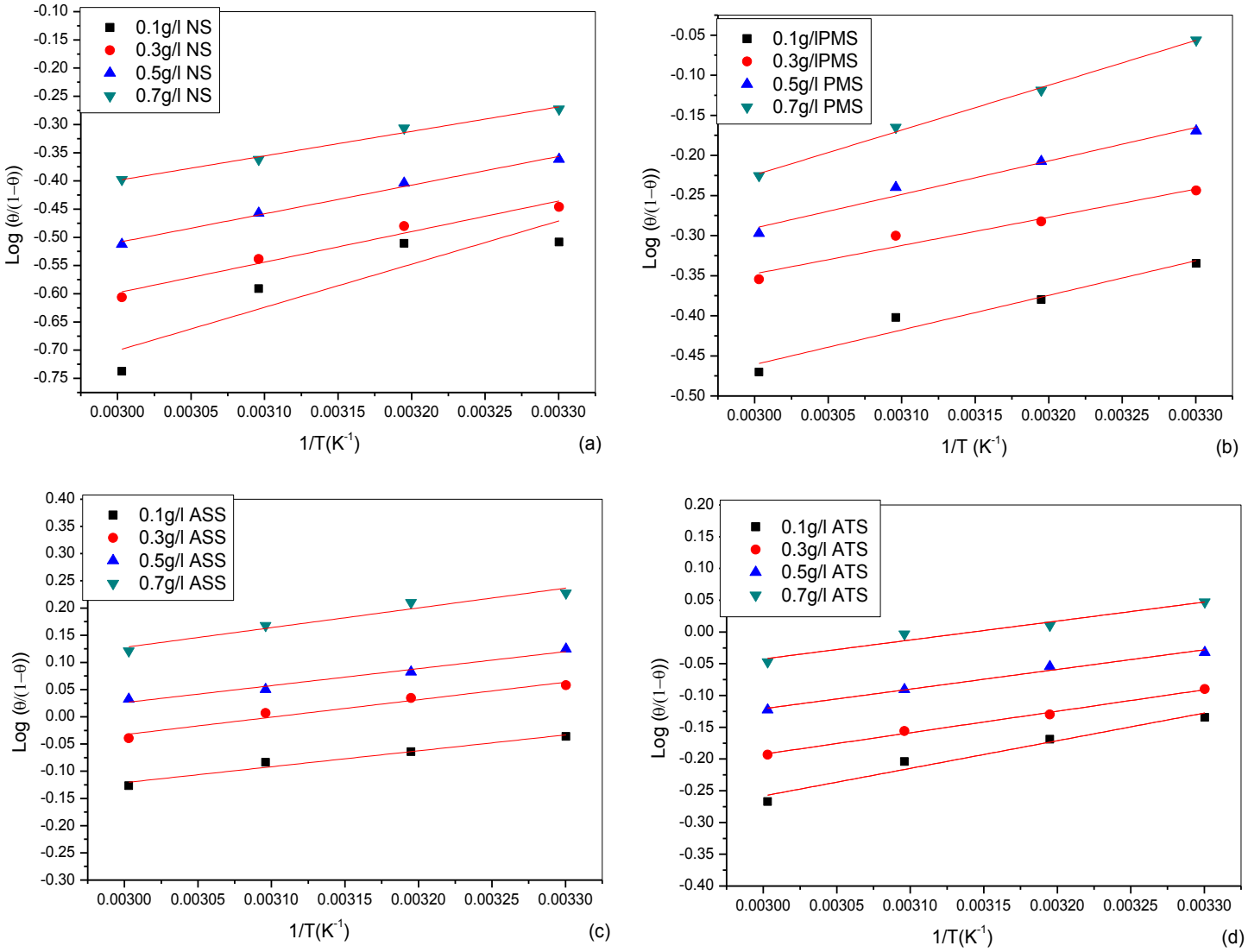

***Figure 4.65**: Adsorption isotherm plot for log (Ɵ/1-Ɵ) versus1/T for the corrosion of galvanised steel in 1 M HCL in the absence and presence of (a) Natural starch, (b) Physical modified starch, (c) Alkaline treated starch and (d) Acid treated starch.*

4.25 Calculated Values of Kinetic/Thermodynamic Parameters for Mild Steel in 0.25M H_2SO_4 in the Absence and the Presence of NS, PMS, ASS and ATS from Gravimetric Studies

Inhibitor	$E_a(kJmol^{-1})$	$\Delta H(kJmol^{-1})$	$\Delta S(kJmol^{-1})$	$Q_{ads}(kJmol^{-1})$
Blank	31.625	29.146	8.16	
0.1g/l NS	34.309	32.114	8.83	-11.14
0.3g/l NS	34.797	32.593	8.96	-11.95
0.5g/l NS	34.733	32.535	8.89	-9.92
0.7g/l NS	34.547	32.363	8.78	-8.23
0.1g/l PMS	36.016	33.818	9.17	-11.15
0.3g/l PMS	36.766	34.565	9.36	-12.15
0.5g/l PMS	36.809	34.604	9.3	-11.07
0.7g/l PMS	37.956	35.714	9.54	-10.45
0.1g/l ASS	49.349	47.357	13.05	-32.46
0.3g/l ASS	51.513	49.464	13.58	-35.54
0.5g/l ASS	50.888	48.813	13.17	-27.89
0.7g/l ASS	42.589	40.502	10.43	-17.33
0.1g/l ATS	37.189	34.910	9.38	-11.96
0.3g/l ATS	36.844	34.546	9.23	-10.44
0.5g/l ATS	35.619	33.340	8.76	-7.15
0.7g/l ATS	35.312	33.531	8.76	-7.14

Table 4.26 Calculated Values of Kinetic/Thermodynamic Parameters for Mild Steel in 1M HCL in the Absence and the Presence of NS, PMS, ASS and ATS from Gravimetric Studies

Inhibitor	E_a(kJmol^{-1})	ΔH(kJmol^{-1})	ΔS(kJmol^{-1})	Q_{ads}(kJmol^{-1})
Blank	43.251	40.598	11.60	
0.1g/l NS	46.654	43.987	12.53	-31.196
0.3g/l NS	45.994	43.336	12.30	-18.539
0.5g/l NS	47.384	44.734	12.62	-16.739
0.7g/l NS	46.415	43.754	12.28	-11.082
0.1g/l PMS	46.611	43.949	12.30	-9.789
0.3g/l PMS	49.255	46.534	12.94	-13.844
0.5g/l PMS	52.707	49.924	13.85	-18.656
0.7g/l PMS	52.928	50.192	13.90	-18.402
0.1g/l ASS	44.927	42.264	11.56	-3.430
0.3g/l ASS	45.153	42.474	11.54	-3.038
0.5g/l ASS	45.125	43.087	11.67	-4.567
0.7g/l ASS	44.780	42.168	11.26	-2.351
0.1g/l ATS	43.823	41.172	11.28	-1.672
0.3g/l ATS	45.329	42.685	11.67	-1.530
0.5g/l ATS	47.986	45.328	12.40	-2.591
0.7g/l ATS	48.840	46.189	12.60	-3.473

Table 4.27 Calculated Values of Kinetic/Thermodynamic Parameters for Galvanised Steel in 0.25M H2SO4 in the Absence and the Presence of NS, PMS, ASS and ATS from Gravimetric Studies

Inhibitor	E_a(kJmol^{-1})	ΔH(kJmol^{-1})	ΔS(kJmol^{-1})	Q_{ads}(kJmol^{-1})
Blank	32.456	29.72	8.567	-
0.1g/l NS	33.853	31.12	8.907	-13.508
0.3g/l NS	33.673	30.95	8.844	-10.639
0.5g/l NS	34.906	32.17	9.137	-12.523
0.7g/l NS	35.353	32.61	9.183	-10.164
0.1g/l PMS	36.314	33.57	9.415	-11.867
0.3g/l PMS	36.525	33.78	9.434	-11.165
0.5g/l PMS	37.277	34.53	9.610	-11.882
0.7g/l PMS	38.310	35.56	9.859	-12.897
0.1g/l ASS	48.868	46.19	12.874	-30.297
0.3g/l ASS	51.296	48.60	13.498	-28.240
0.5g/l ASS	55.593	52.89	14.605	-29.779
0.7g/l ASS	55.316	52.62	14.373	-23.608
0.1g/l ATS	35.046	32.31	8.914	-6.172
0.3g/l ATS	35.713	32.98	9.091	-7.328
0.5g/l ATS	35.771	33.05	9.052	-10.556
0.7g/l ATS	39.047	36.33	9.970	-12.630

Table 4.28 Calculated Values of Kinetic/Thermodynamic Parameters for Galvanised Steel in 1M HCL in the Absence and the Presence of NS, PMS, ASS and ATS from Gravimetric Studies

Inhibitor	E_a(kJmol^{-1})	ΔH(kJmol^{-1})	ΔS(kJmol^{-1})	Q_{ads}(kJmol^{-1})
Blank	34.932	32.29	9.272	-
0.1g/l NS	37.812	35.16	9.963	-14.653
0.3g/l NS	37.329	34.68	9.788	-10.379
0.5g/l NS	37.554	34.91	9.818	-9.749
0.7g/l NS	37.566	34.91	9.768	-8.317
0.1g/l PMS	37.282	34.64	9.716	-8.263
0.3g/l PMS	37.191	34.55	9.631	-6.742
0.5g/l PMS	37.893	35.24	9.801	-8.010
0.7g/l PMS	39.420	36.77	10.202	-10.710
0.1g/l ASS	37.476	34.83	9.558	-5.604
0.3g/l ASS	38.049	35.41	9.649	-6.151
0.5g/l ASS	38.183	35.54	9.636	-5.981
0.7g/l ASS	39.097	36.44	9.798	-6.946
0.1g/l ATS	36.630	35.50	9.859	-8.335
0.3g/l ATS	37.648	35.01	9.664	-6.482
0.5g/l ATS	37.638	34.99	9.606	-5.929
0.7g/l ATS	37.799	35.16	9.586	-5.720

CHAPTER FIVE

CONCLUSIONS AND RECOMMENDATIONS

5.1 Conclusions

This research evaluated the use of the unmodified and modified sweet potato starch as corrosion inhibitors for mild steel and galvanised steel metal in acidic media (0.25M H_2SO_4 and 1M HCL). FTIR studies, gravimetric measurements and potentiodynamic polarization measurements were used in this study. From the result and discussions in this thesis, the following conclusions were derived;

That the modification processes effected changes on the functionality of the sweet potato starch, and these modifications enhanced their inhibition efficacy.

The FTIR spectra of the modified starches (physical modified starch, acid treated starch and alkaline treated starch) proofed that the modifications done on the starch samples were achieved.

The inhibition efficacy of the four starch samples showed that the performance of the starch samples were governed by the structural modification carried out on the starch. Inhibition efficiency values increasing with increase in concentration of the starch samples for both mild steel and galvanised steel following the order; NS < PMS < ATS < ASS.

The inhibition efficacy values of the starches (NS, PMS, ATS and ASS) were low (< 70 %), but in combination with 0.4 g/l KI inhibition efficiency values greater than 80 % was achieved. Hence, the effect of potassium iodide on corrosion

inhibition behaviour of the unmodified and modified starches appears to be synergistic in nature.

AFM, and FTIR studies also revealed the formation of a protective film adsorbed on the mild steel surface.

The results of potentiodynamic polarization measurements show that the unmodified sweet potato and modified sweet potato starches were of mixed type inhibitor.

The inhibition mechanism is explained by adsorption. The adsorption of the four inhibitors in the acid corrodent obeyed Langmuir adsorption isotherm.

The thermodynamic parameters calculated from the adsorption isotherms proposed physical adsorption from the trend of inhibition efficiency with temperature.

5.2 Recommendation

The following recommendations are made for future researchers who may wish to undertake studies on the use of biopolymers; starch to be precise, in corrosion control:

To investigate the inhibitive efficacy of the modified starches in neutral and alkaline environment

Carry out other methods of treatment on sweet potato starch to broaden its functionality as an industrial biopolymer.

Incorporate the modified starches in the formulation of anticorrosive paints

5.3 Contribution to Knowledge

A non-toxic, cost effective polymer whose inhibition efficacy remains unchanged for a prolonged interval has been developed.

Iodide is able to improve efficacy of the polymer without affecting its stability over time.

REFERENCES

Abdallah, M., Megahed, H. E., El-Etre, A. Y., Obied, M. A. & Mabrouk, E. M. (2004). Polyamide compounds as inhibitors for corrosion of aluminium in oxalic acid solutions. *Bulletin of Electrochemistry*. *20*(6). 277-28.

Abdel-Gaber, A. M., Abd-El-Nabey, B. A., Sidahmed, I. M., El-Zayady, A.M. & Saadawy, M. (2006). Inhibitive action of some plant extracts on the corrosion of steel in acidic media, *Corrosion Science*. *48*(9). 2765 - 2779.

Abd El Rehim, S .S., Sayyah, S. M., El-Deeb, M. M., Kamal, S. M. & Azooz, R. E. (2010). Poly (o-phenylenediamine) as an inhibitor of mild steel corrosion in HCl solution. *Materials, Chemistry and Physics. 123*(1). 20-27.

Al Juhaiman, L. A., Mustafa, A. A., & Mekhamer, W. K. (2012). Polyvinyl Pyrrolidone as a Green Corrosion Inhibitor of Carbon Steel in Neutral Solutions Containing NaCl: Electrochemical and Thermodynamic Study. *International Journal Electrochemical Science, 7*(9), 8578-8596.

Altwaiq A, Khouri S. J, Al-luaibi, S., Lehmann, R., Drücker, H. & Vogt, C. (2011) The Role of Extracted Alkali Lignin as Corrosion Inhibitor *Journal of Materials and Environmental Science*, *2*(3), 259-270.

Aly, K. I. & Hussein, M. A. (2010). New polymer syntheses, part 45: Corrosion inhibition behavior of novel polyurea derivatives based on diarylidenecycloalkanone moieties in the polymers backbone. *Journal of Polymer Research, 17*(5), 607-620.

Angelier, H., Dufresne, A. and Molina-Boisseau, S. (2005). Mechanical Properties of Waxy Maize Starch Nanocrystals Reinforced Natural Rubber, *Macromolecules. 38*. 9161-9170.

Aramaki, K. & Hackerman, N. (1969). Inhibition Mechanism of Medium-Sized Polymethyleneimine. *Journal of Electrochemical Society*. *116*. 568.

Arukalam, I. O. & Obidiegwu, M. U. (2011). The Inhibition of Aluminium Corrosion in Hydrochloric Acid Solution by Hydroxyethylcellulose *Academic Research International. 1* (3) 484-491

Arukalam, I. O., Nleme, I. K. & Anyanwu, A. (2011). Comparative Inhibitive Effect of Hydroxyethylcellulose on Mild Steel and Aluminium Corrosion in 0.5M HCl Solution. *Academic Research International. 1*(3). 492 – 498.

Arukalam, I. O., Madufor, I. C., Ogbobe, O. & Oguzie, E. E. (2014) Acidic Corrosion Inhibition of Copper by Hydroxyethyl Cellulose *British Journal of Applied Science & Technology. 4*(9). 1445-1460,

Ashassi-Sorkhabi, H., Ghalebsaz-Jeddi, N., Hashemzadeh, F. & Jahani, H. (2006). Corrosion inhibition of carbon steel in hydrochloric acid by some polyethylene glycols. *Electrochimica Acta. 51*(18). 3848-54.

Ashassi-Sorkhabi, H. & Ghalebsaz-Jeddi, N. (2005). Inhibition effect of polyethylene glycol on corrosion of carbon steel in sulphuric acid. *Materials Chemistry and Physics. 92*(2-3) 480-6.

Atta, A. M., El-Azabawy, O. E., Ismail, H. S. & Hegazy, M. A. (2011). Novel dispersed magnetite core-shell nanogel polymers as corrosion inhibitors for carbon steel in acidic medium. *Corrosion Science. 53*(5). 1680-9.

Banerjee, S. S. & Chen, D. H. (2007). Fast removal of copper ions by gum arabic modified magnetic nano-adsorbent *Journal of Hazardous Material 147*(3) 792-799.

Banerjee, S., Srivastava, V. & Singh, M. M. (2012). Chemically modified natural polysaccharide as green corrosion inhibitor for mild steel in acid medium. *Corrosion Science. 59*. 35-41.

Belkaid, S., Tebbji, K., Mansri, A., Chetouani, A. & Hammouti, B. (2012). Poly (4-vinylpyridine-hexadecyl bromide) as corrosion inhibitor for mild steel in acid chloride solution. *Research on Chemical Intermediates. 38*(9). 2309- 2325.

Bello, M., Ochoa, N., Balsamo, V., López-Carrasquero, F., Coll, S. & Monsalved, A. et al (2010) Modified Cassava Starches as Corrosion Inhibitors of Carbon Steel. An Electrochemical and Morphological Approach. *Carbohydrate Polymers. 82*(3). 561–568

Benabdellah, M., Ousslim, A., Hammouti, B,. Elidrissi, A., Aouniti, A. & Dafali, A. *et al*. (2007). Effect of poly (vinyl caprolactone-co-vinyl pyridine) and poly(vinyl imidazo-co-vinyl pyridine) on the corrosion of steel in H_3PO_4 media. *Journal of Applied Electrochemistry. 37*(7). 819-826.

Bentrah, H., Rahali, Y. & Chala, A. (2014). Gum Arabic as an eco-friendly inhibitor for API 5L X42 pipeline steel in HCl medium. *Corrosion Science. 82*. 426-31.

Berski, W., Ptaszek, A., Ptaszek, P., Ziobro, R., Kowalski, G., Grzessik, M., & Achremowicz, B. (2011). Pasting and rheological properties of oat starch and its derivatives. *Carbohydrate Polymers, 83*(2), 665-671.

Bouklah, M.,& Hammouti, B. (2006). Thermodynamic characterization of steel corrosion for the corrosion inhibition of steel in sulphuric acid solutions by Artemisia. *Portugaliae Electrochimica Acta 24.* 457-468.

Buchweishaija, J. (2009). Plants as a Source Of Green Corrosion Inhibitors: The Case Of Gum Exudates From Acacia Species (A. Drepanolobium and A. Senegal) *Tanzanian Journal of Science. 35*. 93 - 105

Buchweishaija, J. & Mhinzi, G. S. (2008). Natural products as a source of environmentally friendly corrosion inhibitors: The case of natural tree gum exudates from Acacia seyal var seyal. *Portugaliae. Electrochimica. Acta 26*. 257-265.

Burrell MM. (2003) Starch: the need for improved quality or quantity - An overview. *Journal of Experimental Botany. 54*. 451-6.

Camire, M. E., Camire, A., & Krumhar, K. (1990). Chemical and nutritional changes in foods during extrusion. *Critical Reviews in Food Science and Nutrition. 29*(1). 35-57.

Cael, J. J., Koenig, J. L. & Blackwell, J., (1975). Infrared and Raman spectroscopy of carbohydrates. Normal coordinate analysis of V-amylose. *Biopolymers. 14.* 1885

Chen, Z. (2003) Physicochemical properties of sweet potato starches and their application in noodle products Ph.D dissertation No 90-5808-887-1. Wageningen University, Netherlands.

Chetouani, A., Medjahed, K., Benabadji, K. E., Hammouti, B., Kertit, S. & Mansri, A. (2003). Poly (4-vinylpyridine isopentyl bromide) as inhibitor for corrosion of pure iron in molar sulphuric acid. *Prog Organic Coating; 46*(4). 312-6.

Chetouani, A., Medjahed, K., Sid-Lakhdar, K. E., Hammouti, B., Benkaddour, M. & Mansri, A. (2004). Poly(4-vinylpyridine-poly(3-oxide- ethylene) tosyle) as an inhibitor for iron in sulphuric acid at 80°C. *Corrosion Science. 6*(10). 2421-30.

Christopher, G. O. (1997). Towards an understanding of starch granule structure and hydrolysis. *Trends in Food Science & Technology. 8*. 375–382.

Dong-fang, Z., Ben-zhi, J., Shu-fen, Z. & Jin-zong, Y. (2005). Progress in the synthesis and application of green chemicals, carboxymethyl starch sodium Proceeding of the 3rd International Conference on Functional Molecules. 25-30. Dalian, China: Dalian University of Technology

Dubey, A. K. & Singh, G. (2007). Corrosion inhibition of mild steel in sulphuric acid solution by using polyethylene glycol methyl ether (PEGME). *Portugaliae Electrochimica Acta*. *25*. 221-35.

Ebenso, E. E., Ekpe, U. J., Ita, B. I., Offiong, O. E., & Ibok, U. J. (1999). Effect of molecular structure on the efficiency of amides and thiosemicarbazones used for corrosion inhibition of mild steel in hydrochloric acid. *Materials Chemistry & Physics. 60*(1). 79-90.

Ebenso, E. E. (2003). Effect of Halide ions on the corrosion inhibition of mild steel in H_2SO_4 using methyl red. *Bulletin of Electrochemistry. 19*(1). 209-216.

Ebenso, E. E., Ekpe, U. J., Umoren, S. A., Jackson, E., Abiola, O. K., & Oforka, N. C. **(2006)**.Synergistic effect of halide ions on the corrosion inhibition of aluminum in acidic medium by some polymers. *Journal of Applied Polymer Science, 100*(4), 2889-2894.

El-Haddad, M. N. (2013). Chitosan as a green inhibitor for copper corrosion in acidic medium. *Internaional Journal of Biological Macromolecules. 55.* 142-149.

Fang, J. M., Fowler, P. A., Sayers, C. & Williams, P. A. (2004). The chemical modification of a range of starches under aqueous reaction condition. *Carbohydrate Polymers. 55*. 283–289.

Fares, M. M., Maayta, A. K. & Al-Qudah, M. M. (2012). Pectin as promising green corrosion inhibitor of aluminum in hydrochloric acid solution *Corrosion Science. 60*. 112-117.

Fares, M. M., Maayta, A. K. & Al-Mustafa, J. A. (2012). Corrosion inhibition of iota-carrageenan natural polymer on aluminium in presence of zwitterions mediator in HCl media. *Corrosion Science. 65*. 223-230.

Fekry, A. M. & Mohamed, R. R. (2010). Acetyl thiourea chitosan as an eco-friendly inhibitor for mild steel in sulphuric acid medium. *Electrochimica Acta. 55*(6). 1933-1939.

Fiedorowicz, M., Tomasik, P., & Lii, C. Y. (2001). Degradation of starch by polarised light. *Carbohydrate Polymers. 45*. 79–87.

Finch, K.A. (1983) Chemistry and technology of water-soluble polymers Plenum Press, New York, 321-329

Finsgar, M., Fassbender, S., Nicolini, F. & Milosev, I. (2009). Polyethyleneimine as corrosion inhibitor for ASTM 420 stainless steel in near neutral water. *Corrosion Science. 51*(3). 526-33.

Han, J.A. & Lim, S. T. (2004) Structural changes in corn starches during alkaline dissolution by vortexing. *Carbohydrate Polymers. 55*. 193–199.

Hasan, H. H., Abdelghani, E. & Amin, M. A. (2007). Inhibition of mild steel corrosion in hydrochloric acid solution by triazole derivatives; Part 1; Polarisation and EIS studies. *Electrochimica Acta. 52*(22). 6359-6366.

Hassan, R. M. & Zaafarany, I. A. (2013). Kinetics of corrosion inhibition of aluminum in acidic media by water-soluble natural polymeric pectates as anionic polyelectrolyte inhibitors. *Materials. 6*(6). 2436-2451

Hasanov, R., Bilge, S., Bilgi, S., Gece, G. & Kilic, Z. (2010). Experimental and theoretical calculations on corrosion inhibition of steel in 1 M H_2SO_4 by crown type polyethers. *Corrosion Science. 52*. 984-990.

Hosseini, M., Mertens, S. F. L., & Arshadi, M. R. (2003). Synergism and antagonism in mild steel corrosion inhibition by sodium dodecylbenzenesulphonate and hexamethylenetetramine. *Corrosion Science. 45*(7). 1473–1489.

Jenkins, P. J. and Donald, A. M. (1997) "The effect of acid hydrolyis on native starch granule structure. *Starch. 49*(7-8). 262–267.

Jeyaprabha, C., Sathiyanarayanan, S. & Venkatachari, G. (2006). Polyaniline as corrosion inhibitor for iron in acid solutions. *Journal of Applied Polymer Science 101*(4). 2144-2153.

Jeyaprabha, C., Sathiyanarayanan, S., Phani, K. L. N. & Venkatachari, G. (2005). Investigation of the inhibitive effect of poly (diphenylamine) on corrosion of iron in 0.5M H_2SO_4 solutions. *Journal of Electroanalytical Chemistry. 585*(2). 250-255

John, S., Kuruvilla, M. & Joseph, A. (2013). Surface morphological and impedance spectroscopic studies on the interaction of polyethylene glycol (PEG) and polyvinyl pyrrolidone (PVP) with mild steel in acid solutions. *Research on Chemical Intermediates. 39*(3). 1169-1182.

Kacurakova, M., Capeka, P., Sasinkova, V., Wellner, N. & Ebringerova, A., (2000). FT-IR study of plant cell wall model compounds: Pectic polysaccharides and hemicelluloses. *Carbohydrate Polymer. 43*(2). 195–203.

Kalaivani R., Thillai Arasu P. & Rajendran S. (2013) Inhibitive Nature of Carboxymethylcellulose with Zn^{2+}. *Chemical Science Transactions. 2*(4). 1352- 1357

Karthikaiselvi, R., Subhashini, S. & Rajalakshmi, R. (2012). Poly (vinyl alcohol-aniline) water soluble composite as corrosion inhibitor for mild steel in 1 M HCl. *Arabian Journal of Chemistry. 5*(4). 517-522.

Karthikaiselvi, R. and Subhashini, S. (2013). Study of adsorption properties and inhibition of mild steel corrosion in hydrochloric acid media by water soluble composite poly (vinyl alcohol-o-methoxy aniline). *Journal of the Association of Arab Universities for Basic & Applied Sciences*. doi.org/10. 1016/j.jaubas.2013.06.002

Karthikaiselvi, R. & Subhashini, S. (2012) The water soluble composite of poly(vinyl pyrrolidone - methylaniline). A new class of corrosion inhibitors of mild steel in hydrochloric acid media. *Arabian Journal of Chemistry.* doi.org/10.1016/j.arabjc.2012.10.024.

Khairou, K. S. & El-Sayed, A. (2003) Inhibition effect of some polymers on the corrosion of cadmium in hydrochloric acid solution. *Journal of Applied Polymer Science. 88*(4): 866-71.

Kim, D. K., Muralidharan, S., Ha, T. H., Bae, J. H., Ha, Y. C. & Lee, H. G. (2006) Electrochemical studies on the alternating current corrosion of mild steel under cathodic protection condition in marine environments. *Electrochimica Acta. 51*(25) 5259-5267.

Kim, B. S. & Lim, S, T. (1999). Removal of heavy metal ions from water by cross-linked carboxymethyl corn starch. *Carbohydrate Polymers. 39*. 217-223.

Klinov, I. Y. (1962). New polymeric materials in anticorrosion technology. The Inter-Higher Educational Institute Scientific Conference on Questions of Fighting Corrosion). *Gostoptekhizdat, Moskva*. 296–303

Kittipongpatana, O.S. & Sirithunyalug, J. (2006). Development of suspending agent from sodium carboxymethyl mungbean starches. Drug Dev. Ind. Pharm. 32. 809-820.

Kizil, J. and Seetharaman, K., (2002). Characterization of irradiated starches by using FT-Raman and FTIR spectroscopy. *Journal of Agricultural and Food Chemistry. 50*. 3912

Li M, Xu J, & Li R. (2014) Simple preparation of aminothiourea modified chitosan as corrosion inhibitor and heavy metal ion adsorbent. *Journal of Colloid Interface Science.* 417. 131-136.

Liang, Y., Zhang, B. S., Yang, L. S., & Gao, D. W. (2004). Chemical reaction activity of tapioca starch with non-crystallized granule state. *Journal of Zhengzhou Institute of Technology. 25*. 9–13.

Liu, Y., Himmelsbach, D. S. & Barton, F. E. (2004). Two-dimensional Fourier transform Raman correlation spectroscopy determination of the glycosidic linkages in amylose and amylopectin. *Applied Spectroscopy, 58*, 745.

Lopez, O. V., Zaritzky, N. E., & Garcia, M. A. (2010). Physicochemical characterisation of chemically modified corn starches related to rheological behaviour, retrogradation and film forming capacity. *Journal of Food Engineering*, *100*(1), 160-168.

Martinez, M. M., Roscell, C. M., & Gomez, M. (2014). .Modification of wheat flour functionality and digestibilitythrough different extrusion conditions. *Journal of Food Engineering, 143*, 74-79.

Martinez, S. & Stern, I. (2001). Inhibitory mechanism of low carbon steel corrosion by mimosa tannin in sulphuric acid solution. *Journal of Applied Electrochemistry*, *31*, 973.

Manimaran, N., Rajendran, S., Manivannan, M., Thangakani Angelin, J. & Suriya Prabha, A. (2013). Corrosion Inhibition By Carboxymethyl Cellulose. *European Chemical Bulletin. 2*(7). 494-498.

Manivel, P., & Venkatachari, G. (2006). Inhibitive effect of p-aminobenzoic acid and its polymer on corrosion of iron in 1 M HCl solution. *Journal of Materials Science and Technology*. *22*(3): 301-305.

Mekki Daouadji, M. & Chelali, N. (2004). Influence of molecular weight of poly (ortho- ethoxyaniline on the corrosion inhibition efficiency of mild steel in acidic media. *Journal of Applied Polymer Science. 91*(2). 1275-1284.

Mobin, M. & Khan, M. A. (2014). Adsorption and corrosion inhibition behavior of polyethylene glycol and surfactants additives on mild steel in H_2SO_4. *Journal of Materials Engineering and Performance. 23*(1). 222-229

Mobin, M., Parveen, M., & Khan, M. A. (2011). Inhibition of mild steel corrosion using l-tryptophan and synergistic surfactant additives *Portugaliae Electrochimica Acta. 29*(6). 391-403

Mobin, M., Parveen, M. & Rafiquee, M. Z. A. (2013). Inhibition of mild steel corrosion using l-histidine and synergistic surfactants additives. *Journal of Materials Engineering and Performance. 22*(2). 548-556

Mobin, M., Khan, M. A. & Parveen, M. (2011). Inhibition of mild steel corrosion in acidic medium using starch and surfactants additives. *Journal of Applied Polymer Science. 121*. 1558–1565.

Moorthy, S.N., 2002. Physicochemical and functional properties of tropical tuber starches: A review. *Starch. 54*(12):559-592.

Mu, G., Li, X., & Liu, G. (2005). Synergistic inhibition between tween 60 and NaCl on the corrosion of cold rolled steel in 0.5M sulfuric acid, *Corrosion Science 47(8)*. 1932–1952.

Nabais, T., Brouillet, F., Kyriacos, S., Mroueh, M. & Amores, P. *et al*., (2007). High amylose carboxymethyl starch matrices for oral sustained drug-release: In vitro and in vivo evaluation. *European Journal of Pharmaceuticals and Biopharmaceuticals. 65*. 371-378.

Nattapulwat, N., Purkkao, N. & Suwithayapan O. (2009) Preparation and application of carboxymethyl yam (Dioscorea esculenta) starch. *PharmSciTech. 10*(1): 193–198

Noor, E. A. & Al-Moubaraki, A. H. (2008). Thermodynamic study of metal corrosion and inhibitor adsorption processes in mild steel/1-methyl-4 [4′(-X)-styryl pyridinium iodides/hydrochloric acid systems. *Materials Chemistry & Physics*, *110*(1), 145-154.

Ochoa, N., Marisela, B., SancristóbalI, J., Balsamo, V., Albornoz, A., & Joaquin L. *et al.* (2013). Modified cassava starches as potential corrosion inhibitors for sustainable development. *Materials Research.* 1556-1565 doi.org/10.1590/S1516-14392013005000126.

Oki, M., Charles, E., Alaka, C. & Oki, T. K. (2011). Corrosion inhibition of mild steel in hydrochloric acid by tannins rom rhizophora racemosa. *Scientific Research. 2*(6).

Okoro, C. C. (2007). Effect of process modification on the physio-chemical and sensory quality of fufu-flour and dough. *African Journal of Biotechnology. 6* (16) 1949-1953

Oguzie, E. E. (2008). Corrosion inhibitive effect and adsorption behaviour of hibiscus sabdaiffa extract on mild steel in acid media. *Portugaliae Electrochemica Acta*. *26*(3). 303 – 314.

Oguzie, E. E. (2004). Influence of halide ions on the inhibitive effect of congo red dye on the corrosion of mild steel in sulphuric acid solution. *Materials Chemistry & Physics. 87*. 212.

Oguzie E., Onuoha G., & Onuchukwu A. (2004), Influence of halide ions on inhibitive effect of congo red dye on the corrosion of mild steel in sulphuric acid solution, *Materials Chemistry and Physics 89*. 305.

Orubite, K. O., & Oforka, N. C. (2000). Inhibition of the corrosion of mild steel in HCl solutions by the extracts of leaves of Nypa fruticans wurmb, *Materials Letters. 58*(11). 1768-1772

Pawar, P., Gaikwad, A. B., & Patil, P. P. (2007). Corrosion by protective aspects of electrochemically synthesized poly(o-anisidine –co-otoluidine) coatings on copper, *Portugaliae Electrochimica Acta*. *52*. 5958-67

Parveen, M. & Mobin, M. (2013). Novel corrosion inhibiting formulations involving amino acids and surfactants for mild steel in acid medium *International Journal of Scientific & Engineering Research. 4*(12) 167-175.

Popova, A., Sokolova, E., Raicheva, S., & Christov, M. (2003). AC and DC study of the temperature effect on mild steel corrosion in acid media in the presence of benzimidazole derivatives. *Corrosion Science*. *45*(1). 33–58.

Qian, B., Wang, J., Zheng, M., & Hou, B. (2013). Synergistic effect of polyaspartic acid and iodide ion on corrosion inhibition of mild steel in H_2SO_4. *Corrosion Science. 75*. 184-192.

Quraishi, M. A. & Sharma, H. K. (2003). 4- Amino-3-butyl-5-mercapto-1,2,4-triazole;A new corrosion inhibitor for mild steel in sulphuric acid. *Materials Chemistry and Physics 78* (1), 18-21

Rafiquee, M. Z. A., Saxena, N., Khan, S., & Quraishi, M. A. (2008) Influence of surfactants on the corrosion inhibition behaviour of 2-amoniumphenyl-5-mercapto-1-oxo-3,4-diazole (AMOD) on mild steel . *Materials Chemistry & Physics. 107*(2-3) 528-533.

Ragheb, A. A., El-Sayiad, H. S. & Hebeish, A. (1997). Preparation and characterization of carboxymethyl starch (cms) products and their utilization in textile printing. *Starch. 49*. 238-245

Raja, P. B., & Sethuraman, M. G. (2008). Natural products as corrosion

inhibitor for metals in corrosive media — A review. *Materials Letters, 62*(1), 113-116.

Rajendran, S., Sridevi, S. P., Anthony, N. & Amairaj, A. J. (2005). Corrosion behavior of carbon steel in polyvinyl alcohol. *Anti-Corrosion Methods & Materials. 52*(2). 102-107.

Rajeswari, V., Kesavan, D., Gopiraman, M. & Viswanathamurthi, P. (2013). Physicochemical studies of glucose, gellan gum, and hydroxypropyl cellulose - inhibition of cast iron corrosion. *Carbohydrate Polymers. 95*(1). 288-294.

Rani, B. E. A. & Basu, B. B. J. (2012). Green inhibitors for corrosion protection of metals and alloys: An Overview. *International Journal of Corrosion. 38*(17). 105-120.

Refaey, S. A. M., Taha, F. &. Abd El-Malak, A. M. (2004) Inhibition of stainless steel pitting corrosion in acidic medium *Applied Surface Science, 236*(1). 175-185.

Ren, Y., Luo, Y., Zhang, K., Zhu, G., and Tan, X.. (2008).Lignin terpolymer for corrosion inhibition of mild steel in 10% hydrochloric acid medium. *Corrosion Science. 50*(11). 3147-3153.

Rosliza R. & Wan Nik, W.B. (2013). Improvement of corrosion resistance of AA6061 alloy by tapioca starch in seawater. *Current Applied Physics. 10* (1) 221–229

Rosliza, R., Wan Nik, W.B. & Senin, H.B. (2008). The effect of inhibitor on the corrosion of aluminum alloys in acidic solutions. *Materials Chemistry & Physics. 107*. 281–288.

Sakhri, A., Perrin, F. X., Benaboura, A., Aragon, E. & Lamouric, S. (2011).

Corrosion Protection of Steel by Sulfo-Doped Polyaniline-Pigmented Coating. *Progress in Organic Coatings.72*(3), 473-479

Saravanamoorthy, S. & Velmathi, S. (2013). Physiochemical interactions of chiral schiff bases on high carbon steel surface. corrosion inhibition in acidic media. *Progress in Organic coating. 76*:1527-1535.

Sevenou, O., Hill, S. E., Farhat, I. A. & Mitchell, J. R., (2002). Organisation of the external region of the starch granule as determined by infrared spectroscopy. *International Journal of Biological Macromolecules, 31*, 79

Shi, A. M., Li, D., Wang, L. J., Li, B. Z., & Adhikari, B. (2011) Preparation of starch-based nanoparticles through high-pressure homogenization and miniemulsion cross-linking: Influence of various process parameters on particle size and stability. *Carbohydrate Polymers. 83*. 1604–1610

Shinde, V., Sainkar, S. R. & Patil, P. P. (2005). Corrosion by protective Poly(o-toluidine) Coatings on copper. *Corrosion Science. 47*.1352-1369.

Solomon, M. M., Umoren, S. A., Udosoro, I. I. & Udoh, A. P. (2010). Inhibitive and adsorption behaviour of carboxymethyl cellulose on mild steel corrosion in sulphuric acid solution. *Corrosion Science. 52*(4). 1317–1325

Soest, J. J. G. Tournois, H., Wit, D. & Vliegenthart, J. F. G., (1995). Short-range structure in (partially) crystalline potato starch determined with attenuated total reflectance Fourier-transform IR spectroscopy. *Carbohydrate Research, 279,* 201

Souza de S. (2007), Smart coating based on polyanline acrylic blend for corrosion protection of different metals. *Surface Coating Technology. 201*. 7574-81

Sugama, T. & Cook, M. (2000). Poly (itaconic acid)-modified chitosan coatings for mitigating corrosion of aluminum substrates. *Progress in Organic Coatings, 38*(2). 79–87

Sugama, T. & Milian-Jimenez, S. (1999). Dextrine-modified chitosan marine polymer coatings. *Journal of Materials Science. 34*(9). 2003- 2014.

Sugama, T., & DuVall, J. E. (1996). Polyorganosiloxane-grafted potato starch coatings for protecting aluminum from corrosion. *Thin Solid Films. 289*(1-2), 39–48

Sugama, T. (1997). Oxidized Potato-starch Films as Primer Coatings of Aluminium. *Journal of Materials Science, 32*(15), 3995- 4003

Sugama, T. (1995). Pectin Copolymers with Organosiloxane Grafts as Corrosion-protective Coatings for Aluminium. *Materials Letters, 25,* (5-6) 291-299

Sathiyanarayanan, S. K., Balakrishnan, K., Dhawan, S. K. & Trivedi, D. C. (2005). Influence of poly(aminoquinone) on corrosion inhibition of iron in acid media. *Applied Surface Science 252*. 966-975.

Selvaraji, S. K., Kennedy, A. J., Amalraj, A. J., Rajendran, S. & Palaniswamy, N. (2004). Corrosion behaviour of carbon steel in the presence of polyvinylpyrrolidone. *Corrosion Rev 22*(3): 219-32.

Shukla, J., Pitre, K. S., & Jain, P. (2003). Inhibitive effect of PEG on the corrosion of aluminium in acidic medium. Indian Journal of Chemistry Section A; Inorganic, Physical,Theoretical, & Analytical Chemistry. 42(11). 2784-2787.

Sloan, J. W., Mehltretter, C.I. & Senti, R.F. (1962). Carboxymethyl high amylose starch. *Journal of Chemical Engineering Data*. *7* (1). 156-158.

Sharmin, E., Ahmad, S. & Zafar, F. (2012). Renewable resources in corrosion resistance; Dr Shih (Ed.). Corrosion Resistance, *InTech*, www.intechopen.com/books/corrosion-resistance/renewable-resources-in-corrosion-resistance.

Soheila, J., Ali, Y. & Jaber, N. (2013.) Synergistic effect of mixed cationic and anionic surfactants on the corrosion inhibitor behaviour of mild steel in 3.5% NaCl. *Applied Surface Science*. *285*(15). 674–681

Stojanovic, Z., Jeremic, K. & Jovanovic, S. (2000). Synthesis of carboxymethyl starch. *Starch/Starke*. *52*(11). 413-419.

Tang, H., Mitsunaga, T. & Kawamura, Y. (2004). Relationship between functionality and structure in barley starches. *Carbohydrate Polymers. 57.* 145–152.

Torresi, R. M., Solange, S., Pereira da Silva, J. E., Susana, T. & Torresi, C. (2005). Galvanic coupling between metal substrate and polyaniline acrylic blends. Corrosion protection mechanism. *Electrochimica Acta. 50.* 2213-2218

Ubong, M. E. & Mazen, M. K. (2014). Corrosion protection of steel sheets by chitosan from shrimp shells at acid pH. *Cellulose*

Ugwoke, C. E. C., Nzekwe, U., & Ameh, G. I. (2010). Phytochemical constituents and ethnobotany of the leaf extract of bitter leaf (Vernonia amygdalina). *Journal of Pharmaceutical and Allied Sciences 7*(3)

Ulbrich, M., Nathan, C., & Floter, C. (2014). Acid modification of wheat, potato and pea starch applying gentle conditions- impacts on starch properties. *Starke, 66*(9-10), 903-913.

Umoren, S. A., Ebenso, E. E., Okafor, P. C., & Ogbobe, O. (2006). Water soluble polymers as corrosion inhibitors of mild steel in acidic medium. *Pigment Resin Technology 35*(6): 346-52.

Umoren SA, & Obot IB. (2008) Polyvinyl pyrrolidone and polyacrylamide as corrosion inhibitors for mild steel in acidic medium. *Surface Review and Letters.* 25(3): 277-284

Umoren, S. A. (2008). Inhibition of aluminium and mild steel corrosion in acidic medium using gum Arabic. *Cellulose. 15*. 751-61.

Umoren, S. A., Ogbobe, O., Ebenso, E. E., & Okafor, P. C. (2007). Polyethylene glycol and polyvinyl alcohol as corrosion inhibitors for aluminium in acidic medium. *Journal of Applied Polymer Science 105*(6): 3363-70.

Umoren, S. A., Obot, I. B., Ebenso, E. E., Okafor, P. C., Ogbobe, O., & Oguzie, E. E. (2006). Gum arabic as a potential corrosion inhibitor for aluminium in alkaline medium and its adsorption characteristics. *Anti-Corrosion Methods and Materials 53*(5): 277-82.

Umoren, S. A. & Ebenso, E. E. (2008). Blends of polyvinyl pyrrolidone and polyacrylamide as corrosion inhibitors for aluminium in acidic medium *Industrial Journal of Chemical Technology 15*. 355-363.

Umoren , S. A. , Banera, M. J. , Alonso-Garcia, T. , Gervasi, C. A. & Mirifico, M. V. (2013). Inhibition of mild steel corrosion in HCl solution using chitosan. *Cellulose. 20*. 2529-2545.

Umoren, S. A. & Gasem, Z. M. (2013). Influence of molecular weight on mild steel corrosion inhibition effect by polyvinyl alcohol in hydrochloric acid solution. *Journal of Dispersion Science and Technology* 254-260

Umoren, S. A. & Solomon, M. M. (2010). Effect of halide ions additives on the corrosion inhibition of aluminum in HCl by polyacrylamide. *The Arabian Journal for Science and Engineering. 35*. 115 -129

Valdez, B., Schorr, M., Zlatev, R., Carrillo, M., Stoytcheva, M. & Alvarez, L., *et al*. (2013). Corrosion Control in Industry. *Intech. 10*, 72 -87.

Vasco, P. D., Blackwell, J. & Koenig, J. L., (1972) Infrared and Raman spectroscopy of carbohydrates. Part II: Normal coordinate analysis of α-D-glucose. *Carbohydrate Research, 23*, 407.

Vatanasuchart, N., Naivikul O., Charoenrein S. & K. Sriroth, (2003). Effects of different UV irradiations on properties of cassava starch and biscuit expansion. *Journal of .Nature Science, 37*: 334-344.

Vatanasuchart, N., Naivikul O., Charoenrein S. & Sriroth K., (2005). Molecular properties of cassava starch modified with different UV irradiations to enhance baking expansion. *Carbohydrate Polymers. 61*. 80-87.

Vera, R., Schrebler, R., Cury, P. & DelRio, R. (2007). Corrosion protection of carbon steel and copper by polyaniline and poly(ortho- methoxyaniline) films in sodium chloride medium. Electrochemical and morphological study. *Journal of Applied Electrochemistry. 37*. 519-525.

Wang, Y. J., Truong, V. D. and Wang, L.(2003). Structures and rheological properties of corn starch as affected by acid hydrolysis. *Carbohydrate Polymers. 52*(3). 327–333,

Williams, D. N., Gold, K. A., Pulliam Holoman, T. R., Ehrman S. H. & Wilson Jr O. C. (2006). *Journal of Nanoparticle Research 8*(5) 749-753.

Yurt, A., Butun, V. & Duran, B. (2007). Effect of the molecular weight and structure of some novel water soluble triblock copolymers on the electrochemical behaviour of mild steel. *Materials Chemistry & Physics. 105*. 114-121.

Zhang, D. Q., Xie, B., Gao, L. X., Joo, H. G. & Lee, K. Y. (2011). Corrosion inhibition of ammonium molybdate for AA6061 in NaCl solution and its synergestic effect with calcium gluconate. *Journal of Applied Electrochem*istry 481- 491.